

# Properties and clinical relevance of osteoinductive biomaterials

Pamela Habibovic

“Properties and clinical relevance of osteoinductive biomaterials”

The research described in this thesis was financially supported by the European Commission (FP5 project “IntelliScaf” G5RD-CT-2002-00697).

This publication was sponsored by:



Printed by: Febodruk b.v., Enschede, The Netherlands.

ISBN 90-365-2266-8

PhD Thesis, University of Twente, Enschede, The Netherlands

Copyright P. Habibovic, Bilthoven, The Netherlands, 2005. Neither this book nor its parts may be reproduced without written permission of the author.



# PROPERTIES AND CLINICAL RELEVANCE OF OSTEOINDUCTIVE BIOMATERIALS

DISSERTATION

to obtain

the doctor's degree at the University of Twente,

on the authority of the rector magnificus,

prof. dr. W.H.M. Zijm,

on account of the decision of the graduation committee,

to be publicly defended

on Thursday, November 17<sup>th</sup>, 2005 at 13.15

by

Pamela Habibović

born on March 12<sup>th</sup>, 1977

in Tuzla, Bosnia and Herzegovina

**Promoters:** Prof. Dr. Klaas de Groot  
Prof. Dr. Clemens A. van Blitterswijk

## List of publications

This thesis is based upon the following publications:

### Peer reviewed papers:

Habibovic P and de Groot K, Osteoinductive biomaterials, properties and relevance in bone repair, *submitted to Current Opinion in Solid State & Materials Science (COSSMS), special issue on Biomimetics and Tissue Engineering, 2005.*

Habibovic P, Woodfield TBF, de Groot K, and van Blitterswijk CA, Predictive value of in vitro assays in the research on bone and cartilage regeneration, what do they really tell us about the clinical performance?, *submitted to Advances in Experimental Medicine and Technology, 2005.*

Habibovic P, van der Valk CM, Meijer G, van Blitterswijk CA, and de Groot K. Influence of octacalcium phosphate coating on osteoinductive properties of biomaterials. *J Mater Sci Mater Med, 2004; 15(4): 373-380.*

Habibovic P, Li J, van der Valk CM, Meijer G, Layrolle P, van Blitterswijk CA, and de Groot K. Biological performance of uncoated and octacalcium phosphate coated Ti6Al4V. *Biomaterials, 2005; 26(1): 23-36.*

Habibovic P, Yuan H, van der Valk CM, Meijer G, van Blitterswijk CA, and de Groot K. 3D microenvironment as essential element for osteoinduction by biomaterials. *Biomaterials, 2005; 26(17): 3565-75.*

Habibovic P, Sees TM, van de Doel M, van Blitterswijk CA, and de Groot K, Osteoinduction by biomaterials: physico-chemical and structural influences, *submitted to Journal of Biomedical Materials Research A, 2005.*

---

Habibovic P, Yuan H, van de Doel M, Sees TM, van Blitterswijk CA, and de Groot K, Relevance of osteoinductive biomaterials in a critical-sized orthotopic defect, *submitted to Journal of Orthopaedic Research*, 2005.

**Selected abstracts:**

Habibovic P, van der Valk CM, de Groot K, and Layrolle P. Osteo-integration of plasma-spray, biomimetic octacalcium phosphate and carbonated apatite coatings on titanium implants, *Bioceramics 15*, Sydney, Australia, 2002.

Habibovic P, Li JP, van der Valk CM, and de Groot K. Osteoinduction by octacalcium phosphate coated porous Ti6Al4V implants, *Cells, Ceramics and Tissues*, Faenza, Italy, 2003.

Habibovic P, Yuan H, van der Valk CM, van Blitterswijk CA, and de Groot K. Influence of sintering temperature on the osteoinductive properties of calcium phosphate ceramics, *Bone*, Maastricht, The Netherlands, 2003.

Habibovic P, van der Valk CM, and de Groot K. Influence of octacalcium phosphate coating on osteoinductive properties of biomaterials, *18<sup>th</sup> European Conference on Biomaterials*, Stuttgart, Germany, 2003.

Habibovic P, van der Valk CM, van Blitterswijk CA, and de Groot K. Biological performances of uncoated and octacalcium phosphate coated porous Ti6Al4V, *7<sup>th</sup> World Biomaterials Conference*, Sydney, Australia, 2004.

Habibovic P, Yuan H, van der Valk CM, van Blitterswijk CA, and de Groot K. Influence of sintering temperature on osteoinductive properties of two types of calcium-phosphate ceramics, *7<sup>th</sup> World Biomaterials Conference*, Sydney, Australia, 2004.

---

Habibovic P, Yuan H, Sees TM, van den Doel M, van Blitterswijk CA, and de Groot K, Biological performances of osteoinductive and non-osteoinductive biphasic calcium phosphate ceramics in a critical-sized orthotopic defect in goats, *19<sup>th</sup> European Conference on Biomaterials*, Sorrento, Italy, 2005.

Other publications related to this thesis:

Habibovic P, Barrere F, van Blitterswijk CA, de Groot K, and Layrolle P, Biomimetic hydroxyapatite coating on metal implants. *J Amer Ceram Soc*, 2002; 85(3): 517-522.

Habibovic P, Barrere F, and de Groot K, Biomimetic hydroxyapatite coatings, in "Fifteen years of clinical experience with hydroxyapatite coatings in joint arthroplasty", JA Epinette and MT Manley, Editors. 2004; 87-97.

Barrere F, Habibovic P, and de Groot K, Biological activities of biomimetic calcium phosphate coatings, in "Fifteen years of clinical experience with hydroxyapatite coatings in joint arthroplasty", JA Epinette and MT Manley, Editors. 2004; 53-67.

Habibovic P, Barrere F, and de Groot K, New biomimetic coating technologies and incorporation of bioactive agents and proteins, in "Learning from nature how to design new implantable biomaterials", RL Reis and S Weiner, Editors. 2004; 105-21.

---

---

"I have not failed. I have found 10.000 ways that won't work."

Thomas Alva Edison (1847-1931)

---

---

## Table of contents

Abbreviations and definitions.....	10
<b>Chapter 1</b>	
General introduction.....	15
<b>Chapter 2</b>	
Predictive value of in vitro assays for osteoconduction and osteoinduction.....	41
<b>Chapter 3</b>	
Influence of octacalcium phosphate coating on osteoinductive properties of biomaterials.....	63
<b>Chapter 4</b>	
3D microenvironment as essential element for osteoinduction by biomaterials.....	77
<b>Chapter 5</b>	
Osteoinduction by biomaterials: physico-chemical and structural influences.....	97
<b>Chapter 6</b>	
Biological performance of uncoated and octacalcium phosphate coated Ti6Al4V.....	123
<b>Chapter 7</b>	
Relevance of osteoinductive biomaterials in a critical-sized orthotopic defect.....	149
<b>Chapter 8</b>	
General discussion.....	167
<b>Chapter 9</b>	
General conclusions and future perspectives.....	175
Summary.....	180
Samenvatting.....	183
Kratki sadržaj.....	186
References.....	189
Acknowledgements.....	211
Curriculum Vitae.....	213
Selected colour figures.....	214

---

## Abbreviations and definitions

### List of abbreviations:

AHO	Albright hereditary osteodystrophy
ALP	alkaline phosphatase
AMP	adenosine monophosphate
BCP	biphasic calcium phosphate
BET	Brunauer, Emmett and Teller
BMP	bone morphogenetic protein
BSP	bone sialoprotein
CA	carbonated apatite
CaP	calcium phosphate
CG	calcein green
Coll	collagen
DBM	demineralized bone matrix
EDX	energy dispersive x-ray
ESC	embryonic stem cell
ESEM	environmental scanning electron microscope
FGF	fibroblast growth factor
FOP	fybrodisplasia ossificans progressiva
FTIR	fourier transform infra red
G-CSF	granulocyte colony-stimulating factor
GM-CSF	granulocyte-macrophage colony-stimulating factor
HA	hydroxyapatite
IGF	insuline-derived growth factor
IL	interleukin
LM	light microscope
MP	mercury porosimetry
OC	osteocalcin
OCP	octacalcium phosphate



---

ON	osteonectin
OP	osteopontin
OSF2	osteoblast-specific factor 2
Osx	osterix
OTC	oxytetracycline
PDGF	platelet-derived growth factor
PEO	poly(ethylene glycol)- terephthalate
PBT	poly(butylene terephthalate)
PGE	prostaglandin
(P)MMA	(poly)methylmethacrylate
POH	progressive osseous heteroplasia
(Poly)HEMA	(poly)hydroxyethylmethacrylate
PS	plasma-spraying
PTH	parathyroid hormone
PTH-r	parathyroid hormone receptor
PU	polyurethane
Q-PCR	quantitative polymerase chain reaction
RBMC	rat bone marrow cell
RF	radio-frequency
RT-PCR	reverse transcription-polymerase chain reaction
SBF	simulated body fluid
SCS	simulated calcifying solution
Ta	tantalum
TE	tissue-engineering
TGA	thermogravimetry analysis
TGF- $\beta$	transforming growth factor beta
Ti6Al4V	titanium6aluminum4vanadium alloy
vol.%	volume percent
wt.%	weight percent
XRD	x-ray diffraction
XO	xlenol orange
$\beta$ -TCP	beta tricalcium phosphate

**List of relevant definitions as used in this thesis:**

<i>Biomaterial</i>	<p>A non-viable material used in a medical device, intended to interact with biological systems.</p> <p>Material intended to interface with biological systems to evaluate, treat, augment or replace any tissue, organ or function of the body.</p>
<i>Biomimetic material</i>	<p>any material that is structurally or chemically analogous to a component of plant or animal tissue and which can be incorporated into any product whose use is based on the characteristics of that tissue component.</p>
<i>Bone</i>	<p>the hard, rigid form of connective tissue constituting most of the skeleton of vertebrates, composed chiefly of calcium salts embedded in collagen fibers.</p>
<i>Ceramic</i>	<p>type of material chemically derived from the combination of one or more metallic elements with one or more non-metallic elements, usually ionically bound but with a contribution from covalent bonding, characterized in the solid state by extreme brittleness.</p>
<i>Coating</i>	<p>deposited layer or covering on a biomaterial or medical/dental device which is intended to protect or enhance the performance of the device or biomaterial.</p>
<i>Ectopic</i>	<p>located away from normal position.</p>
<i>Femur</i>	<p>the thigh bone.</p>
<i>Graft</i>	<p>piece of viable tissue or collection of viable cells transferred from a donor site to a recipient site for the purpose of reconstruction of the recipient site. Bone grafts can be substituted by biomaterials.</p>
<i>Iliac wing</i>	<p>the upper and largest part of bony pelvic girdle.</p>
<i>Implant</i>	<p>medical device made from one or more biomaterials that is intentionally placed within the body, either totally or partially buried beneath the epithelial surface.</p>

---

<i>Interconnectivity</i>	the degree to which a single phase within a medium is joined to form continuous paths.
<i>Macropore</i>	pore with the diameter larger than 10 micrometers.
<i>Micropore</i>	pore with the diameter smaller than 10 micrometers.
<i>Orthotopic</i>	occurring at the normal place.
<i>Osteoconduction</i>	<ul style="list-style-type: none"><li>• The process through which bone is directed into material structures such as pores, channels and pipes.</li><li>• Spreading of bone over the surface proceeded by ordered migration of differentiating osteogenic cells.</li></ul>
<i>Osteogenesis</i>	bone formation by determined osteoprogenitor cells (DOPCs).
<i>Osteogenic</i>	relating to or derived from the tissue from which bone is developed.
<i>Osteoinduction</i>	<ul style="list-style-type: none"><li>• The mechanism of cellular differentiation towards bone of one tissue due to the physicochemical effect or contact with another tissue.</li><li>• The induction of undifferentiated inducible osteoprogenitor cells (IOPCs) that are not yet committed to the osteogenic lineage to form osteoprogenitor cells.</li></ul>
<i>Osteointegration</i>	the concept of a clinically asymptomatic attachment of a biomaterial to bone, under conditions of functional loading.
<i>Pore</i>	small space between solid parts or particles within a material.
<i>Porosity</i>	the collection of pores making up the void space within a porous material.
<i>Specific surface area</i>	category unit in $\text{m}^2/\text{kg}$ .



## Chapter 1

### General introduction

Pamela Habibovic, Clemens A. van Blitterswijk and Klaas de Groot

University of Twente, Institute for Biomedical Technology,  
Professor Bronkhorstlaan 10D, 3723 MB, Bilthoven, The Netherlands

#### 1.1 Biomineralization

Some 540 million years ago, within a period of a few million years, a multitude of primarily multicellular organisms began to produce mineralized skeletal structures. During this crucial period in the evolution of biomineralization, the basic structural patterns for skeletal formation were fixed, although it has been suggested that some of the underlying principles used for mineralization itself were acquired from ancestral organisms [1].

Today the phenomenon of biomineralization is widespread. Almost all living organisms can deposit minerals that serve a wide variety of functions: magnetotactic bacteria deposit iron oxide enclosed in organic sheaths, mollusks form calcite crystals in their shells, and vertebrates generate the apatite crystals found in bones and teeth. More than sixty different minerals are known to be formed by living organisms, including amorphous minerals, inorganic crystals and crystals including organic compounds. Calcium minerals represent some 50% of all known biogenic minerals and the two major skeleton-reinforcing minerals are calcium carbonate and calcium phosphate [2].

The most common use of crystals is in the form of multicrystalline arrays, primarily to form skeletal structures. The order of the crystals in these arrays can largely differ between different organisms. In the next paragraphs, an overview of the known facts regarding the development of crystalline mineral deposition is given [2].

The current understanding of biomineralization *in vivo* is still very limited and the underlying principles involved are for the most part derived from observations *in vitro*.

Understanding how a whole ordered array of macromolecules and crystals can make biological materials is still far beyond our knowledge. However, there are some well known and generally accepted facts that can help in understanding the mechanism of biomineralization and potentially using this knowledge for purposes of developing intelligent synthetic biomaterials.

It is generally accepted that physiologic mineral, i.e. the formation of mineral in an organized fashion in shells, teeth and bones, does not occur without a matrix. The matrix provides an oriented support for mineral deposition, and may participate directly in the mineralization process by serving as nucleator, or holding and orienting ions which become incorporated into the mineral crystals [3].

The matrix is not the same in all mineralized tissues. Even in vertebrates where type I collagen is the predominant component of dentin, cementum and bone, the calcified cartilage matrix is distinct, containing types II, IX and X collagen as well as proteoglycans, and the enamel matrix is even more unique. The matrices which contain type I collagen also show individual variations. For example, dentin contains dentin phosphoprotein, dentin phosphophoryn and dentin sialoprotein, while none of these exist in bone [4].

The mineral itself is also not the same in all mineralized tissues. For example, calcium carbonates, silicates and oxalates are found in invertebrates, while calcium phosphate apatitic minerals are found in enamel, dentin and bone. The formation of the stable apatitic structure which comprises physiologic mineral of i.e. bone is preceded by a less stable calcium-phosphate phase. There are reports suggesting that this phase is amorphous calcium-phosphate. In addition, dicalcium phosphate and octacalcium phosphate have been proposed as possible precursors of the final bone mineral [1].

The mechanisms underlying mineral deposition can be different too. A key step in the control of mineralization employed by almost all organisms is the initial isolation of a space. Then, under controlled conditions minerals are induced to form within the space. The space is usually delineated by cellular membranes and vesicles [2]. In the case of bone, minerals start to nucleate in the spaces isolated by the collagen fibrils. This heterogeneous nucleation is catalyzed by the phosphated ester- and carboxylate groups present in collagen fibrils. The growth of the crystals consequently takes place along the collagen fibrils, interconnecting them [5, 6]. However, in turkey tendons for

example, matrix vesicle and collagen mineralization start simultaneously at different sites. In other tissues, sulphate-rich proteins, such as bone sialoproteins or proteoglycans, appear to be sites of initial mineralization [4]. In many invertebrates, and in enamel, there are no extracellular matrix vesicles, suggesting that other processes are involved in enamel mineralization. Recently, it was proposed that during mineralization of enamel, linear aggregates of polarized, self-assembled amelogenin nanospheres form a negatively charged template that induces apatite formation [3].

Biom mineralization is thus a complex and only partially understood phenomenon. Further research into mechanisms of biom mineralization, which probably needs to be conducted at micro- and even nanolevel, will be of great importance for the development of successful synthetic bone grafts.

## **1.2 Bone**

Bone is a highly specialized form of connective tissue that is nature's provision for an internal support system in most higher vertebrates. Bone provides for the attachment of the muscles and tendons essential for locomotion, protects the vital organs of the cranial and thoracic cavities, and it encloses the bloodforming elements of the bone marrow. In addition to these mechanical functions, bone plays an important metabolic role as a mobilizable store of calcium and phosphate, which can be drawn upon when needed in the homeostatic regulation of the calcium and phosphate in blood and other fluids of the body [7].

By weight, bone contains approximately 60% mineral, 10% water and about 30% organic matrix. Type I collagen constitutes approximately 90% of the organic matrix; the remaining 10% is composed of proteoglycans and numerous noncollagenous proteins, such as osteocalcin, osteopontin, osteonectin, bone sialoprotein, decorin and biglycan [8, 9]. Bone mineral has a structure similar to type AB carbonated calcium-phosphate apatite. In addition, bone mineral apatite contains non-apatitic carbonate and phosphate groups, which are, from the structural and physical point of view, unstable and very reactive. The high reactivity potential of these groups plays an important role in the formation and degradation of the bone tissue [10-12].

Morphologically there are two forms of bone: cortical (compact) bone and cancellous (trabecular) bone. Compact bone, which is rigid and dense, is found mainly in the middle shaft of long bones or shells of other bones. Found predominantly in epiphysis, ribs and spine, cancellous bone has a highly porous structure (>75%), with numerous small bone trusses or trabeculae interconnected with each other, and tends to orient along the principal directions in adaptation to the external loading environment.

Bone is composed of four different cell types. Osteoblasts, osteoclasts and bone lining cells are present on bone surface, whereas osteocytes permeate the mineralized interior. Osteoblasts, osteoclasts and bone lining cells originate from local osteoprogenitor cells, whereas osteoclasts arise from the fusion of mononuclear precursors, which originate in the various hemapoietic tissues. Osteoblasts are the fully differentiated cells responsible for the production of the bone matrix and regulation of its mineralization. The osteocyte is a mature osteoblast within the bone matrix and is responsible for the matrix maintenance. Bone lining cells are flat, elongated cells that cover bone surfaces that are undergoing neither bone formation nor resorption. Little is known regarding the function of these cells, however, it has been speculated that bone lining cells can be precursors for osteoblasts. Osteoclasts are large, multinucleated cells, which are able of resorbing bone mineral.

### **1.3 Current methods of bone repair**

The improvement of the quality of life and consequent increase of life expectancy are accompanied by the expanding demand for the repair of damaged and degraded organs and tissues. Bone tissue regeneration remains an important challenge in the field of orthopaedic- and maxillofacial surgery. Spinal fusions and repairs of bone defects caused by traumas, tumors, infections, biochemical disorders and abnormal skeletal development, are some examples of the frequently performed surgeries in the clinic. For most of these surgeries, there is a great need for grafting materials. Below, an overview of the existing bone graft substitutes is given.



### **1.3.1 Natural bone grafts**

Autologous bone is still considered the golden standard for bone repair and regeneration, in particular because of the absence of immunogenic reaction after the surgery [13-17]. In addition, autologous bone grafts possess a great biological performance in terms of osteogenicity (supply of bone forming cells by the bone marrow) [18], osteoinductivity (initiation of the differentiation of mesenchymal stem cells towards the osteogenic lineage by e.g. bone morphogenetic proteins (BMPs) present in the graft) [14, 17-19] and osteoconductivity (facilitation of cell- en nutrient infiltration through the 3D porous structure) [17, 18, 20]. Although autologous bone grafting meets many requirements for bone regeneration, its use is also associated with some important drawbacks. The harvest of the graft requires an additional invasive surgical procedure that may lead to donor site morbidity [14, 16-18], chronic post-operative pain [17, 21-23], hypersensitivity [17] and infection [18, 23, 24]. Another important drawback of the use of autograft is the limited availability. Unlike autologous bone, allogeneic and xenogeneic grafts are widely available and do not require an additional surgery on the patient. However, allogeneic bone has to undergo processing techniques such as lyophilization, irradiation or freeze-drying to remove all immunogenic proteins in order to avoid any risk of immunogenic reaction [25, 26]. In turn, these processing techniques have a negative effect on osteoinductive and osteoconductive potential of the allografts [27], which consequently decreases their biological performance as compared to autografts [21, 28-30].

### **1.3.2 Synthetic bone graft substitutes**

Because of the above-mentioned drawbacks of natural bone grafts, a large number of synthetic graft substitutes have been developed. Synthetic bone graft substitutes are largely available, they do not cause antigenic response and can easily be tailored depending on the intended application. Synthetic bone graft substitutes are based on the biomaterials, which are defined as “non-viable materials used in a medical device, intended to interact with biological systems” [31].

As shown in the chart in figure 1, based on their chemical composition, biomaterials can be divided into four groups:

- Metallic implants, such as titanium and its alloys, stainless steel and cobalt-chromium alloys,
- Ceramics, such as calcium-phosphate-, alumina-, carbon- and glass ceramic,
- Polymers like poly (methyl methacrylate), poly (urethane), ultra high molecular weight poly ethylene, silicon and polylactide,
- Composites of first three groups such as calcium-phosphate ceramic coatings on metallic implants or polymer-ceramic composites.

Diverse calcium-phosphate containing biomaterials and metals, as well as the combinations of the two are most frequently used for bone repair and replacement.

### **1.3.2.1 Calcium phosphate biomaterials**

Calcium-phosphate (CaP) biomaterials, with the chemical composition similar to that of bone and teeth mineral, are the most widely used synthetic bone graft substitutes. In addition to an excellent biocompatibility, their bioactivity is remarkable.

As reviewed by Damien and Parsons [17], various CaP biomaterials have shown some distinct clinical successes. Both hydroxyapatites of natural origin (coral- and bovine bone derived) and synthetic hydroxyapatites have widely been tested and successfully used for clinical applications. Due to its low resorption rate, hydroxyapatite has proven to be a good material for alveolar ridge augmentation, pulp capping, and filling of periodontal defects, where the use of autologous bone has been found to be less than optimal. In orthopaedics, porous hydroxyapatite blocks have been used for filling defects remaining after tumor excision, for spinal fusion of vertebral bodies and for the canine defects. Dental applications of tricalcium phosphate ceramics include the filling of defects due to periodontal loss, as well as repairing cleft palates. In orthopaedics, tricalcium phosphate remains an implant material for defect filling where a resorbable material is indicated. A ceramic receiving much attention is biphasic calcium phosphate, consisting of hydroxyapatite and tricalcium phosphate. This ceramic is clearly biocompatible and osteoconductive, while having a resorption rate between that of

pure hydroxyapatite and pure tricalcium phosphate. By altering the ratio of hydroxyapatite to tricalcium phosphate, variable rates of degradation can be achieved. Clinically, biphasic calcium phosphate has been tested for treatment of patient with scoliosis and for filling defects after tumor removal.

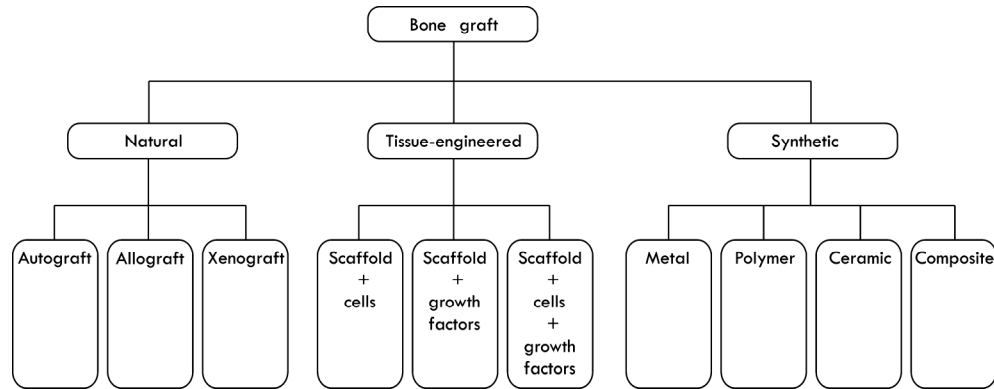


Figure 1: an overview of bone grafts and bone graft substitutes.

The concept of developing CaP cement was introduced by LeGeros et.al. and Chow et.al. CaP cements consist of solid and liquid components, and the product obtained after the setting of the cement is dependent on the reaction between these two components. A great advantage of the cements above other CaP materials is that they are injectable [32].

Investigations of the biological performances of glass ceramics and bioactive glass have also shown favorable bone-bonding characteristics, due to their ability to form a CaP rich layer on their surface. However, their inherent weakness limits their use to non-loadbearing sites and alveolar ridge reconstruction [17, 33, 34].

### 1.3.2.2 Metals

Metallic implants like titanium and its alloys are biocompatible [35, 36] and have excellent mechanical properties, which makes them suitable for load-bearing

applications [37]. However, high stiffness of the metals often leads to stress-shielding from residual bone, which may result in detrimental resorptive bone remodeling [38], and consequently to a poor fixation of the implant. Recent developments in metallic implant designs therefore focus on adapting the mechanical properties of metals to those of biological systems, by e.g. introduction of a porous structure. Although they are widely used in load-bearing application, the ability of metals to bond to bone and to guide new bone formation are distinctly smaller as compared to the earlier described CaP materials.

Heat-, acidic and alkaline treatments of metals, and sputtering of their surfaces with e.g. corundum are all meant to increase the surface roughness of and even to introduce microporosity into their structures. By doing so, the surface of metallic implant harbors nucleation sites for the formation of calcium-phosphate crystals in a saturated environment, which in turn, can significantly influence the metal's bioactivity. Similarly, aluminum oxide powder can be used to make highly macro- and microporous metallic ceramics, with improved bioactivity as compared to other metals.

### **1.3.2.3 Composites**

Composites consist of two or more different biomaterials which are combined with the aim to improve their properties in terms of mechanical strength, osteoconductivity, etc. For example, in order to decrease stiffness of CaP ceramics without losing their osteoconductive properties, composites of collagens [39] and synthetic polymers [40, 41] with CaPs are made.

Another example of composites are CaP ceramic coatings that have been developed in order to be combined with e.g. metallic implants. Thereby, mechanical properties of metals are combined with the osteoconductivity of CaPs. Plasma sprayed coatings, mainly hydroxyapatite, on titanium alloy (Ti6Al4V) prostheses have widely been used in orthopaedic surgery to reconstruct hip and knee joints. Earlier investigations have shown that these coatings can successfully enhance clinical success to less than 2% failures after 10 years [42]. Despite excellent clinical performances, the plasma spray process is limited by intrinsic drawbacks. For instance, this line-of-sight process takes place at high

temperatures. The process is, therefore, limited to thermally stable phases like hydroxyapatite, and the incorporation of growth factors that stimulate bone healing is impossible. Furthermore, the process of plasma-spraying cannot provide even coatings on porous metal surfaces. Recently, other techniques have been studied to improve the quality of coatings, such as electrophoretic deposition [43], sputter deposition [44], and sol-gel [45]. Nevertheless, the deposition of apatite coatings from simulated body fluids offers the most promising alternative to plasma-spraying and other coating methods. The biomimetic approach has four main advantages: it is a low temperature process applicable to, besides metals, any heat-sensitive substrate including polymers [46], it forms bone-like apatite or octacalcium phosphate crystals having high bioactivity and good resorption characteristics [47], it is evenly deposited on or even into porous or complex implant geometries and it can incorporate bone growth stimulating factors [48, 49].

### **1.3.3 Tissue-engineered hybrids**

Despite intensive research and continuous improvements of synthetic biomaterials, so far these materials do not perform as good as autologous bone grafts. Bone conduction over the material surface and the replacement by bone as well as their mechanical properties are usually inferior to autologous bone grafts [17, 29, 50-52]. In order to bring the biological performance of synthetic biomaterials closer to that of autologous bone, a new interdisciplinary research field has developed: tissue engineering. In 1993 Langer and Vacanti defined tissue engineering as an: “interdisciplinary field that applies principles of engineering and life sciences toward the development of biological substitutes that restore, maintain, or improve tissue function” [53]. With regard to bone regeneration, mainly two strategies have been implemented to generate new tissue: 1) chemical stimulation of bone formation through the use of bone inducing substances and 2) the construction of hybrid implants composed of osteogenic cells/tissue and a biomaterial scaffold [53].

To date numerous growth factors have been identified and subsequently produced by recombinant gene technology, such as bone morphogenetic proteins (BMPs) and other

members of the transforming growth factor  $\beta$  (TGFs- $\beta$ ) family, fibroblast growth factors (FGFs), platelet-derived growth factors (PDGFs) and insulin derived growth factors (IGFs). Various studies have shown that bone growth factors have several regulating effects on cells from the osteoblastic lineage and in vivo studies have demonstrated that some factors can induce bone formation and/or stimulate bone healing. Kirker-Head has reviewed the application of BMPs in a number of animal models at various orthotopic sites, such as spinal fusion, long bone defects, mandibular and cranial bone defects, fracture healing, as well as in periodontal regeneration, alveolar ridge augmentation and osteointegration of dental implants [54]. In addition, various preclinical and clinical studies have shown positive effects of BMP in nonunions and segmental defects, like traumatic tibial defect [55, 56] and femoral defects [57].

The combination of autologous cells with carriers is another way to produce tissue-engineered hybrids. Various cell types such as calvarial [58, 59] and periosteal [60, 61] cells, osteoblasts of trabecular bone [62, 63], chondrocytes [64] and vascular pericytes [65] have been tested as potential sources of bone forming cells. Nevertheless, the most widely used source of osteogenic cells is bone marrow. Bone marrow has been recognized as a source of osteoprogenitor cells that can differentiate towards bone forming cells when cultured under adequate conditions [66-69]. In addition, bone marrow has been shown to be the most abundant source of osteoprogenitors, which possess high proliferative ability and great capacity for differentiation [70, 71]. Studies in rodents have shown the feasibility of the tissue-engineered hybrids, consisting of a carrier and bone marrow stromal cells, after ectopic [72, 73] and orthotopic implantation [72-76]. In larger animals, there are a few studies showing the biological performance of the TE hybrids, in ectopic [77-80] and orthotopic sites [80-82].

Although both growth factors-based and cell-based tissue-engineered constructs have shown the capability to enhance bone formation when implanted orthotopically, their biological performance is for a big part dependent on the construct carrier. For example, when BMPs are implanted without a carrier, they are reported to diffuse too rapidly to be able to induce or to enhance new bone formation. Furthermore, the amount of BMP necessary to achieve a certain dose in vivo is also carrier dependent [83-85]. Similarly, a suitable carrier is a prerequisite for the success of a cell-based tissue-engineered construct. For instance, recent studies have shown that bone formation

in tissue-engineered constructs is restricted to confined areas of the scaffold. Furthermore, bone bridging between individual tissue-engineered material granules is exceptional. In addition, the findings of the clinically relevant studies suggest that the effect of tissue engineering is moderate and may be irrelevant at long-term implantation intervals [86]. The tissue engineering technique is also associated with some drawbacks. The production of recombinant growth factors, collection and transport of the biopsies, culture of autologous cells are some of the factors that make tissue engineering time-, money- and labor-consuming.

The real challenge of the bone regeneration research field still lies in the development of synthetic bone graft substitutes. Further improvement of biomaterials is needed in order to make tissue engineering more successful, and ideally, even unnecessary. Fully synthetic “intelligent” biomaterials should be able to perform at least as good as autologous bone graft. A group of potentially “intelligent” biomaterials are osteoinductive biomaterials.

#### **1.4 Backgrounds on osteoinduction**

Bone and cartilage formation has been found in extraskelatal tissues after implantation of devitalized tissue and tissue extracts as early as in the beginning of the 20<sup>th</sup> century [87-91]. At that time however, consistent results have rarely been obtained and little was known about elements involved in this process.

In 1958 Bridges and Pritchard performed a screening study in rabbits in order to examine the fate of a variety of devitalized tissues and other substances introduced in the rabbit soft tissue and to study the histological changes occurring after procedures which consistently resulted in bone or cartilage formation [92]. The results of this study showed that tissues containing hypertrophic cartilage consistently induced bone if devitalized with alcohol, acetone, hydrochloric acid or heating to 55 °C, while skeletal and cardiac muscle and tissues containing smooth muscle, which were devitalized with alcohol and acetone, consistently induced cartilage followed by bone. It was concluded that induction was due to liberation of chemical substances, possibly of protein nature,

from the implants, and that these substances may be identical in hypertrophic cartilage and muscle.

In 1965 Urist set a landmark in the research into osteoinduction by publishing a report in which osteoinduction by hydrochloric acid-decalcified diaphyseal bone was consistently shown in muscles of rabbits, rats, mice and guinea pigs [19]. Urist illustrated that bone formation in extraskeletal implants of decalcified bone matrix occurs in the interior of cavities, and that new osteoblasts are not derived from elements of the donor tissue, but from proliferating pluripotent, ingrowing cells of the host.

Another highly valuable report in osteoinduction was published by Friedenstein in 1968 in which bone induction by transitional epithelium was described [93]. The author defined osteoinduction as “the induction of undifferentiated inducible osteoprogenitor cells (IOPCs) that are not yet committed to the osteogenic lineage to form osteoprogenitor cells”. This induction only takes place in the presence of inducing substances, such as transitional epithelium or demineralized bone.

Later work by Urist and coworkers led to the conclusion that a discrete protein within the demineralized bone matrix (DBM) was the sole inducer of bone formation. This finding was published in 1971 and this protein was named Bone Morphogenetic Protein (BMP) [94]. BMP was shown to be involved in the bone formation cascade of chemotaxis, mitosis, differentiation, callus formation and finally bone formation. Different groups showed that BMPs have the ability to induce de novo endochondral bone formation when implanted in ectopic sites of different experimental animals. Proof that BMP could be extracted from demineralized bone matrix and still retain its ability to form bone came in 1977 [95].

#### **1.4.1 Osteoinduction by Bone Morphogenetic Proteins**

To date 15 BMPs are known (BMP1-15) [96]. Besides BMP-1, which is a metalloprotease [97], BMPs belong to the Transforming Growth Factor beta (TGF- $\beta$ ) superfamily [98, 99]. When DBM (or BMPs) are implanted ectopically in rodents, a cascade of events, similar to embryonic bone formation and fracture healing is initiated. First, the chemotaxis of undifferentiated mesenchymal cells occurs, followed by cell



proliferation. Then, these cells differentiate into chondroblasts and chondrocytes, followed by the formation of cartilaginous extracellular matrix including type II collagen and proteoglycans. The chondrocytes mature and become hypertrophic, and cartilage starts to mineralize. Following the period of chondrogenesis, blood vessels appear at the implantation site. Bone-forming cells are consequently observed, and while calcified cartilage is removed by osteoclasts, bone matrix is produced. Once bone has been formed, hemopoietic bone marrow appears within the bone. Finally, bone undergoes remodeling [100]. In figure 2, a sequence of events during osteoinduction by BMPs is illustrated.

Although it is generally thought that BMP-induced bone formation is endochondral [101], recent reports have shown that, depending on the carrier on which BMPs are implanted in the body, osteoinduction by BMPs can be either endochondral or intramembranous. For example, fibrous collagen membrane [102], hydroxyapatite [103] and biomimetic CaP coatings [104] in combination with BMP have shown intramembranous bone induction. In contrast, BMPs on fibrous glass membrane and insoluble bone matrix showed that ectopic bone was formed following the process of endochondral ossification [102, 103]. The exact reason for the observed difference between different carriers is not completely understood yet. It has been proposed that differences in vascularization as well as differences in local oxygen concentrations might be of importance in the process of differentiation of the undifferentiated cells into either chondroblasts or directly into osteoblasts [105]. For both optimal vascularization and oxygen levels, the ultrastructure of the carrier has been proposed to be relevant [106]. Osteoinductive capacity of BMPs has mostly been tested in rodents, either subcutaneously or intramuscularly. In comparative studies, more bone was induced intramuscularly than subcutaneously or intra-fatty, suggesting again the importance of vascularization in ectopic bone formation, as it is generally accepted that the level of vascularization is higher in the muscle as compared to other investigated soft tissues [107, 108]. Only a few reports describe osteoinduction by BMPs in higher animals, namely in monkeys and baboons [109-112]. Besides the observations of the differences in response to BMPs between different species [112], there are reports showing differences in response to ectopically implanted BMPs, between individuals of the same species, probably due to genetic differences [113].

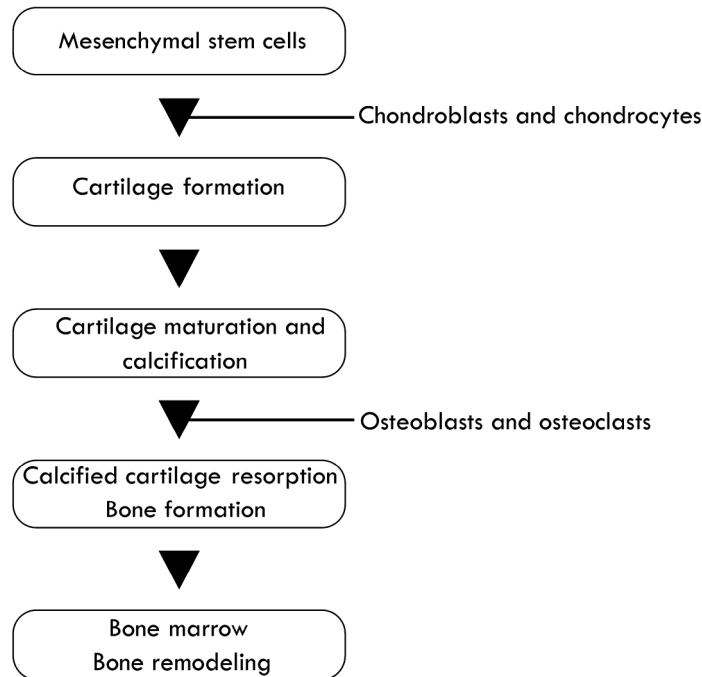


Figure 2: the sequence of events in endochondral bone formation.

#### 1.4.2 Osteoinduction by biomaterials

Soon after Urist's description of osteoinduction by DBM and the suggestion that BMPs are responsible for the process of osteoinduction, Winter and Simpson described an observation of bone induction by a sponge made of polyhydroxyethylmethacrylate (poly-HEMA), that was at that time used for e.g. breast augmentations, in soft tissue of pigs [114]. The authors observed that the implanted sponge became calcified prior to bone formation. Calcification of the used sponge was also observed after subcutaneous implantation in rats. The observed phenomenon of bone induction by the polymeric sponge could not be explained by the Urist's theory, as the sponge neither contained nor produced BMPs. Interestingly, in earlier reports it was observed that bone was induced by tendons and arteries only if they were first calcified *in vivo*, as reviewed by de Groot [115]. Although the exact underlying phenomenon was not known, these

observations suggested that calcification, and hence calcium-phosphates might play an important role in the process of osteoinduction.

In the last decade, a large number of publications illustrated osteoinduction by diverse CaP biomaterials, such as synthetic hydroxyapatite ceramic in dogs [116-120], coral derived hydroxyapatite ceramic in dogs, monkeys and baboons [117, 121-123],  $\alpha$ -tricalcium phosphate,  $\beta$ -tricalcium phosphate-, biphasic calcium phosphate-,  $\alpha$ -pyrophosphate- and  $\beta$ -pyrophosphate ceramics [122, 124-130]. In addition, CaP cements [124, 131] and coatings [132, 133] were shown to be osteoinductive in various animal models. Besides CaP containing biomaterials, osteoinduction was also observed in alumina ceramic [134], titanium [135, 136] and glass ceramics [137]. The last group of materials was shown to be able to precipitate a CaP layer on their surface in a Ca- and P-rich environment, and their in vivo ectopic bone formation was preceded by the process of calcification.

Until now the exact mechanism of osteoinduction by biomaterials is still largely unknown. It is furthermore questionable whether the mechanisms of osteoinduction by BMPs and osteoinduction by biomaterials are the same. In some reports by Ripamonti and coworkers it is hypothesized that endogenous BMPs are collected in the biomaterial post-implantation and that they consequently induce bone formation ectopically [138, 139]. The authors, however, failed in giving a conclusive evidence for their hypothesis. In the pilot study by Yuan and coworkers it was suggested that BMPs do play a role in osteoinduction by biomaterials, although this role does not seem to be essential [140]. The limited number of animals used in this pilot study limited the reliability of its results. The three apparent differences in osteoinduction by BMPs and biomaterials are that 1) bone induced by biomaterials is always intramembranous [121, 129] while BMP-induced bone is mostly formed via the endochondral pathway [101], 2) in small animals such as rodents bone is very rarely induced by biomaterials [116, 141-144], but easily by BMPs [145-147] and 3) while bone is never observed on the periphery of the biomaterials and it is always formed inside their pores, bone formation by BMPs is regularly seen on the outside of the carrier and even in the soft tissue distant from the carrier surface [104, 148].

The exact processes involved in the mechanism of osteoinduction by biomaterials are still largely unknown. The work by many groups has, however, shown that biomaterials need to meet very specific requirements in terms of (I) macro-, (II) microstructure and (III) chemical composition in order to be osteoinductive.

From the literature, the following is known about the relevance of the above material characteristics in the process of osteoinduction:

(I) Macrostructure:

- CaP ceramics: Bone induction by CaP ceramics was never observed on flat ceramic surfaces. All osteoinductive ceramics had either a porous macrostructure [116, 118, 119, 121, 122, 124-126, 128, 149] or a macrostructure that contained well-defined concavities [138]. Bone formation was never observed on the peripheries of porous implants, and was always found inside the pores or concavities, aligning the surface.
- CaP cements: Bone induction in CaP cements was only observed in the pores and surface crevices formed due to degradation of cements [124, 131]. Bone formation was never observed on the flat cement surfaces.
- CaP coatings: Bone induction by the biomimetically produced octacalcium phosphate was only observed when the coating was applied on porous scaffolds and solely in their center [132, 133]. Similarly, bone formation was observed inside the octacalcium phosphate coated hollow titanium cylinders, contrary to the dense coated titanium cylinders [132].
- Glass ceramic [137], alumina ceramic [134], polymeric sponge [114] and titanium [135, 136]: osteoinductive glass ceramic, alumina ceramic and synthetic poly-HEMA sponge all possessed a porous macrostructure. Osteoinductive titanium was macroporous having a complex macrostructure produced by sputter technique. The same porous metal, produced in the form of fibrous mesh, i.e. with a more simple porous structure, was not osteoinductive [135].

**(II) Microstructure:**

- Unfortunately, in many reports on osteoinduction, microstructures of the used materials were poorly characterized. The following reports gave an indication of the importance of microstructure:
- CaP cements: pores and surface crevices in which the bone induction took place had a rough microstructure [124, 131].
- CaP coatings: bone induction was observed on the octacalcium phosphate coated porous Ta implants, in contrast to the carbonated apatite coated ones [132]. Apart from the chemical composition difference between the two CaP phases, the two coatings differed significantly in their surface morphologies. Octacalcium phosphate coating had a rough morphology, due to its large crystals perpendicularly grown on the substrate surface, in contrast to a more smooth morphology of carbonated apatite.
- Glass ceramic, alumina ceramic, titanium and glass [134, 137]: all materials possessed a rough surface due to the used production techniques. Only chemically/thermally treated titanium implants induced bone [135, 136]. The result of such a treatment was the formation of micropores on the metal surface, which was absent on the untreated implants.

**(III) Chemical composition (presence of CaP):**

- CaP ceramics, cements and coatings and glass ceramic all contained CaP. Poly-HEMA sponge, alumina ceramic and titanium did not contain CaPs initially. Nevertheless, all these materials are known to be able to calcify in vitro when immersed in SBF [135]. A similar process of calcification, that is possibly a precursor of bone formation, is expected to take place in vivo [114, 134, 135, 137].

Based on the knowledge of the importance of structural and physico-chemical properties of the material in the process of osteoinduction, a hypothesis of the mechanism of osteoinduction by biomaterials is given in a flowchart (figure 3).

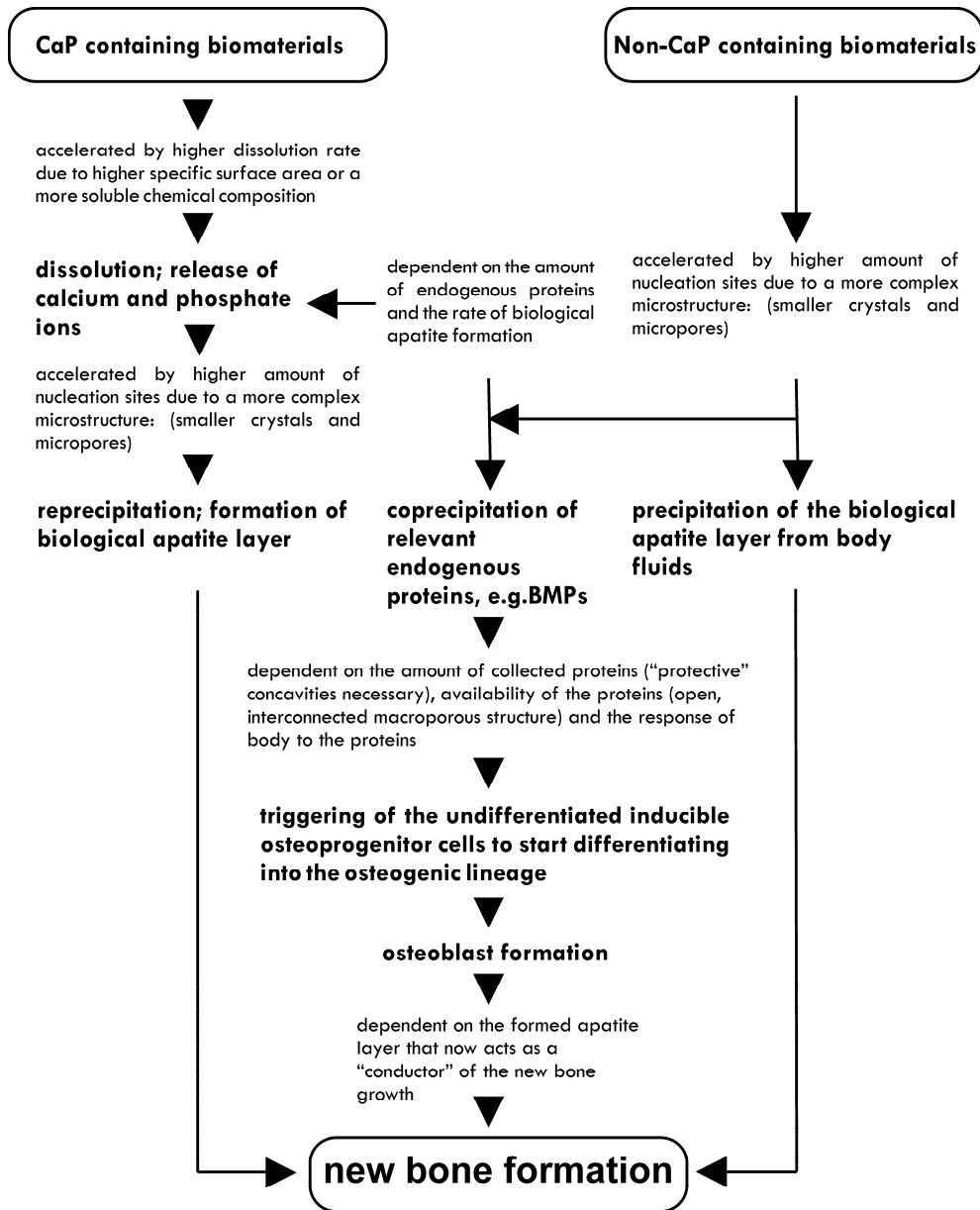


Figure 3: flowchart of the proposed mechanism of osteoinduction by biomaterials.

The interest in osteoinductive biomaterials is based on the hypothesis that a material that is able to induce bone ectopically will also perform better at orthotopic sites.

However, because of the lack of understanding of the mechanism of osteoinduction by biomaterials, at present, many studies still focus on ectopic implantations, as this is the only way to give the evidence of osteoinductive potential of a biomaterial.

Therefore, the number of studies in which osteoinductive potential of a material is directly linked to its performance orthotopically is very limited, and even more limited is the number of studies in which osteoinductive materials are tested in clinically relevant orthotopic defects.

## **1.5 Heterotopic ossification**

The phenomenon of osteoinduction cannot be discussed without shedding light upon a frequently observed clinical problem which closely resembles osteoinduction: heterotopic ossification. Heterotopic ossification, sometimes also called pathological ossification is often simply defined as the presence of bone in soft tissue, where bone normally does not exist. This condition should not be confused with metastatic calcification, such as observed with hypercalcemia, and dystrophic calcification, which occurs in morbid tissues such as tumors.

Heterotopic ossification can roughly be divided into two forms. The first, acquired form is often associated with trauma (fracture, total hip arthroplasty, muscular trauma) or has a neurogenic cause (spinal cord or central nervous system injuries) and is most common. In addition, there is the rare hereditary form, including fibrodysplasia ossificans progressiva (also known as myositis ossificans progressiva), progressive osseous heteroplasia and Albright hereditary osteodystrophy [150].

### **1.5.1 Acquired heterotopic ossification**

The most common, acquired form of heterotopic ossification may occur after virtually any type of musculoskeletal trauma. For example, heterotopic ossification may occur after orthopaedic procedures such as hip-, knee-, elbow- or shoulder arthroplasty, fractures, joint dislocations, or soft-tissue trauma, with the musculus quadriceps femoris

and musculus brachialis often involved. Heterotopic ossification includes the specific posttraumatic variant myositis ossificans, in which patients often have soft-tissue ossification at sites of trauma adjacent to long bones. Less commonly encountered sites of posttraumatic heterotopic ossification are abdominal incisions, wounds, the kidneys, the uterus, the cardiac valves, the corpora cavernosa and gastrointestinal tract. The other common traumatic form of heterotopic ossification occurs after injury to the nervous system, usually without direct injury to the soft tissue where bone formation will occur, and is therefore known as posttraumatic neurogenic heterotopic ossification. Heterotopic ossification often occurs among patients with recent spinal cord injury and it develops only in sites distal to the level of the injury. Closed head injuries, strokes and brain tumors also may lead to heterotopic ossification. Notable, but more rare, are the cases of heterotopic ossification after burns, sickle cell anemia, hemophilia, tetanus, poliomyelitis, multiple sclerosis and toxic epidermal necrolysis.

The clinical signs and symptoms of heterotopic ossification may appear as early as three weeks or as late as twelve weeks after the musculoskeletal trauma, spinal cord injury or other. Loss of joint mobility and resulting loss of function are the most important complications of heterotopic ossification. Other complications include peripheral nerve entrapment and pressure ulcers.

The transformation of mesenchymal cells, present in the connective tissue septa within muscle, into osteogenic cells is thought to be the pathogenesis of heterotopic ossification. The differentiation of the mesenchymal cells into the osteogenic lineage is postulated to be induced by the bone morphogenetic protein that is liberated from normal bone in response to venous stasis, inflammation, or diseases of connective tissue attachments to bone, conditions that often accompany immobilization or trauma. Some investigators proposed the involvement of a centrally mediated factor. The role of prostaglandin E2 (PGE2) has also been suggested as a mediator in the differentiation of the mesenchymal cells of the soft tissue into the osteogenic lineage. Observations showed that the heterotopic bone formation often starts at some distance from normal bone, later moving towards it [150-152].



### 1.5.2 Pathological heterotopic ossification

Hereditary forms of heterotopic ossification, such as fibrodysplasia ossificans progressiva, progressive osseous heteroplasia and Albright hereditary osteodystrophy do not go accompanied with traumas and severe injuries.

Fibrodysplasia ossificans progressiva (FOP) is a severely disabling, autosomal dominant disorder that is characterized by congenital malformation of the great toes and by postnatal progressive heterotopic ossification of tendon, ligament, fascia and skeletal muscle. FOP has three distinguished features: (I) congenital malformation of the great toes, (II) heterotopic ossification of soft connective tissues and (III) temporal progression of osteogenesis in characteristic anatomic patterns. Patients who have FOP have two skeletons: a normotopic one formed during embryogenesis and heterotopic one formed after birth. Although heterotopic bone forms independently of the skeleton, maturing heterotopic bone generally forms rigid synostoses with the normotopic skeleton, thus further restricting motion and exacerbating disability.

Congenital malformation of the great toes along with postnatal heterotopic endochondral osteogenesis strongly suggests that FOP is a disorder of defective induction of endochondral osteogenesis. The earliest histopathological finding is an intense perivascular lymphocytic infiltration, followed by death of skeletal muscle and replacement by highly vascular fibroproliferative soft tissue. The soft tissue rapidly matures through an endochondral process to form heterotopic bone.

The autosomal dominant inheritance of FOP has been documented, but the gene or genes responsible for this disorder are unknown. BMP-4 is overexpressed in lymphocytes and lesional cells of patients who have FOP, but mutations have not been detected in the FOP genes, and recent linkage studies exclude the BMP-4 locus. The molecular cause of FOP may be in a component of the BMP signaling pathway or in some other gene whose product controls BMP-4 production [152, 153].

Albright hereditary osteodystrophy (AHO) is an autosomal dominant disorder of the skin, skeletal and endocrine system, with variable features that may include pseudohypoparathyroidism, multiple hormone resistance, obesity, short stature, round facies and cutaneous and subcutaneous ossification. In most patients with AHO, the disease is caused by heterozygous mutations in *GNAS1*, a gene of human chromosome

20 encoding the  $\alpha$ -subunit of the stimulatory G protein of adenylyl cyclase. This genetic defect leads to the impaired activation of adenylyl cyclase and impaired cyclic adenosine monophosphate (AMP)-mediated signal transduction [154].

Progressive osseous heteroplasia (POH) is a developmental disorder of mesenchymal differentiation characterized by dermal ossification during infancy and by progressive heterotopic ossification of cutaneous, subcutaneous and deep connective tissue during childhood. The disorder can be distinguished from FOP by the presence of cutaneous ossification, by the absence of congenital skeletal malformations, by the asymmetric mosaic distributions of lesions, by the absence of predictable regional patterns of heterotopic ossification and by the predominance of intramembranous rather than endochondral ossification. POH can be distinguished from AHO by the progression of heterotopic ossification from skin and subcutaneous tissue into skeletal muscle, by the absence of morphological features associated with AHO and by the presence of normal endocrine function. As already mentioned, heterotopic ossification in POH occurs predominantly through an intramembranous pathway, although there are few reports describing observed islands of endochondral ossification.

Although it is still largely unknown what the pathogenesis of POH is, the involvement of the presence of a mutant gene in mesenchymal stem cells destined for widespread distribution has been suggested. Observations in patients with POH suggest that such mesenchymal stem cells or more committed osteogenic precursors are present in skin, subcutaneous fat, muscle, tendon and ligament tissue [154].

In summary, heterotopic ossification, as a general name for the bone formation in extraskeletal sites often observed in the clinic, can be divided into two forms: acquired and hereditary. The first, acquired form of heterotopic ossification, is most often caused by traumas and severe injuries, and is most probably induced by BMPs released from the surrounding bone as a reaction to inflammation and other consequences of the trauma. This form of heterotopic ossification should therefore not get the label pathological. Hereditary form of heterotopic ossification involves diseases. In the case of FOP, the involvement of BMP-4 is suggested, while AHO and POH most probably have other underlying mechanisms.

Obviously, the involvement of BMPs in some types of heterotopic ossification suggests close resemblance with osteoinduction by BMPs. In the basis, osteoinduction and

heterotopic or pathological ossification are two names for the same phenomenon, but used in a different manner. While the word osteoinduction is used to express the ability of a substance to induce new bone formation, the word pathological ossification is used to refer to the problem that bone growth at abnormal sites can cause. Whether osteoinduction by biomaterials also represents the same phenomenon is, as discussed earlier, not completely understood yet. Bone formation in osteoinductive materials is found in soft tissue far away from the skeleton, which excludes release of BMPs from the surrounding bone as in the case of a trauma or a spinal cord injury. That endogenous BMPs are locally produced as the reaction of the body to the surgery is possible, but does not explain the fact that one type of the materials does and another type does not induce bone formation. Besides, the lack of bone induction on the periphery of the materials, lack of bone induction in small animals and consistent intramembranous ossification all suggest that osteoinduction by biomaterials is (partially) different from osteoinduction by either added or locally produced BMPs.

### **1.6 Aims and approach of the thesis**

The full understanding of the phenomenon of osteoinduction should help us developing better bone graft substitutes by teaching us the parameters that nature needs in order to start producing bone. It is thereby important to use the knowledge of fundamental biological processes and to combine it with materials science knowledge. In this thesis, we have attempted to come a step closer to the unraveling of the mechanism of osteoinduction.

This thesis mainly focuses on achieving two goals: (I) gathering relevant information on the parameters which are important in the process of osteoinduction by biomaterials in order to unravel this, so far largely not understood, phenomenon and (II) investigating the relevance of osteoinductive biomaterials orthotopically in order to get more insight into their potential use in the clinic.

In order to achieve these goals, the following questions need to be answered:

- What is the influence of chemical composition, microstructure and surface morphology on the osteoinductive properties of materials? The dynamics of the

interaction between a material and the in vivo surrounding can be influenced by either changing its chemical compositions (e.g. addition of a more soluble compound) or by changing its specific surface area (e.g. by introducing micropores or by coating the surface with a highly crystalline phase). Changes of the interaction between the material and its in vivo environment are hypothesized to be of influence on the material's osteoinductive properties.

- Is there an influence of implant size and implantation site on the relative amount of induced bone? Osteoinduction by biomaterials always takes place inside the implant and never on its periphery. A smaller implant has relatively more periphery than a larger implant, which could be a reason for more micromotion in the center of the smaller implant. Besides, there is relatively more surface available for infiltration of cells and nutrients within a large implant as compared to a small implant. A larger implant is therefore hypothesized to induce relatively more bone ectopically than a smaller implant of the same type. Vascularization is hypothesized to be of great importance in osteoinduction by biomaterials. It is therefore expected that the implantation of a material intramuscularly will result in more bone formation than the implantation of the same material subcutaneously.
- What occurs on or near the surface of an osteoinductive material during ectopic implantation? After implantation, on the surface of a CaP-containing material, release of calcium and phosphate ions takes place, followed by the reprecipitation of a more stable carbonated apatite layer. During the formation of the apatite layer, endogenous proteins are coprecipitated into the layer. These events lead to the initiation of the differentiation of the undifferentiated cells into the osteogenic lineage. It is hypothesized that on the surface of a material with a high specific surface area, the process of dissolution-reprecipitation/coprecipitation will take place faster and will be more pronounced than on the similar material with a lower specific surface area.
- What is the performance of osteoinductive biomaterials at orthotopic implantation sites? It is hypothesized that a material that is able to induce bone formation ectopically, i.e. an osteoinductive material, has the ability to increase

the amount of bone formed orthotopically, in comparison with a non-osteoinductive material.

In order to answer the above questions, two material types are used as a model: biomimetically produced octacalcium phosphate coating applied on surfaces of porous metals, polymers and ceramics and sintered porous ceramics based on hydroxyapatite. The phenomenon of osteoinduction by biomaterials is complex and still largely unknown, which makes it difficult to use simplified in vitro models to study its mechanism. Uncontrollable interactions between the material and the cell culture medium, difficulties in choosing the right cell sort and culture conditions are only few examples of the problems one is confronted with when trying to study a complex phenomenon such as osteoinduction in vitro.

Because of the above shortcomings on the in vitro systems, in this thesis, the in vivo model in goats is chosen. As previously mentioned, osteoinduction by biomaterials is rarely observed in rodents and other small animals, which was a reason to choose a large animal as a model. In addition, a large animal model is needed to be able to test osteoinductive materials in clinically relevant critical-sized orthotopic defects. The choice of goat as a model was made because of the large availability in The Netherlands.

Chapter 2 of this thesis is a review on limitations of different in vitro models to study bone repair by biomaterials and complex biological phenomena involving bone formation such as osteoconduction and osteoinduction.

Chapters 3, 4 and 5 deal with physico-chemical parameters which are of importance in the mechanism of osteoinduction. In Chapter 3, it is investigated whether a relatively simple application of biomimetic octacalcium phosphate coating can improve osteoinductive properties of a range of different porous biomaterials. In Chapters 4 and 5, influence of chemical composition (pure hydroxyapatite and biphasic calcium phosphate ceramic in Chapter 4 and different hydroxyapatite to  $\beta$ -tricalcium phosphate weight ratios in biphasic calcium phosphate ceramic and carbonated apatite ceramics in Chapter 5) and microstructure (and hence specific surface area) on osteoinductivity of biomaterials are investigated. In addition, Chapter 5 deals with implant size and implantation site effect on the amount of induced bone and with changes occurring on the surface of osteoinductive biomaterials after intramuscular implantation.

In Chapters 6 and 7 the performance of osteoinductive biomaterials at orthotopic implantation sites is investigated. In Chapter 6, uncoated and octacalcium-phosphate coated porous titanium alloy scaffolds as well as porous biphasic calcium-phosphate ceramic scaffolds are implanted in diaphyseal femur of goats. In Chapter 7, implantations of osteoinductive and non-osteoinductive biphasic calcium phosphate ceramic are performed in critical-sized iliac wing defects.

In Chapter 8 the results of all studies are discussed.

In Chapter 9 some general conclusions and recommendations for future research are given.

## Chapter 2

### **Predictive value of in vitro assays for osteoconduction and osteoinduction**

Pamela Habibovic, Klaas de Groot and Clemens A. van Blitterswijk

University of Twente, Institute for Biomedical Technology,  
Professor Bronkhorstlaan 10D, 3723 MB, Bilthoven, The Netherlands

#### **2.1 Abstract**

Increasing demand for synthetic scaffolds and matrices that can be used in bone repair and regeneration raises the need for fast and reliable preclinical screening tests. In vitro organ culture- and cell culture systems, originally developed as tools to study the effects of hormones and cytokines on the attachment, proliferation and differentiation of cells, are also attractive for screening of biomaterials, because they are relatively simple, and allow for work in a controlled environment. Besides, in vitro assays are preferred above the in vivo ones from an ethical and financial point of view.

However, as the established in vitro bone formation assays have been developed for a different purpose, they do not take into account possible effects of the presence of a biomaterial in the in vitro system. An important question that needs to be answered is, therefore, whether the established in vitro systems as such are suitable for the biomaterials research and to which extent the results from in vitro studies are predictive for the final performance of the material in vivo and in the clinic.

In this paper, we review a number of studies in which potential synthetic bone grafts have been tested in vitro and consequently in vivo in order to investigate to which extent their results correlate with each other.

Today's in vitro assays in which potential synthetic bone graft substitutes are tested often give inconclusive results and their predictive value for the in vivo performance of the graft is limited, which may be caused by a number of reasons such as a biomaterial-

cell culture medium interaction, which is absent in vivo and a wrong cell- and assay choice.

The increasing number of new synthetic bone grafts will demand more fast and reliable in vitro assays. However, the existing assays will need adjustments in order have a predictive value for the in vivo behavior of biomaterials.

Keywords: in vitro assays, biomaterials, osteoconduction, osteoinduction.

## **2.2 Introduction**

The continuous increase of life expectancy leads to an expanding demand for repair and replacement of damaged and degraded organs and tissues. Recent completion of a first version of the human genome sequence means a great breakthrough for the field of pharmaceuticals. It is conceivable that new developments in pharmaceutical research will result in a large number of novel and improved medicines. A similar development is expected in the field of biomaterials used for bone repair and replacement. Spinal fusions and repairs of bone defects caused by traumas, tumors, infections, biochemical disorders and abnormal skeletal development, are some examples of the frequently performed surgeries in the clinic. For most of these surgeries, there is a great need for grafting materials.

This expanding amount of newly developed biomaterials is accompanied by an increased need for the high-throughput screening systems which are reliable in predicting the performance of the material in the function it was developed for. For example, recently, a method was developed for rapid, microscale screening of polymer-cell interaction by using microarrays [155].

In the research into new bone graft substitutes, in general two types of preclinical assays are used: in vitro assays using a cell- or an organ culture system (i.e. in vitro bone formation assays) and in vivo assays, using experimental animal models. In vitro assays have initially been developed to study the influence of growth factors and hormones on e.g attachment, proliferation, differentiation and mineralization of cells. Subsequently, investigators started to use these in vitro assays in the biomaterials research. Instead of studying the influence of e.g. growth factors on the differentiation



of cells, the behavior of cells in the presence of the testing material is studied. However, in general, it is ignored that the in vitro setting may significantly be changed by the presence of a material due to e.g. material-cell culture medium interaction. If such an interaction is not expected in vivo, the question raises what the predictive value of the in vitro assay is for the in vivo performance of the material.

Besides the increasing need for reliable in vitro assays to test biomaterials prior to implanting them in animals and humans, investigators need tools which are helpful in unraveling mechanisms of complex in vivo phenomena. In vitro assays are attractive because of their simplicity, but, at the same time, their simplicity is an important limitation. It is of course impossible to fully simulate the in vivo situation in a culture dish and yet, in many publications, rather strong conclusions about the in vivo performance of biomaterials and about mechanisms of complex phenomena are drawn from the in vitro studies.

In this paper, we try to give an idea of the predictive value of in vitro assays today by reviewing a number of studies in which different in vitro assays were used to test the performance of biomaterials for bone repair and replacement and comparing their results with the results of the in vivo studies. We should mention that the question whether in vivo assays in small and large animals are predictive for the performance of biomaterials clinically is at least as important as the question whether in vitro assays are predictive for their in vivo performance. However, few studies show clinical follow-up data which can be related to the results of animal studies. Therefore, this paper is limited to reviews of the studies in which first in vitro and consequently in vivo animal assays were performed.

In the first part, we give some backgrounds on in vitro bone formation assays in general, and an overview of organs and cells which are commonly used in in vitro bone formation assays. We then give an overview of a number of in vitro and in vivo studies performed with similar materials for bone repair. Finally, we try to point out the shortcomings of the existing in vitro assays and give some recommendation for the improvement of the frequently used assays.

### 2.3 Backgrounds on in vitro bone formation assays

In vitro bone formation assays have initially been developed as tools to study the effects of hormones and cytokines in a controlled environment [156]. Despite the inherent diversity in these systems, most of them share some common features. For example, the basic culture environment (medium composition, serum type and concentration, supplements, temperature and antibiotics) and methods of routine maintenance (feeding, subculturing, cloning) are very similar in all systems. Gronowicz and Raisz [156] have given an overview of the culture conditions which are generally applicable for different in vitro bone formation culture systems. The fact that they give a simplified reflection of the in vivo situation and allow for the research in a controlled environment are primary reasons for the use of in vitro assays. In addition, from a financial and ethical point of view, in vitro assays are preferred above the in vivo ones. The existing bone formation assays can be divided into two groups: organ culture systems and bone cell culture systems.

As reviewed by Gronowicz and Raisz [156], tissues used for bone formation assays in bone organ culture systems vary in source and age including fetal, newborn and occasionally adult bone. Chicken, mouse and rat bones are most common, although human bone fragments have also been used. Bone from calvaria and limb is the most frequently cultured tissue. Fetal calvaria are characterized by intramembranous bone formation, while growth of long bones is mainly endochondral. However, as intramembranous and endochondral bone may have different responses to hormones, growth factors and environmental conditions, most in vitro organ culture systems have limitations and may not give a similar response as endochondral bone and adult bone cells.

In addition to organ culture systems, the in vitro isolation and culture of bone-derived cell populations has substantially enhanced our ability to understand factors important for the proliferation and differentiation of cells of the osteogenic lineage. As recently reviewed by Kartsogiannis and Ng [157], commonly employed model systems include either primary cultures of osteoblastic cells derived from fetal calvaria and subperiosteal fetal long bones or established cell lines that can be divided into clonal

cell lines from cells isolated from bone tumors (osteosarcomas), non-transformed cell lines, experimentally immortalized cell lines and bone marrow cultures.

## **2.4 Cells and cell sources of bone formation assays**

### **2.4.1 Primary cells**

Primary bone cell culture systems were mainly designed to study the functions and regulatory mechanisms of mature osteoblasts, i.e. the synthesis, secretion, organization and mineralization of bone extracellular matrix. Most osteoblast-like cell culture systems use cells in early primary or early passage cultures after isolation from bones of fetal or neonatal mice, rats, chickens and cattle. Tissues from such young animals are considered good sources of cells for culture as they proliferate readily in vitro and the rapid growth of bone during this phase of life ensures that the tissue contains a large number of active, phenotypically mature osteoblasts. Calvarial bones are particularly favorable since they are easy to dissect cleanly, show limited development of marrow and are not yet fully mineralized [158]. Besides functions of mature osteoblasts, another important aspect in bone formation research is developmental potential of osteoprogenitor cells and their relationships with other cell lineages such as chondrocytes, myoblasts and fibroblasts. It is important to investigate the factors that trigger the differentiation of osteoprogenitor cells along an osteogenic or alternative pathway and the reversibility of these pathways. Bone cell culture systems focusing on osteoprogenitor cells often use, in addition to bone, periosteum, bone marrow stroma and periodontal ligament as their cell source as reviewed by Majeska [158].

### **2.4.2 Cell lines**

Extensive overviews of different cell lines which are commonly used in in vitro bone formation systems are given by Majeska [158] and by Kartsogiannis and Ng [157]. Below, a short summary is given.

The earliest cell lines to be characterized as osteoblastic and used for in vitro studies were derived from rat osteosarcomas. The family of clonal cell line ROS was derived from a spontaneous tumor in an ACI rat. The most commonly used group is ROS 17/2 which exhibits adenylate cyclase activity in response to Parathyroid Hormone (PTH) as well as a high Alkaline Phosphatase (ALP) activity which is regulated by PTH and Vitamin D3 (1,25(OH)2D3). Subclone ROS 17/2.8 subsequently expresses Osteocalcin (OC) mRNA and calcifies in vivo when implanted in a diffusion chamber. In addition, ROS17/2.8 cells respond to Transforming Growth Factor- $\beta$  (TGF- $\beta$ ) with increase of ALP, Collagen Type I (Coll-I), Osteopontin (OP) and Osteonectin (ON) mRNA. Cell lines designated UMR106 were isolated from  $^{32}\text{P}$ -orthophosphate-induced tumors in rats. Several cell lines derived from human osteosarcoma are SaOS, TE-85 and MG-63 and OHS-4 cells. A recently characterized new osteosarcoma cell line CAL72 is more closely related to normal osteoblasts than other osteosarcoma cell lines. CAL72 expresses mRNA coding for Interleukin-6 (IL-6), Granulocyte-macrophage colony-stimulating factor (GM-CSF) and Granulocyte colony-stimulating factor G-CSF and thus appears to be closer to primary osteoblastic cells than e.g. SaOS and MG-63.

In addition to cells derived from osteosarcomas, a number of osteoblast-like cell lines have been established from normal bone. Early clonal lines were derived from rodent tissues and included a series (designated RCJ) derived from normal rat calvarial cell preparations and a clonal cell line, designated MC3T3-E1, derived from mouse calvaria. This cell line has been shown to increase cyclic AMP in response to PTH and express high ALP activity which is regulated by PTH, 1,25(OH)2D3 and Prostaglandin-E2 (PGE-2) and is capable of collagen synthesis. The cells represented by CRP 4/7, CRP 7/4, CRP 7/7, CRP 10/3 and CRP 10/30 also belong to the group of non-transformed osteoblastic cell lines.

The treatment of cells by a transfection with a recombinant retrovirus containing cDNA has been used to establish immortalized osteoblastic cells lines. These cell lines have the advantage of having a more fully characterized immortalization mechanism. RCT-1 and RCT-3 cells are examples of immortalized cell lines which express osteoblastic traits. Human osteoblast-like cells (hOB) are an example of cell lines established by transfecting normal human osteoblast-like cells, with a large and small T antigen against

SV40. They express mRNA for (I)-procollagen, OP, TGF- $\beta$ , and IL-1  $\beta$ , while treatment with 1,25(OH) $_2$ D $_3$  results in increased expression of OC and ALP mRNA and protein.

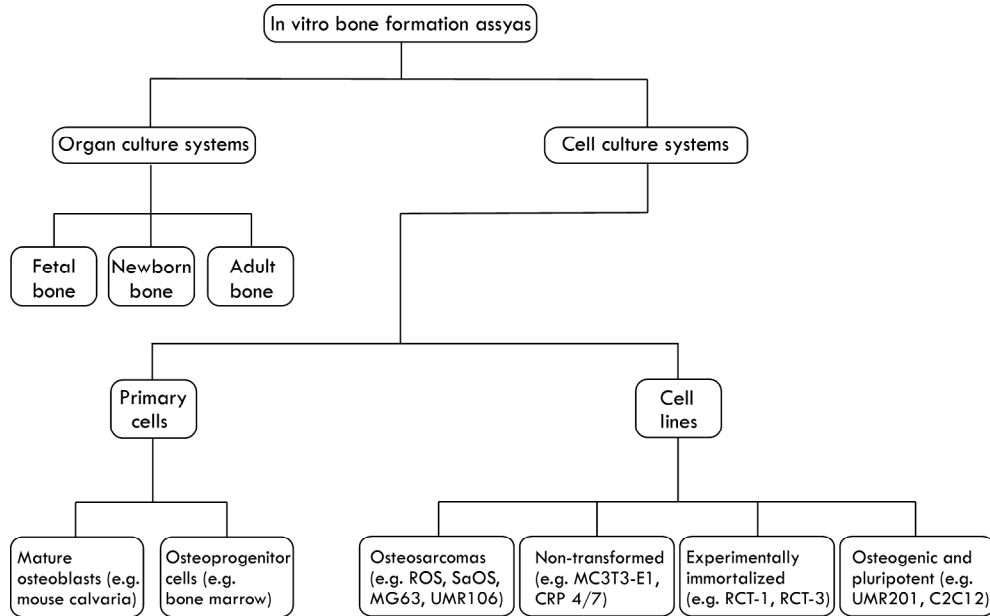


Figure 1: an overview of in vitro bone formation assays.

Examples of cell lines that can be used to study osteogenic differentiation from progenitor cell populations are UMR-201 cells, established from neonatal rat calvaria and MBA-15 cells originating in bone marrow stroma. Another group of cells that can be used as a useful model to study the osteogenic differentiation and its regulation by hormones and growth factors are pluripotent mesenchymal cells. Pluripotent mesenchymal cells are capable of differentiating into different lineages: osteoblasts, chondroblasts, adipocytes, myoblasts and fibroblasts. One example of a widely used pluripotent cell line is “murine C2C12 mesenchymal precursor”. When C2C12 cells are cultured in the presence of TGF $\beta$ -1, terminal differentiation into myotubes is blocked. Similarly, when C2C12 cells are treated with Bone Morphogenetic Protein-2 (BMP2), myogenic differentiation is blocked, but osteoblast differentiation is stimulated. Another example of a pluropotent mesenchymal cell line is C3H10T1/2. For these cells it is

known that recombinant N-terminal sonic hedgehog (NShh) abolishes adipocytic differentiation both in presence and absence of BMP-2, while committing these cells into the osteogenic lineage.

Another group of cells with a high potential to be a helpful tool in studying the principles of osteogenic differentiation and the factors influencing differentiation of cells towards osteoblasts are pluripotent embryonic stem cells (ESCs). ESCs have an unlimited potency to self renew and maintain their pluripotency in culture [159, 160]. Although the application of ESCs in bone development research is still at the early stage, there are reports showing successful differentiation of mouse ESCs into the osteogenic lineage in response to specific growth factors [161-164].

An overview of organs and cells used for in vitro bone formation assays is given in figure 1.

## **2.5 In vitro models for assaying bone graft substitutes**

As mentioned before, the expanding development of (synthetic) biomaterials for support, replacement and regeneration of bone has created the need for in vitro systems in which the potential in vivo performance of these materials can be assayed. In vitro cell- and organ culture assays are in the first place used to investigate the “safety” of the material in terms of e.g. cytotoxicity and biocompatibility. In addition, in vitro bone formation assays are used in order to predict the performance of the material in vivo in its role of e.g. bone filler. In this case, the potential osteoconductivity of the material is tested. Finally, in vitro cell culture systems are used to study complex and not yet fully unraveled “biologically driven” phenomena such as osteoinduction. Below, we give a few examples of in vitro studies in which materials cytotoxicity, osteoconductivity and osteoinductivity were assayed. In addition, the results and authors’ conclusions drawn from these studies are compared to the results in vivo, where similar materials were tested.

### 2.5.1 Cytotoxicity

Hyakuna et.al. investigated changes in calcium-, phosphate-, magnesium- and albumin content of cell culture medium after immersion of different biomaterials [165]. The results of this study showed that monocrystalline and polycrystalline alumina ceramics did not have any influence on the surrounding medium. Two types of apatite containing glass ceramics (A W-GC and A W CP-GC) showed a slight decrease of phosphorus and a slight increase of calcium ion concentration in the culture medium. Hydroxyapatite (HA) ceramics sintered at 600°C and 900°C with a very high specific surface area showed a high and rapid adsorption of calcium- and phosphate ions and albumin from the medium. Changes of calcium and phosphate concentrations of the medium were suggested to be the reason for the poor attachment of V79 Chinese hamster fibroblasts, and hence for a higher apparent cytotoxicity of the HA ceramics sintered at 600°C and 900°C and the two glass ceramics as compared to the tissue culture plastic and alumina ceramics.

Norman et.al. compared the attachment of MC3T3-E1 osteoblast-like cells on porous (sintered) and dense (unsintered) HA ceramic with the attachment on polystyrene culture discs [166]. Their observation was a significantly higher attachment on plastic as compared to the two ceramics. Furthermore, more cells attached on the porous in comparison to the dense ceramic, which was explained by 1) higher specific surface area of the porous ceramic, thus more available space for cells to attach and 2) lower reactivity of the surface of the porous ceramic in comparison to the unsintered ceramic, possibly a lower uptake of calcium- and phosphate ions from the culture medium and hence a lower cytotoxic effect on the cells.

Suzuki et.al. prepared ceramics with Ca/P ratios varying from 1.50 to 1.67 by mixing different amounts of HA and tricalcium phosphate (TCP) ceramics and observed variations of zeta-potentials of different surfaces after immersion in the cell culture medium [167]. Decrease of calcium- and phosphate ions in the culture medium was always observed, but its intensity depended on the Ca/P ratio of the ceramics and so did the change of the pH of the medium. Changes of the ions concentrations and pH of

the medium were suggested to be of influence on the attachment of L-929 cells on the ceramic surfaces, and thus on the cytotoxicity of the material.

Knabe and coworkers performed a similar study, in which they compared attachment and proliferation of rat bone marrow cells (RBMCs) on highly resorbable CaP ceramics [168] and on glassy materials with different rates of resorbability [169]. Interestingly, while in the previously described studies above authors observed a decrease of calcium- and phosphate ions from the medium and suggested this decrease to be the reason for a poor attachment and growth of the cells, Knabe and coauthors suggested that the inhibitory effect on cellular growth on some of their materials was associated with an increased concentration of phosphorus ions released into the medium by these materials and the formation of a phosphorus-rich layer on their surface. Daily refreshment of the medium increased the osteoblast attachment on some, but not on all tested ceramics.

In later work of this group, in which highly resorbable CaP cements and CaP ceramics were compared, it was suggested that increased levels of phosphate- and potassium ions, decreased levels of calcium ions and hence elevated pH of the medium were reasons for poor attachment and proliferation of RBMCs.

The above described examples of studies in which safety of materials in terms of cytotoxicity is tested all emphasized the presence of the biomaterial-cell culture medium interaction, which seems to be responsible for, or at least of influence on the behavior of cells. Although material-medium interactions are sometimes of great influence on the behavior of cells *in vitro*, in the *in vivo* environment they might be less important if observed at all, as, unlike in a culture dish, in the body there is a continuous supply and thus refreshment of nutrients and body fluids. For the cytotoxicity tests, this probably means that the *in vitro* settings give a more “negative” reflection of *in vivo* situation.

### **2.5.2 Osteoconduction**

Osteoconduction, defined as “spreading of bone over the surface proceeded by ordered migration of differentiating osteogenic cells” [170], is supposed to be driven by physico-chemical properties of the material, having its origin in



dissolution/reprecipitation or precipitation of a calcium-phosphate layer on the surface of the material [171, 172]. An important aspect is thereby the direct bonding of bone to the materials without fibrous tissue deposition, so-called contact or bonding osteogenesis [170]. In a few studies, these properties of the materials were tested first in vitro and then in vivo.

De Bruijn et.al. used an in vitro rat bone marrow cell culture system to study various types of calcium-phosphates [173]. Besides the elaboration of different interfaces, mineralization occurred at a later time on slow degrading materials such as fluoroapatite, than on fast degrading materials such as tricalcium phosphate. Authors therefore suggested that a more dynamic interface is formed on degrading materials that could be favorable for bone formation to occur. This hypothesis was further tested by implanting various plasma-sprayed calcium-phosphate coatings in rat femoral bone for relatively short period of time [174]. The results of this study indeed suggested that initially higher amount of bone was formed on fast degrading amorphous hydroxyapatite as opposed to the slow degrading highly crystalline hydroxyapatite.

Similar to the study of de Bruijn et.al., in a study by ter Brugge et.al., the effect of the crystallinity of thin radio frequency (RF) magnetron sputtered calcium-phosphate coatings on the attachment, proliferation and mineralization of rat bone marrow cells was studied [175]. Authors observed proliferation, differentiation and mineralization of cells on uncoated titanium and crystalline calcium-phosphate coating, while no proliferation or differentiation was observed on the fast degrading amorphous calcium-phosphate coating. It was observed that the thin, RF magnetron sputtered amorphous calcium-phosphate coating was completely dissolved in a relatively short period of time, which was suggested to be a reason for poor growth and mineralization of cells. Obviously, the in vitro effect of crystallinity on rat bone marrow cells differs between thick, plasma-sprayed and thin magnetron sputtered calcium-phosphate coatings.

In a study by Hulshoff et.al., amorphous and crystalline plasma-sprayed calcium-phosphate coatings, and amorphous and crystalline RF magnetron sputtered coatings were applied on titanium surfaces and compared in a rat bone marrow cell culture system [176]. Uncoated titanium was used as a control. In this study, no significant difference was found in attachment and proliferation of cells on various substrata. In addition, crystalline and amorphous magnetron sputtered coating and amorphous

plasma-sprayed coating showed the formation of the mineralized extracellular matrix after 18 days of culture, in contrast to the crystalline plasma-sprayed coating. When similar coatings on titanium substrata were compared in a rabbit femoral condyle model [177], at 6 and 9 weeks of implantation, no difference in bone contact was found between different types of coating. Regarding the amount of bone found at a certain distance from the implant, crystalline RF magnetron sputtered coating showed a better performance than other coatings. However, the observed difference was only significant after 6 weeks of implantation. This study showed that the in vitro observed difference in the formation of extracellular matrix between crystalline plasma-sprayed coating and other coating types could not be translated to the amount of bone contact in vivo. And further, a higher amount of bone at a certain distance from the implant which was observed in crystalline RF magnetron sputtered coating as compared to other coating types, could not be explained by any of the in vitro observations.

In a study by Gaillard et.al. [178] PEO/PBT copolymers were provided with calcium ions by incubation in a  $\text{CaCl}_2$  solution ("calcium-containing PEO/PBT"). Subsequently, they were either incubated in an alkaline phosphate containing solution that resulted in precipitation of HA/ $\beta$ -TCP crystals on implant surface ("surface precalcification") or in an acidic phosphate-containing solution resulting in the formation of calcium pyrophosphate crystals just underneath the implant surface ("matrix precalcification"). These materials, together with the untreated PEO/PBT copolymer were first tested in a rat bone marrow culture system. This study showed that control PEO/PBT material did not change calcium concentration of the culture medium. "Calcium-containing PEO/PBT" showed a fast release of calcium ions into the medium. While "matrix precalcified" PEO-PBT gradually released calcium ions into the medium, "surface precalcified" PEO-PBT showed an uptake of calcium ions from the medium. During a 3-week rat bone marrow culture, the non-treated PEO/PBT copolymer showed a nodule formation, but no mineralization of the extracellular matrix was observed. The "calcium-containing" PEO/PBT showed mineralized foci formation already after 2 weeks of culture. On the surface of the two precalcified copolymers, instead of nodules, two or three continuous cell layers were formed and mineralization was observed after 2 weeks. Longer culture period resulted in more mineralization in close contact with the copolymer surface. Based on these results the authors concluded that the availability of calcium ions or

calcium phosphate crystals in PEO/PBT copolymers stimulates mineralization in bone marrow cell culture, which is an indication for improved bone-bonding characteristics in vivo. The four groups of materials, i.e. non-treated PEO/PBT, “calcium-containing” PEO/PBT, “surface precalcified” PEO/PBT and “matrix-precalcified” PEO/PBT were subsequently implanted in the femora of rats [179]. The results from this in vivo study revealed that “calcium-containing” PEO-PBT did not show an increase in calcification rate as compared to the non-treated PEO/PBT. Authors concluded that a too fast release of calcium ions was the reason for the inability of the “calcium-containing” PEO/PBT to stimulate calcification. The results further showed that the thickness of the calcified layer on the two “precalcified” copolymers did not increase during the implantation period as was observed in the in vitro study. Furthermore, the total amount of formed bone did not differ between the four implant types, but the percentage of bone contact was higher in “surface precalcified” implants as compared to the other three implant types. The authors suggested that the main reason for this observation lies in dissolution of calcium and phosphorus ions, leading to an increased concentration of the local ion concentrations and consequent precipitation of the biological apatite layer on the material surface.

A recent report by Wang and coworkers described a comparison of proliferation and differentiation of SaOS-2 osteoblastic cell line on HA ceramics sintered at three different temperatures (1200°C, 1000°C and 800°C) [180]. Results of this study showed that cell proliferation rate on HA ceramic sintered at 1200°C was the highest. In addition, BSP, OC and ON protein levels after 12-day-culture were significantly higher on HA sintered at 1200°C as compared to HA ceramics sintered at 1000°C and 800°C respectively. Authors therefore concluded that HA ceramic sintered at 1200°C, which had a significantly lower specific surface area than the other two ceramics, was the best candidate to be used as a bone graft. They suggested that the ceramic sintered at higher temperature possibly had a less reactive surface and hence a lower cytotoxicity as compared to the other two tested ceramics. These results were in accordance with the results of the in vitro study of Hyakuna et.al. [165]. In a study by our group [181] however, biphasic calcium phosphate (BCP, consisting of HA and  $\beta$ -TCP) ceramics sintered at 1150°C and at 1300°C were implanted in a critical-sized iliac wing defect

of goats. Significantly more bone was found in the orthotopically implanted BCP sintered at 1150°C as compared to BCP sintered at 1300°C (figure 2) [181]. The two materials had similar compositions and macroporosities and they only differed in their microporosities. BCP1150 with its higher microporosity and hence higher specific surface area in comparison with BCP1300 was suggested to have a higher surface reactivity, which was consequently the reason for a higher bone regenerative potential. These in vivo results were thus in conflict with the in vitro data given by Hyakuna et.al. [165] and Wang et.al. [180], in which ceramics sintered at higher temperatures showed a more pronounced cell proliferation and osteogenic differentiation.

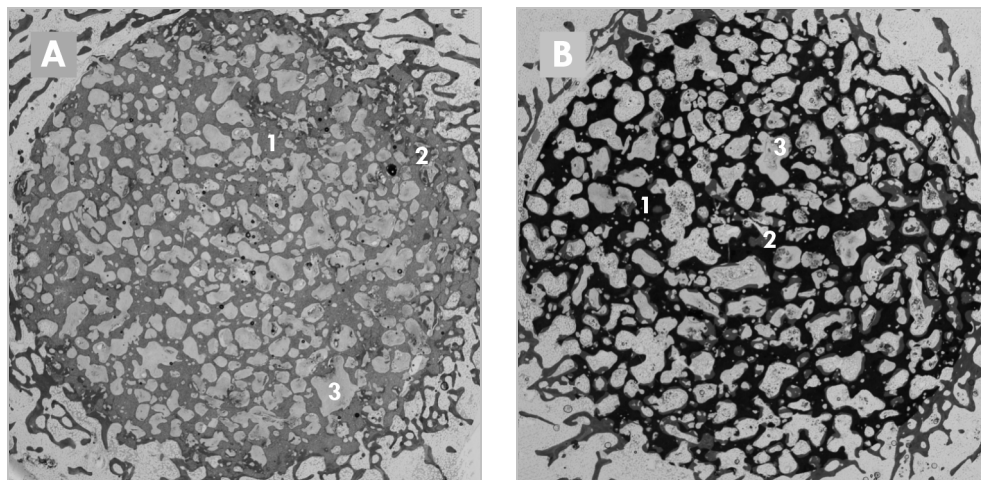


**Figure 2:** digital photographs of BCP1300 (A) and BCP1150 (B) after implantation in goat iliac wing defect for 12 weeks.

(1) = ceramic, (2) = bone, (3) = fibrous tissue.

Only a small ridge of new bone has formed along the host bone bed in the BCP1300 disc (A),

while bone has grown deeply inside the BCP1150 disc (B). → p214.

The above described are only a few examples of the studies in which in vitro bone formation assays were used to predict the performance of biomaterials in vivo. As can be seen, in some studies, in vitro results completely fit the in vivo results, while in the others, differences observed in vitro could not be found in vivo or were in full contrast with the in vivo data. In the reviewed studies, both in vitro and in vivo studies were performed with similar biomaterials. This is, however, not always the case. Sometimes,

only in vitro results are presented, and authors use these to draw conclusions on the performance of materials in vivo, which makes it impossible to elaborate on the predictive value of the in vitro assays.

### **2.5.3 Osteoinduction**

Osteoinduction is an even less understood phenomenon as compared to osteoconduction. In the sixties, osteoinduction was defined as “the differentiation of the undifferentiated inducible osteoprogenitor cells that are not yet committed to the osteogenic lineage to for osteoprogenitor cells” [93]. In other words, osteoinductivity is the ability of a cytokine or a material to induce bone formation ectopically. Extensive research of Urist and others led to the conclusion that a discrete protein within the demineralized bone matrix (DBM) was the sole inducer of bone formation. This finding was published in 1971 and this protein was named Bone Morphogenetic Protein (BMP) [94]. BMP was shown to be involved in the bone formation cascade of chemotaxis, mitosis, differentiation, callus formation and finally bone formation. Besides the BMP-driven osteoinduction, many investigators have shown that also some biomaterials that neither contain nor produce BMPs are also able to induce ectopic bone formation [124, 128, 129, 135, 138, 182, 183]. Despite the extensive research, the underlying mechanism of osteoinduction is still largely unknown and reliable assays to study this phenomenon are needed. Below, a few in vitro studies on osteoinduction are described.

Adkisson et.al. [184] developed a “rapid quantitative bioassay of osteoinduction” by using SaOS-2 osteosarcomas and studies cell proliferation rates under influence of DBM. However, correlation between cell proliferation and osteoinduction was not strong. Osteogenic factors, like BMP are not commonly associated with mitogenic response. Zhang et.al. [185] and Wolfinbarger and Zhang [186] used human periosteal cells and human dermal fibroblasts to relate cellular ALP activity to DBM osteoinductivity. In these studies, the authors failed to show a clear correlation between in vitro assays and in vivo bone formation.

Carnes et.al. used an immature osteoprogenitor cell line, 2T9 to investigate the effect of DBM on the cell differentiation [187]. They failed to show any effect on differentiation

and concluded that there are no soluble factors being released from DBM into the culture medium.

Han et.al. assayed ALP activity of the C2C12 cells in a culture in presence of DBM, and succeeded correlating it with the in vivo bone formation [188]. The last study mimics the in vivo situation more than other described studies, although the expression of ALP is not the most sensitive marker for the osteogenic differentiation.

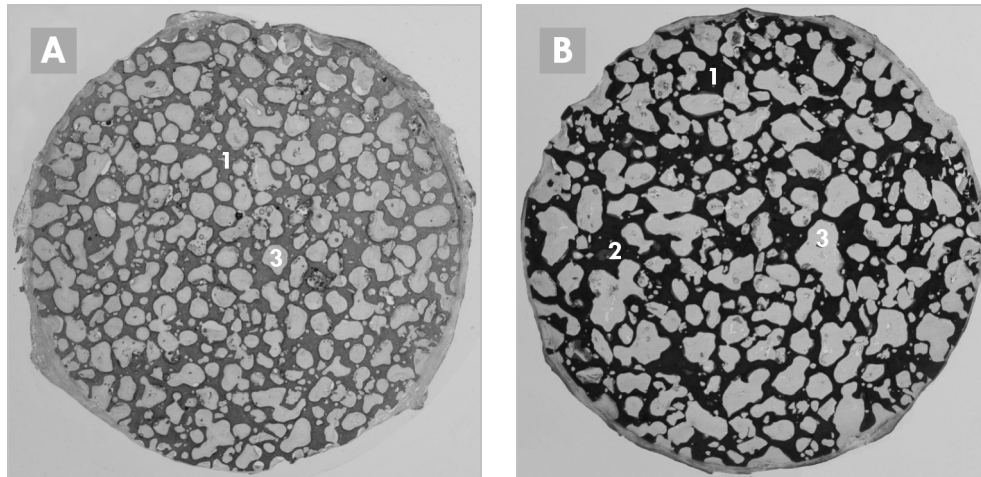


**Figure 3:** digital photograph of histological slides of BCP1300 (A) and BCP1150 (B) after 12-week intramuscular implantation in goat.

(1) = ceramic, (2) = bone, (3) = fibrous tissue.

In BCP1300, the ceramic is extensively filled with fibrous tissue, but no signs of bone formation are observed.

In BCP1150 (B) bone has formed in the pores of the implant, aligning its surface. → p215.

Regarding the mechanism of osteoinduction by biomaterials a very limited amount of studies is performed and published. In our group, an extensive number of studies has been performed in vivo. In addition, we have tried to perform a number of in vitro studies as well, however, their results were either inconclusive, or in contrast with the in vivo observations. Below, a few examples of the performed studies are given.

In an earlier published study [183], HA ceramics sintered at 1150°C and 1250°C together with biphasic calcium phosphate (BCP, consisting of HA and  $\beta$ -TCP) ceramics sintered at 1100°C, 1150°C and 1200°C were implanted intramuscularly in goats and

we found that HA sintered at 1150°C induced bone formation intramuscularly, while no bone was induced by HA sintered at 1250°C. Furthermore, the amount of induced bone by the BCP ceramics increased with decreasing sintering temperatures.

In another study [181], BCP ceramics sintered at 1150°C and at 1300°C were implanted intramuscularly in goats. Ectopic bone formation was only found in the BCP sintered at lower temperature (figure 3) [181]. The presence of microporosity in BCP1150 was suggested to be responsible for a higher osteoinductive potential in comparison with BCP1300 ceramic.

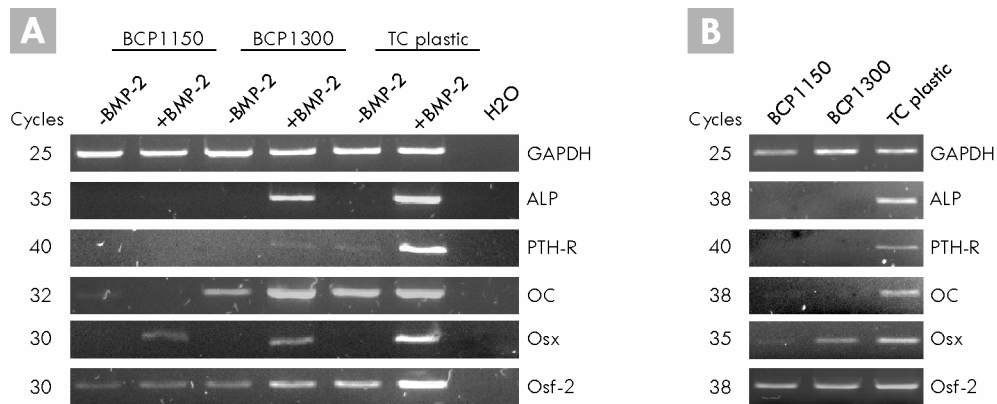


**Figure 4:** RT-PCR data showing the temporal expression of osteogenic mRNA by C2C12 cells cultures with and without BMP-2 (100ng/ml) (A) and MC3T3-E1 cells cultured without ascorbic acid (B) for 6 days on BCP1300 and BCP1150 discs (Ø25 x 5 mm<sup>3</sup>). The expression of most osteogenic markers by C2C12 cells (A) is increased when cells are cultured in presence of BMP-2. In both presence and absence of BMP-2, the expression of most markers is highest when the C2C12 cells are cultured on tissue culture plastic. Cells show a higher expression of osteogenic markers when cultured on BCP1300 as compared to BCP1150. Similar to C2C12 cells, the expression of all investigated osteogenic markers by MC3T3-E1 cells (B) is the highest on TC plastic, followed by BCP1300 and then BCP1150.

In order to compare BCP1150 and BCP1300 in vitro, we cultured MC3T3-E1 osteoblastic-like cells and C2C12 pluripotent mesenchymal cells (in presence and in absence of BMP-2) on BCP1150 and BCP1300 ceramics and consequently investigated the expression of various osteogenic markers (mRNA for ALP, OC, ON, OSF-2 and Osx) by using RT-PCR. For both cell types, a higher expression of most markers was observed on BCP1300 than on BCP1150 (figure 4). Furthermore, the expression of these markers

was the highest by cells cultured on TC plastic. Measurements of calcium- and phosphate contents of the medium after 3 hours of soaking showed a decrease of calcium concentration with 22% and a decrease of phosphate concentration with 18% in presence of BCP1300, while the decrease of calcium and phosphate concentrations in presence of BCP1150 was 62% and 60%, respectively. After 3 days of soaking, which is the normal time point at which culture medium is refreshed, calcium- and phosphate contents of the culture medium further decreased with 8% for both ceramics.

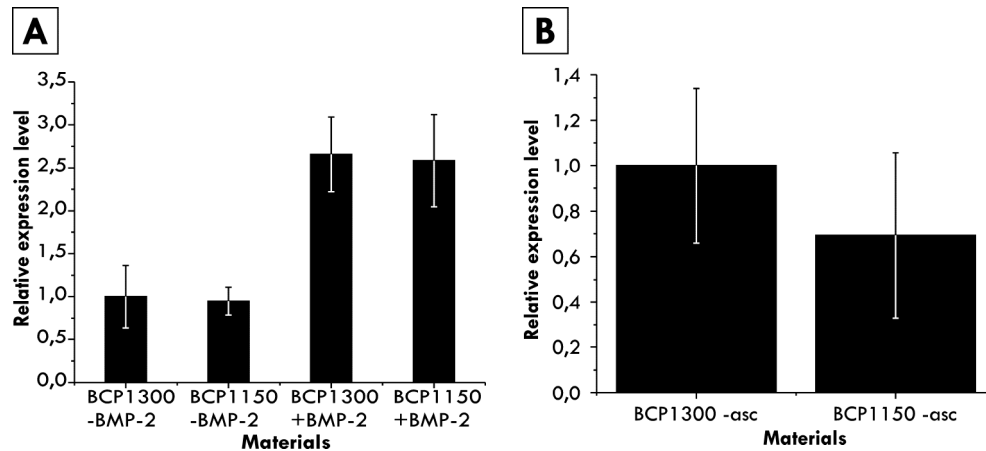


**Figure 5:** Q-PCR data (n=3) showing relative expression of Osteocalcin mRNA by C2C12 cells cultured with and without BMP-2 (100ng/ml) (A) and MC3T3-E1 cells cultured without ascorbic acid (B) for 6 days on BCP1300 and BCP1150 particles (1-2  $\mu$ m). The Osteocalcin expression by C2C12 cells (A) is significantly increased when cells are cultured in presence of BMP-2 on both BCP1300 and BCP1150 ceramic. There are no significant differences in the Osteocalcin expression between cells cultured on BCP1300 and BCP1150 for neither cell type. However, the trend for both cell types is the same, namely a slight downregulation of Osteocalcin on BCP1150 as compared to BCP1300.

No changes in calcium- and phosphate contents of the medium in the absence of ceramics were observed.

In order to decrease the change of the contents of the medium, we repeated the experiment with MC3T3-E1 and C2C12 cell lines by using considerably smaller ( $\pm 100$  times lower volume) amount of BCP1150 and BCP1300 scaffolds in the same volume of medium. This time, the amount of calcium decreased with 7% and the amount of phosphate with 11% in presence of BCP1300 scaffold after 72 hours of soaking.



Decrease of calcium concentration was 36% and that of phosphate 40% in presence of BCP1150. Although differences in the expression of OC (figure 5, Q-PCR data) for MC3T3-E1 and C2C12 cells between BCP1150 and BCP1300 were smaller this time, the trend of expression remained the same. Differentiation of cells towards the osteogenic lineage was higher on BCP1300 as compared to BCP1150, while in vivo significantly more bone was induced by BCP1150 in comparison to BCP1300.

A similar study was performed with mouse embryonic stem cells (to be published separately), and interestingly, in this study, the expression of mRNA for OC and BSP was higher on BCP1150 as compared to BCP1300. Whether these results mean that the effect of the material is only visible in very early stages of differentiation, or simply that ESCs react differently to the changes of the medium caused by the presence of ceramics as compared to C2C12 and MC3T3-E1 cells, needs to be further investigated.

## **2.6 Limitations of in vitro models for assaying bone graft substitutes**

All examples described above suggest that the use of the existing in vitro assays in biomaterials research might not always be valuable. Sometimes, the in vitro data are completely in accordance with the in vivo findings, especially when rather simple physico-chemically guided processes are studied. In other studies, in which more complex, biologically driven processes are studied, in vitro and in vivo results are in full contrast with each other. The question that needs to be answered is what the cause of these inconclusive results is. First of all it is important to note that in most cell culture and organ culture systems involving biomaterials there is, in addition to cell-biomaterial interaction, often a very important biomaterial-cell culture medium interaction which often markedly influences the outcomes of the study. In the in vivo environment these interactions might be less important if observed at all, as, unlike in a culture dish, in the body there is a continuous supply and thus refreshment of nutrients and body fluids.

Although most examples given above are studies performed on CaP containing biomaterials, the changes in the medium can also be caused by non-CaP materials (certain polymeric sponges [114], alumina ceramics [134], porous titanium [136] scaffolds are able of forming a CaP layer when immersed in a CaP-rich environment).

Release of calcium, phosphate, magnesium, and other ions from highly resorbable materials, uptake of different ions from the culture medium by a high surface area of a material, changes of pH and Z-potentials on the surfaces, formation of phosphorus and/or calcium rich layers on the surfaces, adsorption of all, or selected proteins from the serum-containing cell culture media, are only few observations from this type of studies. Obviously, all these changes of the medium differ significantly between the tested materials and raise therefore the question if such in vitro systems are applicable for the comparative types of experiments. Different studies focus on comparing material A with material B by studying cell attachment, proliferation, differentiation and mineralization on their surfaces. However, if the interaction between material A and the culture medium is different from the interaction between material B and the medium, the cells will attach, grow and differentiate in different environments and can therefore not be compared with each others when similar biomaterial-body fluid interactions are not expected in vivo. In addition, changes which take place in the medium due to the presence of a biomaterial will influence different cell types in a different manner, which makes comparisons between different studies difficult, if not impossible.

In addition to taking into account possible side effects of the presence of biomaterials in in vitro cell culture systems, the choice of cells is of great importance for the reliability of the results. For example, if one would like to compare two biomaterials and to be able to draw some conclusions regarding their potential performance as bone filler, would the attachment and proliferation of primary rat osteoblasts then be the right assay knowing that in vivo osteoblasts are not the cells which are initially in contact with biomaterial surface? The choice is probably even more difficult when one is trying to investigate a largely unknown phenomenon in vitro, such as osteoinduction by BMPs or even less understood osteoinduction by biomaterials. Obviously, in order to study the mechanism of osteoinduction by biomaterials, it is probably not sufficient to choose osteoblasts or osteoblast-like cells as osteoinduction is the process of differentiation of cells that are not yet committed to the osteogenic lineage to form osteoprogenitor cells. Therefore, murine pluripotent mesenchymal C2C12 cells could be better candidates than osteoblasts. However, it is well-known that ectopic bone formation by biomaterials is only very rarely found in mice [141-144], making cells of murine origin possibly a bad choice. In addition, it is hard to decide whether the culture of C2C12 cells on

osteoinductive biomaterials should be performed in presence or in absence of e.g. BMP-2, as it is suggested, but not proven yet [138, 139], that BMPs play a role in the process of osteoinduction by biomaterials. Similar questions of the choice of cell origin and culture conditions should be answered if one would choose to use ESCs to study the phenomenon of osteoinduction by biomaterials in vitro.

## **2.7 How to improve the existing in vitro assays?**

In conclusion, in our opinion, the in vitro assays which are nowadays used to study the potential performance of biomaterials in vivo, have a largely limited predictive value. It should be emphasized again the existing in vitro assays have originally been designed to test the influence of growth factors, cytokines and hormones on the behavior of cells and organs. In these in vitro assays, the presence of a material has never been taken into account. However, in the studies involving biomaterials, there is, in addition to the material-cell interaction, which is supposed to be studied, often a material-medium interaction, which can be of high importance for the results and should therefore not be ignored. Prior to starting an experiment, the following questions should be answered: 1) is there an interaction between the testing material and the medium?, 2) does this interaction have the consequence for the results of the study? and 3) is a similar interaction expected in vivo? If the biomaterial-cell culture medium seems to be an artifact of the used system, this effect of biomaterial-medium interaction should be removed. Knabe and coworkers suggested for example preincubation of the material in the medium prior to the start of cell culture and daily medium replenishment [168]. Although possibly successful for some biomaterials, this solution might be expensive, in particular if the cell culture is performed in presence of e.g. growth factors. Another possible solution could be the use of bioreactors in in vitro systems, with continuous monitoring and adjustment of the changing contents of the medium. Only if cells grow in the same medium, their interactions with different biomaterials can be compared in a useful way, and only then some careful conclusion regarding their potential in vivo performance can be drawn.

As already mentioned, the choice of cells and assays can be of great importance on the outcomes of in vitro studies. This is important when e.g. osteoconductive potential of a biomaterial is studied. Instead of using mature osteoblasts, which are responsible for the appositional bone growth rather than for de novo bone formation in vivo, the use of inducible and determined osteoprogenitor cells, as present in the bone marrow, might be more useful. When studying the not yet unraveled complex biological phenomena such as osteoinduction, initially a pluripotent cell line should be used. The use of a homogeneous cell population can give an insight into processes governing osteoinduction. In the next step, adult mesenchymal stem cells from the recipient site (mostly muscle, or perivascular cells) should be used, as they are most probably involved in the process of osteoinduction.

## **2.8 Conclusions**

Today's in vitro assays in which potential synthetic bone graft substitutes are tested often give inconclusive results and their predictive value for the in vivo performance of the graft is limited. Most important limitations of the existing in vitro assays, which have initially been developed for a different purpose, are: 1) in in vitro systems there is often a biomaterial-cell culture medium interaction which can be of influence on the results of the in vitro study and is undesired as it is often not expected to occur in vivo in the same way and 2) cells used in in vitro systems are often not representative for the in vivo situation, in particular when complex biological phenomena, such as osteoinduction are investigated.

## **2.9 Acknowledgements**

Authors would like to thank Gilles Bluteau and Jerome Guicheux (INSERM UMRS 9903, Faculty of Dental Surgery, Nantes, France) for their help with cell culture and RT-PCR analysis and Sanne Both (University of Twente, Institute for Biomedical Technology, Bilthoven, The Netherlands) for performing the QPCR analysis.

## Chapter 3

### Influence of octacalcium phosphate coating on osteoinductive properties of biomaterials

Pamela Habibovic<sup>1</sup>, Chantal M. van der Valk<sup>2</sup>, Gert Meijer<sup>3</sup>,  
Clemens A. van Blitterswijk<sup>1</sup> and Klaas de Groot<sup>1</sup>

<sup>1</sup>University of Twente, Institute for Biomedical Technology,  
Professor Bronkhorstlaan 10D, 3723 MB, Bilthoven, The Netherlands

<sup>2</sup>IsoTis SA, Professor Bronkhorstlaan 10-D, Bilthoven, 3720 MB, The Netherlands

<sup>3</sup>University Medical Center Utrecht, PO Box 85500, Utrecht, 3508 GA,  
The Netherlands

#### 3.1 Abstract

In this study, we investigated the influence of octacalcium phosphate (OCP) coating on osteoinductive properties of various biomaterials. Porous titanium alloy (Ti6Al4V), hydroxyapatite (HA), biphasic calcium phosphate (BCP) and polyethylene glyco terephthalate/polybutylene terephthalate (PEGT-PBT) copolymer, all uncoated and coated with biomimetically produced OCP, were implanted in paraspinal muscles of 10 goats for 6 and 12 weeks. Uncoated Ti6Al4V and HA did not show bone formation after intramuscular implantation. All OCP coated implants, except PEGT-PBT, induced bone in the soft tissue. Both uncoated and OCP coated BCP induced bone. However, bone incidence was higher in the coated BCP implants as compared to the uncoated ones. Biomimetic OCP coating might be a helpful tool for designing more advanced orthopaedic and dental implants.

Keywords: biomimetic coatings, octacalcium phosphate (OCP), osteoinduction.

### 3.2 Introduction

Osteoinduction can be defined as the process of bone formation in extraskeletal sites. Osteoinduction includes a process of differentiation of non-osteogenic cells into osteoblasts and bone morphogenesis.

Various calcium phosphate (CaP) containing biomaterials, produced in the form of ceramics, cements and coatings, have been shown to induce ectopic bone formation in various animal models. In the last decade, a few reports showed osteoinduction by synthetic hydroxyapatite (HA) in dogs [116-120], coral derived HA ceramic in dogs, monkeys and baboons [117, 121, 122], synthetic  $\alpha$ - and  $\beta$ -tricalcium phosphate ( $\alpha$ -TCP,  $\beta$ -TCP), biphasic calcium phosphate ceramics (BCP),  $\alpha$ -pyrophosphate ceramics and  $\beta$ -pyrophosphate ceramics [125-129, 149]. Besides many reports of osteoinduction by CaP ceramics, Yuan et.al. [189] showed ectopic bone formation by a CaP cement in muscles of dogs. Recently, Yuan et.al., [140] and Barrere et.al. [132] reported osteoinduction by octacalcium phosphate (OCP) coating on porous tantalum (Ta) implants in dogs and goats, respectively.

Composite of CaP coatings and metal implants is an example of combining different biomaterials in order to improve intrinsic properties of the final implant. Combination of sufficient mechanical properties of metals with bioactivity of CaPs makes CaP coated implants suitable for, e.g. total hip arthroplasty and other load bearing applications. The conventional technique of providing metal implants with a CaP coating is plasma-spraying (PS). Although PS coated implants have shown some great clinical successes [42], the method of producing them shows many disadvantages. PS coating process takes place at very high temperatures, limiting this method to stable CaP phases. Furthermore, it is not possible to coat geometrically complex and porous implants by using the PS method, while introduction of porosity into orthopaedic implants is becoming more important, as mechanical interlocking might enhance bone-implant integration process.

Recently, other techniques have been studied to improve the quality of coatings, such as electrophoretic deposition [43], sputter deposition [44] and sol-gel [45]. Nevertheless, the deposition of CaP coatings from Simulated Body Fluids (SBF) [190] offers the most

promising alternative to PS and other methods. The biomimetic coating method is inspired by the bone mineralization process of collagen fibers. As a result of the paraphysiological conditions of this technique, various CaP phases such as OCP [191] and carbonated apatite (CA) [192] can be deposited. The biomimetic coating process is performed in a solution, which allows for coating of geometrically irregular and porous implants.

The aim of this in vivo study was to investigate the influence of biomimetic OCP coating on osteoinductive properties of various biomaterials.

### **3.3 Materials and methods**

#### **3.3.1 Implants**

In this study, we used four kinds of porous materials: Ti6Al4V, HA, BCP and PEGT-PBT. All materials, except PEGT-PBT were used with and without biomimetic OCP coating. Ti6Al4V implants were produced by a positive replica method as described earlier [193]. In short, 70 wt% of titanium alloy powder (Northwest Non-Ferrous Institute of China) consisting of spherical particles with a diameter lower than 44 $\mu$ m (325 mesh) was mixed with H<sub>2</sub>O (20 wt%). Polyethylene glycol (PEG) and methylcellulose were used as binders (8 wt%). Dolapix (CE 64, Germany) and ammonia solution (2 wt%) were added to improve the rheological property of the slurry. Porous titanium alloy bodies were made by impregnation of polymeric (PU) sponges (35-45 pores per inch) (Coligen Europe B.V., Breda, The Netherlands). When the slurry reached the designed viscosity range (3000-5000 cp), Polyurethane (PU) foams were dipped into the slurry and then extracted to dry. The dipping-drying process was repeated until the struts of the PU foam were coated with titanium alloy slurry. The superfluous slurry was removed by using a roller under pressure, to get an evenly distributed coating on the foam. After final drying, the samples were first heated to 500°C to burn out foam, then, they were sintered in a vacuum furnace at 1250°C with holding time of 2h. Cylinders ( $\varnothing$ 5 x 10 mm<sup>3</sup>) were machined by using the electric sparking method. The ultrastructure of porous titanium alloy was characterized by using an environmental scanning electron

microscope (ESEM; XL30, ESEM-FEG, Philips, The Netherlands) in the secondary electron mode. The porosity of the material was determined from the histological slides using an image analysis PC-based system equipped with KS400 version 3.0 software (Carl Zeiss Vision, Oberkochen, Germany). Average pore size was measured on the 2D cross-section by using the automatic ruler of the ESEM. Pore interconnectivity was visually analyzed by the ESEM on the material cross-sections.

Porous HA implants were produced by using the dual phase mixing method described earlier [129]. In this method, commercially available HA powder (Merck, Amsterdam, The Netherlands) was used. The processing route consisted of three steps. In the first step, HA slurry was prepared by mixing 2/3 wt% of calcined HA powder with 1/3 wt% water containing deflocculant (Dolapix CE 64, Germany) and binder (carboxymethyl cellulose, Pomosin BC, The Netherlands). In the second step, two immiscible phases were mixed: water-based HA slurry and polymethyl methacrylate (PMMA) resin with a volume ratio of 1:1. The PMMA resin consisted of PMMA powder, MMA monomer and an additional fugitive pore maker ( $<10$  v/v%) such as naphthalene or wax particles. In the final step, the mixture was mould-shaped, polymerized, dried, pyrolysed and sintered in air at  $1250^{\circ}\text{C}$  for 8 hours. Cylinders ( $\text{Ø}5 \times 10 \text{ mm}^3$ ) were machined using a lathe. The structure of porous HA was characterized by an ESEM. Porosity, pore size and pore interconnectivity were analyzed by the same techniques as described for the Ti6Al4V implants. Composition and crystal structure of the material were determined by using Fourier transform infra red spectroscopy (FTIR; Spectrum100, Perkin Elmer Analytical Instruments, Norwalk, CT) and X-ray diffraction (XRD; Miniflex, Rigaku, Japan).

Porous BCP implants were prepared by using the  $\text{H}_2\text{O}_2$  foaming method as published earlier [129]. For the preparation of the ceramic, in-house made BCP powder was used. Porous green bodies were produced by mixing the BCP powder with 2%  $\text{H}_2\text{O}_2$  solution (1.0 g powder /  $1.2 \pm 0.05$  ml solution) and naphthalene (Fluka Chemie, The Netherlands) particles (710-1400  $\mu\text{m}$ ; 100 g powder / 30 g particles) at  $60^{\circ}\text{C}$ . The naphthalene was then evaporated at  $80^{\circ}\text{C}$  and the porous green bodies were dried. Subsequently, porous green bodies were sintered at  $1200^{\circ}\text{C}$  for 8 h and machined into cylinders ( $\text{Ø}5 \times 10 \text{ mm}^3$ ) by using a lathe. The structure of porous BCP was



characterized by an ESEM. Porosity, pore size and pore interconnectivity were analyzed by the same techniques as described for the Ti6Al4V implants. Composition and crystal structure were determined by using FTIR and XRD. HA/ $\beta$ -TCP ratio in the BCP was determined by comparing the BCP XRD pattern to the calibration patterns prepared from the powders with the known HA/ $\beta$ -TCP weight ratios.

PEGT-PBT copolymers were obtained from IsoTis SA (Bilthoven, The Netherlands) with a composition denoted as aPEGTbPBTc, where a represents PEG molecular weight, and b and c wt% of PEGT and PBT blocks, respectively. Final materials were prepared by using the compression molding and particle-leaching method described earlier [46]. In brief, PEGT-PBT granules with a size of 500-600  $\mu\text{m}$  were homogeneously mixed with sodium chloride grains and sieved to obtain particles ranging in size from 400-600  $\mu\text{m}$ . The amount of the salt was adjusted to a desired final volume percentage of 75%. The mixture was heated to 180°C for 3 min and subsequently compression molded for 1 min at 2.9 MPa in a hot press (THB 008, Fontijne Holland BV, The Netherlands) resulting in a block with dimensions of 120 x 100 x 10 mm<sup>3</sup>. The block was then immersed into demineralized water for 48 h to remove the sodium chloride, and dried under reduced pressure in vacuum oven. Final implants with a size of  $\varnothing 5$  x 10 mm<sup>3</sup> were cored out of bigger blocks. The structure of porous PEGT-PBT was characterized by an ESEM. Porosity, pore size and pore interconnectivity were analyzed by the same techniques as described for other implants.

### 3.3.2 Coating process

Prior to the coating process, porous implants were ultrasonically cleaned in acetone, ethanol and water, subsequently. Next, they were soaked in SBF for 24h at 37°C to seed the metal surface with calcium phosphate nuclei. The used SBF solution was 5 times more concentrated than Kokubo's SBF solution [190] (table 1) in order to increase the rate of the coating process. In order to produce crystalline OCP coating, the implants were then immersed in simulated calcifying solution (SCS) (table 1) for 48 hours at 37°C with one replenishment.

**Table 1:** inorganic composition (mM) of Kokubo's SBF, supersaturated SBFx5 and SCS.

	Ion concentration (mM)							
	Na <sup>+</sup>	K <sup>+</sup>	Ca <sup>2+</sup>	Mg <sup>2+</sup>	Cl <sup>-</sup>	HPO <sub>4</sub> <sup>2-</sup>	HCO <sub>3</sub> <sup>-</sup>	SO <sub>4</sub> <sup>2-</sup>
<b>SBF</b>	142.0	5.0	2.5	1.5	148.8	1.0	4.2	0.5
<b>SBFx5</b>	714.8	--	12.5	7.5	723.8	5.0	21.0	--
<b>SCS</b>	140.4	--	3.1	--	142.9	1.86	--	--

The biomimetic method of producing the OCP coating has previously been described in detail [191]. The coating composition and crystallinity were investigated by using FTIR and XRD. Coating thickness was measured on 2-D implant cross-sections by the automatic ESEM ruler.

### 3.3.3 In vivo experiments

This study was approved by the Dutch Animal Care and Use Committee. Ten adult Dutch milk goats were housed at Central Animal Laboratory Institute (GDL), Utrecht, The Netherlands, at least four weeks prior to surgery.

Before the surgical procedure, a dose of 0.1ml in 5ml of physiologic saline solution ( $\pm$  1ml/25kg body weight) of Domosedan (Pfizer Animal Health BV, Capelle a/d IJssel, The Netherlands) was administered by intravenous injection. The surgical procedure itself was performed under general inhalation anesthesia of the animals. Thiopental (Nesdonal,  $\pm$  400mg/70kg of body weight, on indication, Rhone Merieux, Amstelveen, The Netherlands) was injected intravenously, and anesthesia was maintained with a gas mixture of nitrous oxide, oxygen and Halothane (ICI-Farma, Rotterdam, The Netherlands).

After shaving the lumbar area and disinfection with iodine, the left muscle fascia was exposed and cut. Using blunt dissection, intramuscular pockets were created, and filled with one of the each above described implants: Ti6Al4V, OCP Ti6Al4V, HA, OCP HA, BCP, OCP BCP and OCP PEGT-PBT. Subsequently, the fascia was closed with a non-resorbable suture to facilitate implant localization at explantation. The skin was closed in two layers. After 6 weeks, the same procedure was repeated in the right back muscle. Table 2 gives an overview of the implanted materials.

Immediately after the surgery, pain relief was given by buprenofine (Temgesic; Schering-Plough, Kenilworth, NJ).

12 weeks after the first implantation (i.e. implantation times 6 and 12 weeks), each animal was sacrificed by an overdose of pentobarbital (Euthesaat, Organon, Oss, The Netherlands) and potassium chloride.

Intramuscular implants with surrounding tissue were explanted by sharp dissection and fixed in Karnovsky's fixative. All implants were dehydrated in a graded ethanol series (70-100%) and transferred into MMA solution that polymerized at 37°C within 1 week. Longitudinal sections (10-15µm) were made by using the modified interlocked diamond saw (Leica Microtome, Nussloch, Germany). Sections were stained with 1% methylene blue and 0.3% basic fuchsin after etching with HCl/ethanol mixture. Qualitative analysis was performed on all retrieved implants by using a light microscope (E600 Nikon, Japan).

**Table 2:** implantation scheme.

<b>Material</b>	<i>Ti6Al4V</i>	OCP <i>Ti6Al4V</i>	HA	OCP HA	BCP	OCP BCP	OCP PEGT-PBT
<b>6 weeks</b>	10	10	10	10	10	10	10
<b>12 weeks</b>	10	10	10	10	10	10	10

### 3.4 Results

#### 3.4.1 Implant characterization

As determined from the material cross-sections by using an image analysis system, the average porosity of the porous Ti6Al4V implants was  $79 \pm 5\%$  and the pores varied in diameter between 400 and 1300 µm. Observations by the ESEM showed that the pores were well interconnected. Figure 1a illustrates the macrostructure of the uncoated porous Ti6Al4V. Higher magnification ESEM photograph (figure 1b) shows the rough metal surface, caused by the sintering of the alloy powder particles.

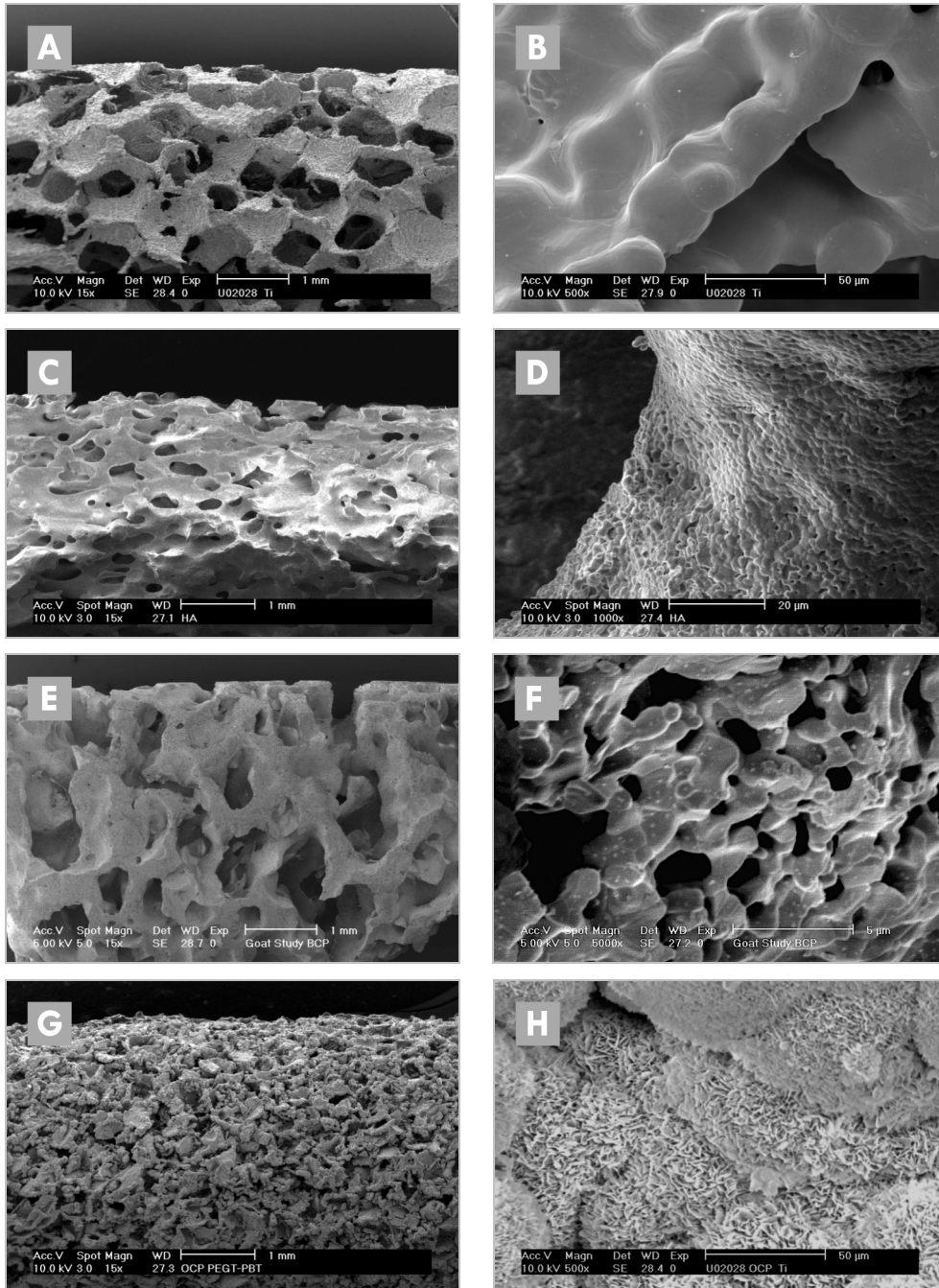


**Figure 1:** ESEM photographs of Ti6Al4V magnification 10x (A), and 500x (B), HA 10x (C) and 1000x (D), BCP 10x (E) and 5000x (F), OCP PEGT-PBT 10x (G) and 500x (H).

High magnification OCP PEGT-PBT photograph is representative for the structure of OCP coating on all implants.

Average macroporosity of the porous HA implants was  $46 \pm 8\%$  with pores varying in size between 100 and 800  $\mu\text{m}$ . Mercury porosimeter measurements showed that the average microporosity ( $<10\mu\text{m}$ ) was around 1.3%. ESEM observations revealed that the pores were well interconnected. ESEM photograph at low magnification (figure 1c) illustrates macroporous structure of HA, while the higher magnification photograph (figure 1d) shows its rough microstructure. XRD and FTIR analysis (results not shown) showed that the HA ceramic consisted of pure HA.

BCP implants revealed a well-interconnected macroporous structure (figure 1e), with pores varying in size between 100 and 800  $\mu\text{m}$ . Image analysis of the material cross-sections gave an average macroporosity of  $54 \pm 4\%$ . Higher magnification ESEM analysis (figure 1f) showed that macropore walls contained micropores (pore size  $<10\mu\text{m}$ ). As measured by mercury porosimeter, average microporosity was around 24%. XRD pattern and FTIR spectrum analyses (results not shown) of the produced material showed a biphasic chemistry consisting of 88% HA and 12%  $\beta$ -TCP. The material was highly crystalline.

Final composition of PEGT-PBT implants was 1000PEGT70PBT30, meaning the PEG molecular weight of 1000 and the weight percentage of PEGT/PBT being 70 and 30, respectively. The average porosity of these implants was  $75 \pm 5\%$  and their pore size varied between 500 and 600  $\mu\text{m}$ . Figure 1g is a low magnification ESEM photograph of the OCP coated PEGT-PBT implant. High magnification photograph (figure 1h), that is representative for all OCP coated implants, shows the highly crystalline and rough structure of the final OCP coating.

ESEM observations revealed that in all coated implants, the material surface was homogeneously covered with a CaP layer. However, the thickness of the coating was not the same throughout the implant. The average thickness varied between 20  $\mu\text{m}$  at the interior of the implant and 60  $\mu\text{m}$  at the implant periphery. Large OCP crystals were oriented perpendicularly to the surface of the implants, as illustrated by the high magnification ESEM photograph of the coated PEGT-PBT (figure 1h). FTIR spectra and XRD patterns (not shown) were typical for a pure, highly crystalline OCP phase.

### 3.4.2 Bone induction

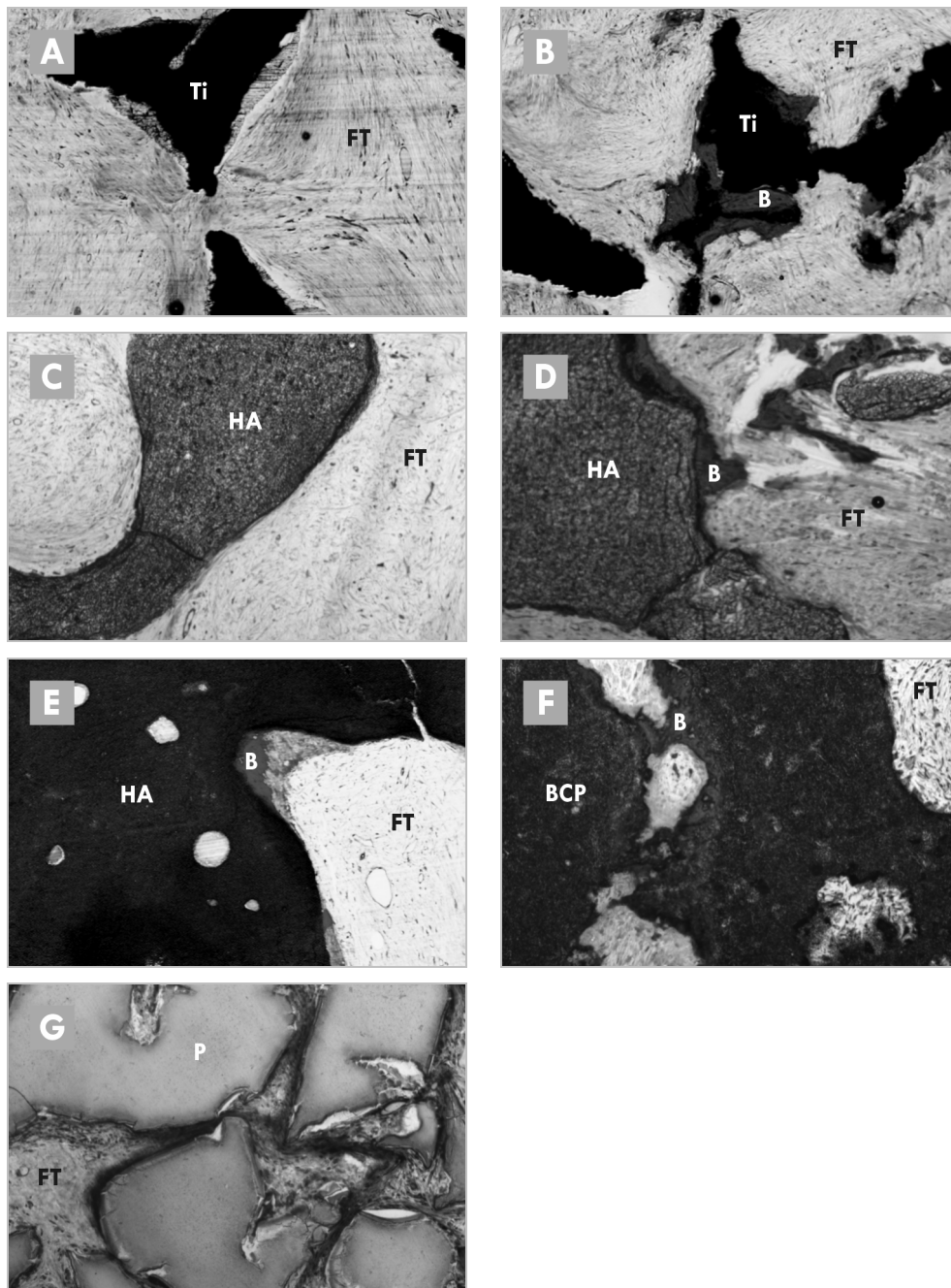
At retrieval, all implants were surrounded by highly vascularized muscle tissue. Histology showed no evidence for toxicity of the implants nor was a deviating inflammatory reaction observed.

Table 3 shows bone incidence in all implants after 6 and 12 weeks of intramuscular implantation. As can be seen, uncoated Ti6Al4V and uncoated HA implants did not show any ectopic bone formation after 6 and 12 weeks of implantation. Bone could be observed in the uncoated BCP implants. All OCP coated implants, except PEGT-PBT, sporadically induced bone after both 6 and 12 weeks of intramuscular implantation. The amount of induced bone was limited.

Table 3: bone incidence after intramuscular implantation.

<b>Material</b>	<i>6 weeks</i>	<i>12 weeks</i>
<b>Ti6Al4V</b>	0/10	0/10
<b>OCP-Ti6Al4V</b>	4/10	6/10
<b>HA</b>	0/10	0/10
<b>OCP-HA</b>	2/10	0/10
<b>BCP</b>	3/10	6/10
<b>OCP-BCP</b>	4/10	6/10
<b>OCP-PEGT/PBT</b>	0/10	0/10

Ti6Al4V, HA and OCP PEGT-PBT (figure 2a, c, and g respectively) were extensively filled with fibrous tissue, but no signs of bone formation were observed. The bone formed in OCP Ti6Al4V, OCP HA, BCP and OCP BCP (figure 2b, d, e and f, respectively) was always observed in the macropores inside the implants and never on the implant periphery or in surrounding soft tissue. The formed bone was normal in appearance, aligned with osteoblasts, and with mineralized bone matrix and osteocytes clearly visible. The OCP coating was often incorporated inside the newly formed bone. In the areas without bone, the OCP coating had extensively dissolved after 6 weeks, and could only occasionally be observed after 12 weeks of implantation. In the areas where the coating was still visible, signs of its resorption by multinucleated cells were observed.



**Figure 2:** LM photographs (magnification 10x) after 12 weeks of intramuscular implantation of Ti6Al4V (A), OCP Ti6Al4V (B), HA (C), OCP HA (D), BCP (E), OCP BCP (F) and OCP PEGT-PBT (G).

Ti=titanium alloy, HA=hydroxyapatite, BCP=biphasic calcium phosphate, P=PEGT-PBT, FT=fibrous tissue and B=bone. → p216.

### 3.5 Discussion

In this *in vivo* study, we investigated the effect of OCP coating on osteoinductive potential of various biomaterials.

Because of the low bone incidence, and a low quantity of bone formed in this study, only a qualitatively analysis of ectopic bone formation was performed.

All implants used in this study had a macroporous structure. The reason for this choice of structure was the fact that in all previous studies on osteoinduction by CaP biomaterials, ectopic bone formation was never observed on the non-porous implants or on the peripheries of the implants, suggesting the presence of porosity to be a prerequisite of osteoinduction.

In this study, uncoated Ti6Al4V implants did not induce bone in any of the animals, while bone was induced after application of the CaP coating on their surface. This finding suggests that the presence of CaPs is another prerequisite for ectopic bone formation. Although Yuan et.al. [134] and Fujibayashi et.al. [135] have shown osteoinduction by alumina ceramic and chemically treated porous titanium, it is well known that both alumina ceramic and pretreated titanium are able to calcify when immersed in SBF *in vitro*. It has been suggested that the same process of calcification occurs *in vivo*, preceding the process of bone formation. Although CaP seems to be of importance in the process of osteoinduction, the presence of a CaP phase alone is not enough, as is suggested by the fact that no bone was found in uncoated the HA implants.

Besides macroporosity and the presence of CaPs, microstructure of the material is believed to influence its osteoinductive properties as well. In the present study we compared different CaP phases (HA, BCP and OCP) as well as different macro- and microstructures. In the case of bulk ceramics, sintering process is often responsible for the formation of micropores inside the macropore walls. Increase of microporosity is responsible for the increase of the specific surface area of the ceramic. In the case of the OCP coating, we cannot speak of microporosity. However, also here, the specific surface area of the material is increased due to the presence of large crystals that perpendicularly grow on the implant surface.

Obviously all three described material properties, i.e. chemical composition, macro- and microstructure are of great importance for osteoinductive potential of a material.



As shown in table 3, the presence of OCP coating increased osteoinductive potential of all tested biomaterials. Uncoated Ti6Al4V and HA, that did not show ectopic bone formation in this study, became osteoinductive after the application of the OCP coating on their surface. Similarly, bone incidence of BCP increased in the presence of OCP coating. The fact that uncoated BCP did and uncoated HA did not show any bone induction is probably due to the differences in their chemistry and structure as earlier reported by Yuan et.al. [129]. The reason for the poor osteoinductive performance of the coated polymer might be explained by the fact that, due to the chosen composition, this implant was soft and unable to retain its porous shape after implantation. Continuous movement of the muscle caused too much pressure on the PEGT-PBT implant, making the implant flat and its pores closed.

Although our knowledge on the parameters which are of influence on osteoinductive behavior of biomaterials is increasing [127-129, 194], the exact mechanism of osteoinduction remains unknown. Concerning this mechanism, we hypothesize: 1) osteoinductive materials exert a direct effect on the growth and differentiation of relevant cells that attach to them, a 2) the surface of osteoinductive materials helps collecting relevant proteins, which in their turn exert an osteoinductive effect on the recruited cells.

In both cases, the presence of porosity plays an important role. Nutrients can easily be supplied through the interconnected porous structure. On the other hand, microporous walls provide a protected area, without strong fluid movements, giving cells the space to differentiate towards the osteogenic lineage. The presence of CaP leads to a dissolution process, and therewith release of calcium and phosphate ions. This process results in a CaP supersaturation in the vicinity of the implant surface, eventually causing precipitation of bone like carbonated apatite layer, possibly accompanied with coprecipitation of relevant proteins from body fluids. Consequently, undifferentiated cells start differentiating into osteoblasts, finally forming new bone.

An interesting observation from this study is a large difference in the amount of bone induced between individual animals, i.e. one goat was "more inductive" than another goat, for all implanted materials. The reason for this difference could be either genetic or pathological, but as long as the mechanism of osteoinduction itself is not clear, this phenomenon will be hard to explain. In addition to the intraspecies difference observed

in this study, it is well known that osteoinductive potential of a biomaterial varies between different species [116, 143].

This study shows that we are able to produce an OCP coating on various kinds of porous implants by following a biomimetic route. OCP coating can improve the osteoinductive potential of various materials. It has previously been suggested that osteoinductive materials show more bone formation when implanted orthotopically as compared to the non-osteoinductive biomaterials [195], which suggests the importance of osteoinductivity in bone repair. The biomimetic coating method might be an elegant tool of producing more advanced orthopaedic and dental implants.

### **3.6 Acknowledgements**

A part of this study was financially supported by the EU “IntelliScaf” Project (G5RD-CT-2002-00697).

## Chapter 4

### 3D microenvironment as essential element for osteoinduction by biomaterials

Pamela Habibovic<sup>1</sup>, Huipin Yuan<sup>2</sup>, Chantal M. van der Valk<sup>2</sup>, Gert Meijer<sup>3</sup>,  
Clemens A. van Blitterswijk<sup>1</sup> and Klaas de Groot<sup>1</sup>

<sup>1</sup>University of Twente, Institute for Biomedical Technology,

Professor Bronkhorstlaan 10D, 3723 MB, Bilthoven, The Netherlands

<sup>2</sup>IsoTis SA, Professor Bronkhorstlaan 10-D, Bilthoven, 3720 MB, The Netherlands

<sup>3</sup>University Medical Center Utrecht, PO Box 85500, Utrecht, 3508 GA, The Netherlands

#### 4.1 Abstract

In order to unravel the mechanism of osteoinduction by biomaterials, in this study we investigated the influence of the specific surface area on osteoinductive properties of two types of calcium phosphate ceramics. Different surface areas of the ceramics were obtained by varying their sintering temperatures.

Hydroxyapatite (HA) ceramic was sintered at 1150 and 1250 °C. Biphasic calcium phosphate (BCP) ceramic, consisting of hydroxyapatite and beta tricalcium phosphate ( $\beta$ -TCP), was sintered at 1100, 1150 and 1200 °C.

Changes in sintering temperature did not influence the chemistry of the ceramics; HA remained pure after sintering at different temperatures and the weight ratio of HA and  $\beta$ -TCP in the BCP was independent of the temperature as well. Similarly, macroporosity of the ceramics was unaffected by the changes of the sintering temperature. However, microporosity (pore diameter  $<10\mu\text{m}$ ) significantly decreased with increasing sintering temperature. In addition to the decrease of the microporosity, the crystal size increased with increasing sintering temperature. These two effects resulted in a significant

decrease of the specific surface area of the ceramics with increasing sintering temperatures.

Samples of HA1150, HA1250, BCP1100, BCP1150 and BCP1250 were implanted in the back muscles of Dutch milk goats and harvested at 6 and 12 weeks post implantation. After explantation, histomorphometrical analysis was performed on all implants.

All implanted materials except HA1250 induced bone. However, large variations in the amounts of induced bone were observed between different materials and between individual animals.

Histomorphometrical results showed that the presence of micropores within macropore walls is necessary to make a material osteoinductive. We postulate that introduction of microporosity within macropores, and consequent increase of the specific surface area, affects the interface dynamics of the ceramic in such a way that relevant cells are triggered to differentiate into the osteogenic lineage.

Keywords: hydroxyapatite (HA), biphasic calcium phosphate (BCP), sintering temperature, macrostructure, microstructure, specific surface area, osteoinduction.

## 4.2 Introduction

Osteoinduction can be defined as the “induction of undifferentiated inducible osteoprogenitor cells that are not yet committed to the osteogenic lineage to form osteoprogenitor cells” [93]. In order to prove the osteoinductive potential of a biomaterial, soft tissue implantation i.e. implantation in the absence of cells with direct bone forming capacity, can be used. First evidence of osteoinduction was given by Urist in 1965 [19], after implantation of demineralized bone matrix (DBM) in soft tissue of rabbits, rats, mice and guinea pigs. Later studies [101, 196, 197] suggested that DBM contained morphogenetic factors capable of inducing the differentiation of resident extraskeletal mesenchymal cells firstly into chondrocytes and then into osteoblasts, i.e. osteoinduction. At present, highly purified native bone morphogenetic proteins (BMPs)

and recombinant human BMPs are available and in many studies their osteoinductive potential has been shown [198-200].

The general idea that BMPs are always necessary for triggering bone induction was challenged by Winter's and Simpson's discovery [114] of osteoinduction by a polymeric sponge. In this study it was observed that prior to the process of bone formation, the calcification of a polymeric sponge had taken place, suggesting the importance of the *in vivo* calcification, and thereby calcium-phosphates (CaPs) in the process of osteoinduction.

The importance of CaPs in osteoinduction has been supported by the reports of various groups in the last decade. Some examples are studies that showed bone induction in synthetic HA ceramic in dogs [116-120], in coral derived HA ceramic in dogs, monkeys and baboons [117, 121, 122], in  $\alpha$ -TCP-,  $\beta$ -TCP-, BCP-,  $\alpha$ -pyrophosphate- and  $\beta$ -pyrophosphate ceramics [122, 124-129]. In addition to the CaP containing biomaterials, there have also been a few reports showing osteoinduction by alumina ceramic [134] and titanium [135] in dogs. Similar to Winter's and Simpson's observation [114], the *in vivo* calcification of these materials is believed to be the precursor of bone induction.

Because the mechanism of osteoinduction by biomaterials is not completely understood, it is unknown whether it is the biomaterial, or possibly an interaction between the biomaterial and the relevant proteins present in body that is responsible for the process of bone induction. Since most implants do not induce bone, specific material properties are apparently needed for starting the process of bone induction. To start the differentiation of the undifferentiated inducible osteoprogenitor cells into bone forming cells, it has been suggested that not only the chemistry, but also geometry of the biomaterial in contact with these cells are critical factors [124, 128, 129, 134, 135]. In other words, the microenvironment around the cells is crucial. As earlier reported, changing the sintering temperature of a CaP ceramic has a consequence for its microstructure and crystal size, i.e. its specific surface area. This in turn not only influences mechanical strength [201] and initial bone-bonding of the ceramic [202], but also the microenvironment and thus possibly the ceramic osteoconductive properties [203]. An indicator of the influence of sintering temperature on ceramic osteoconductive properties is that the expressions of relevant markers, such as alkaline phosphatase and

osteocalcin, have been reported to be different for varying sintering temperatures [204].

The goal of the current in vivo study was to try to unravel the possible mechanism of osteoinduction by investigating the influence of the microenvironment around the undifferentiated inducible cells on the osteoinductive capacity of the CaP ceramics. The specific surface area was used to quantify the microenvironment. The tool used to vary the specific surface area was the sintering temperature of the ceramics. In order to avoid possible influence of the chemical composition, not one but two types of CaP ceramics, namely HA and BCP, were chosen. Osteoinduction was evaluated by implantation in back muscles of adult Dutch milk goats.

### **4.3 Materials and methods**

#### **4.3.1 Implants**

Porous HA implants were produced by using the dual phase mixing method described earlier [129]. In this method, commercially available HA powder (Merck, Amsterdam, The Netherlands) was used. The processing route consisted of three steps. In the first step, HA slurry was prepared by mixing 2/3 wt% of calcined HA powder with 1/3 wt% water containing deflocculant (Dolapix CE 64, Germany) and binder (carboxymethyl cellulose, Pomosin BC, The Netherlands). In the second step, two immiscible phases were mixed: water-based HA slurry and polymethyl methacrylate (PMMA) resin with a volume ratio of 1:1. The PMMA resin consisted of PMMA powder, MMA monomer and naphthalene (<10 v/v%) as an additional fugitive pore maker. In the final step, the mixture was mould-shaped, polymerized, dried and pyrolyzed. Finally, the materials were divided into two groups and sintered in air at 1150 and 1250 °C, respectively, for 8 hours. A lathe was then used to produce cylinders ( $\varnothing 5 \times 10\text{mm}^3$ ).

Ultrastructures of the porous HA ceramics were characterized by an environmental scanning electron microscope (ESEM; XL30, ESEM-FEG, Philips, The Netherlands) in the secondary electron mode. Macroporosities and average pore sizes of the ceramics were determined by using histological slides (10 cross-sections for 6-week- and 10

cross-sections for 12-week-implantation). First, the labels of the sections were covered. Then, high resolution (300dpi), low magnification (10x) digital micrographs were made of these sections. Using Adobe Photoshop 7.0, bone and material were pseudocoloured, red and green respectively. Image analyses were carried out with a computer-based system equipped with KS400 version 3.0 software (Carl Zeiss Vision, Oberkochen, Germany). Prior to measurements the system was geometrically calibrated with an image of a block of known dimensions. A program was developed in KS400 to quantify the pore diameter for individual pores and the total macroporosities of the ceramics. The macroporosity was determined as:  $[(\text{total implant surface} - \text{scaffold surface}) / \text{total implant surface}] * 100\%$ . Microstructures of the ceramics were analyzed by using a mercury intrusion porosimeter (MP, AutoPore IV 9500, Micromeritics Instrument Cooperation, Norcross, Georgia). For a good comparison, the microporosity of each ceramic was expressed as total incremental pore volume (ml) per g of the material for the pores with a diameter lower than 10  $\mu\text{m}$ . Specific surface areas of the ceramics were determined from the mercury porosimeter results, as the cumulative surface area ( $\text{m}^2/\text{g}$ ) when all the pores were filled with mercury. Pore interconnectivity was visually analyzed by an ESEM on the material cross-sections.

Compositions and crystal structures of the ceramics were determined by using Fourier Transform Infra Red Spectroscopy (FTIR; Spectrum100, Perkin Elmer Analytical Instruments, Norwalk, CT) and X-Ray Diffraction (XRD; Miniflex, Rigaku, Japan).

Porous BCP implants were prepared by using the  $\text{H}_2\text{O}_2$  method as published earlier [129]. For the preparation of the ceramic, in-house made BCP powder was used. Porous green bodies were produced by mixing this powder with 2%  $\text{H}_2\text{O}_2$  solution (1.0g powder /  $1.2 \pm 0.05\text{ml}$  solution) and naphthalene (Fluka Chemie, The Netherlands) particles (710 - 1400  $\mu\text{m}$ ; 100g powder/ 30g particles) at 60°C. The naphthalene was then evaporated at 80°C and the green porous bodies were dried. They were divided into three groups and sintered at 1100, 1150 and 1200 °C respectively for 8 hours. Finally, a lathe was used to produce cylinders with a size of  $\text{Ø}5 \times 10\text{mm}^3$  for BCP1200 and  $\text{Ø}7 \times 7\text{mm}^3$  for BCP1100 and BCP1150. Due to the differences in the production techniques, BCP implants sintered at 1100 and 1150 °C had a different size from the BCP sintered at 1200°C and HA implants. Although the influence of the implant size

cannot be completely excluded, the results of this study suggest that we can reliably make the comparison between all implanted ceramics. Ultrastructures of the porous BCP ceramics were characterized by an ESEM. Porosities, pore sizes, pore interconnectivity and specific surface areas were analyzed by the same techniques as described for the HA implants. Ceramic chemical compositions and crystal structures were determined by using an FTIR and XRD. HA/ $\beta$ -TCP weight ratios in the BCP ceramics were calculated by comparing the BCP XRD patterns to the calibration patterns prepared from the powders with the known HA/ $\beta$ -TCP weight ratios.

### **4.3.2 Animals and implantation**

This study was approved by the Dutch Animal Care and Use Committee. In total, ten adult Dutch milk goats were used. The animals were housed in Central Animal Laboratory Institute (GDL), Utrecht, The Netherlands, at least 4 weeks prior to surgeries. Before surgical procedures, a dose of 0.1 mL in 5 mL of physiologic saline solution ( $\pm$  1 mL/25 kg body weight) of Domosedan (Pfizer Animal Health BV, Capelle a/d IJssel, The Netherlands) was administered by intravenous injection. Surgical procedures were performed under general inhalation anesthesia of the animals. Thiopental (Nesdonal,  $\pm$  400 mg/70 kg of body weight, on indication, Rhone Merieux, Amstelveen, The Netherlands) was injected intravenously, and anesthesia was maintained with a gas mixture of nitrous oxide (66 v/v%), oxygen (33 v/v%) and Halothane (1 v/v%) (ICI-Farma, Rotterdam, The Netherlands).

Besides the implantations described in this study, the animals were used for a different study, to be published separately. Different groups of implants were assumed not to influence each other's behavior, as they were implanted either at a different implantation site or at a sufficient distance from each other as approved by the Dutch Animal Care and Use Committee.

After shaving the lumbar areas and disinfection with iodine, left muscle fascias were exposed and cut. Using blunt dissection, intramuscular pockets were created, and filled with one of each above-mentioned implants: HA1150, HA1250, BCP1100, BCP1150 and BCP1200. Subsequently, fascias were closed with nonresorbable sutures to



facilitate implant localization at explantation. The skin was closed in two layers. After 6 weeks, the same procedure was repeated in the right back muscle of each of the ten goats. Table 1 shows the total amounts of implanted materials for both time points.

Immediately after surgeries, pain relief was given by buprenofine (Temgesic; Schering-Plough, Kenilworth, NJ).

Twelve weeks after the first implantations (i.e. implantation times 6 and 12 weeks), each animal was sacrificed by an overdose of pentobarbital (Euthesaat, Organon, Oss, The Netherlands) and potassium chloride.

**Table 1:** overview of the total amounts of the implanted ceramics.

<b>Material</b>	<i>6 weeks</i>	<i>12 weeks</i>
<b>HA1150</b>	10	10
<b>HA1250</b>	10	10
<b>BCP1100</b>	10	10
<b>BCP1150</b>	10	10
<b>BCP1250</b>	10	10

#### **4.3.3 Retrieval of the implants, histology and histomorphometry**

The implants with surrounding tissue were explanted by sharp dissection and fixed in Karnovsky's fixative. They were dehydrated in a graded ethanol series (70%-100%) and transferred into a methylmethacrylate (MMA) solution that polymerized at 37°C within one week. Longitudinal sections (10-15µm in thickness) were made by using the modified interlocked diamond saw (Leica Microtome, Nussloch, Germany). Sections were stained with 1% methylene blue and 0.3% basic fuchsin after etching with HCl/ethanol mixture.

For histomorphometry, the same image analysis method was used as previously described for the measurement of material macroporosities. In the computer-based image analysis system, a program was developed to quantify different parameters concerning bone formation:

- Percentage of bone occupying available pore area (%b.),

- Percentage of available scaffold outline (in 3D surface of the scaffold) in contact with bone: [%contact = (bone-scaffold contact length / scaffold outline length) \* 100%] in the total area of the implant (%b.cont. in implant), and
- Percentage of available scaffold outline in contact to bone in the peripheral area that was defined by drawing a line 40 pixels central from the outer contour (corresponds with a distance of 350  $\mu\text{m}$ ) (%b.cont. in outer zone).

In addition to the measurements of the amounts of induced bone in the available pore areas, the bone contact measurements were performed as this parameter can give additional information on the bone growth direction in time [78, 205]. Measurements of the bone contact in both total area of the implant and in the peripheral area were performed in order to get more insight into preferable location for bone induction and consequently into the possible mechanism of this phenomenon.

#### **4.3.4 Statistical analysis**

Statistical calculations were done with the SPSS (Chicago, IL) 9.0 software. We found large variances between the individual animals. However, the trend within each animal was similar (material A induced more bone than material B in all goats). Because the distribution of the data was not normal, we chose non-parametric tests to perform the statistical analysis. Friedman rank test, followed by a post-hoc test [206] was chosen to make the comparisons between all ceramics at both time points.

The Wilcoxon signed rank test [207] for paired comparisons was used to analyze the difference in bone formation per material between the two time points and the difference in bone contact per material between the total implant and the peripheral zone.

In both tests, the significance level was set at  $p=0.05$ .

## 4.4 Results

### 4.4.1 Material characterization

HA ceramics, sintered at both 1150 and 1250 °C consisted of pure HA, as shown by the FTIR spectra and XRD patterns (figure 1a and 1b, respectively). No differences could be found in FTIR spectra and XRD patterns between the HA ceramics sintered at the either temperatures. Observations by the stereomicroscope and by the ESEM showed that both ceramics had similar macrostructures, consisting of well-interconnected macropores.

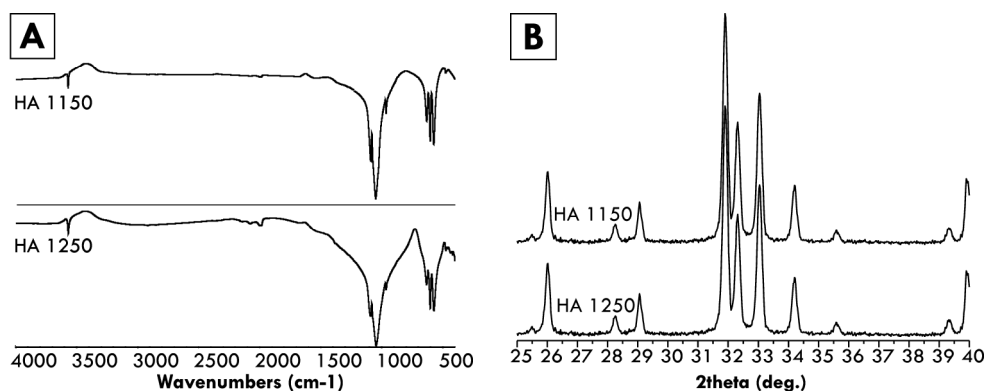
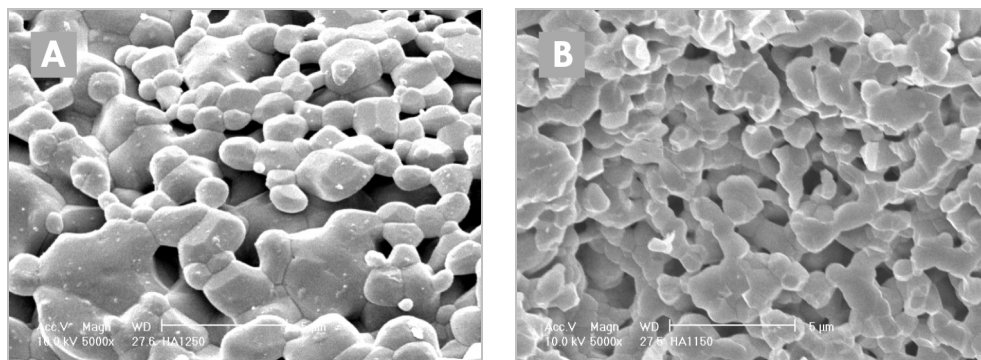


Figure 1: FTIR spectra (A) and XRD patterns (B) of HA1150 and HA1250.

Macropore diameters for both ceramics were similar ranging between 200 and 400  $\mu\text{m}$ , with an average of  $249\pm 38$   $\mu\text{m}$  (table 2). However, microstructures of the two ceramics differed: HA1250 had a rough microstructure, with only few micropores (pore diameter  $< 10$   $\mu\text{m}$ ) (figure 2a), while macropore walls of HA1150 contained many micropores (figure 2b).

Furthermore, the average crystal size of the HA1250 was higher as compared to HA1150. These observations were confirmed by the porosity measurements. Macroporosities of ceramics were  $47\pm 3\%$  as determined from the material cross-

sections (table 2). For the pores with the pore diameter lower than 10  $\mu\text{m}$ , large differences in the total pore volume between the HA1150 and HA1250 were observed. As can be seen in figure 3, for both temperatures, most micropores had a diameter of around 0.5  $\mu\text{m}$ . However, the total incremental volume of micropores, i.e. the microporosity is much higher for HA1150 as compared to HA1250.



**Figure 2:** ESEM photographs (magnification 5000x) of HA1250 (A) and HA1150 (B).  
Decrease in the sintering temperature results in an increase of the amount of micropores  
and a decrease in the crystal size of a ceramic.

**Table 2:** macroporosity and specific surface area overview.

<b>Material</b>	<i>Macroporosity (%)</i>	<i>Diameter macropores (<math>\mu\text{m}</math>)</i>	<i>Specific Surface Area (<math>\text{m}^2/\text{g}</math>)</i>
<b>HA1150</b>	47.5 $\pm$ 1.2	243.9 $\pm$ 38.7	1.32
<b>HA1250</b>	46.5 $\pm$ 4.9	248.4 $\pm$ 51.0	0.07
<b>BCP1100</b>	50.9 $\pm$ 3.0	367.1 $\pm$ 44.7	1.60
<b>BCP1150</b>	54.3 $\pm$ 8.0	380.2 $\pm$ 60.6	1.02
<b>BCP1200</b>	53.7 $\pm$ 4.2	371.1 $\pm$ 63.9	0.71

The specific surface area of HA1150 was 1.32  $\text{m}^2/\text{g}$  and of HA1250 0.07  $\text{m}^2/\text{g}$  (table 2).

BCP ceramics sintered at 1100 $^{\circ}\text{C}$ , 1150 $^{\circ}\text{C}$  and 1200 $^{\circ}\text{C}$  exhibited similar FTIR spectra and XRD patterns as is shown in the figures 4a and 4b respectively. As can be seen from the XRD pattern, there is a peak at  $2\theta = 31.2^{\circ}$  typical of  $\beta$ -TCP, and absent on the XRD pattern of pure HA (figure 1b). Compositions of the three BCP ceramics were

the same, all consisting of 88% HA and 12%  $\beta$ -TCP. Similar to the two HA ceramics, BCP ceramics also consisted of highly interconnected macropores ranging in the size between  $320\mu\text{m}$  and  $470\mu\text{m}$ , with an average of  $373\pm 56\mu\text{m}$  (table 2). LM and ESEM observations showed similar macrostructures for BCP1100, BCP1150 and BCP1200.

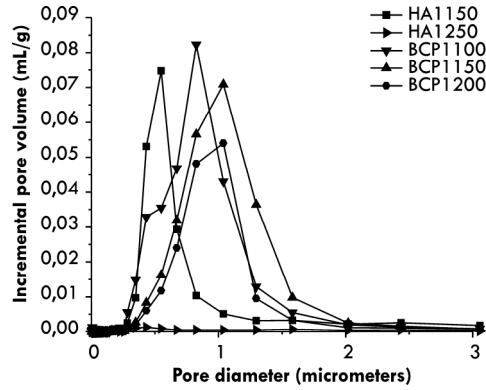


**Figure 3:** total incremental pore volume of the implanted ceramics.

Decrease in the sintering temperature results in an increase of the total micropore volume, i.e. microporosity of the ceramic.

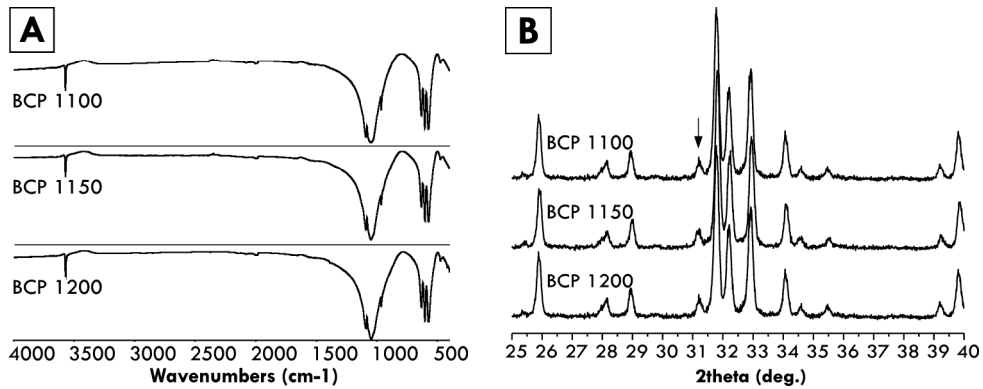


**Figure 4:** FTIR spectra (A) and XRD patterns (B) of BCP1100, BCP1150 and BCP1200.

Microstructures of the BCP ceramics sintered at the three temperatures did differ. As can be seen from the high magnification ESEM photographs (figures 5a, 5b and 5c), lowering the sintering temperature increased the amount of micropores within

macropore walls and decreased ceramic's crystal size. Measurements on cross-sections showed similar macroporosities for the three ceramics of  $53\pm 5\%$  (table 2).

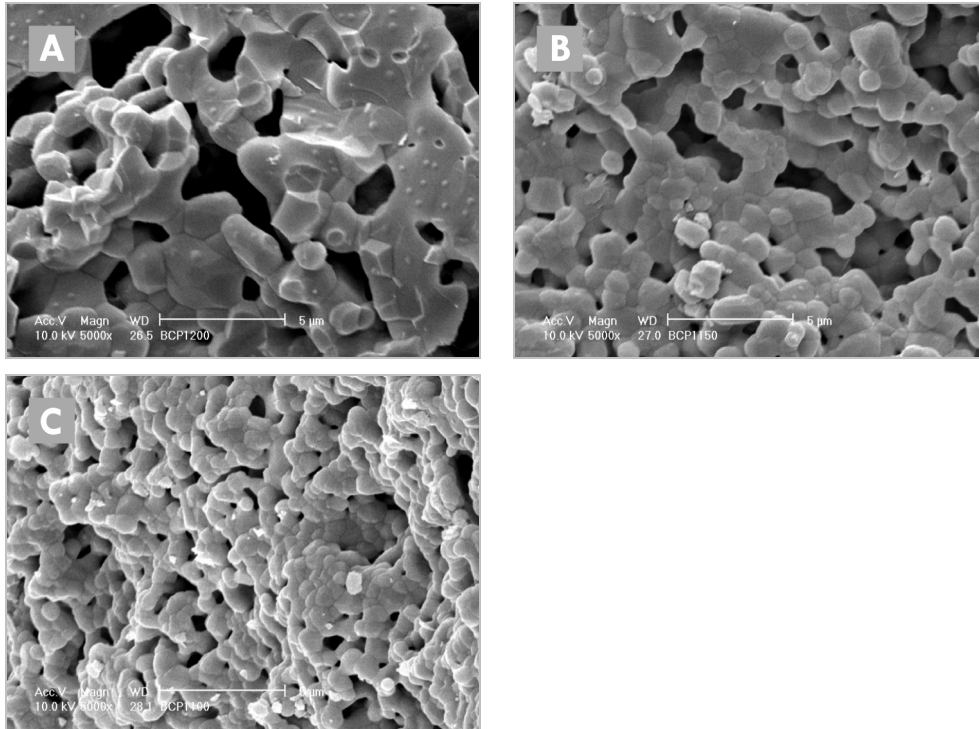


**Figure 5:** ESEM photographs (magnification 5000x) of BCP1200 (A), BCP1150 (B) and BCP1100 (C).  
Decrease in the sintering temperature results in an increase of the amount of micropores  
and a decrease in the crystal size of a ceramic.

As illustrated by figure 3, most micropores of the three BCPs had a diameter of around  $1\mu\text{m}$ . Figure 3 also shows that the increase in the sintering temperature resulted in a decreased total incremental micropore volume per gram of the material (microporosity), resulting, in turn, in a decreased specific surface area: BCP1100 =  $1.60\text{ m}^2/\text{g}$ , BCP1150 =  $1.02\text{ m}^2/\text{g}$  and BCP1200 =  $0.71\text{ m}^2/\text{g}$  (table 2).

Material characterization results of this study can be summarized as follows:

- Macroporosities of all implanted ceramics were similar (~50%). Average macropore size of HAs was around 245  $\mu\text{m}$  and that of BCPs around 370  $\mu\text{m}$  in diameter.
- Specific surface areas: BCP1100 (1.60  $\text{m}^2/\text{g}$ ) > HA1150 (1.32  $\text{m}^2/\text{g}$ ) > BCP1150 (1.02  $\text{m}^2/\text{g}$ ) > BCP1200 (0.71  $\text{m}^2/\text{g}$ ) > HA1250 (0.07  $\text{m}^2/\text{g}$ ).
- Chemical composition: 88wt% HA / 12wt%  $\beta$ -TCP in BCP versus 100wt% HA.

#### 4.4.2 Intramuscular implantation

There were no surgical complications and all implants were retrieved. At retrieval, all implants were surrounded by well-vascularized muscle tissue. Histology showed no evidence for toxicity of the implants, or signs of an inflammatory tissue response directly related to the implants.

**Table 3:** bone incidence after 6 and 12 weeks of implantation.

<b>Material</b>	<b>6 weeks</b>	<b>12 weeks</b>
<b>HA1150</b>	5/10	7/10
<b>HA1250</b>	0/10	0/10
<b>BCP1100</b>	6/10	8/10
<b>BCP1150</b>	7/10	6/10
<b>BCP1200</b>	3/10	6/10

Table 3 gives an overview of the bone incidence after 6 and 12 weeks of implantation. In some animals bone was not induced at all, while in the others (2 out of 10 after 6 weeks, and 5 out of 10 after 12 weeks) bone induction was considerable (>2% bone contact) as compared to the results of the similar studies in the same model. Because of the large variations in the amounts of induced bone between individual animals (non-normal data distribution), calculations of the average values and the standard errors of the mean for bone contact and bone area were not possible. To illustrate the large differences, we plotted the data found for %b.cont. in total implant for goats 1 and 3 (figure 6).

HA1250 was the only ceramic that did not induce bone formation in any of the animals. Table 4 gives an overview of the significant differences ( $p < 0.05$ ) between the ceramics for each of the measured parameters and for both time points.

Significant differences ( $p < 0.05$ ) between 6 and 12 weeks of implantation were only found for BCP1100 and HA1150, for all three measured parameters.

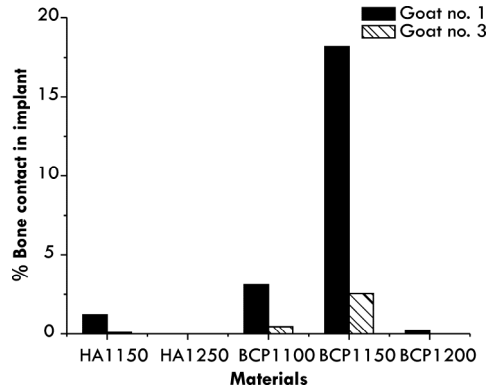


**Figure 6:** histomorphometrical results: % bone contact with the implant surface in the total area of the implant in goats 1 and 3 after 6 weeks of implantation.

Variations in the amount of formed bone are large between the individual animals, but the order of osteoinductive potential of the materials remains similar.

**Table 4:** overview of the implanted ceramics between which a significant differences ( $p < 0.05$ ) was observed after 6 and 12 weeks of implantation for the three measured parameters according to the Friedman's rank test.

\* $p = 0.05$

	6 weeks	12 weeks
<b>%b.</b>	BCP1100>HA1250 BCP1150>HA1250	BCP1100>HA1250 BCP1150>HA1250 BCP1100>BCP1200 BCP1150>BCP1200 HA1150>=HA1250*
<b>%b.cont. implant</b>	BCP1100>HA1250 BCP1150>HA1250 HA1150>=HA1250*	BCP1100>HA1250 BCP1150>HA1250 BCP1100>BCP1200 BCP1150>BCP1200
<b>%b.cont. peripheral zone</b>	BCP1100>HA1150 BCP1150>HA1150 BCP1100>HA1250 BCP1150>HA1250	BCP1100>HA1250



Significant differences ( $p < 0.05$ ) between %b.cont. in total implant and %b.cont. in peripheral zone were found for two ceramics: %b.cont. in total implant was significantly higher than %b.cont. in peripheral zone after both 6 and 12 weeks of implantation for HA1150 and only after 6 weeks of implantation for BCP1150.

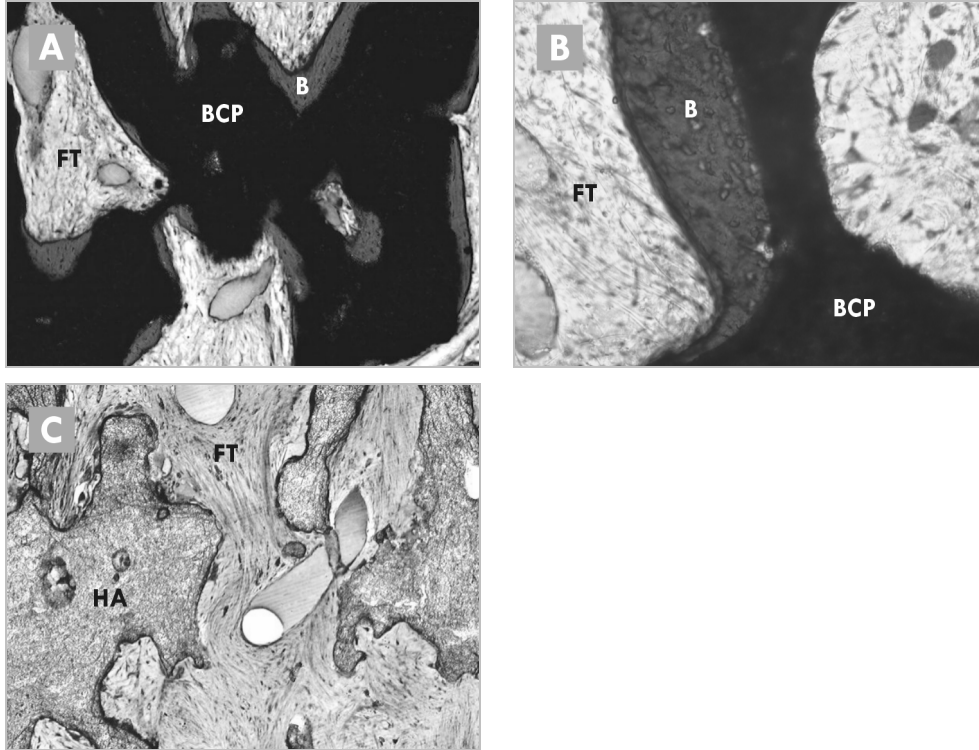


**Figure 7:** LM photographs of BCP1150 (magnification 4x) (A), BCP1150 (magnification 20x) (B), and HA1250 (magnification 4x) (C) after 12 weeks of implantation.

B=bone, FT=fibrous tissue BCP=BCP1150 ceramic, HA=HA1250 ceramic

The induced bone is formed in the pores of the implant, aligning its surface (A). The formed bone is normal in appearance, aligned with osteoblasts and with osteocytes and osteoid clearly visible (B).

The non-inductive ceramic is filled with fibrous tissue, but no signs of bone formation are observed (C). → p217.

No bone was observed on the outside of the implants. Bone formation was limited to inside the pores. Figure 7a illustrates new bone formation in BCP1150 after 12 weeks of implantation. The formed bone was normal in appearance as illustrated by figure

7b. Figure 7c is a histological slide of HA1250 after 12 weeks of implantation, the ceramic that did not induce bone in any of the animals.

Bone induction results of this study can be summarized as follows:

- Bone induction: (BCP1100, BCP1150) > (BCP1200, HA1150) > HA1250 (no induction at all).
- Bone induction in individual animals: >2% bone contact in goats no. 1 and 3 after 6 weeks and in goats no. 1, 2, 3, 4, and 6 after 12 weeks of implantation. Hardly any bone induction in goats no. 7, 8 and 10.

#### **4.5 Discussion**

Winter's and Simpson's observation of bone induction by a polymeric sponge [114] after soft tissue implantation in pigs could not be explained by the Urist's BMP theory [94], as the implanted polymeric sponge initially neither contained nor produced BMPs. An interesting finding of the Winter's and Simpson's study was that the implanted polymer showed *in vivo* calcification prior to the process of bone formation, suggesting the significance of CaPs in the process of osteoinduction. In a large number of publications, osteoinduction by CaP biomaterials in the form of ceramics [116-119, 121, 122, 124-126, 128, 149, 208], cements [124, 126, 131], coatings [132, 133, 182, 209] and glass ceramics [137] has been shown. In addition to CaP containing biomaterials, osteoinduction has also been observed in alumina ceramic [134] and titanium [135].

Although osteoinduction by biomaterials is obviously a real phenomenon, its mechanism is still largely unknown. This and previous work indicate some of the parameters necessary for making a biomaterial osteoinductive. In turn, these parameters suggest the mechanisms involved in the phenomenon of osteoinduction.

The presence of macropores, or concavities [138] is shown to be a prerequisite for osteoinduction by biomaterials. The presence of a well-interconnected macroporous structure is important for a good supply of the body fluids with nutrients throughout the implant. Accompanied with this supply, the release of calcium- and phosphate ions, that is believed to be the origin of the bioactivity of CaP biomaterials [171, 172, 210], took

place, followed by the precipitation of a biological apatite layer [211]. The precipitation of this apatite layer took place when the concentration of calcium- and phosphate ions had reached the supersaturation level in the material vicinity. This might explain the fact that the bone induction always takes place in the pores in the center of implant and not on the implant periphery [205]. The diffusion of the released calcium- and phosphate ions might occur too fast at the implant periphery, and therefore not allow for the ion concentration increase required for the biological apatite formation.

It is expected that a material with a higher dissolution rate will release calcium- and phosphate ions faster, followed by a faster formation of the biological apatite layer. One way to influence the in vivo dissolution rate of a material is by changing its specific surface area. This study showed, for the first time, that HA1250, which possessed very few micropores, and hence a low specific surface area, did not induce any bone, while HA1150, having the same chemical composition but a much higher specific surface area, did induce bone. Similarly, the amount of bone induced by BCP1200 was significantly lower than the amount of bone induced by both BCP1100 and BCP1150. However, no significant differences in the amounts of bone induced between BCP1100 and BCP1150 were found, although they had different specific surface areas, which suggest the existence of an optimal specific surface area. Materials with a specific surface area below the optimum will degrade slower, and will finally induce less bone. Materials with a specific surface area above the optimum might degrade too fast, losing thereby the shape and stability that is necessary to facilitate bone formation. Finally, there is a minimum threshold in the amount of micropores and hence specific surface area below which bone will not be induced.

Also the changes of the material chemical composition can influence its in vivo degradation. Both BCP1100 and BCP1150 performed significantly better than HA1250. Moreover BCP1150 induced more bone than HA1150. Although they were sintered at the same temperature, the specific surface area of the HA ceramic was slightly higher than that of BCP. From the conclusion on the effect of specific surface area drawn above one would expect more bone in HA1150 than in BCP1150. Therefore it is evident that there are other factors influencing osteoinductive capacity of a ceramic. In addition to the difference in the average macropore diameter of about 100 microns between BCP1150 and HA1150, the most important difference between

the two materials was the presence of  $\beta$ -TCP in BCP. Although we cannot exclude the importance of the macropore size, based on the earlier research we hypothesize that the effect of the presence of the more soluble  $\beta$ -TCP in BCP, and subsequently faster dissolution of BCP is more relevant than the difference in macropore size between the two materials.

In the biomaterials that initially do not contain CaPs, like alumina ceramic and titanium, the formation of the biological apatite layer will take longer than in biomaterials that do contain CaPs. In the non-CaP biomaterials, calcium- and phosphate ions from the body fluids will precipitate onto the microporous surface of the material. The microporous surface acts as the collection of nucleation sites for this precipitation.

The formed bone-like biological CaP layer could be a physico-chemical trigger for the cells to differentiate into the osteogenic lineage similar to being in a bony environment. However, there is another important observation from this study: the large variation in osteoinductive potential of individual animals, in addition to the inter-species variation [117]. If the process of osteoinduction by biomaterials is only based on the above described dissolution-precipitation process of calcium- and phosphate ions, it would not be likely to observe such a large difference between individual animals. No reports describing large variations between individuals' response to CaP biomaterials in an orthotopic context could be found. On the other hand, in addition to the difference in the response to BMPs between the higher animals and rodents [112], there are reports of differences in the response to BMPs between the individuals of the same species, probably due to genetic factors [113]. Similar differences were also observed in humans [56]. Thus, it seems plausible that endogenous BMPs, or other relevant proteins play a role in osteoinduction by biomaterials. This means that precipitation of the biological apatite layer in vivo could be accompanied by the coprecipitation of the relevant proteins (e.g. BMPs), which in turn trigger the recruited cells to differentiate into the osteogenic lineage. The amounts of coprecipitated proteins, that vary with the amounts of endogenous proteins, in conjunction with the variations in the body response to these proteins, could explain the observed intra-species differences. We have summarized our ideas in figure 8. In conclusion, from the results of this study we postulate that the undifferentiated inducible osteoprogenitor cells are triggered to start differentiating into the osteogenic lineage by the BMPs or other relevant proteins that

are coprecipitated in the newly formed biological apatite layer, and that consequently this biological apatite layer acts as the conductor of the bone formed by the induced cells. Further reading (figure 8): [212-215].

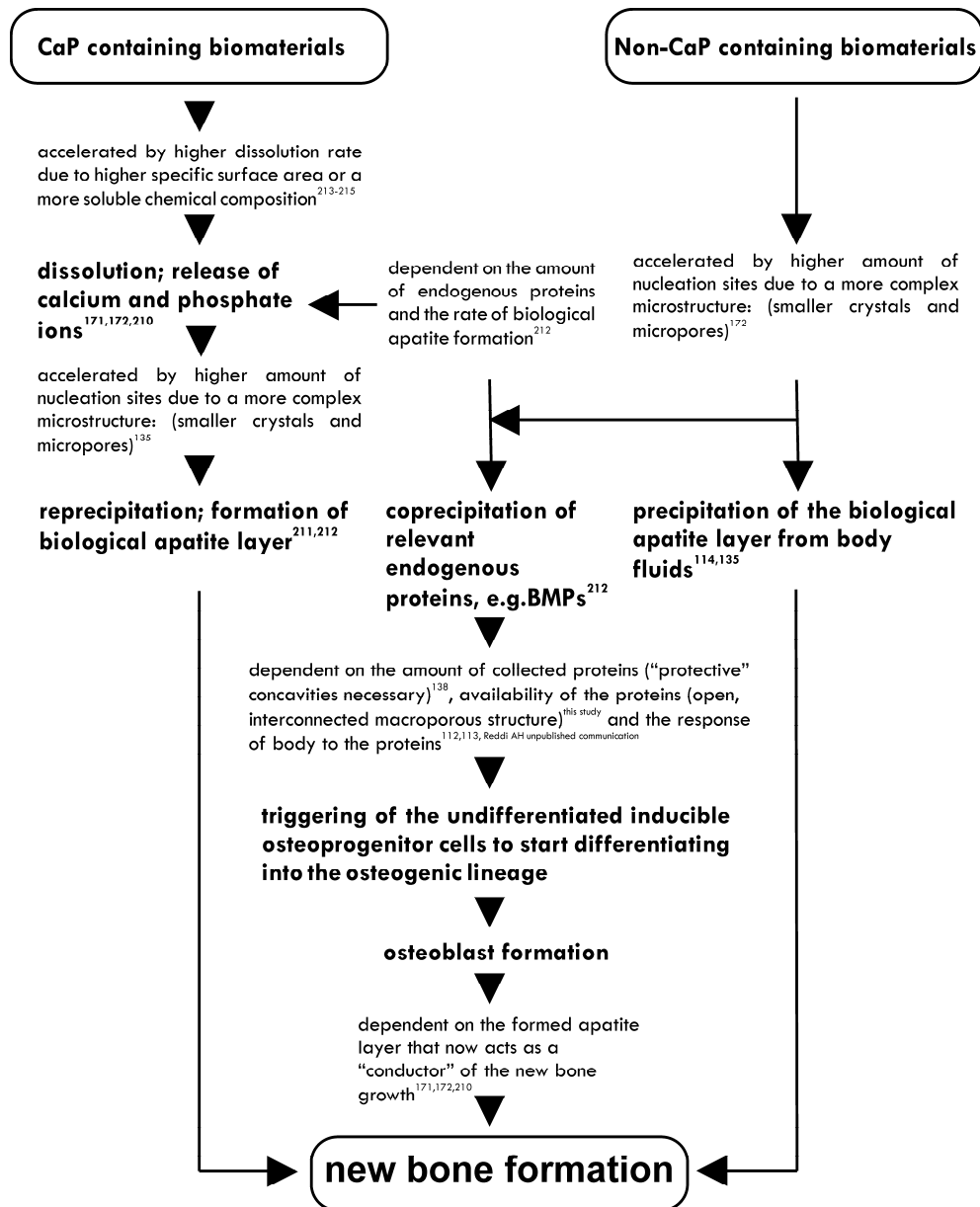


Figure 8: flow chart of the proposed mechanism of osteoinduction by biomaterials.

#### **4.6 Conclusion**

This study shows that, in addition to macropores, a minimum amount of micropores within the macropore walls is necessary for a material to be osteoinductive. These micropores are probably required for acceleration of the dissolution-precipitation process of CaPs on the material interface. The large variation in the amounts of induced bone that is observed between the individual animals suggests that some endogenous proteins such as BMPs might also play a role in the mechanism of osteoinduction by biomaterials.

#### **4.7 Acknowledgements**

Authors would like to thank Dr. Maarten Terlou from the Image Analysis Department of the University Utrecht for developing the software used for the histomorphometry and Dr. Paul Westers and Dr. Edwin Martens from the Biostatistics Department for their generous help with statistical analysis.

A part of this study was financially supported by the EU “IntelliScaf” Project (G5RD-CT-2002-00697).

## Chapter 5

### **Osteoinduction by biomaterials: physico-chemical and structural influences**

Pamela Habibovic, Tara M. Sees, Mirella van den Doel,  
Clemens A. van Blitterswijk and Klaas de Groot

University of Twente, Institute for Biomedical Technology,  
Professor Bronkhorstlaan 10D, 3723 MB, Bilthoven, The Netherlands

#### **5.1 Abstract**

Osteoinduction by biomaterials has been shown to be a real phenomenon by many investigators in the last decade. The exact mechanism of this phenomenon is, however, still largely unknown.

This *in vivo* study in goats was performed to get insight into processes governing the phenomenon of osteoinduction by biomaterials and had four main goals: 1) to further investigate influence of physico-chemical properties and structure on a biomaterial's osteoinductive potential, 2) to investigate influence of implant size on the amount of induced bone, 3) to investigate implantation site dependence and 4) to investigate changes occurring on the surface of the material after implantation.

Intramuscular implantations of four different biphasic calcium phosphate (BCP) ceramics, consisting of hydroxyapatite (HA) and  $\beta$ -tricalcium phosphate ( $\beta$ -TCP) and a carbonated apatite (CA) ceramic indicated that, for a maximal osteoinductive potential, there is an optimal specific surface area for each material type.

It was further shown that a decrease of the implant size with a half significantly decreased the relative amount of induced bone.

In addition, subcutaneous implantation did not give rise to bone formation in any of the animals, while bone was induced in most animals intramuscularly.

Analysis of the surfaces of the materials after subcutaneous implantation inside diffusion chambers indicated that the increased specific surface area leads to more surface reactivity, which is hypothesized to be essential for osteoinductivity of biomaterials.

Keywords: osteoinduction, biomaterials, mechanism, biphasic calcium phosphate ceramic, carbonated apatite ceramic.

## 5.2 Introduction

First reports on bone and cartilage formation after implantation of devitalized tissues [89, 92, 216] and tissue extracts [87] ectopically (i.e. in the absence of bone cells) have already been published in the forties and fifties of the previous century. In the late sixties, Urist defined osteoinduction as “the mechanism of cellular differentiation towards bone of one tissue due to physico-chemical effect or contact with another tissue” [26]. A year later, Friedenstein defined osteoinduction as “the induction of undifferentiated inducible osteoprogenitor cells (IOPCs) that are not yet committed to the osteogenic lineage to form osteoprogenitor cells” [93]. Later work of Urist and Reddi [19, 101, 196, 197] resulted in finding bone morphogenetic proteins (BMPs) which were proposed to irreversibly induce differentiation of perivascular mesenchymal-type cells into osteoprogenitor cells to finally form cartilage and bone [197]. Although osteoinduction by certain types of devitalized tissues and thus BMPs has been extensively investigated, the exact mechanism is not fully understood yet.

The search for the explanation of the mechanism of osteoinduction was further complicated by Winter’s and Simpson’s early finding of ectopic bone formation after implantation of a polyhydroxyethylmethacrylate (poly-HEMA) sponge that neither contained nor produced BMPs [114]. In this study, authors observed that osteoinduction was preceded by the *in vivo* calcification of the polymeric sponge. Up to now, many groups reported osteoinduction by various synthetic biomaterials such as synthetic hydroxyapatite (HA) ceramic in dogs [116-120], coral derived HA ceramic in dogs, monkeys and baboons [117, 121, 122],  $\alpha$ -tricalcium phosphate ( $\alpha$ -TCP),  $\beta$ -TCP-, BCP-,  $\alpha$ -pyrophosphate- and  $\beta$ -pyrophosphate ceramics [122, 124-130, 181, 183, 209].



Besides calcium-phosphate (CaP) bulk ceramics, ectopic bone formation was also found in CaP cements [124, 131] and in various porous implants coated with biomimetic octacalcium phosphate (OCP) [132, 182, 209]. In addition to the CaP containing biomaterials, there are a few reports showing osteoinduction by glass ceramic [137], alumina ceramic [134] and titanium in dogs [135, 136], all of which have the ability to calcify in a CaP rich environment. These reports all give further evidence that osteoinduction by biomaterials is a real phenomenon.

Although both BMPs and biomaterials can lead to ectopic bone formation, it is unknown whether they (partially) follow the same pathway. In contrast to the, mainly endochondral, BMP- triggered osteoinduction [101], cartilage formation as a precursor of the final bone formation has never been observed in osteoinduction by biomaterials without added BMPs [121, 124, 129, 138, 183], and is thus intramembranous. Another difference between BMP- and biomaterials guided osteoinduction is their incidence in different animal models: bone is abundantly induced in soft tissue of rats and mice by using BMP-2 and BMP-7 (OP-1) [145-147], but hardly by synthetic biomaterials [116, 141-144]. Ripamonti and coworkers suggested the influence of BMPs in osteoinduction by biomaterials, but did not prove this hypothesis by experimental data [138, 139].

During the last decade, experiments by various investigators in large animal models have shown parameters which are of great importance in the process of osteoinduction by biomaterials. For instance, it has been shown that the presence of concavities or macropores is one of the prerequisites for osteoinduction [124, 138]. Furthermore, the presence of micropores, by which the specific surface area of the material is increased, seems to be essential too [124, 128, 129, 134, 135, 181, 183]. It has been proposed that the increased specific surface area leads to more surface reactivity in terms of dissolution and reprecipitation of a biological apatite layer, which possibly coprecipitates relevant endogenous proteins, which in turn initiate the differentiation of pluripotent cells into the osteogenic lineage [183].

The present in vivo study was performed in order to get more insight into the processes governing the phenomenon of osteoinduction by biomaterials, by achieving following goals:

- to further investigate the influence of physico-chemical properties and structure on a biomaterial's osteoinductive potential. We compared five CaP ceramics,

four of which were biphasic, consisting of HA and  $\beta$ -TCP, with slightly varying chemical composition and large variations in microstructure, and a carbonated apatite (CA) ceramic, that is, based on its chemistry, closer to bone mineral than the BCP ceramics;

- to investigate the influence of implant size on the amount of induced bone. The availability of the implant for cell and nutrient infiltration, as well as possible micromotion inside the implant could be influenced by the implant size;
- to investigate the influence of implantation site on osteoinduction by biomaterials. Implantation site dependence, i.e. comparison of intramuscular and subcutaneous implantation, could shed light upon the importance of vascularization in the process of osteoinduction;
- to investigate changes occurring on the surface of an osteoinductive and a non-osteoinductive ceramic after implantation inside diffusion chambers. The idea behind this part of the study is to test the earlier given hypothesis that the high specific surface area of osteoinductive biomaterials, which causes a high surface reactivity, is essential for osteoinduction by biomaterials [183].

### **5.3 Materials and methods**

#### **5.3.1 Implants**

In this study, 5 ceramic types were investigated: biphasic calcium phosphate A (BCPA), BCPB, BCPC, BCPD and carbonated apatite (CA). The four BCP ceramics were used to investigate the influence of variations of physico-chemical properties, achieved by differences in preparation methods, on the osteoinductive potential of the ceramics. The osteoinductive properties of the rather novel CA bulk ceramic are interesting because, based on its chemical composition, CA ceramic resembles the bone mineral composition more than BCP ceramics do.

BCPA and BCPB implants were prepared by using the  $H_2O_2$  foaming method as published earlier [129]. For the preparation of the ceramic, in-house made BCP powder

was used. Porous green bodies were produced by mixing this powder with 2% H<sub>2</sub>O<sub>2</sub> solution (1.0 g powder / 1.2 ± 0.05 ml solution) and naphthalene particles (710 - 1400 μm; 100 g powder/ 30 g particles) at 60°C. The naphthalene was then evaporated at 80°C and the green porous bodies were dried. They were divided into two groups and sintered at 1150 °C (BCPA) and 1300 °C (BCPB) respectively for 8 hours.

BCPC, BCPD and CA are novel ceramics, developed in the course of the EU “IntelliScaf” project (G5RD-CT-2002-00697).

A lathe was used to produce cylinders with a size of Ø6.5 x 10 mm<sup>3</sup> (all ceramic types) and Ø6.5 x 5 mm<sup>3</sup> (BCPA and BCPB). All implants were cleaned in ultrasonic baths and sterilized by gamma irradiation.

Composition and crystal structure of the ceramics were determined by using fourier transform infra red spectroscopy (FTIR) and X-ray diffraction (XRD). HA/β-TCP weight ratios in the BCP ceramics were determined by comparing the BCP XRD patterns to the calibration patterns prepared from the powders with the known HA/β-TCP weight ratios.

Prior to implantation, ultrastructure of all ceramics was characterized by an environmental scanning electron microscope (ESEM) in the secondary electron mode. ESEM, coupled with an image analysis system was used to determine macroporosities (pore diameter >10 μm) of the ceramics. In addition, total-, macro- and microporosities (pore diameter < 10μm) as well as average pore sizes and pore size distributions were determined by using a mercury intrusion porosimeter (MP). Specific surface areas of the ceramics were determined from the MP results, as the cumulative surface area (m<sup>2</sup>/g) when all pores were filled with mercury.

### **5.3.2 Animals and implantation**

This study was approved by the Dutch Animal Care and Use Committee. In total, ten adult Dutch milk goats (18-30 months) were used. The animals were housed in the Central Animal Laboratory Institute (GDL), Utrecht, The Netherlands, at least 4 weeks prior to surgery.

Surgical procedures were performed under general inhalation anesthesia of the animals preceded by an intravenous injection of Thiopental (Nesdonal,  $\pm$  400mg/70kg of body weight, on indication).

For the comparison of osteoinductive potentials of the five used ceramic types, all materials were implanted intramuscularly in all animals. For intramuscular implantation, fascia incisions were created in the paraspinal muscles (L1-L3). Using blunt dissection, intramuscular pockets were created, and filled with one of the above described ceramic cylinders ( $\varnothing$ 6.5 x 10 mm<sup>3</sup>): BCPA, BCPB, BCPC, BCPD and CA. Subsequently, fascias were closed with nonresorbable sutures to facilitate implant localization at explantation. The skin was closed in two layers.

For investigation of implantation site and implant size dependence on the amount of induced bone, we used BCPA and BCPB ceramics as a model. For the investigation of the implant size dependence, in addition to the above described intramuscularly implanted cylinders with the size  $\varnothing$ 6.5 x 10 mm<sup>3</sup>, smaller cylinders ( $\varnothing$ 6.5 x 5 mm<sup>3</sup>) of both BCPA and BCPB were implanted.

In order to investigate the implantation site dependence, BCPA and BCPB cylinders were, besides intramuscularly, also implanted subcutaneously. For subcutaneous implantations, separate blunt incisions were made in the skin of the back area, one cylinder with a size of  $\varnothing$ 6.5 x 5 mm<sup>3</sup> of each BCPA and BCPB ceramic was inserted, after which the skin was closed in two layers.

Pain relief was given by Durogesic 25 (fentanyl transdermal system CII patches).

8, 10 and 11 weeks after first surgery, in all animals, cylinders ( $\varnothing$ 6.5 x 10 mm<sup>3</sup>) of BCPA and BCPB ceramics inside diffusion chambers were implanted subcutaneously by following the same procedure as described above. Because of a relatively small impact on animals, during these surgeries, local anesthesia (subcutaneously injected Lidocaine) was used. Diffusion chambers in which the ceramics were placed prior to implantation, consisted of a Plexiglas ring on both ends of which  $\varnothing$  0.45  $\mu$ m Durapore® HV filters were pasted using the MF cement for diffusion chamber (Diffusion chamber kit, Millipore) as described previously [213]. Implantation of materials inside these semi permeable chambers allows the diffusion of macromolecules and ions into the chamber but blocks the invasion of host cells and tissues.

Table 1 gives an overview of total amounts of the implanted ceramics.

In order to visualize the dynamics of bone growth, the goats received sequential fluorochrome labels at 4 weeks (Calceine green, 10 mg/kg, I.V.), 6 weeks (Oxytetracycline, 32 mg/kg I.M.) and 8 weeks (Xylenol orange, 80 mg/kg, I.V.) [78, 80, 181].

12 weeks after first implantations, each animal was sacrificed by an overdose of pentobarbital (Euthesaat) and potassium chloride.

**Table 1:** overview of the total amounts of the implanted ceramics.

DC = diffusion chamber.

Implant	IM (12 weeks)	SC (12 weeks)	SC (4 weeks)	SC (2 weeks)	SC (1 week)
BCPA	10				
BCPB	10				
BCPC	10				
BCPD	10				
CA	10				
BCPAh	10				
BCPBh	10	10			
DC BCPA			20	20	20
DC BCPB			20	20	20

### 5.3.3 Retrieval of the implants, histology, histomorphometry and material analysis

The implants with surrounding tissue were explanted by sharp dissection and fixed in Karnovsky's fixative. They were dehydrated in a graded ethanol series (70%-100%) and transferred into a methylmethacrylate (MMA) solution that polymerized at 37°C within one week. Longitudinal sections (10-15µm in thickness) were made by using the modified interlocked diamond saw. Sections were either stained with 1% methylene blue and 0.3% basic fuchsin after etching with HCl/ethanol mixture and then qualitatively investigated by using a light microscope (LM) or left unstained for epifluorescence microscopy with a LM equipped with a quadruple filter block (XF57, dichroic mirror 400, 485, 558 and 640 nm).

Histomorphometry was performed on histological sections. First, the labels of the sections were covered. Then, high resolution (300dpi), low magnification digital micrographs were made of these sections. Image analyses on the pseudocolored micrographs were carried out with a computer-based image analysis system. Prior to measurements, the system was geometrically calibrated with an image of a block of known dimensions. In the computer-based image analysis system, a program was developed to quantify two parameters concerning bone formation:

- Percentage of bone occupying available pore area ( $\text{area}_{\text{bone}}/\text{pore}$ );
- Percentage of available scaffold outline (in 3D surface of the scaffold) in contact with bone: [ $\% \text{contact} = (\text{bone-scaffold contact length} / \text{scaffold outline length}) * 100\%$ ] in the total area of the implant ( $\% \text{b.cont}$ ).

The first parameter was chosen in order to allow for comparison with previous studies. The second parameter was chosen as in a study in which the performances of different materials are compared, it seems more appropriate to relate the new bone formation to available scaffold rather than to available pore space. Furthermore, contact percentage is more sensitive for early bone apposition which always occurs on the ceramic surface and has relatively low volume.

After explantation, BCPA and BCPB ceramics, which were implanted subcutaneously inside diffusion chambers, were removed from the chambers and dried at 60 °C in air for 2 days. They were then powdered in a mortar, and the powder was homogenized. One part of the powder was used to perform FTIR and XRD analyses. Other part was used for Thermogravimetry Analysis (TGA). TGA analyses were performed on samples weighing 10-20 mg at a heating speed of 10 °C/min. Weight loss between 30 °C and 200 °C, 200 °C and 450 °C and 450 °C and 900 °C were associated to water, organic compounds and CO<sub>3</sub> respectively. From the weight loss, weight percentages of organic compounds and CO<sub>3</sub> were calculated.

#### **5.3.4 Statistical analysis**

Statistical calculations were done with the SPSS 12.0 software.

In agreement with previous studies, intramuscularly implanted ceramics showed large variances between the individual animals [183, 209]. Hence, the distribution of the data was not normal and that is why the non-parametric Wilcoxon signed rank test [207] for paired comparisons was used to perform the statistical analyses.

For the quantitative TGA data, the two-sided, paired Student's t-test was used to analyze differences between BCPA and BCPB.

For both tests the significance level was set at  $p=0.05$ .

## 5.4 Results

### 5.4.1 Material characterization

FTIR spectra and XRD patterns of the four BCP and the CA ceramic are given in figure 1a and 1b.

All BCP ceramics had similar, biphasic composition, consisting of HA and  $\beta$ -TCP. However, their HA/ $\beta$ -TCP weight ratios differed: BCPA and BCPB ceramics consisted of  $80\pm 3$  wt% HA and  $20\pm 3$  wt%  $\beta$ -TCP, while the contents of HA and  $\beta$ -TCP in BCPC and BCPD were  $70\pm 5$  wt% and  $30\pm 5$  wt% respectively, which is also illustrated by the differences in the height of the main  $\beta$ -TCP peak (at  $2\theta = 31.2^\circ$ ) in the BCP XRD patterns (figure 1b). The FTIR spectrum of the CA ceramic exhibits typical carbonated apatite structure with distinct bands assigned to  $\text{CO}_3^{2-}$  group at  $1497\text{ cm}^{-1}$ ,  $1462\text{ cm}^{-1}$  and  $868\text{ cm}^{-1}$  (figure 1a).  $\text{CO}_3^{2-}$  content (B type >90%) in the CA ceramic was around 8 wt%. All ceramics were highly crystalline.

Different production techniques caused different macrostructures. Macropores of BCPA and BCPB had a somewhat longitudinal shape, with a length/width aspect ratio between 1.5 and 2. BCPC, BCPD and CA possessed macropores with a more regular circular shape, with a length/width ratio close to 1. Despite these differences, all ceramics had a macroporous structure with macropores varying in diameter between 50 and 1000  $\mu\text{m}$ . LM photographs of the ceramics macrostructures prior to implantation are shown in figure 2.

Microstructures of the ceramics differed significantly, as illustrated by figure 3. BCPB contained very few micropores and a larger average crystal size in comparison with other investigated ceramics. Macropores of the CA ceramic on the other hand, contained a large amount of micropores and small crystal size as compared to all other ceramics in this study. Crystal size of BCPA was smaller than that of BCPC, while the amount of micropores in BCPD was lower than the amount of micropores in BCPA and BCPC.

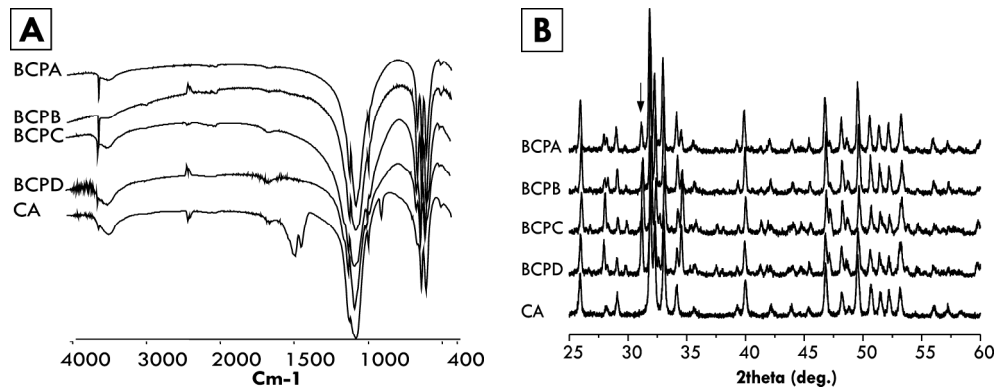


**Figure 1:** FTIR spectra (A) and XRD patterns (B) of BCPA, BCPB, BCPC, BCPD and CA ceramic.

Arrow = main  $\beta$ -TCP peak in BCP ceramics.

Figure 4 exhibits the macro- and microporosities of the ceramics prior to implantation, expressed as differential mercury intrusion as a function of pore size. The diameter of most macropores of BCPA, BCPB and BCPD was around 400  $\mu\text{m}$ , while macropores of CA had a slightly smaller average diameter. Average diameter of BCPC macropores was lower as compared to the other four ceramics.

Both image analysis of ESEM photographs and mercury porosimetry measurements indicated that, prior to implantation, macroporosities of all ceramics were similar,  $58 \pm 5$  %. Most micropores of all five ceramics had a diameter of around 1  $\mu\text{m}$ . In addition, CA ceramic possessed a high amount of micropores with a very small diameter of around 0.1  $\mu\text{m}$ .



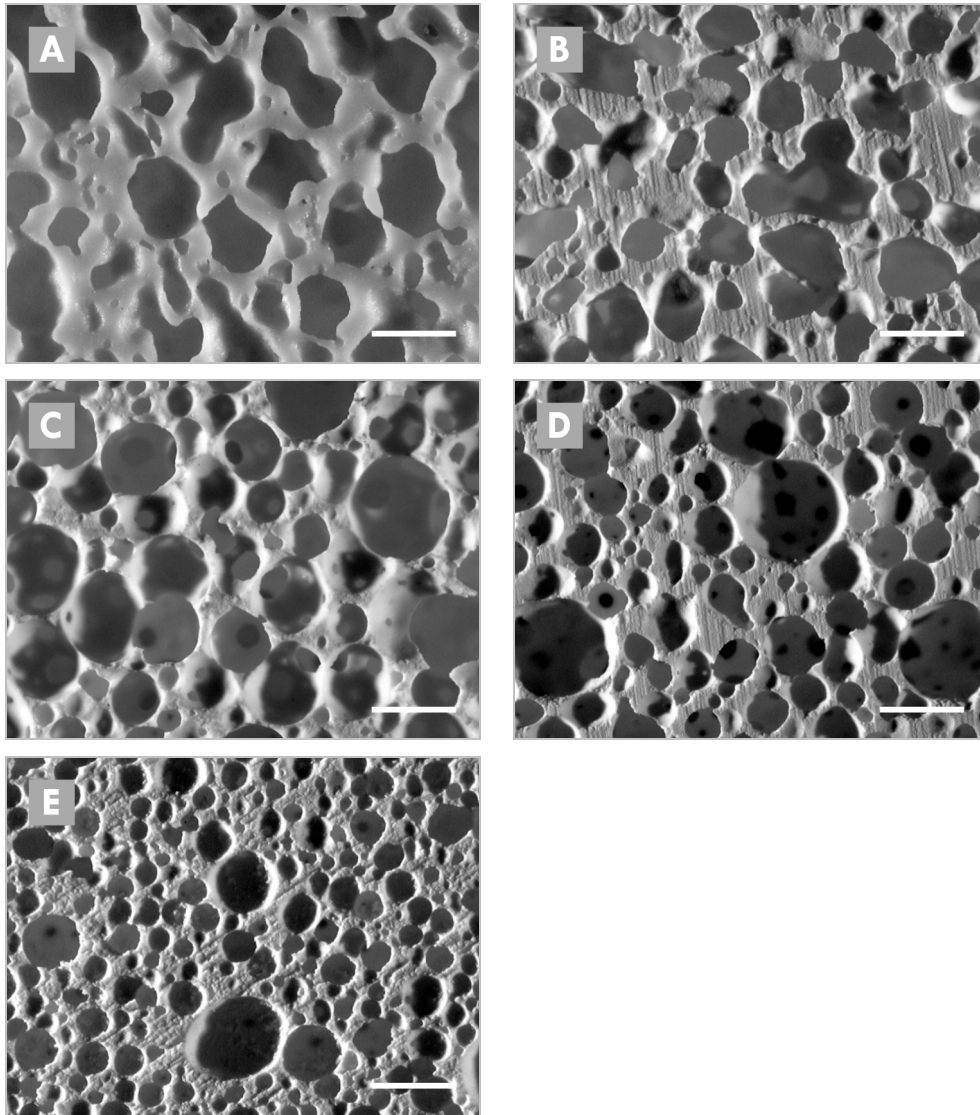


**Figure 2:** LM photographs (magnification 4x) of BCPA (A), BCPB (B), BCPC (C), BCPD (D) and CA (E) ceramic.  
Bar = 1mm.

Microporosities of BCPA, BCPB, BCPC, BCPD and CA were circa 17%, 4%, 24%, 10% and 20% respectively. Total porosities of BCPA, BCPB, BCPC, BCPD and CA were  $75\pm 5\%$ ,  $70\pm 5\%$ ,  $75\pm 5\%$ ,  $75\pm 5\%$  and  $80\pm 5\%$  respectively, as measured by mercury

porosimetry. Data on macro- and microporosity and crystal size can be summarized in specific surface area (SSA) which allows for the comparison of these, slightly different, ceramics. SSAs of the five ceramics were: BCPA ca.  $1.0 \text{ m}^2/\text{g}$ , BCPB ca.  $0.2 \text{ m}^2/\text{g}$ , BCPC ca.  $1.4 \text{ m}^2/\text{g}$ , BCPD ca.  $0.8 \text{ m}^2/\text{g}$  and CA ca.  $9.7 \text{ m}^2/\text{g}$ .

Table 2 gives an overview of material characterization of the investigated ceramics.

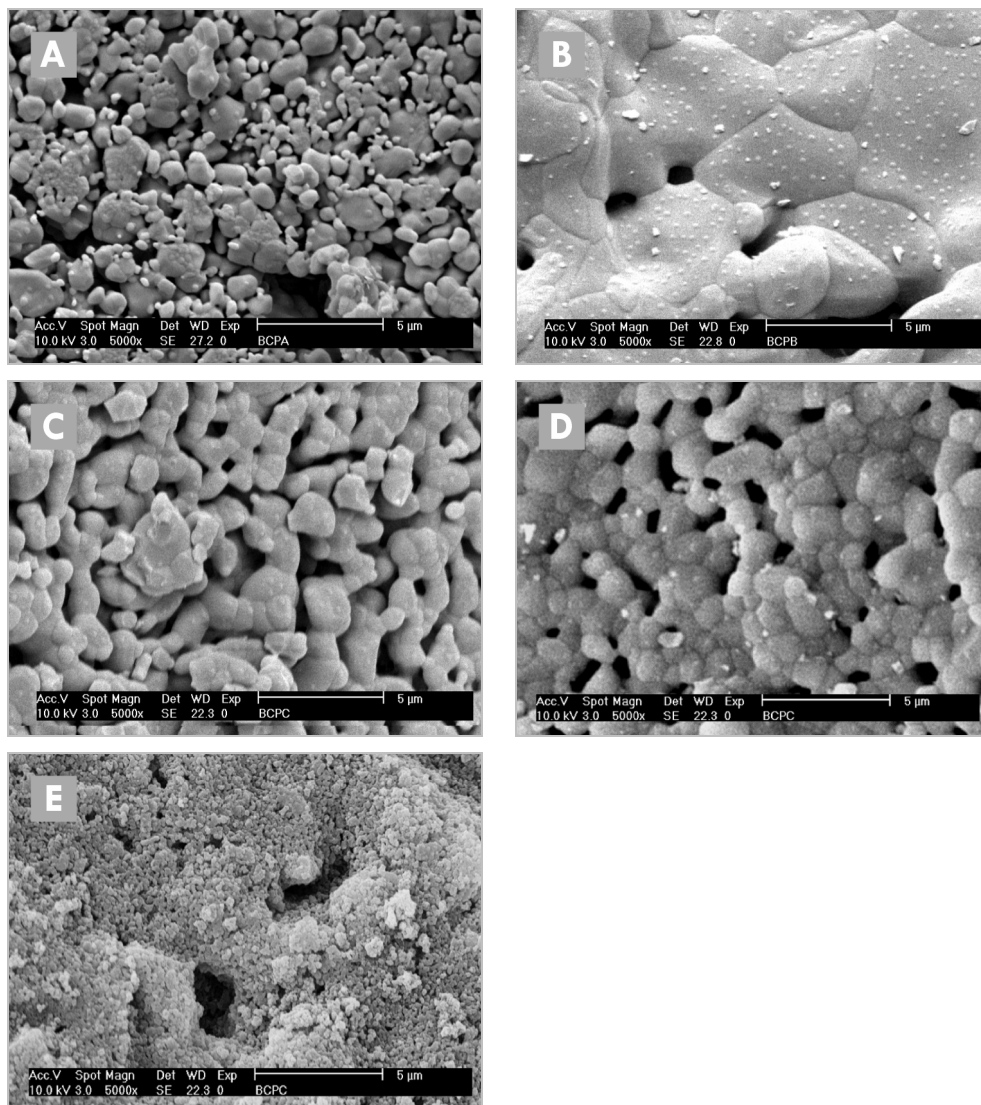


**Figure 3:** ESEM photographs (magnification 5000x) of BCPA (A), BCPB (B), BCPC (C), BCPD (D) and CA (E) ceramic.

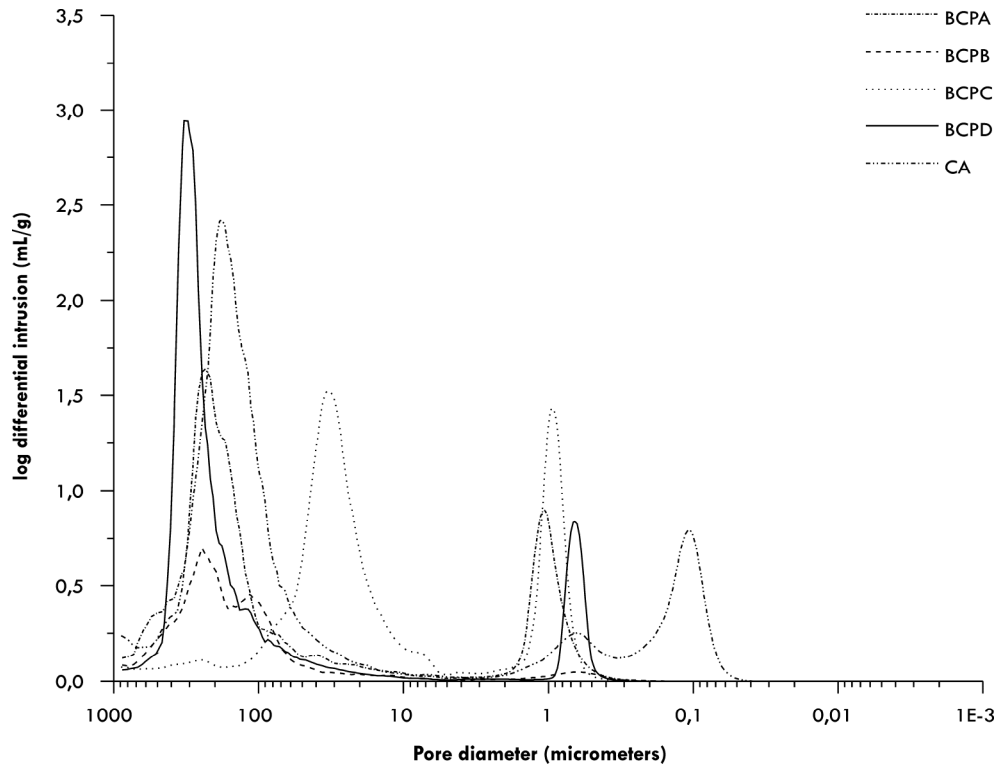


Figure 4: summary of macro- and microporosities and pore size distribution of BCPA, BCPB, BCPC, BCPD and CA ceramic.

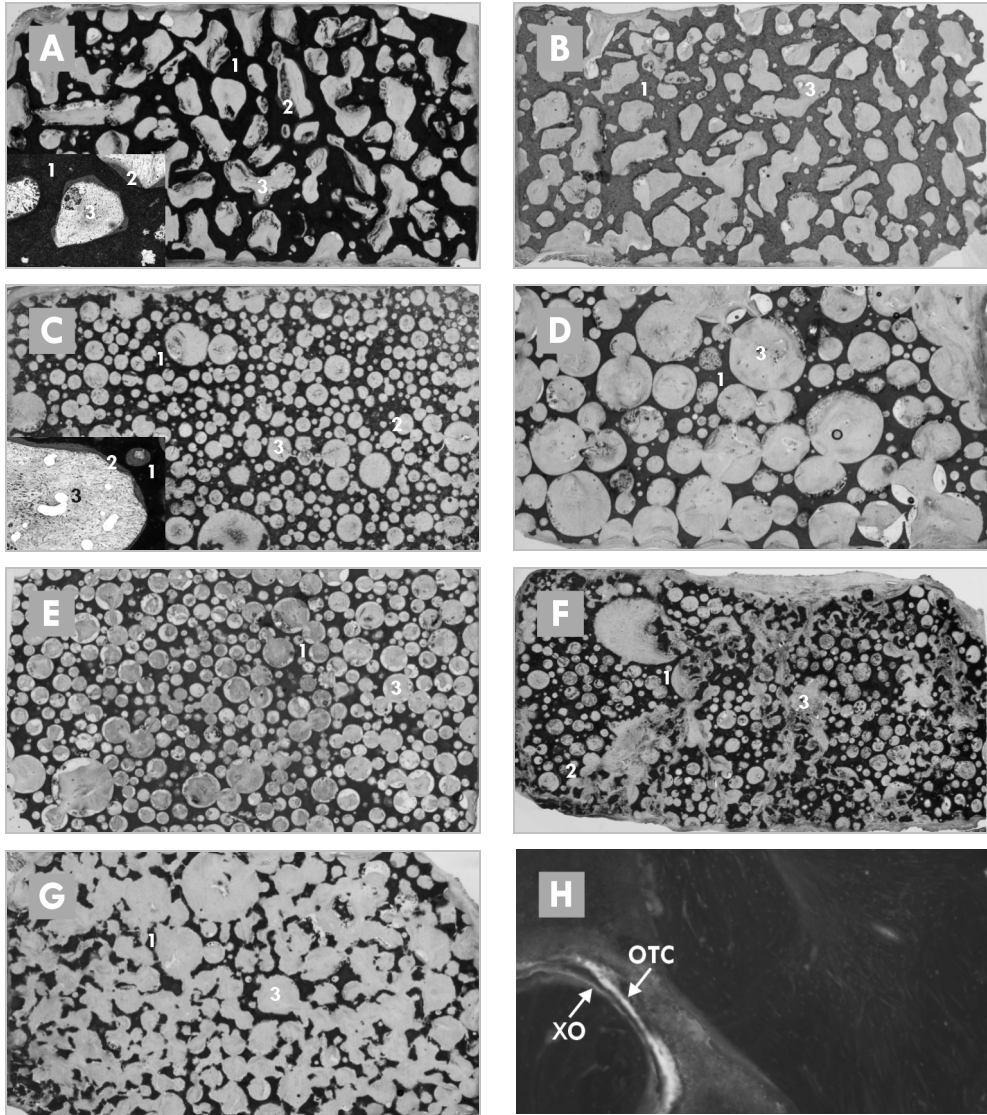
Table 2: summary of chemical compositions, macroporosities, specific surface areas and bone incidence of the investigated ceramics.

Implant	Chemical composition	Macro-porosity (vol.%)	Micro-porosity (vol.%)	S.S.A. (m <sup>2</sup> /g)	Bone incidence IM	Bone incidence SC
<b>BCPA</b>	HA/ $\beta$ TCP	58 $\pm$ 5	17	1.0	9/10	N/A
<b>BCPAh</b>	80wt%/20wt%				7/10	0/10
<b>BCPB</b>	HA/ $\beta$ TCP	58 $\pm$ 5	4	0.2	0/10	N/A
<b>BCPBh</b>	80wt%/20wt%				0/10	0/10
<b>BCPC</b>	HA/ $\beta$ TCP	58 $\pm$ 5	24	1.4	6/10	N/A
	70wt%/30wt%					
<b>BCPD</b>	HA/ $\beta$ TCP	58 $\pm$ 5	10	0.8	0/10	N/A
	70wt%/30wt%					
<b>CA</b>	HA with 8wt% CO <sub>3</sub> <sup>2-</sup> (type B)	58 $\pm$ 5	20	9.7	0/10	N/A

### 5.4.2 Intramuscular implantation

#### 5.4.2.1 Comparison of the materials

There were no surgical complications and all implants were retrieved. At retrieval, all implants were surrounded by well-vascularized muscle tissue.



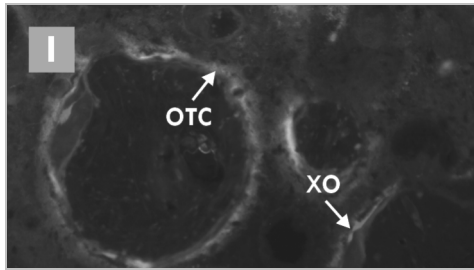


**Figure 5:** digital photograph of histological slides of intramuscularly implanted BCPA (A) (inset = LM photograph magnification 10x), BCPB (B), BCPC (C) (inset = LM photograph magnification 10x), BCPD (D), CA (E), BCPC (F), CA (G) and fluorochrome markers of BCPA (H) and BCPC (I).

(1) = ceramic, (2) = bone, (3) = fibrous tissue, OTC = Oxytetracycline, XO = Xylenol orange.

The induced bone in BCPA and BCPC (A and C respectively) is formed in the pores of the implants, aligning their surface. The bone is normal in appearance, aligned with osteoblasts and with osteocytes and osteoid clearly visible (insets of A and C). BCPB, BCPD and CA ceramics (B, D and E respectively) are extensively filled with fibrous tissue, but no signs of bone formation are observed. In some animals, BCPC ceramic was fragmented and mechanical degradation was observed. Note bone formation only in the non-fragmented part of the implant (F). In some animals, chemical dissolution of CA ceramic was observed (G). Presence of both Oxytetracycline and Xylenol orange marker shows that the bone formation in both BCPA and BCPC (H and I respectively) had started before the sixth week of implantation. → p218/219.

Histology showed no evidence for toxicity of the implants, or an unwanted inflammatory tissue response.

Bone was formed intramuscularly in 9 out of 10 goats in BCPA implants and in 6 out of 10 goats in BCPC implants, while no signs of bone formation were found in BCPB, BCPD and CA implants (table 2). Figures 5a-5e show photographs of the histological slides of the five implanted ceramics. In BCPA and BCPC ceramics, bone was formed in the pores of the implants, aligning the ceramic surface, and was never observed on implant peripheries. The newly formed bone was normal in appearance, aligned with osteoblasts and with osteocytes clearly visible. BCPB, BCPD and CA ceramics were fully infiltrated by fibrous tissue, however, no signs of bone formation were observed.

An interesting observation from the histological slides was the material degradation behavior. As illustrated in figure 5f, in some animals, BCPC exhibited partial fragmentation and delamination of the particles. Interestingly, in these implants bone was only induced in the part of the implant that was not fragmented (left on the photograph). In addition, in some animals, we observed the loss of structure, probably due to chemical degradation of the CA ceramic (figure 5g).

Analyses of the fluorochrome markers confirmed that the bone growth generally started on the surface of the ceramics and continued towards the pore center. For both BCPA (figure 5h) and BCPC (figure 5i) in some animals, both 6-week Oxytetracycline and 8-week Xylenol orange marker could be found, which suggested the start of new bone formation before the 6<sup>th</sup> week of implantation. In other animals, only the Xylenol orange marker was found, which suggests differences in the onset of bone formation between individual goats.

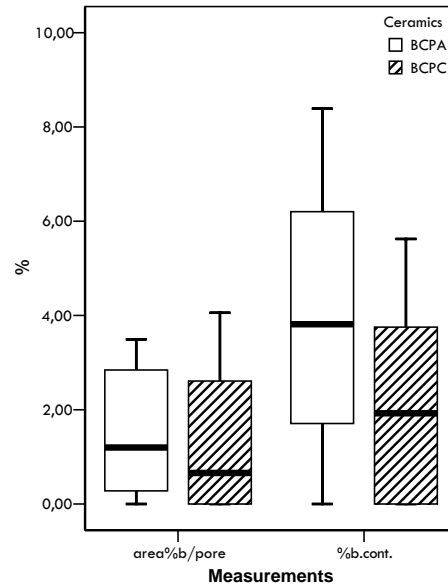


**Figure 6:** histomorphometrical results: boxplots (mean and interquartile values) of area%b/pore and %b.cont. of intramuscularly implanted BCPA and BCPC ceramics.

For both, bone area-related parameter (area%b/pore) and bone contact parameter (%b.cont.) BCPA performed better than BCPC, but the difference was only significant ( $p=0.011$ ) for %b.cont.

The amount of induced bone largely differed between individual goats, for both BCPA and BCPC. For example, percentage of bone occupying available pore area (area%b/pore) in BCPA varied between 0.3% and 3.5%, with an average of  $1.4 \pm 1.5\%$ . area%b/pore in BCPC varied between 0.7% and 4.1%, with an average of  $1.2 \pm 1.3\%$ . Similar to this, area related parameter, percentage of available scaffold

outline in contact with bone (%b.cont.) varied largely between individual goats: %b.cont. in BCPA varied between 1.6% and 8.7% with an average of  $3.9\pm 3.5\%$ ; %b.cont. of BCPC varied between 1.9% and 5.6% with an average of  $2.0\pm 2.0\%$ . Histomorphometrical data are summarized in a boxplot (figure 6). Although for both measured parameters BCPA showed a higher value than BCPC, significant difference between the two was only found for %b.cont ( $p=0.011$ ). Despite large differences in the amount of induced bone between individual goats, an intra-animal consistency was observed. This means that if a relatively large amount of bone was induced by BCPA in goat no.1, in this goat, BCPC induced a large amount of bone as well. And further, if BCPA induced very little bone in goat no.3, in this goat bone was not induced at all by BCPC. Thus, in all goats BCPA induced more bone than BCPC, however, there were “more” and “less” inductive goats, and the effect of inter-animal variations was visible for both BCPA and BCPC.

#### 5.4.2.2 Influence of implant size

In order to investigate the influence of implant size on the amount of induced bone, we compared implants with the size  $\varnothing 6.5 \times 10 \text{ mm}^3$  (BCPA and BCPB) with the implants with the same diameter, but with half of the length (BCPAh and BCPBh). As already mentioned, BCPA with the full length induced bone in 9 out of 10 animals (table 2). Bone incidence in BCPAh was 7 out of 10 (table 2). In both, large and small implants, the quality of the formed bone was similar. Qualitative analyses of the fluorochrome markers (photographs not shown) showed the presence of both 6-week Oxytetracycline and 8-week Xylenol orange label in some BCPA implants, while only the Xylenol orange label was observed in BCPAh implants, suggesting an earlier start of bone formation in the larger implants.

Histomorphometrical data for both measured parameters, percentage of bone occupying available pore area (area%b/pore) and percentage of available scaffold outline in contact with bone (%b.cont.) showed a higher value for BCPA in comparison to

BCPAh, however, this difference was only significant ( $p=0.017$ ) for area%b/pore (figure 7).

Neither BCPB nor BCPBh induced bone in any of the animals.

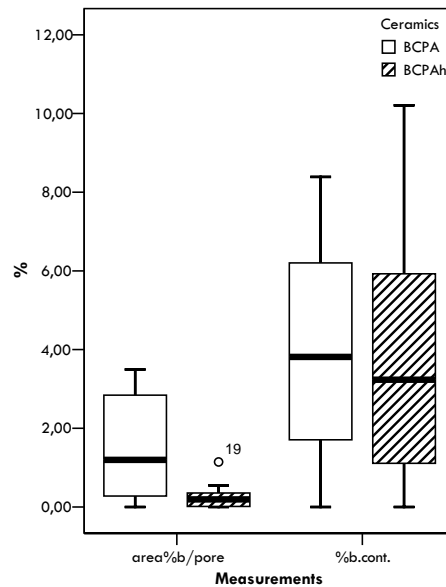


**Figure 7:** histomorphometrical results: boxplots (mean and interquartile values) of area%b/pore and %b. between intramuscularly implanted BCPA and BCPAh ceramics.

(o) = outliers.

For both, bone area-related parameter (area%b/pore) and bone contact parameter (%b.cont.) BCPA implant ( $\varnothing 6.5 \times 10 \text{ mm}^3$ ) showed more bone than a similar, but smaller ( $\varnothing 6.5 \times 5 \text{ mm}^3$ ) implant (BCPAh), however the difference was only significant ( $p=0.017$ ) for area%b/pore.

### 5.4.2.3 Implantation site dependence

BCPAh and BCPBh implants were implanted both intramuscularly and subcutaneously. As mentioned before, bone incidence in intramuscularly implanted BCPAh was 7 out of 10 (table 2), while no bone was observed in any of the subcutaneously implanted BCPAh ceramics. No bone formation was observed in either intramuscularly or subcutaneously implanted BCPBh ceramics.



### 5.4.3 Diffusion chamber study

In order to investigate changes on the surfaces of the ceramics *in vivo*, we subcutaneously implanted BCPA and BCPB ceramics inside diffusion chambers which allowed the diffusion of macromolecules and ions into the chamber but blocked the invasion of host cells and tissues. Diffusion chambers containing BCPA ceramic and BCPB ceramic respectively were implanted for 1, 2 and 4 weeks. Qualitative observation of the two materials after implantation and removal from the chambers showed the macroscopical presence of a glassy layer on the implant surfaces. FTIR spectra of the ceramics after implantation (figure 8) exhibited some changes as compared to the spectra before implantation. Already one week after implantation of BCPA, new small carbonate bands (C-O in  $\text{CO}_3^{2-}$ ) appeared at  $1448\text{ cm}^{-1}$  and  $1475\text{ cm}^{-1}$ , indicating the formation of the AB-carbonated apatitic phase. Additionally, new, more distinct bands appeared at  $1458\text{ cm}^{-1}$  and  $1546\text{ cm}^{-1}$ , which correspond to N-H vibrations and a small band at  $2960\text{ cm}^{-1}$  corresponding to C-H aliphatic vibrations. The appearance of these bands suggested the presence of organic compounds (proteins, peptides) on the surface of the BCPA ceramic. 2 and 4 weeks after implantation the above described bands looked even more pronounced in the BCPA FTIR spectrum.

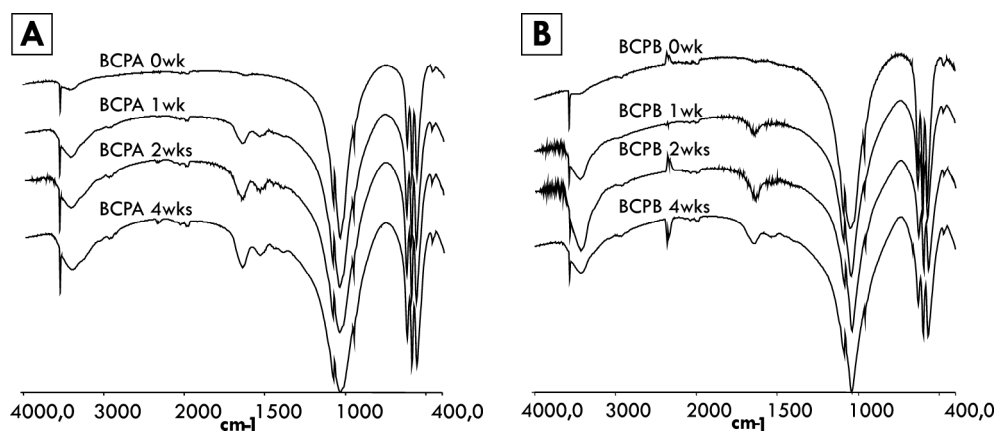
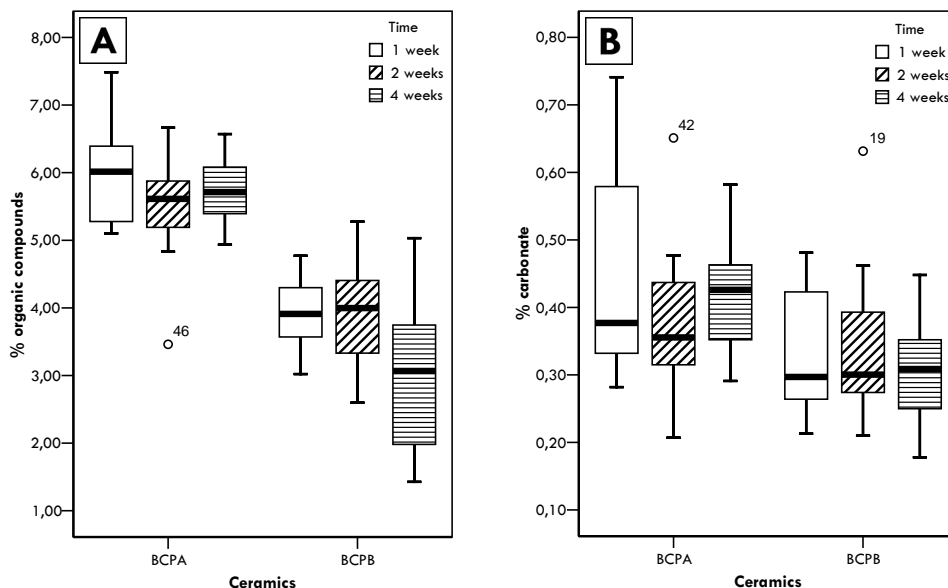


Figure 8: FTIR spectra of BCPA (A) and BCPB (B) implanted subcutaneously inside diffusion chambers for 1, 2 and 4 weeks.

Changes in the FTIR spectrum of BCPB after implantation were similar to those of BCPA ceramic. However, the newly appeared bands looked somewhat smaller on BCPB than on BCPA spectra. There were no noticeable differences between the XRD patterns of the two ceramics made before and after subcutaneous implantation in diffusion chambers (XRD patterns not shown).



**Figure 9:** TGA analysis: boxplots (mean and interquartile values) of %organic compounds (A) and carbonate (B) in subcutaneously implanted BCPA and BCPB ceramic inside diffusion chambers for 1, 2 and 4 weeks.

(o) = outliers.

The amount of both organic compounds and carbonate was significantly higher in BCPA than in BCPB at all implantation time points. No significant difference between the time points was observed for neither of the measured compounds.

TGA analyses of the two ceramics after implantation were performed in a temperature range 30°C – 900 °C. The weight loss observed between  $\pm 200$  °C and  $\pm 540$  °C was attributed to organic compounds, while the weight loss between  $\pm 540$  °C and  $\pm 900$  °C was associated with the presence of carbonate. TGA analysis of the BCPA and BCPB ceramics prior to implantation proved the absence of both organic compounds and carbonate in the initial ceramics. Quantitative data of the TGA analyses are

summarized in figure 9. At all three time points, i.e. 1, 2 and 4 weeks of implantation, a significantly higher (in all cases  $p < 0.01$ ) amount of organic compounds was found on BCPA ceramic surface as compared to the BCPB surface. The amount of carbonate on the surfaces of the ceramics was much smaller than the amount of organic compounds, but also in this case, the carbonate amount on the BCPA surface was significantly higher ( $p = 0.015$  for 1 week,  $p = 0.009$  for 2 weeks and  $p = 0.019$  for 4 weeks of implantation) than that on BCPB surface. No significant differences were observed in the amounts of organic compounds and carbonate between the three time points, for either of the investigated ceramics.

## 5.5 Discussion

Osteoinduction by CaP containing biomaterials in various forms, as well as by materials that initially do not contain CaPs has been shown in various reports in the last decade [116-122, 124-130, 134-136, 181, 183, 209] However, so far, little is known about the exact mechanism of the phenomenon underlying osteoinduction. The results of this study add to the knowledge of parameters which influence material osteoinductive properties.

The first goal of this study was to further investigate the influence of physico-chemical and structural properties of a material on its osteoinductive potential. We compared five CaP ceramics, four of which were BCPs. Although produced from powders with a similar chemical composition, these four ceramics had quite different final properties. As previously described, BCPA and BCPB, with the same chemical composition and macrostructure, differed only in their microstructures due to differences in the temperatures they were sintered at [181]: BCPA had a highly porous microstructure, while hardly any micropores could be found in the macropore walls of BCPB. A consequence of the different microstructures was that the specific surface area of BCPA was about 5 times higher than that of BCPB. After implantation, BCPA induced bone in almost all animals. In contrast, no bone was found in any of the implanted BCPB ceramics. In agreement with previous studies, these findings suggest that below a certain

level of specific surface area, bone will not be induced. Therefore, a “high” specific surface area seems to be of essential importance for osteoinduction by biomaterials.

BCPC and BCPD were produced from the same powder, but using different techniques. They had the same chemical composition, and similar macroporosities, but different microporosities. Although both microporous, the amount of micropores found in BCPC was higher as compared to BCPD. In addition, crystal size of BCPC was smaller than that of BCPD. Similar to the BCPA and BCPB ceramics, a consequence of more micropores and smaller crystal size was an around 2 times higher specific surface area of BCPC than that of BCPD. After implantation, BCPC induced bone in 7 out of 10 animals, while no bone was observed in any of the BCPD implants. Similar to the comparison of BCPA and BCPB, also in this case, an increased specific surface area positively influenced osteoinductive potential of the ceramic.

The comparison of the two osteoinductive ceramics in this study, namely BCPA and BCPC, is slightly more complicated. BCPC contained 10% more  $\beta$ -TCP than BCPA. In addition, the specific surface area of BCPC was around 1.5 times higher than that of BCPA. Both the higher amount of the more soluble component  $\beta$ -TCP and a higher specific surface area obviously increase the surface reactivity of a material, which should, as previously proposed [183], improve its osteoinductive properties. This was, however, not the case in the present study. Besides a lower bone incidence in BCPC, the amount of bone induced in BCPC was lower than the amount found in BCPA. Further differences between these two ceramics, which could possibly explain these unexpected results, are found in their macrostructures. Although both highly macroporous, most macropores of BCPA had a diameter of around 400  $\mu\text{m}$ , while most macropores of BCPC had an average diameter smaller than 100  $\mu\text{m}$ . As recently reviewed by Karageorgiou and Kaplan [217], based on early studies, the minimum requirement for pore size is considered to be  $\pm 100 \mu\text{m}$  due to cell size, migration requirements and nutrient transport [218]. However, pore sizes higher than 300  $\mu\text{m}$  are recommended due to i.e. formation of capillaries. Although these recommendations were based on processes of bone formation which take place orthotopically, it is conceivable that they are also applicable for the process of osteoinduction. It is thus possible, that although the higher surface reactivity of BCPC was preferable for osteoinduction according to

the earlier hypothesized mechanism [183], BCPA's larger macropores were responsible for better nutrient and cell distribution and capillary formation throughout the implant. Nutrient and cell distribution and consequent capillary formation should precede the process of ectopic bone formation and if they are insufficient, this process may be delayed and its result decreased. Furthermore, BCPC ceramic, as is shown in the results paragraph, partially fragmented after implantation in some of the animals. This resulted in the formation of loose particles and debris, and in the loss of macroporous structure. Investigation of histological slides showed that in the fragmented parts of the implant, no bone could be found. This observation could be explained by the fact that in order to facilitate growth of the induced bone, a mechanically stable surface is needed. Micromotion caused by debris and loose particles may negatively influence the bone growth facilitation.

The CA ceramic had a specific surface area which was significantly higher than that of any of the other ceramics used in this study. Furthermore, its chemical composition, which closely resembles that of bone mineral, was different from that of the four BCPs, which makes the comparison more challenging. Although we retrieved all implanted materials, histological slides showed a significant dissolution of the CA ceramic in some animals. This observation suggests that there is a limit in the increase of the specific surface area of the material that positively influences its osteoinductive properties. In the case of CA ceramic, chemical composition and a very high specific surface area might be the reasons for a too high surface reactivity, which leads to an extensive degradation of the material before the bone formation has started. Therefore, although the induction of differentiation towards osteoblasts might have taken place, bone formation could not be facilitated.

In short, the results from the part of the study in which the influence of physico-chemical and structural properties on osteoinduction was investigated showed that on the one hand, bone is not induced below a certain low level of specific surface area and on the other hand, bone formation, although possibly initiated, does not take place above a certain high level of specific surface area due to a fast resorption. These findings suggest that for each material type there is an optimal specific surface area which leads to maximal osteoinduction, if any. In addition, results of this study emphasized previous observations that the right macrostructure (i.e. macropore size,

interconnectivity), which leads to an adequate nutrient and cell supply and vascularization, is of great importance in the process of osteoinduction by biomaterials. Finally, a mechanically stable surface is needed for facilitation of initiated bone formation.

Results of the implant size investigation showed that bone incidence in BCPA implants with the size  $\varnothing 6.5 \times 10 \text{ mm}^3$  was higher than in similar implants with half the length ( $\varnothing 6.5 \times 5 \text{ mm}^3$ ). Histomorphometrical measurements further confirmed that the relative amount of bone in available pore area was relatively higher in bigger than in smaller implants. The observed implant size influence could be explained by the fact that, in comparison to smaller implants, larger implants have a larger periphery surface which allows for more migration of cells and nutrients inside the implant. Furthermore, there is possibly more micromotion in the smaller implants as compared to the larger ones, which could negatively influence the process of attachment, proliferation and differentiation of the cells in the centre of the implant. This implant-size dependence might be, in addition to the well known inter-species genetic and metabolic differences, one of the reasons that explains lack of osteoinduction by biomaterials in rodents, in which obviously only small implants can be inserted.

Comparison of implantation sites showed that intramuscularly implanted BCPA induced bone, while no bone was found in any of the subcutaneously implanted BCPA ceramics, which is possibly due to a better vascularization intramuscularly. These results contrast the findings of Gosain et.al. [124], in which authors compared intramuscular and subcutaneous osteoinduction in sheep after 1 year of implantation, and could not find any significant differences between the two sites. Although a similar type of comparison is made, our study in goats and Gosain et.al.'s study in sheep differed in osteoinductive materials used, implantation time, and most importantly, animal model. Our observation that subcutis was a less inductive implantation site than muscle was however in accordance with the finding of Yang et.al. [143]. Although this study lacked histomorphometrical data, the authors observed a delayed osteoinduction in subcutaneously implanted materials as compared to intramuscularly implanted materials in both pigs and dogs. The observations of the latter study suggest that there might be a difference in "osteoinductive potential" between subcutis and muscle, which is conceivable as it is generally accepted that intramuscularly, there is more

vascularization than subcutaneously. However, the difference between the two sites might only be visible during the early time of implantation. It is plausible that, after a certain implantation time the ectopically induced bone stops growing and starts resorbing as it lacks natural mechanical stimulation. The process of bone resorption occurs earlier intramuscularly than subcutaneously, as the bone formation intramuscularly takes place earlier as well. It is therefore possible that, after 1 year of implantation as in Gosain et.al's study, difference in the amount of bone between subcutaneously and intramuscularly implanted materials is not visible anymore, while in our 3-month-study, this difference was clearly observed.

As mentioned previously, osteoinduction by biomaterials shows large interspecies differences. Bone is hardly ever induced in rats and mice [116, 141-144], is rarely found in rabbits and very frequently in large mammals (i.e. goats, sheep, dogs) and non-human primates such as baboons [117, 124, 129, 130, 143, 219, 220]. However, there is also a difference in osteoinductive potentials between different large animals. The same material implanted intramuscularly in goats and dogs induced more bone in dogs [143]. Similarly, a material implanted in dogs and baboons induced more bone in baboons [117]. To our knowledge, direct comparisons between sheep and goats in the same study have not been made. Comparisons between our study in goats and the studies in sheep are hard to make, as, in addition to the difference in the materials used to study osteoinduction, the implantation time of Gosain et.al.'s study was 1 year and Le Nihouanned et.al.'s [130] study 6 months while implantation time of our study was 3 months. Besides, in the study by Le Nihouanned et.al., the volume of implanted ceramic was around 6 times higher than the volume of the present study, and this, as showed above, might be of importance for the amount of induced bone. When comparing studies on osteoinduction by biomaterials, it is therefore important to take into account that, in addition to the animal model and material used, implantation time, implantation site and the amount of implanted material may be of great importance for the amount of induced bone.

Implantation of osteoinductive and non-osteoinductive ceramic inside diffusion chambers was meant to investigate changes on the material surface, without interference with cells and tissues. Implantation periods of 1, 2 and 4 weeks were chosen because, in this model, ectopic bone formation starts before the sixth week of implantation, as is shown

by the fluorochrome markers. The results of FTIR and TGA analyses on the materials explanted and removed from the diffusion chambers support the hypothesis that in the process of osteoinduction, surface reactivity plays a role. It is proposed that on the surface of the material, a dissolution-reprecipitation process takes place, which is accompanied by coprecipitation of relevant endogenous factors such as cytokines or proteins [183]. On a material with a higher specific surface area, this process of induction is faster and more prominent. The results from the present study indeed show that, during the implantation, more carbonate and more organic compounds were found on the surface of the osteoinductive BCPA ceramic as compared to the non-osteoinductive BCPB ceramic. Whether this process is essential for the osteoinductivity of a material needs to be further proven. However, these results give a direct relationship between specific surface area and the material interaction with its *in vivo* environment. The next step in the finding the mechanism of osteoinduction would be to investigate which organic compounds are present on the material surface, and what their role is in the induction of ectopic bone formation.

## **5.6 Conclusion**

The results of the present study showed that for each material type there is an optimal specific surface area at which the osteoinductive potential of the material is highest. This study further showed that the decrease of the implant size significantly decreases the relative amount of induced bone. In addition, in the model used in this study, the same material induced bone intramuscularly but not subcutaneously, which suggests the importance of vascularization in the process of osteoinduction by biomaterials.

## **5.7 Acknowledgements**

Authors would like to thank Dr. Edwin Martens from the Biostatistics Department of the University Utrecht for his generous help with the statistical analyses. This study was financially supported by the EU "IntelliScaf" Project (G5RD-CT-2002-00697).



## Chapter 6

### Biological performance of uncoated and octacalcium phosphate coated Ti6Al4V

Pamela Habibovic<sup>1</sup>, Jiaping Li<sup>1</sup>, Chantal M. van der Valk<sup>2</sup>, Gert Meijer<sup>3</sup>,  
Pierre Layrolle<sup>4</sup>, Clemens A. van Blitterswijk<sup>1</sup> and Klaas de Groot<sup>1</sup>

<sup>1</sup>University of Twente, Institute for Biomedical Technology,

Professor Bronkhorstlaan 10D, 3723 MB, Bilthoven, The Netherlands

<sup>2</sup>IsoTis SA, Professor Bronkhorstlaan 10-D, Bilthoven, 3720 MB, The Netherlands

<sup>3</sup>University Medical Center Utrecht, PO Box 85500, Utrecht, 3508 GA, The Netherlands

<sup>4</sup>INSERM EM9903, Materials of Biological Interest, Faculty of Dental Surgery, Place Alexis Ricordeau, Nantes, 44042, France

#### 6.1 Abstract

The in vivo behavior of a porous Ti6Al4V material that was produced by a positive replica technique, with and without an octacalcium phosphate (OCP) coating, has been studied both in the back muscle and femur of goats. Macro- and microporous biphasic calcium phosphate (BCP) ceramic, known to be both osteoconductive and able to induce ectopic bone formation, was used for comparison purpose.

The three groups of materials (Ti6Al4V, OCP Ti6Al4V and BCP) were implanted transcortically and intramuscularly for 6 and 12 weeks in 10 adult Dutch milk goats in order to study their osteointegration and osteoinductive potential.

In femoral defects, both OCP Ti6Al4V and BCP were performing better than the uncoated Ti6Al4V, at both time points. BCP showed a higher bone amount than OCP Ti6Al4V after 6 weeks of implantation, while after 12 weeks, this difference was no longer significant.

Ectopic bone formation was found in both OCP Ti6Al4V and BCP implants after 6 and 12 weeks. The quantity of ectopically formed bone was limited as was the amount of animals in which the bone was observed. Ectopic bone formation was not found in uncoated titanium alloy implants, suggesting that the presence of calcium phosphate (CaP) is important for bone induction.

This study showed that CaPs in form of coating on metal implants or in form of bulk ceramic have a significantly positive effect on the bone healing process.

Keywords: porous Ti6Al4V, biomimetic coatings, octacalcium phosphate (OCP), biphasic calcium phosphate (BCP), osteointegration, osteoinduction.

## 6.2 Introduction

Calcium phosphate (CaP) containing biomaterials, in particular hydroxyapatite (HA), beta tricalcium phosphate ( $\beta$ -TCP), and the mixtures of two, are known for having a good biological performance [17, 221-224], but they often lack satisfactory mechanical properties.

Metals, on the other hand, possess great mechanical properties, making them suitable for load-bearing applications [37]. However, high stiffness of the metals often leads to stress-shielding from residual bone, which may result in detrimental resorptive bone remodeling [38], and consequently to a poor fixation of the implant. Recent developments in metallic implant designs therefore focus on adapting the mechanical properties of metals to those of biological systems. Certain metals, such as stainless steel, titanium and its alloys are already widely used in orthopaedics and dentistry because of their good biocompatibility [35, 36], but their ability to bond to bone and to guide bone growth are distinctly smaller as compared to the above mentioned ceramics.

Recent designs of orthopaedic implants therefore often include combinations of metallic and CaP materials. One example is the application of CaP coating on metal implants that combines the mechanical strength of the metal with the ceramics favorable biological properties. In addition to the interfacial bonding to bone introduced by CaP

coatings on dense metal implants, applying a porous structure can even further advance bony integration, whereby mechanical interlocking may also enhance the integration process.

Porous titanium and its alloys have been used in dental and orthopaedic applications since the end of 1960s [225-227]. Many available methods of producing porous titanium and titanium alloy scaffolds include sintering together of the particles [228, 229] or plasma spraying of the powder on a dense substrate followed by the cutting of the porous layer [135]. The shortcoming of these production methods is that they often result in a low porosity (< 50%), low average pore size (< 300  $\mu\text{m}$ ) and poorly interconnected pores. All these factors might have a negative effect on the biologic performance of these materials. Another method includes compacting single titanium fiber into a die to certain porosity, followed by vacuum sintering, resulting in the formation of a so-called titanium fiber mesh [135]. Besides excellent biocompatibility [230], sintered titanium fiber meshes have been shown to act as a good carrier for growth factors [231, 232] and as tissue engineering scaffold [233, 234]. However, in absence of the growth factors and/or osteogenic cells, their osteoconductive performance is limited. In addition to titanium and its alloys, promising reports on the use of porous metals based on tantalum (Ta) for orthopaedic applications have been given [235-237].

Our group has recently developed a porous Ti alloy material by using a positive replica technique. This technique allows us to produce a controllable high porosity structure, with open and interconnected pores [193].

As mentioned earlier, apart from the mechanical interlocking provided by implant porosity, applying a bioactive coating on the metal surface could further enhance its biological performance. The conventional technique to provide metallic implants with a CaP coating is plasma-spraying (PS). Earlier investigations have shown that these coatings can successfully enhance clinical success to a <2% failure rate after 10 years [42]. Despite this clinical performance, the PS method is limited by some intrinsic drawbacks. For instance, the coating is being produced at very high temperatures, limiting this method to stable CaP phases. Furthermore, by using this line-of-sight method, it is impossible to coat geometrically complex and porous implants.

One of the alternative methods uses the so-called biomimetic route, in which the bone mineralization process is mimicked by immersing implants in simulated body fluids (SBF) [190]. As a result of the parapsychological conditions of this technique, various CaP phases such as octacalcium-phosphate (OCP) [191] or bone-mineral like carbonated apatite (CA) [192] can be deposited. A previous study in femoral condyle of goats by Barrère et.al. [132] showed a direct contact between the newly formed bone and the OCP coated porous Ta surface. Between the newly formed bone and uncoated Ta however, a layer of fibrous tissue was often observed. Intramuscular implantation of the OCP coated porous Ta implants also showed the ability of such an implant to induce bone in non-osseous site, i.e. osteoinductive behavior [132, 133, 140].

The objective of this goat study was to investigate the biological performance of a porous titanium alloy (Ti6Al4V) material, produced by a positive replica method, with and without biomimetic OCP coating, in terms of osteointegration and osteoinduction.

## **6.3 Materials and methods**

### **6.3.1 Implants**

Porous titanium alloy (Ti6Al4V) implants were produced by a positive replica method as described earlier [193]. In short, 70 wt% of titanium alloy powder (Northwest Non-Ferrous Institute of China) consisting of spherical particles with a diameter lower than 44  $\mu\text{m}$  (325 mesh) was mixed with H<sub>2</sub>O (20 wt%). Polyethylene glycol (PEG) and Methylcellulose were used as binders (8 wt%). Dolapix and ammonia solution (2 wt%) were added to improve the rheological property of slurry. Porous titanium alloy bodies were made by impregnation of polymeric (PU) sponges (35-45 pores/in) (Coligen Europe B.V., Breda, The Netherlands). When the slurry reached the designed viscosity range (3000-5000 cp), Polyurethane (PU) foams were dipped into the slurry and then extracted to dry. The dipping-drying process was repeated until the struts of the PU foam were coated with titanium alloy slurry. The superfluous slurry was removed by using a roller under pressure, to get an evenly distributed coating on the foam. After final drying, the samples were heated in argon to 500°C to burn out the foam. This

process resulted in a small change of color of the metal, which suggests the formation of a thicker titanium oxide (TiO<sub>2</sub>) layer. Finally, the metal bodies were sintered in a vacuum furnace (10<sup>-5</sup> mbar) at 1250°C with holding time of 2h. The Energy Dispersive X-Ray (EDX) analysis (result not presented) showed a higher oxygen peak in comparison to the green body, confirming the formation of a thicker TiO<sub>2</sub> layer. Cylinders (∅5 x 10 mm<sup>3</sup>) were machined by using a wire electric discharge machine, with demineralized water as medium. The ultrastructure of porous titanium alloy was characterized by using an environmental scanning electron microscope (ESEM; XL30, ESEM-FEG, Philips, The Netherlands) in the secondary electron mode. The porosity of the material was determined by both volume/weight method (n=3) and by image analysis technique on the histological slides (10 cross-sections for 6-week- and 10 cross-sections for 12-week implantation). In the volume/weight method the following calculation is made: 100% - [(weight of the porous implant/ the weight a dense implant with the same size)\*100%]. For the second method, high resolution (300dpi), low magnification (10x) digital micrographs were made of blinded sections. Using Adobe Photoshop 7.0, bone and material were pseudocoloured, red and green respectively. Image analysis was carried out with a PC-based system equipped with KS400 version 3.0 software (Carl Zeiss Vision, Oberkochen, Germany). Prior to measurement the system was geometrically calibrated with an image of a block of known dimensions. A program was developed in KS400 to quantitate the pore size for each pore and the material porosity. The porosity was determined as: [total implant surface - (scaffold surface + bone surface) / total implant surface] \* 100%. Pore interconnectivity was visually analyzed on the material cross-sections by using an ESEM. The compression strength of the material was 10.3 ± 3.1 MPa, as measured and reported earlier [193].

Porous Biphasic Calcium Phosphate (BCP) implants were prepared by using the so-called H<sub>2</sub>O<sub>2</sub> method as published earlier [129]. For the preparation of the ceramic, in-house made BCP powder was used. Porous green bodies were produced by mixing this powder with 2% H<sub>2</sub>O<sub>2</sub> solution (1.0 g powder / 1.2 ± 0.05 ml solution) and naphthalene (Fluka Chemie, The Netherlands) particles (710 - 1400 μm; 100 g powder/ 30 g particles) at 60°C. The naphthalene was then evaporated at 80°C and the green porous bodies were dried. Finally, the bodies were sintered at 1200°C for 8

h. These bodies were machined into cylinders ( $\varnothing 5 \times 10\text{mm}^3$ ) using a lathe. The structure of porous BCP was characterized by using an ESEM. Porosity, pore size and pore interconnectivity were analyzed by the same techniques as described for the Ti alloy implants. Material composition and its crystal structure were determined by using Fourier Transform Infra Red Spectroscopy (FTIR; Spectrum100, Perkin Elmer Analytical Instruments, Norwalk, CT) and X-Ray Diffraction (XRD; Miniflex, Rigaku, Japan). HA/ $\beta$ -TCP weight ratio in the BCP was calculated by comparing the BCP XRD pattern to the calibration patterns prepared from the powders with the known HA/ $\beta$ -TCP weight ratios. The specific surface area of the material was measured by using the Brunauer, Emmett and Teller method (BET, cfDIN66131) (Institut des matériaux de Nantes L.C.S., Nantes, France). The compression strength of the used BCP was  $3.4 \pm 0.8$  MPa [unpublished results].

### 6.3.2 Coating process

Prior to the coating process, porous Ti alloy cylinders were ultrasonically cleaned in acetone, ethanol and water, subsequently. Next, they were soaked in Simulated Body Fluid (SBF) for 24h at 37°C to seed the metal surface with calcium phosphate nuclei. The used SBF solution was 5 times more concentrated than Kokubo's SBF solution [190] (table 1) in order to speed up the coating process. The supersaturation of the SBF solution was achieved by addition of slightly acidic gas CO<sub>2</sub>. The starting pH of the solution was 5.8. At the end of the process, the pH reached a value of 8.3.

In order to produce crystalline OCP coatings, the implants were then immersed at 37°C in Simulated Calcifying Solution (SCS) (table 1) for 48 h with one replenishment. SCS was buffered at pH 7.4 by using the TRIS/HCl. The biomimetic methods of producing the two CaP layers have previously been described in detail [191, 192]. The coating composition and crystallinity were investigated by using FTIR and XRD. Coating thickness was measured on 2D implant cross-sections by the automatic ESEM ruler. The specific surface area of the coating was determined by using the BET method.

**Table 1:** inorganic composition (mM) of Kokubo's SBF, supersaturated SBFx5 and SCS.

	<b>Ion concentration (mM)</b>							
	$Na^+$	$K^+$	$Ca^{2+}$	$Mg^{2+}$	$Cl^-$	$HPO_4^{2-}$	$HCO_3^-$	$SO_4^{2-}$
<b>SBF</b>	142.0	5.0	2.5	1.5	148.8	1.0	4.2	0.5
<b>SBFx5</b>	714.8	--	12.5	7.5	723.8	5.0	21.0	--
<b>SCS</b>	140.4	--	3.1	--	142.9	1.86	--	--

### 6.3.3 Animals

This study was approved by the Dutch Animal Care and Use Committee. Ten adult Dutch milk goats were used in total and housed at Central Animal Laboratory Institute (GDL), Utrecht, The Netherlands, at least 4 weeks prior to surgery.

Before the surgical procedure, a dose of 0.1 ml in 5ml of physiologic saline solution ( $\pm$  1 ml/25 kg body weight) of Domosedan (Pfizer Animal Health BV, Capelle a/d IJssel, The Netherlands) was administered by intravenous injection. The surgical procedure itself was performed under general inhalation anesthesia of the animals. Thiopental (Nesdonal,  $\pm$  400 mg/70 kg of body weight, on indication, Rhone Merieux, Amstelveen, The Netherlands) was injected intravenously, and anesthesia was maintained with a gas mixture of nitrous oxide, oxygen and Halothane (ICI-Farma, Rotterdam, The Netherlands).

Besides the implantations described in this study, the animals were used for a different study, to be published separately. Based on the previous in vivo studies by our group, we hypothesize that different groups of implants could not influence each other's behavior, as they were implanted either at a different implantation site or at a sufficient distance from each other.

### 6.3.4 Orthotopic implantation

The implants were inserted in the left diaphyseal femur of the goats, which was exposed by a lateral skin incision and blunt dissection. The holes were drilled in the lateral cortex using a pneumatically powered orthopaedic drill (drilling speed 150

rpm), under permanent cooling with saline. Each defect was created according to a four-step procedure, to a final diameter of 5.0 mm.

The implants (uncoated Ti6Al4V, OCP Ti6Al4V and BCP) were allocated according to randomized scheme. Using gentle tapping, the implants were press-fit inserted in their designated positions. The incision was routinely closed with sutures. After 6 weeks, the same procedure was repeated in the right diaphyseal femur of all goats. Table 2 gives an overview of the implanted materials.

Table 2: implantation scheme.

Time (weeks)	Femoral diaphysis			Back muscle		
	Ti6Al4V	OCP Ti6Al4V	BCP	Ti6Al4V	OCP Ti6Al4V	BCP
6	10	10	10	10	10	10
12	10	10	10	10	10	10

### 6.3.5 Intramuscular implantation

After shaving the lumbar area and disinfection with iodine, the left muscle fascia was exposed and cut. Using blunt dissection, intramuscular pockets were created, and filled with the above-mentioned implants. Subsequently, the fascia was closed with a nonresorbable suture to facilitate implant localization at explantation. The skin was closed in two layers. After 6 weeks, the same procedure was repeated in the right back muscle. Table 2 shows the amounts of implanted materials.

Immediately after the surgery, pain relief was given by buprenofine (Temgesic; Schering-Plough, Kenilworth, NJ).

12 weeks after the first implantation (i.e. implantation times 6 and 12 weeks), each animal was sacrificed by an overdose of pentobarbital (Euthesaat, Organon, Oss, The Netherlands) and potassium chloride.



### 6.3.6 Retrieval of the implants, histology and histomorphometry

The implants from the retrieved femora were isolated “en block” using a diamond saw, and fixed at 4°C in Karnovsky’s fixative (4% paraformaldehyde, 5% glutaraldehyde). Intramuscular implants with surrounding tissue were explanted by sharp dissection and fixed in Karnovsky’s fixative as well. All implants were dehydrated in a graded ethanol series (70%-100%) and transferred into a methylmethacrylate (MMA) solution that polymerized at 37°C within one week. Longitudinal sections (10-15µm) were made by using the modified interlocked diamond saw (Leica Microtome, Nussloch, Germany). Sections were stained with 1% methylene blue and 0.3% basic fuchsin after etching with HCl/ethanol mixture. The midsections of the implants retrieved from femora were used for histomorphometry. In case of intramuscular implants, only qualitative analysis using a light microscope (E600 Nikon, Japan) was performed.

For histomorphometry of femora implants, high resolution (300dpi), low magnification (10x) digital micrographs were made of blinded sections. Using Adobe Photoshop 7.0, bone and material were pseudocoloured, red and green respectively. Image analysis was carried out with a PC-based system equipped with KS400 version 3.0 software (Carl Zeiss Vision, Oberkochen, Germany). Prior to measurement the system was geometrically calibrated with an image of a block of known dimensions. A program was developed in KS400 to quantitate different parameters concerning bone formation:

- %b.cont. in cortex: percentage of available scaffold outline (which is the surface of the scaffold) in contact to bone: [%contact = (bone-scaffold contact length / scaffold outline length) \* 100%] within the cortical area (area C in figure 1);
- %b.cont. in implant: percentage of available scaffold outline in contact to bone: [%contact = (bone-scaffold contact length / scaffold outline length) \* 100%] in the total implant area (area B in figure 1);
- %b.cont. in outer zone: percentage of available scaffold outline in contact to bone: [%contact = (bone-scaffold contact length / scaffold outline length) \* 100%] in an outer zone of cortical area that is defined as the area of the

implant within the cortical area with a thickness of 350  $\mu\text{m}$  measured from the edges of the implant (area E in figure 1);

- %b.cont. in inner zone: percentage of available scaffold outline in contact to bone: [%contact = (bone-scaffold contact length / scaffold outline length) \* 100%] in the inner zone, that is defined as the area of implant in the total cortical area and excludes the outer zone E (area D in figure 1);
- %b.cont. bone marrow: percentage of available scaffold outline in contact to bone: [%contact = (bone-scaffold contact length / scaffold outline length) \* 100%] in the bone marrow area (area F in figure 1);
- %b. in cortex: the percentage of bone in available pore area within cortical area (area C in figure 1);
- %b. in implant: the percentage of bone in available pore area in the total implant area (area B in figure 1).

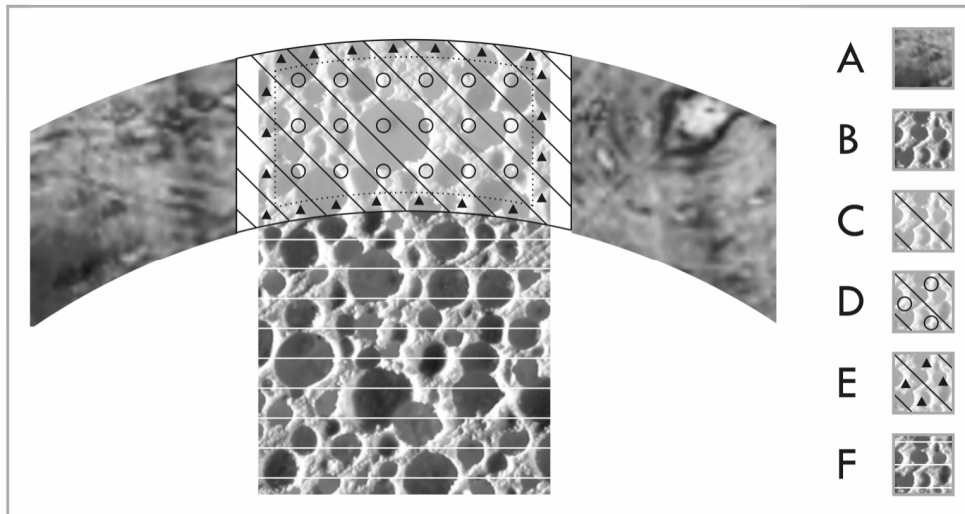


**Figure 1:** zones of histomorphometrical analysis: (A) host cortical bone, (B) total implant area; (C) cortical area, (D) inner zone of the cortical area, (E) outer zone of the cortical area and (F) bone marrow area.

We measured de novo bone formation in different areas of the formed defect in order to distinguish new bone formation in the cortical area, where the defect should be

healed from the part of the implant that was situated in the bone marrow. Furthermore, we distinguished the outer zone of the cortical area with a thickness of 350  $\mu\text{m}$ , from the inner zone (the rest of the implant) to get more insight into the osteoconductive properties of the materials.

### **6.3.7 Statistics**

Statistical calculations were done with the SPSS (Chicago, IL) 9.0 software. We found large variances between the individual animals and the data received were not normally distributed. That is why we chose the non-parametric tests to perform the statistical analysis. Friedman rank test, followed by a post-hoc test [206] was chosen to make the comparisons between the materials at both time points. Friedman test computes a Friedman two-way analysis of variance on selected variables. This test is a nonparametric extension of the paired t test, where, instead of two measures, each subject has n measures ( $n > 2$ ). In other terms, it is a nonparametric analog of repeated measures analyses of variance with one group. The Friedman test is often used for analyzing ranks of three or more objects by multiple judges or like in the case of this study, various materials implanted in all animals.

We used the Wilcoxon signed rank test [207] to analyze the difference in bone formation per material between the two time points. The Wilcoxon test compares the rank values of the selected variables, pair by pair, and displays the count of positive and negative differences. For ties, the average rank is assigned. It then computes the sum of ranks associated with positive differences and the sum of ranks associated with negative differences. The test statistic is the lesser of the two sums of ranks.

In both cases, the significance level was set at  $p=0.05$ . As can be seen from the descriptions above, the two used statistical tests are both based on ranks, instead of average or median values. However, the results of histomorphometry in this paper are presented in graphs with the average values with standard error of the mean (SEM), in order to make the results more recognizable and comparable with previous studies. And although the asterisks indicating the significant differences are illustrated on these graphs, they are based on the above-mentioned rank tests.

## 6.4 Results

### 6.4.1 Implant characterization

#### 6.4.1.1 Uncoated Ti6Al4V

As determined from the material cross-sections, and by the volume/weight method, the porosity of the Ti alloy implants was  $79\pm 5\%$  and the pore size between 400 and 1300  $\mu\text{m}$ . Observations by the ESEM showed that the pores of the implant were well interconnected. Figure 2a shows the structure of the non-coated porous Ti alloy. Higher magnification photograph (figure 2b) shows the rough metal surface, caused by the sintering of the alloy particles.

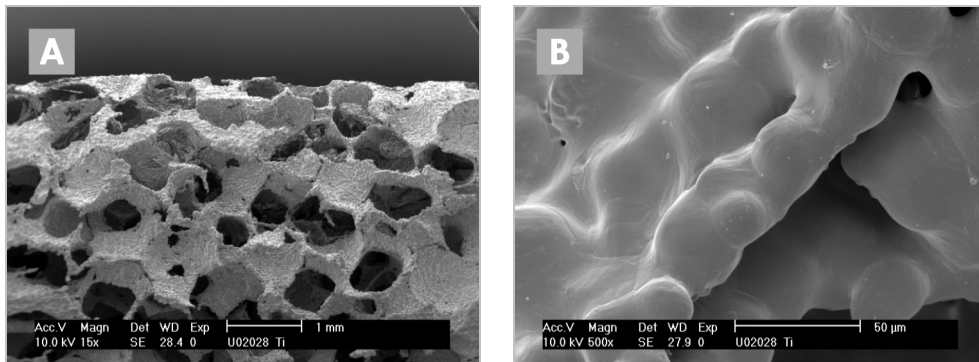


Figure 2: ESEM photographs of porous Ti6Al4V implant magnification 15x (A) and 500x (B).

#### 6.4.1.2 OCP coated Ti6Al4V

As observed by the ESEM, in the coated implants, the surface of the Ti alloy was homogeneously covered with a CaP layer. Figure 3a is a low magnification photograph of the coated Ti6Al4V implant. However, the thickness of the coating was not the same throughout the implant. It varied between 20  $\mu\text{m}$  at the interior of the implant and 60  $\mu\text{m}$  at the implant periphery. Large OCP crystals were oriented perpendicularly to the

surface of the metal. Figure 3b illustrates the crystalline structure of the coating. FTIR spectrum and XRD pattern (figures 4a and 4b, respectively) were typical of the pure, highly crystalline OCP phase. The specific surface area of the coating was  $7.2 \pm 0.1$  m<sup>2</sup>/g.

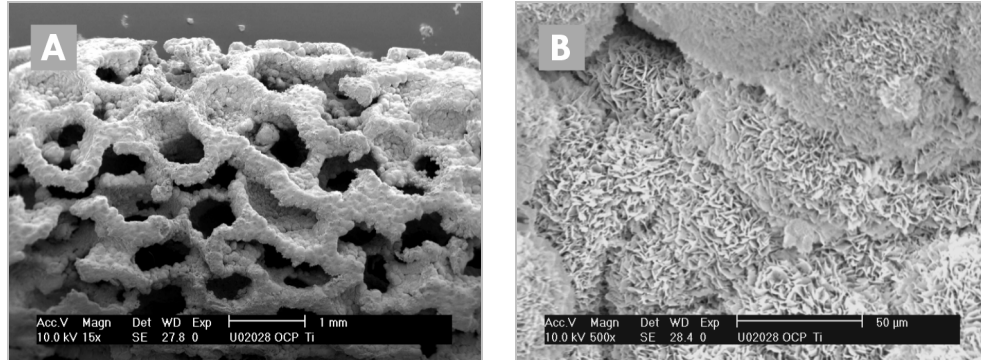


Figure 3: ESEM photographs of OCP coated porous Ti6Al4V implant magnification 15x (A) and 500x (B).

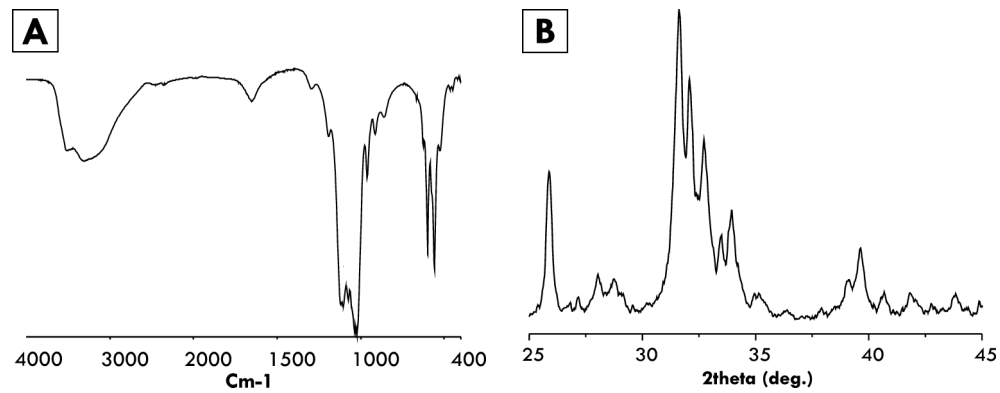


Figure 4: FTIR spectrum (A) and XRD pattern (B) of the OCP coating.

#### 6.4.1.3 BCP

As observed by the ESEM, BCP implants consisted of a well-interconnected macroporous structure, with a pore size varying between 100 and 800 μm. Histomorphometry on

cross-section and determination by the volume/weight method gave an average macroporosity of  $54\pm 4\%$ . Higher magnification ESEM analysis showed that macropore walls contained micropores (pore size  $< 10\mu\text{m}$ ). Figure 5a illustrates the macroporous structure of the BCP, while higher magnification photograph (figure 5b) shows its micropores. FTIR and XRD analysis of the produced material (figures 6a and 6b respectively) showed a biphasic chemistry consisting of  $\pm 88\text{ wt}\%$  HA and  $\pm 12\text{ wt}\%$   $\beta$ -TCP. The material was highly crystalline. The specific surface area of the ceramic was  $1.2\pm 0.1\text{ m}^2/\text{g}$ .

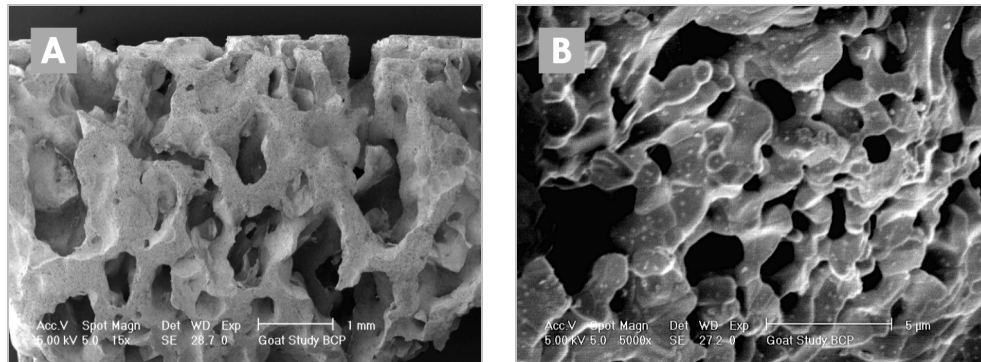


Figure 5: ESEM photographs of BCP implant magnification 15x (A) and 5000x (B).

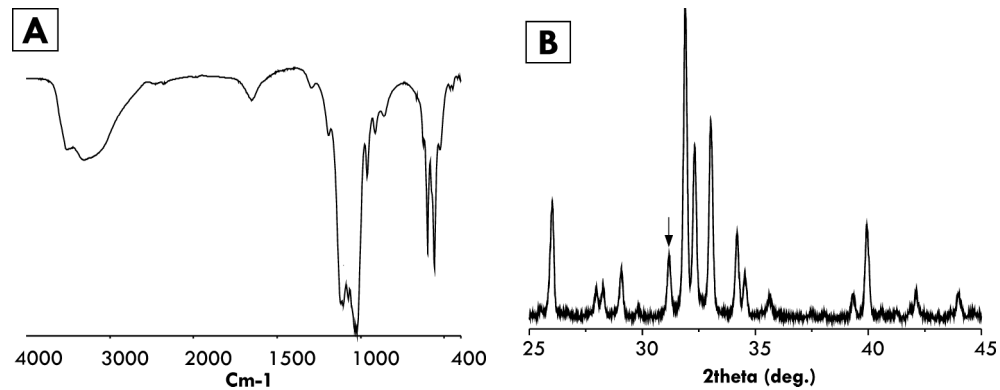


Figure 6: FTIR spectrum (A) and XRD pattern (B) of BCP ceramic.

Arrow indicates the main  $\beta$ -TCP peak in BCP.

## 6.4.2 Transcortical implantation

There were no surgical complications and all implants were retrieved. No macroscopic or microscopic signs of infection were found.

### 6.4.2.1 Comparison of the materials

As can be seen from the results shown in the figures 7a and 7b of the measurements in the total implant area, both OCP Ti6Al4V and BCP gave a significantly higher amount of bone as compared to the uncoated Ti6Al4V after 6 weeks of implantation, looking at both, %b.cont. in implant and %b. in implant. Furthermore, BCP performed significantly better than OCP Ti6Al4V after 6 weeks. After 12 weeks of implantation, the difference between Ti6Al4V and OCP Ti6Al4V and Ti6Al4V and BCP was still significant, while this was no longer the case for the difference between OCP Ti6Al4V and BCP.

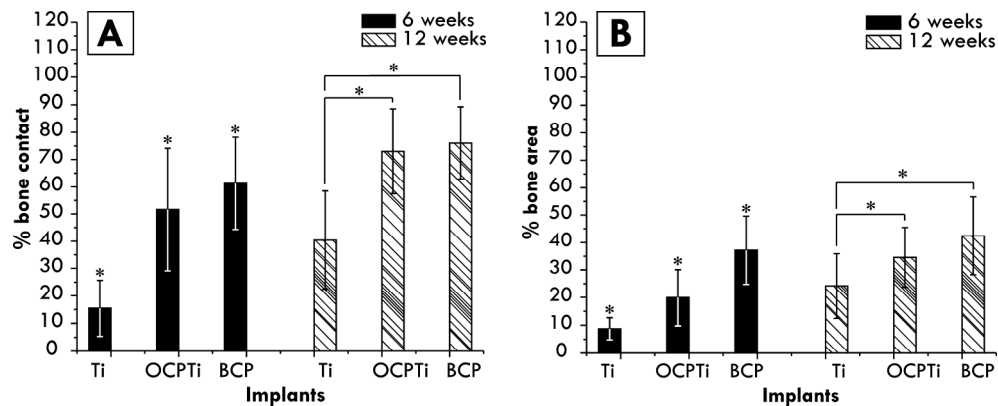


**Figure 7:** histomorphometrical results of the %b.cont. (A) and %b. (B) in total implant area.

For both parameters after 6 weeks significant difference ( $p < 0.001$  for %b.cont. and  $p = 0.001$  for %b.) can be found between OCP Ti6Al4V and Ti6Al4V, between BCP and Ti6Al4V and between BCP and OCP Ti6Al4V.

After 12 weeks, significant differences exist between OCP Ti6Al4V and Ti6Al4V and between BCP and Ti6Al4V for both parameters ( $p = 0.002$  for %b.cont. and  $p = 0.008$  for %b.).

According to the Wilcoxon test, significant difference between 6 and 12 weeks was found for the uncoated Ti6Al4V for both %b.cont. ( $p = 0.022$ ) and %b. (0.009) and for OCP Ti6Al4V only for parameter %b. ( $p = 0.005$ ).

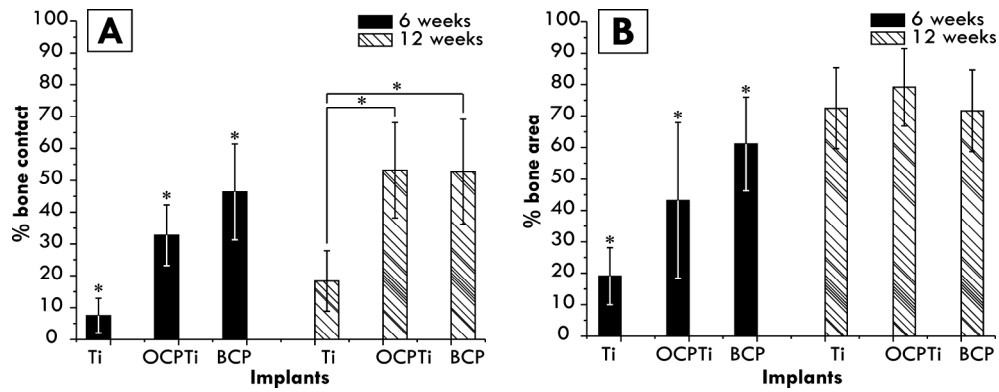


**Figure 8:** histomorphometrical results of the %b.cont. (A) and %b. (B) in the cortical area.

For parameter %b.cont, after both 6 ( $p < 0.001$ ) and 12 ( $p = 0.020$ ) weeks significant difference is found between OCP Ti6Al4V and Ti6Al4V and between BCP and Ti6Al4V. For the parameter %b., after 6 weeks significant difference ( $p = 0.002$ ) is found between OCP Ti6Al4V and Ti6Al4V, between BCP and Ti6Al4V and between BCP and OCP Ti6Al4V.

After 12 weeks, no significant differences ( $p = 0.273$ ) is found between different implants.

The Wilcoxon signed rank test showed significant difference between 6 and 12 weeks for the uncoated Ti6Al4V for both %b.cont. ( $p = 0.007$ ) and %b. ( $p = 0.005$ ). Similarly, for OCP Ti6Al4V there was a significant difference between 6 and 12 weeks in both %b.cont. ( $p = 0.017$ ) and %b. ( $p = 0.008$ ).

Figure 8a represents %b.cont. in cortex. After 6 weeks of implantation we can see that the differences between Ti6Al4V and OCP Ti6Al4V and Ti6Al4V and BCP are significant. However, there is no significant difference between OCP Ti6Al4V and BCP that was observed in the graph of the total implant area. Concerning the % b. in the available pore space of the cortical area (figure 8b), both OCP Ti6Al4V and BCP are significantly higher than the uncoated Ti6Al4V, and BCP is significantly higher than OCP Ti6Al4V after 6 weeks of implantation. After 12 weeks, however, there are no differences between the three kinds of implants. Figures 9 a, c and e illustrate an example of the bone ingrowth in the cortical area after 6 weeks of implantation in uncoated Ti6Al4V, OCP Ti6Al4V and BCP, respectively.



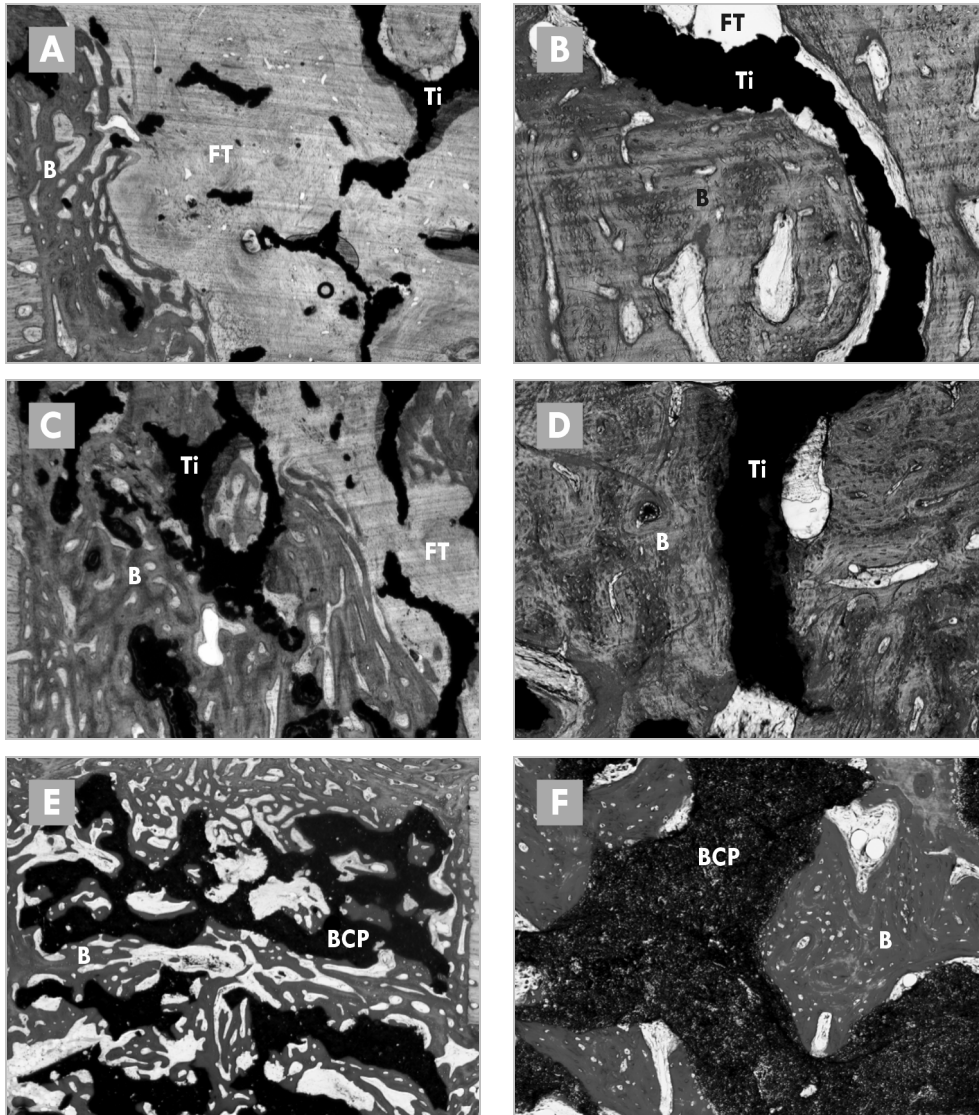


**Figure 9:** LM photographs of histological slides of uncoated Ti6Al4V after 6 weeks (magnification 2x) (A) and 12 weeks (magnification 10x) (B); OCP coated Ti6Al4V after 6 weeks (magnification 2x) (C) and 12 weeks (magnification 10x) (D) and BCP after 6 weeks (magnification 2x) (E) and 12 weeks (magnification 10x) (F) of transcortical implantation.

Ti=Ti6Al4V, B=bone, FT=fibrous tissue, BCP=ceramic.

More bone has grown in the OCP Ti6Al4V and BCP (A and C) implants in comparison to the uncoated Ti6Al4V implant (E). Similarly, there is more direct bone contact between the newly formed bone in OCP Ti6Al4V and BCP implants (B and D) in comparison with the uncoated Ti6Al4V implants (F). → p220.

In the case of uncoated Ti6Al4V (figure 9a) bone ingrowth starts from the host bone bed towards the implant. In the OCP Ti6Al4V implant (figure 9c), new bone had grown deeply into the center of the implant. Similarly, newly formed bone had bridged the formed defect within the BCP implant (figure 9e). From the analysis of the histology slides of the implants after 12 weeks of implantation by the light microscope, we observed a lower amount of bone as well as less direct bone contact in the uncoated Ti alloy implants in comparison to both OCP Ti6Al4V and BCP. Figure 9b is a high magnification of the uncoated Ti alloy after 12 weeks of implantation showing a poor direct contact between metal and bone. Figures 9d and 9f, illustrating OCP Ti6Al4V and BCP after 12 weeks of implantation respectively, show a direct contact between the bone and the material.

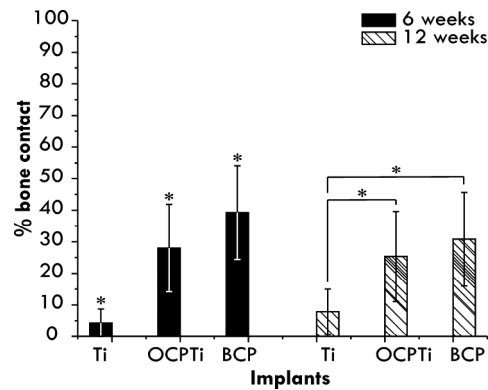


**Figure 10:** histomorphometrical results of the %b.cont. in bone marrow area.

After 6 weeks significant difference ( $p < 0.001$ ) is found between OCP Ti6Al4V and Ti6Al4V, between BCP and Ti6Al4V and between BCP and OCP Ti6Al4V. After 12 weeks ( $p = 0.001$ ), significant differences exist between OCP Ti6Al4V and Ti6Al4V and between BCP and Ti6Al4V. The Wilcoxon signed rank test did not show significant differences between 6 and 12 weeks for any of the implant groups.

When looking at the results illustrated by the figure 10, we can see significant differences in %b.cont. between Ti6Al4V and OCP Ti6Al4V and between Ti6Al4V and BCP at both time points.

Measurements of %b.cont. in inner and outer zone of the cortical area (not illustrated) showed a significantly higher %b.cont. in the outer zone than in the inner zone after 6 weeks of implantation for each kind of implant. After 12 weeks, however, this

difference could only be found for BCP. Differences between the individual materials in both zones were similar to the differences found in the total cortical area (see figure 8a), meaning that for both time points in both zones, OCP Ti6Al4V and BCP showed a significantly higher amount of bone contact than the uncoated Ti6Al4V, while there was no difference between BCP and OCP Ti6Al4V.

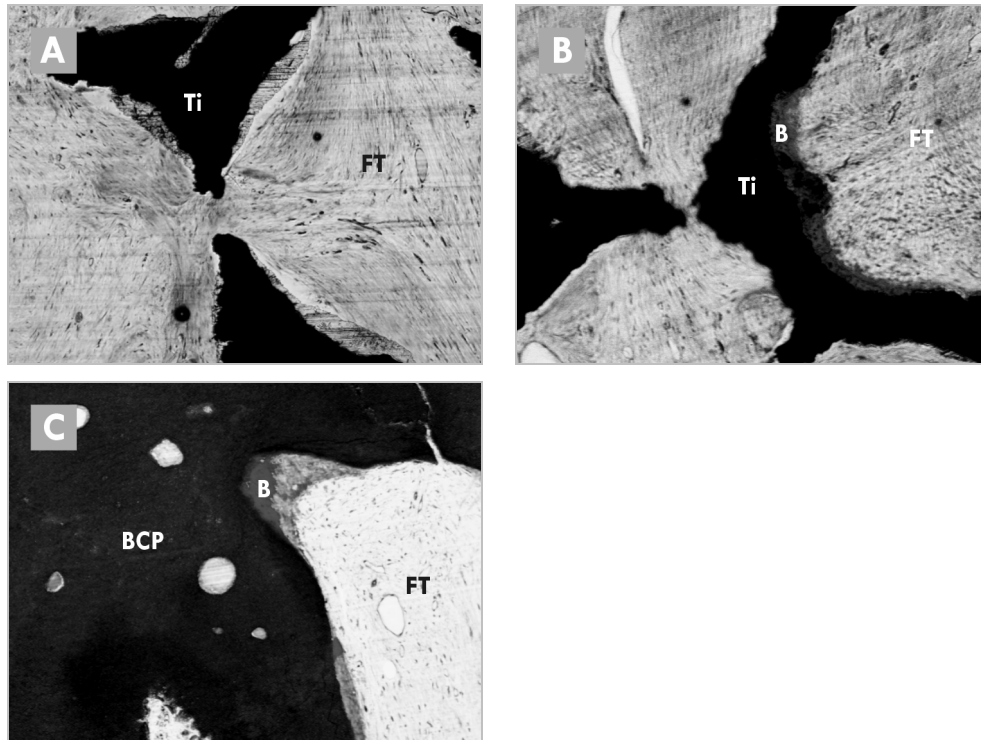


**Figure 11:** LM photographs of histological slides magnification 10x of uncoated Ti6Al4V (A), OCP coated Ti6Al4V (B) and BCP (C) after 12 weeks of intramuscular implantation.

Ti=Ti6Al4V, B=bone, FT=fibrous tissue, BCP=ceramic. → p221.

#### 6.4.2.2 Time dependence

The Wilcoxon test was used to statistically compare individual materials at the two time points. The test showed significant difference between 6 and 12 weeks of implantation for the uncoated Ti6Al4V in the parameters: %b.cont. in cortex, %b. cortex, %b.cont. in

implant, %b. in implant and %b.cont. in inner zone. Significant difference in the OCP Ti6Al4V was found in the parameters: %b.cont. in cortex, %b. in cortex, %b. in implant and %b.cont. in inner zone. No difference between 6 and 12 weeks of implantation in the BCP implants could be found for any of the measured parameters.

### 6.4.3 Intramuscular implantation

At retrieval, all implants were surrounded by well-vascularized muscle tissue. Histology showed no evidence for toxicity of the implants nor were the signs of an inflammatory tissue response specifically related to the implants observed.

As observed by light microscopy, uncoated Ti alloy implants did not induce bone in the soft tissue. The implants were, however, extensively filled with fibrous tissue, which is illustrated by figure 11a.

Both OCP coated Ti alloy and BCP (figure 11b and 11c), on the other hand, did show extraskeletal bone formation. Although bone was consistently observed, it occurred in small volumes only. Table 3 gives an overview of the bone incidence in time. In the case of both OCP Ti6Al4V and BCP, more goats showed bone formation after 12 weeks than after 6 weeks. Furthermore, although the bone areas were not measured, the LM analyses of the histological slides suggested an increased amount of formed bone after 12 weeks of implantation when compared to 6 weeks of implantation. The bone was never observed on the implant periphery, and was always found inside the pores. The formed bone was normal in appearance, aligned with osteoblasts, and with mineralized bone matrix and osteocytes clearly visible. In the case of OCP coated Ti alloy implants, the coating was often incorporated into the newly formed bone.

Observations of the histological slides of the coated Ti6Al4V implants by LM showed that the OCP coating had extensively dissolved after 6 weeks, and could only occasionally be observed after 12 weeks of implantation, in particular on the periphery of the implant, where the initial coating was the thickest. OCP coating has a typical crystalline structure that can easily be distinguished from bone on histological slides. The exact dissolution of the coating was however, not measured. Similar in vivo dissolution behavior of the OCP coating has previously been described [132]. Figures 12a and

12b are examples of dissolved OCP coating after 6 and 12 weeks of implantation respectively. In the areas where the coating was still visible, signs of its resorption by multinucleated cells could be observed, as shown in figure 12c. In vitro resorption of OCP coating has previously been shown by Leeuwenburgh et.al. [47].

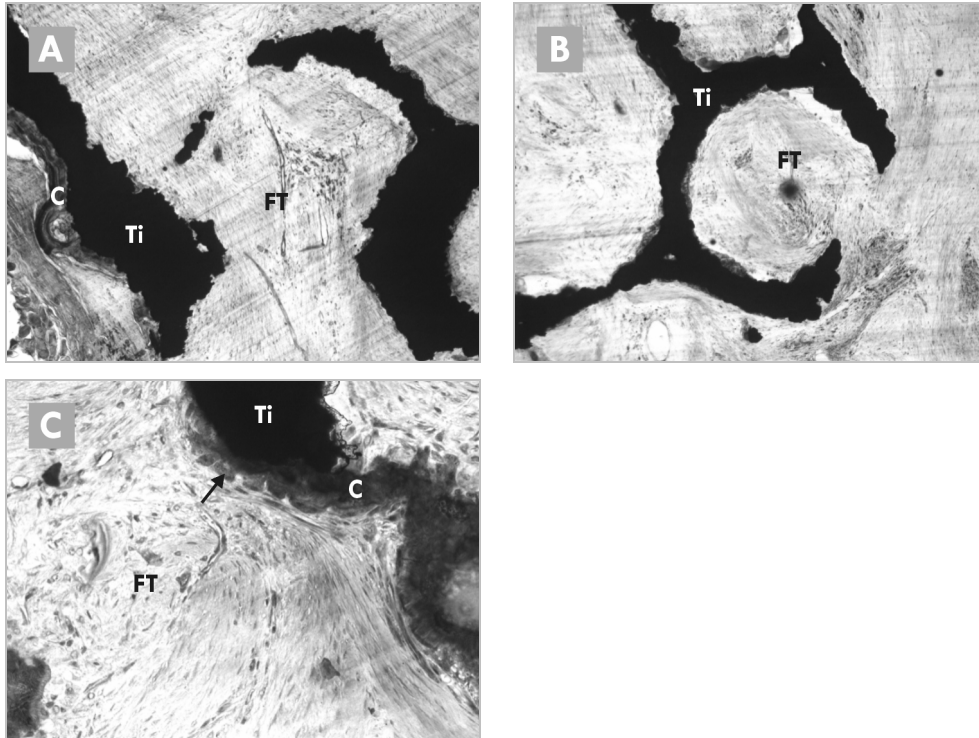


**Figure 12:** LM photographs of histological slides magnification 5x of the OCP Ti6Al4V after 6 weeks (A) and 12 weeks (B) of implantation, and magnification 20x after 6 weeks of implantation.

Ti=Ti6Al4V, B=bone, FT=fibrous tissue, C=OCP coating; BCP=ceramic.

In (A) there is still some coating present on the periphery of the implant after 6 weeks of implantation, in (B) after 12 weeks of implantation the coating is further degraded, in (C) multinucleated cells (see arrow) are resorbing the coating left after 6 weeks of implantation. → p222.

## 6.5 Discussion

In this goat study, we investigated the in vivo behavior of a porous Ti6Al4V material, produced by a positive replica method, uncoated and coated with a biomimetic OCP

coating, in ectopic and orthotopic locations. We chose BCP ceramic as a reference, because previous animal studies have shown that this material has a large osteoinductive potential [124, 129, 143, 220] and could possibly be good bone filler in the clinic [238].

We introduced a porous structure into all used implants in order to improve mechanical interlocking, and therewith also the bone integration process. However, because of different production techniques, the porosity and the average pore size varied between the metal and the ceramic implants.

As we did not find any signs of toxicity or deviating inflammation related to the implants, we can conclude that our novel material has an acceptable biocompatibility as bone filler. However, the ability of metal itself to guide new bone formation and to form a tight bond with the newly formed bone, i.e. its osteoconductivity [34] is limited. By modification of its surface chemistry and topography, through the application of a CaP coating, we tried to enhance its bioactivity.

Although BCP ceramic, with its high osteoinductive potential and good performance as a bone filler was a good positive control in this study, it is important to note that it had a lower porosity and average pore size than Ti6Al4V and OCP Ti6Al4V. The chemistry of the BCP, that is a mixture of HA and  $\beta$ -TCP, and the biomimetically produced OCP differed as well. Furthermore, due to the sintering process, BCP ceramic macropore walls consisted of micropores, increasing therewith the surface roughness. Such a microporosity was not present in the OCP coating. Nevertheless, OCP coating surface was rough as well, due to the large crystals that were perpendicularly oriented to the metal surface.

The above-mentioned material characteristics: chemical composition, macroporosity, crystallinity and surface roughness are all of great importance for the bone integration process. The release of calcium and phosphate ions is believed to be at the origin of the bioactivity of CaPs [171, 172, 210]. This dissolution is followed by the precipitation of a biological CaP layer [211]. In addition, organic compounds are incorporated into this newly formed layer, and cells like osteoprogenitor cells, osteoblasts and osteoclasts colonize the biomaterial [239, 240].

Transcortical implantation results of this study confirmed a well-known fact that the application of a CaP layer on a metal surface significantly increases its bioactivity.

Biomimetically produced OCP coating applied on our porous Ti6Al4V metal enhances its osteoconductive properties, while keeping its mechanical strength. Differences in the amount of newly formed bone between the coated and the uncoated Ti alloy implants were significant in the cortical area of the defect as well as in the bone marrow, suggesting a high osteoconductive potential of the OCP coating. We found a significant difference between Ti6Al4V and OCP Ti6Al4V after 12 weeks of implantation in the contact between the newly formed bone and the implant surface, but this difference could not be found in the amount of formed bone in the available pore area. In order to get a full overview of both osteoconductive properties of a material and defect healing process by the material, both histomorphometric methods should be used.

BCP as bulk ceramic caused a faster bone growth, when looking at both bone contact and bone area, in comparison to the OCP as coating on the metal implant. The BET measurements showed that OCP had a specific surface area that was about 5 times higher than that of BCP. Furthermore, the solubility isotherms of various CaPs show that OCP powder is slightly more soluble than  $\beta$ -TCP powder, and significantly more soluble than HA powder [212]. Both characteristics suggest a higher dissolution rate of OCP in comparison to the BCP that should be followed by a faster carbonated apatite formation of the material surface and consequently by a faster bone formation. However, as mentioned earlier, the OCP Ti6Al4V implants had a much higher porosity and pore size as compared with BCP. The lower porosity and average pore size of BCP might have been more suitable for bone ingrowth, possibly because of a better balance between a sufficient nutrient and blood supply into the implant on one hand and a protected area that is necessary to reach the supersaturation of  $\text{Ca}^{2+}$  and  $\text{PO}_4^{3-}$  ions, in order to initiate the formation of carbonated apatite layer on the other, in comparison to the OCP coated Ti6Al4V implant. This is a possible explanation of the observations from this study. However, due to the many differences in material chemistry and morphology between OCP and BCP, further investigations are needed to fully understand their effect on the bone ingrowth.

The difference in the bone amount formed in BCP and OCP Ti6Al4V disappeared after 12 weeks of implantation, which suggests that, on longer term, both CaP materials have the same effect on the bone integration process. This could be explained by the fact that, on longer term, surface of both materials is covered by a bone like carbonated

apatite layer, and that the effect of dissolution behavior of the initial materials became less relevant. In the case of OCP, the coating is fully replaced by the newly formed bone within approximately 12 weeks, and bone continues to grow until the defect is filled. The bulk ceramic, on the other hand, will undergo the same process, but in this case material degradation will continue as well, although very slowly. Comparison of the amount of formed bone between 6 and 12 weeks showed a difference for Ti6Al4V and OCP Ti6Al4V but not for BCP. This once again supports our observation that the bone formation in BCP scaffolds is taking place faster than in the other two materials.

From the results of the intramuscular implantation, we can conclude that uncoated Ti alloy was not osteoinductive in this study, while both OCP Ti6Al4V and BCP did show some extraskeletal bone formation. The amount of formed bone, and the number of animals in which the bone was induced, was similar for the both biomaterials. Although the bone was consistently found, its amount was limited.

It is interesting to note that very large differences were observed between the amount of bone that was induced in individual animals, i.e. one goat was “more inductive” than another goat, for all implanted materials. The reason for these differences could be searched in genetic as well as in pathological backgrounds, but as long as the mechanism of osteoinduction itself is not clear, this phenomenon will be hard to explain. Because of such a limited amount of induced bone, any statistical analysis was impossible to perform. The only conclusion is therefore that both BCP and OCP Ti6Al4V have an osteoinductive potential, and that a non-inductive material such as Ti alloy can become inductive by combining it with a CaP coating. The findings from this study would therefore suggest that the presence of CaP is a critical factor in the process of osteoinduction. And although Yuan et.al. [134] and Fujibayashi et.al. [135] showed the possibility of bone induction by alumina ceramic and chemically treated porous titanium respectively, most of the biomaterials that were shown to induce bone consist of CaP. Although we know that many different material characteristics (chemistry, composition, macro and microstructure) may be important for its osteoinductive behavior [127-129, 194], the exact mechanism of osteoinduction remains unknown. Concerning this mechanism, we hypothesize: 1) Osteoinductive materials exert a direct effect on the growth and differentiation of relevant cells that attach to them, and 2) The surface of osteoinductive materials helps collecting relevant proteins, which in their turn exert an



osteoinductive effect on the recruited cells. To test these hypotheses, and to investigate which cells are important in the process of osteoinduction, additional research needs to be performed.

In our study, CaP containing materials are performing better than the bare metal both ectopically and orthotopically, but from our observation, we cannot draw the conclusion that osteoinductivity improves the ingrowth in orthotopic sites, because of the fact that Ti6Al4V is not only non-inductive, but its conductive properties are limited as well. Nevertheless, it has been reported that osteoinductive materials are performing better orthotopically than the non-inductive materials [195]. This suggests that increased bone ingrowth in OCP Ti6Al4V is not only due to increased osteoconductivity but also due to osteoinductivity of the OCP coating.

## **6.6 Conclusion**

In our study we introduced a porous Ti6Al4V material, produced by a novel technique, with sufficient mechanical properties and biocompatibility. Furthermore, we have shown that the application of OCP coating on the metal implants can improve its performance in bone healing process. BCP ceramic showed better osteoconductive properties than both, uncoated and OCP coated Ti alloy. Finally, both OCP Ti6Al4V and BCP showed an osteoinductive potential in the muscles of goats.

## **6.7 Acknowledgments**

Authors would like to thank Dr. Maarten Terlou from the Image Analysis Department and Dr. Paul Westers and Dr. Edwin Martens from the Biostatistics Department of the University Utrecht for developing the software used for the histomorphometry and the help with statistical analysis.

A part of this study was financially supported by the EU “IntelliScaf” Project (G5RD-CT-2002-00697).



## Chapter 7

### Relevance of osteoinductive biomaterials in a critical-sized orthotopic defect

Pamela Habibovic, Huipin Yuan, Mirella van den Doel, Tara M. Sees,  
Clemens A. van Blitterswijk and Klaas de Groot

University of Twente, Institute for Biomedical Technology,  
Professor Bronkhorstlaan 10D, 3723 MB, Bilthoven, The Netherlands

#### 7.1 Abstract

Several publications have shown the phenomenon of osteoinduction by biomaterials to be real. However, it has been questioned whether the ability of a biomaterial to initiate bone formation in ectopic implant sites improves the performance of such osteoinductive biomaterial in clinically relevant orthotopic sites. Until now, no studies have been published in which osteoinductive potential of a biomaterial is directly related to its performance orthotopically.

In this study, we compared an osteoinductive and a non-osteoinductive biphasic calcium-phosphate (BCP) ceramic ectopically and in a clinically relevant critical-sized orthotopic defect in goats.

The two materials compared in this study, BCP1150 and BCP1300, had similar chemical composition, crystallinity and macrostructure, but their microstructure differed significantly. BCP1150, sintered at a lower temperature, had a large amount of micropores, small average crystal size and hence a high specific surface area. In contrast, BCP1300 with few micropores, had a significantly lower specific surface area as compared to BCP1150.

12-week-intramuscular implantation in goats (n=10) showed that bone was induced in all BCP1150 implants, while no signs of bone formation were found in any of the BCP1300 implants.

After 12 weeks of implantation in a bilateral critical-sized iliac wing defect in the same goats, the osteoinductive BCP1150 showed significantly more bone than the non-osteoinductive BCP1300. In addition, the analysis of fluorochrome markers, which were administered to the animals 4, 6 and 8 weeks after implantation in order to visualize the bone growth dynamics, showed an earlier start of bone formation in BCP1150 as compared to BCP1300.

Significantly better performance of osteoinductive ceramic in a critical-sized orthotopic defect in a large animal model in comparison to the non-osteoinductive ceramic suggests osteoinduction to be clinically relevant. Further improvement of a material's osteoinductive properties is thus a significant step forward in the search for alternatives for autologous bone graft.

Keywords: osteoinduction, biphasic calcium-phosphate ceramic, critical-sized defect, bone repair.

## 7.2 Introduction

The role of biomaterials in osteoinduction, i.e. "the induction of undifferentiated inducible osteoprogenitor cells (IOPCs) that are not yet committed to the osteogenic lineage to form osteoprogenitor cells" [93] has been investigated by various groups during the last decade. Osteoinduction has been shown by a number of calcium-phosphate (CaP) containing bulk ceramics such as hydroxyapatite- (HA) [116-122, 183],  $\alpha$ -tricalcium phosphate- ( $\alpha$ -TCP),  $\beta$ -TCP-, BCP,  $\alpha$ -pyrophosphate- and  $\beta$ -pyrophosphate [116, 122, 124, 125, 127-129, 140, 182, 183, 209, 241], in soft tissues of various animal models. Furthermore, ectopic bone formation has been observed by octacalcium phosphate (OCP) coated porous biomaterials [132, 182, 209], CaP cements [124, 131] and glass ceramics [137]. In addition to the CaP-

containing biomaterials, there have also been a few reports showing osteoinduction by porous alumina ceramic [134] and titanium [135, 136].

The presence of concavities on implant surfaces or macropores is shown to be a prerequisite for osteoinduction by biomaterials [138]. In addition, a certain, not yet well-defined microstructure seems to be an essential element in the mechanism of osteoinduction [124, 128, 129, 134, 135, 183]. Despite the extensive research into osteoinductive properties of various biomaterials, the mechanism of osteoinduction remains largely unknown.

An important clinical question that needs to be answered is whether an osteoinductive material that is able to induce bone formation ectopically is also able to accelerate the growth and increase the amount of the newly formed bone orthotopically. In that case, osteoinductive biomaterials might perform better than most of the currently used synthetic bone graft substitutes and could be better alternatives for the “golden standard” i.e. the autologous bone graft without the well-known complications of the harvesting procedure [24, 242], extended surgical procedure and limited availability.

Therefore, in the present study we compared bone formation by an osteoinductive [183] and a non-osteoinductive BCP ceramic in an established orthotopic critical-sized defect model that allows paired comparisons [29], as well as ectopically with the aim of answering the question whether osteoinduction is a clinically relevant property for bone repair.

### **7.3 Materials and methods**

#### **7.3.1 Implants**

Porous BCP implants were prepared by using the H<sub>2</sub>O<sub>2</sub> foaming method as published earlier [129]. For the preparation of the ceramic, in-house made BCP powder was used. Porous green bodies were produced by mixing this powder with 2% H<sub>2</sub>O<sub>2</sub> solution (1.0 g powder / 1.2 ± 0.05ml solution) and naphthalene (Fluka Chemie, Zwijndrecht, The Netherlands) particles (710 - 1400 μm; 100 g powder/ 30 g particles) at 60°C. The naphthalene was then evaporated at 80°C and the green porous bodies were dried.

They were divided into two groups and sintered at 1150 °C and 1300 °C respectively for 8 hours.

Compositions and crystal structures of the ceramics were determined by using Fourier transform infra red spectroscopy (FTIR; Spectrum100, Perkin Elmer Analytical Instruments, Norwalk, CT) and X-ray diffraction (XRD; Miniflex, Rigaku, Japan). HA/ $\beta$ -TCP weight ratios of the BCP ceramics were determined by comparing the BCP XRD patterns to the calibration patterns prepared from the powders with the known HA/ $\beta$ -TCP weight ratios.

A lathe was used to produce ceramic discs with a size of  $\varnothing 17 \times 6 \text{ mm}^3$ . All implants were cleaned in ultrasonic baths and sterilized by gamma irradiation (Isotron Nederland BV, Ede, The Netherlands).

Prior to implantation, ultrastructures of the porous BCP ceramics were characterized by an environmental scanning electron microscope (ESEM; XL30, ESEM-FEG, Philips, Eindhoven, The Netherlands) in the secondary electron mode. Total-, macro- (pore diameter  $>10 \mu\text{m}$ ) and microporosities (pore diameter  $< 10\mu\text{m}$ ) as well as average pore sizes and pore size distributions were determined on ESEM photographs by an image analysis system and by using a mercury intrusion porosimeter (MP; Auto Pore IV 9500, Micromeritics European Analysis Service, Mönchengladbach, Germany). For a good comparison, the microporosity of each ceramic was expressed as total incremental pore volume (ml) per gram of the material for the pores with a diameter lower than  $10 \mu\text{m}$ . Specific surface areas of the ceramics were determined from the MP results, as the cumulative surface area ( $\text{m}^2/\text{g}$ ) when all pores were filled with mercury.

After implantation, macroporosities of the ceramics were measured again, by using histological sections [183, 209]. First, the labels of the sections were covered. Then, high resolution (300dpi), low magnification digital micrographs were made of these sections. Image analyses on the pseudocolored micrographs were carried out with a computer-based system equipped with KS400 version 3.0 software (Carl Zeiss Vision, Oberkochen, Germany). Prior to measurements, the system was geometrically calibrated with an image of a disc of known dimensions. A program was developed in KS400 to quantify macroporosities of the ceramics. The macroporosity was determined as:  $[(\text{total implant surface} - \text{scaffold surface}) / \text{total implant surface}] * 100\%$ .

### 7.3.2 Animals and implantation

This study was approved by the Dutch Animal Care and Use Committee. In total, ten adult Dutch milk goats (18-30 months) were used. The animals were housed in the Central Animal Laboratory Institute (GDL), Utrecht, The Netherlands, at least 4 weeks prior to surgeries.

Surgical procedures were performed under general inhalation anesthesia of the animals preceded by an intravenous injection of Thiopental (Nesdonal,  $\pm$  400mg/70kg of body weight, on indication, Rhone Merieux, Amstelveen, The Netherlands). After shaving and disinfection of the dorsal thoracolumbar area, a central skin incision at T8-L5 was made to expose the muscle fascia. Both iliac wings were identified and cleared of muscle tissue. Using constant saline cooling, central guide holes were drilled before  $\varnothing$ 17 mm trephine holes were made [29]. BCP1150 and BCP1300 implants were press-fit inserted into the defects according to a randomized scheme. The muscles were then tightly sutured to the remaining fascia on the wings.

For intramuscular implantation, separate fascia incisions were created in the paraspinal muscles (L1-L3). Using blunt dissection, intramuscular pockets were created, and filled with one BCP1150 and one BCP1300 ceramic disc. Subsequently, fascias were closed with nonresorbable sutures to facilitate implant localization at explantation. The skin was closed in two layers.

Pain relief was given by Durogesic 25 (fentanyl transdermal system CII patches; Janssen-Cilag EMEA, Beerse, Belgium).

In order to visualize the dynamics of bone growth, the goats received sequential fluorochrome labels at 4 weeks (Calceine green, 10 mg/kg, i.v., Sigma Aldrich, Zwijndrecht, The Netherlands), 6 weeks (Oxytetracycline, 32 mg/kg i.m., Engemycine, Mycofarm, Amersfoort, The Netherlands) and 8 weeks (Xylenol orange, 80 mg/kg, i.v. Sigma Aldrich, Zwijndrecht, The Netherlands) [78, 80].

12 weeks after the implantations, each animal was sacrificed by an overdose of pentobarbital (Euthesaat, Organon, Oss, The Netherlands) and potassium chloride.

### 7.3.3 Retrieval of the implants, histology and histomorphometry

The iliac wing implants with surrounding bone were removed by using an oscillating saw. The intramuscular implants with surrounding tissue were explanted by dissection. All explanted implants were fixed in Karnovsky's fixative, dehydrated in a graded ethanol series (70%-100%) and transferred into a methylmethacrylate (MMA) solution that polymerized at 37°C within one week.

In order to obtain histological sections, orthotopic implants were ground in the plane parallel to the iliac wing, until the outer circular margin of the implant on the anterior side of the iliac wing appeared. Then, 3 mm below the ground surface three central sections with a thickness of 10-15µm were made by using the modified interlocked diamond saw (Leica Microtome, Nussloch, Germany). Sections were stained either with 1% methylene blue and 0.3% basic fuchsin after etching with HCl/ethanol mixture for routine histology and histomorphometry or left unstained for epifluorescence microscopy with a light microscope (LM; E600 Nikon, Japan) equipped with a quadruple filter block (XF57, dichroic mirror 400, 485, 558 and 640 nm, Omega Filters, Didam, The Netherlands). Intramuscular implants underwent the same procedure of sectioning (three central sections 3 mm below the surface of the disc) and staining as did the orthotopic implants.

For histomorphometry, the same image analysis method was used as previously described for the post-implantation measurement of material macroporosities. In the computer-based image analysis system, a program was developed to quantify different parameters concerning bone formation:

- Percentage of bone occupying available pore area (area%b/pore);
- Percentage of available scaffold outline in contact with bone: [%contact = (bone-scaffold contact length / scaffold outline length) \* 100%] in the total area of the implant (%b.cont).

The first parameter was chosen in order to allow for comparison with previous studies. The reason for the choice of the second parameter, %b.cont., was that in a study in which the performances of two materials are compared, it seems more appropriate to relate the new bone formation to available scaffold rather than to available pore



space. Furthermore, contact percentage is more sensitive for early bone apposition which generally occurs on the ceramic surface and has a relatively low volume.

In order to get insight into healing of the defect, in the iliac wing implants, the histomorphometry was not only performed in the total implant area, but also in the central area of the implant with the diameter of 8.5 mm (half of the total implant diameter).

#### **7.3.4 Statistical analysis**

Statistical calculations were done with the SPSS (Chicago, IL) 12.0 software.

For orthotopic implants, the two-sided, paired Student's t-test was used to analyze differences between BCP1150 and BCP1300.

In agreement with previous studies [183, 209], intramuscularly implanted ceramics showed large variances in the amount of induced bone between the individual animals. Hence, the distribution of the data was not normal and that is why the non-parametric Wilcoxon signed rank test for paired comparisons [207] was used to perform the statistical analyses.

For both tests the significance level was set at  $p=0.05$ .

### **7.4 Results**

#### **7.4.1 Material characterization**

FTIR spectra (figure 1 a) and XRD patterns (figure 1 b) of both BCP1150 and BCP1300 ceramics were similar and characteristic of a biphasic CaP composition. Both ceramics were fully crystalline and consisted of  $80\pm 3$  % HA and  $20\pm 3$  %  $\beta$ -TCP. As observed by LM and ESEM, both ceramics consisted of highly interconnected macropores, with an average pore size of around 400  $\mu\text{m}$  (figures 2a and 2b). Both image analysis of ESEM photographs and mercury porosimetry measurements indicated that prior to

implantation total porosity of BCP1150 was  $76\pm 2\%$  and that of BCP1300  $68\pm 2\%$ . Macroporosity of the two materials was similar,  $55\pm 5\%$ .

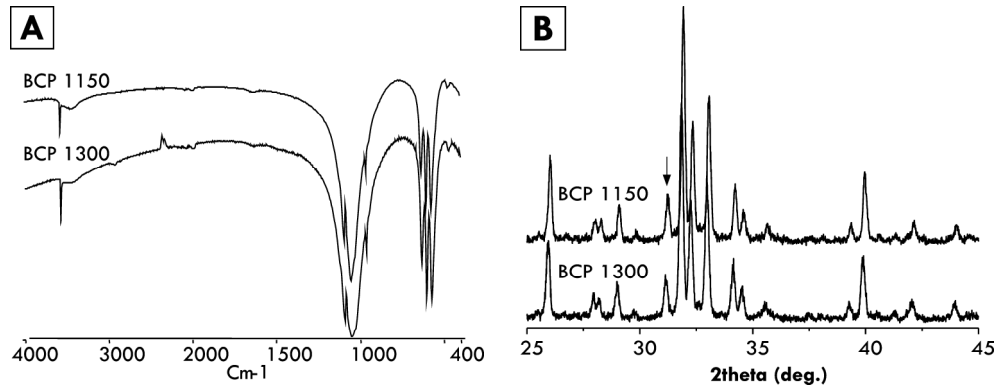


Figure 1: FTIR spectra (A) and XRD patterns (B) of BCP1150 and BCP1300.

Arrow indicates the main  $\beta$ -TCP peak.

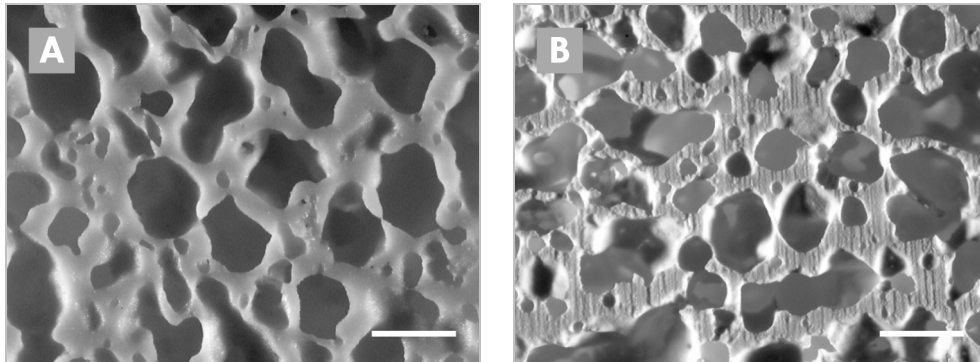
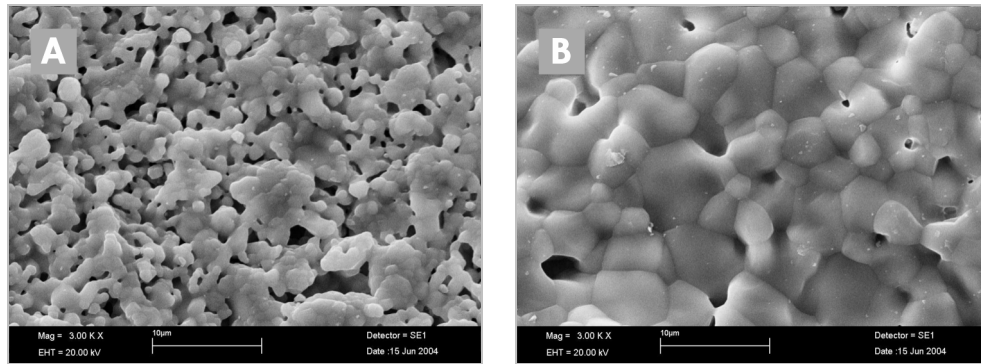


Figure 2: LM photographs (magnification 4x) of BCP1150 (A) BCP1300 (B).

Bar = 1 mm.

Unlike other material characteristics, the microstructures of the two ceramics were different. As shown by the high magnification ESEM photographs of BCP1150 and BCP1300 (figures 3a and 3b respectively), changes of the sintering temperature changed the materials microstructures. The macropore walls of BCP1150 contained more micropores than BCP1300. In addition, crystals of BCP1150 were smaller than

those of BCP1300. These observations were confirmed by the mercury porosimetry results that are shown in figure 4. As can be seen in figure 4, most micropores of BCP1300 had a diameter of around 0.7  $\mu\text{m}$ , whereas the diameter of the BCP1150 micropores was around 1  $\mu\text{m}$ . Figure 4 further demonstrates that the total incremental volume of micropores, i.e. the microporosity, was much higher for BCP1150 as compared to BCP1300. Microporosity of BCP1150 was ca. 17 % and that of BCP1300 ca. 3 %. Macro- and microstructure characterizations of the two ceramics can be summarized by their specific surface areas. The specific surface areas of BCP1150 and BCP1300 were about 1  $\text{m}^2/\text{g}$  and 0.2  $\text{m}^2/\text{g}$ , respectively.



**Figure 3:** ESEM photographs (magnification 3000x) of BCP1150 (A) and BCP1300 (B).

Decrease in the sintering temperature results in an increase of the amount of micropores and a decrease in the crystal size of a ceramic.

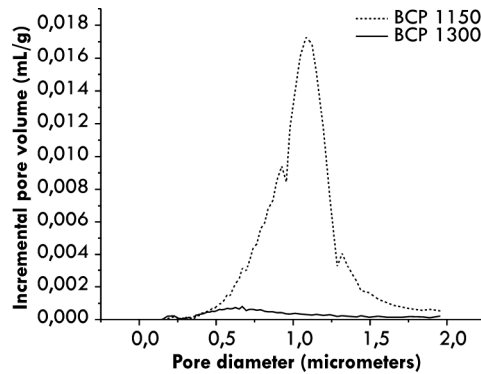


**Figure 4:** total incremental micropore volume for BCP1150 and BCP1300.

Decrease in the sintering temperature results in an increase of the total micropore volume, i.e. microporosity of a ceramic.

### 7.4.2 Ectopic implantation

There were no surgical complications and all implants were retrieved. All explanted ceramics were surrounded by well-vascularized muscle tissue and no macroscopic or microscopic signs of inflammation were found.

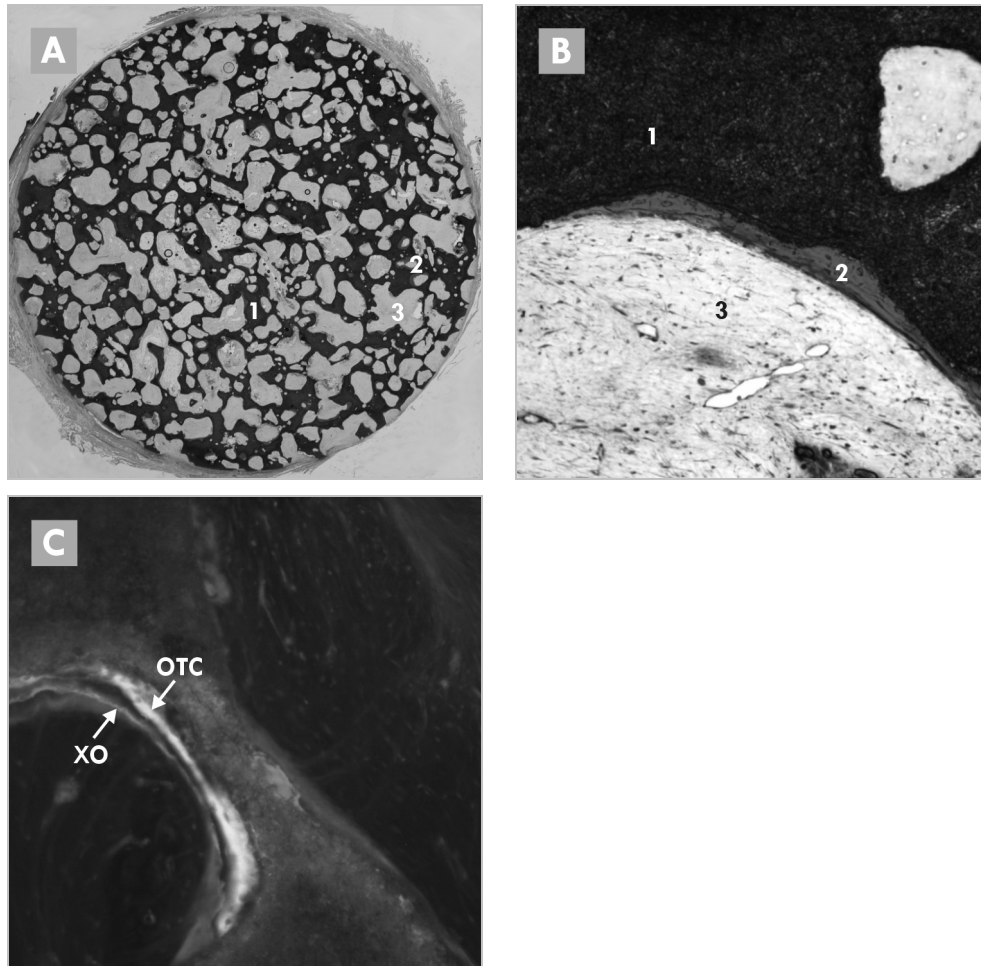


**Figure 5:** digital photograph (A), LM photograph (magnification 10x) of a histological slide (B) and fluorochrome markers (C) of intramuscularly implanted BCP1150.

(1) = ceramic, (2) = bone, (3) = fibrous tissue, OTC = Oxytetracycline, XO = Xylenol orange.

The induced bone is formed in the pores of the implant, aligning its surface (A). The bone is normal in appearance, aligned with osteoblasts and with osteocytes and osteoid clearly visible (B). The presence of both Oxytetracycline and Xylenol orange marker shows that the bone formation had started before the sixth week of implantation (C). → p223.

Macroporosities of the two ceramics measured after implantation, were similar to those before implantation ( $58\pm 5\%$ ), indicating that no substantial resorption of either of the materials had taken place during the 12-week-implantation period.

Bone formation was observed in all implanted BCP1150 discs. Histology showed small foci of bone aligning the ceramic surface as is illustrated in figure 5a. Bone had formed throughout the implants, but was however never observed on the implant exteriors. The formed bone was normal in appearance, aligned by an osteoblast layer and with osteocytes well visible (figure 5b). Fluorescence microscopy confirmed observations from previous studies that bone formation started on the implant surface and continued towards the pore center. In some BCP1150 implants, both Oxytetracycline and Xylenol orange marker were observed, suggesting that bone formation had started before the sixth week of implantation (figure 5c). In other BCP1150 implants, only Xylenol orange marker was visible, emphasizing again the observed intra-species differences.

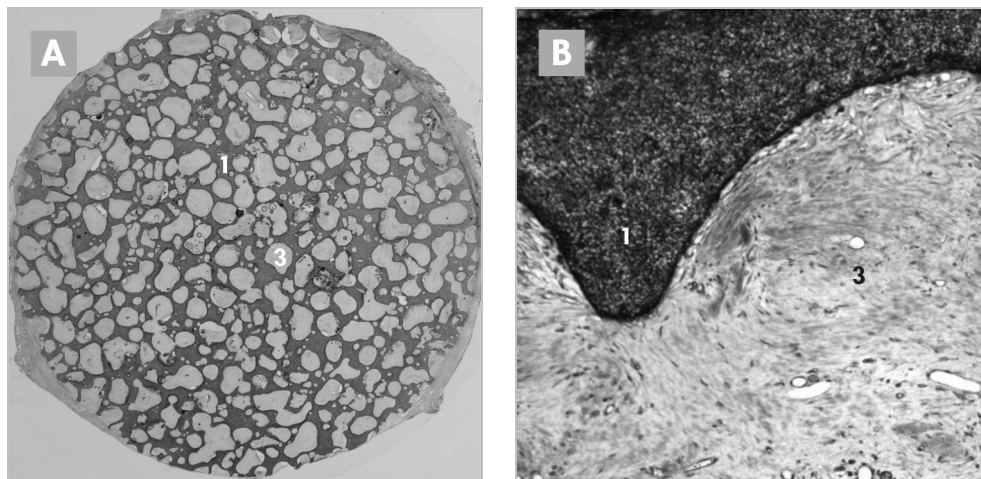


**Figure 6:** digital photograph (A) and LM photograph (magnification 10x) (B) of a histological slide of the intramuscularly implanted BCP1300.

(1) = ceramic, (3) = fibrous tissue.

The ceramic is extensively filled with fibrous tissue, but no signs of bone formation are observed. → p224.

Although bone was observed in all BCP1150 implants, in agreement with previous studies [183, 209], the amount of formed bone varied significantly between the

individual animals. For example, percentage of bone area occupying available pore area (area%b/pore) varied between ca. 0.05% and ca. 6% with an average of  $1.5 \pm 2.0\%$ . Similarly, percentage of available scaffold outline in contact with bone (%b.cont) varied between ca. 0.5% and ca. 10% giving an average of  $2.9 \pm 3.8\%$ .

All BCP1300 implants were extensively filled with fibrous tissue as is shown by figures 6a and 6b. However, no bone formation was observed in any of the implants. As expected, the Wilcoxon signed rank test showed that for both measured parameters, BCP1150 performed significantly better ( $p=0.018$ ) than BCP1300.

### 7.4.3 Orthotopic implantation

There were no surgical complications and all implants were retrieved. At retrieval, iliac wing implants of all animals were overgrown by tissue and could neither visually nor manually be detected (no motion). Histology showed no evidence for toxicity of the implants, or signs of an inflammatory tissue response. All implants were totally integrated in the surrounding cancellous bone, without interposition of fibrous tissue.

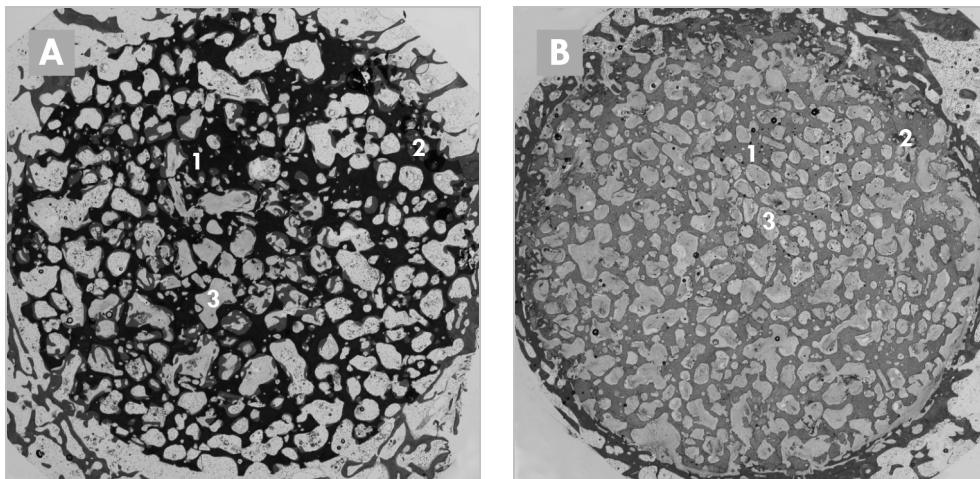


**Figure 7:** digital photographs of BCP1150 (A) and BCP1300 (B) after explantation from the iliac wing defect.

(1) = ceramic, (2) = bone, (3) = fibrous tissue.

Bone has grown deeply inside the BCP1150 disc (A) while only a small ridge of new bone has formed along the host bone bed in the BCP1300 disc (B). → p225.

Similar to the intramuscular implants, no significant resorption of either of the materials had taken place during the 12-week-implantation period orthotopically.

As shown in figure 7a, a considerable amount of bone had formed in the pores of BCP1150 implants. In all animals, new bone had grown deeply inside the BCP1150 discs and most defects were almost completely filled with bone. In BCP1300 implants, however, a relatively small amount of bone had formed (figure 7b). The new bone formation had taken place in the areas of the implant close to the host bone bed, while no bone could be observed in the center of any of the BCP1300 discs.

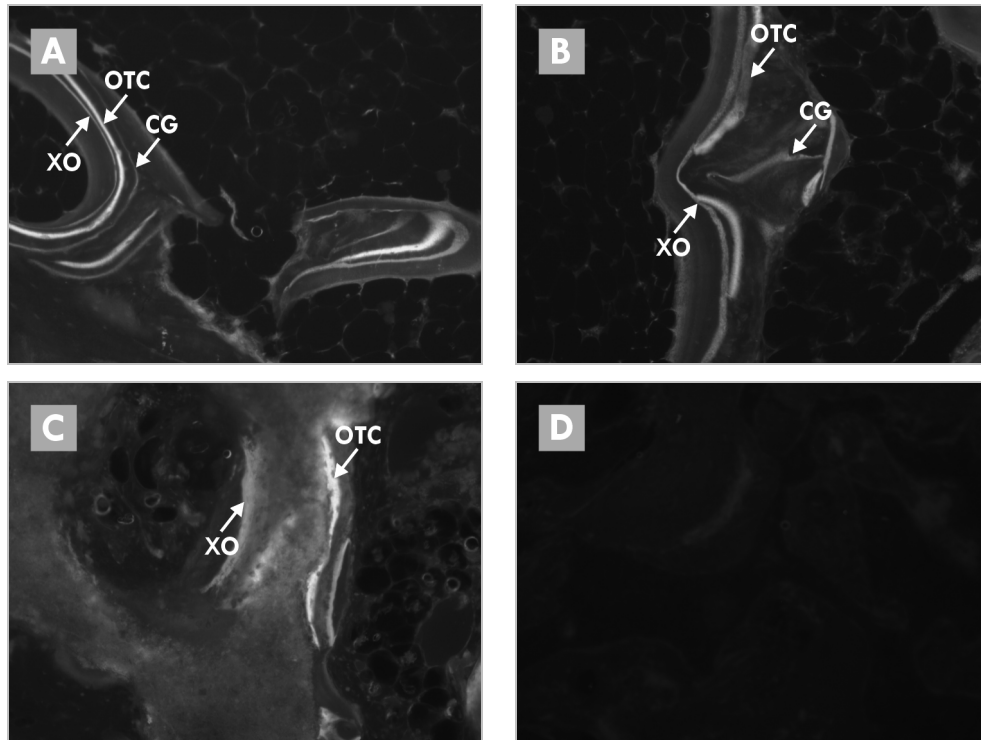


**Figure 8:** LM photographs (magnification 10x) of the fluorochrome markers on the periphery of BCP1150 (A) and BCP1300 (B) and in the center of BCP1150 (C) and BCP1300 (D) discs explanted from the iliac wing defects.

CG = Calcein green, OTC = Oxytetracycline, XO = Xylenol orange.

On the peripheries of both BCP1150 (A) and BCP1300 (B) all markers can be seen, which shows that in both ceramics bone formation near the host bone bed had started before the fourth week of implantation.

The presence of the Oxytetracycline and Xylenol orange marker in the center of BCP1150 disc (C) shows that the bone formation far away from the host bone bed had started before the sixth week of implantation. Absence of any of the markers in the center of BCP1300 (D) illustrates the absence of new bone within the first eight weeks of implantation. → p226.

Analyses of the presence of the fluorochrome markers indicated that in both ceramics, the bone apposition generally started at the ceramic surface and continued away from the surface, towards the pore center. In the peripheral areas of both implant types, the presence of the Calcein green label indicated that the bone growth had started before the fourth week of implantation (figures 8a and 8c). In BCP1150, however, more Calcein green label could be observed, suggesting more early bone formation on BCP1150 than on BCP1300 ceramic surface. In the central part of BCP1150 implants, Xylenol orange marker could be observed indicating the start of bone formation before the eighth week of implantation. In addition to the Xylenol orange marker in some of the implants, Oxytetracycline marker was observed, indicating an even earlier bone formation in the central area of BCP1150 (figure 8b). In the central areas of most BCP1300 implants, the absence of any of the used markers confirmed the absence of bone formation within the first 8 weeks of implantation as is shown in figure 8d.

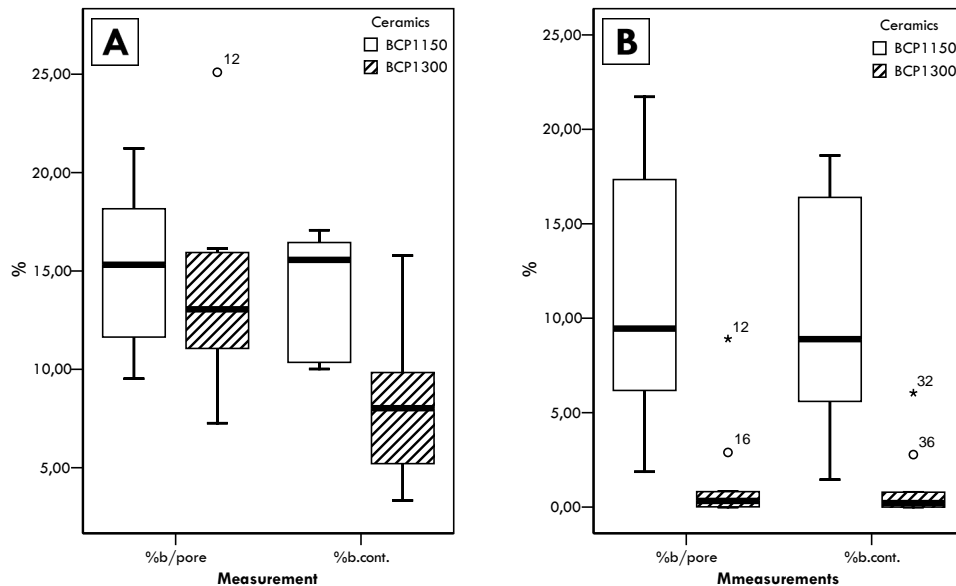


**Figure 9:** histomorphometrical results: boxplots (mean and interquartile values) of area%b/pore and %b.cont. in the total (A) and central (B) area of the orthotopically implanted BCP1150 and BCP1300 discs.

(o) = outliers, (\*) = extreme outliers.

In the total implant area (A) BCP1150 performed better than BCP1300 for both measured parameters. The difference was however only significant ( $p < 0.01$ ) for %b.cont. In the central implant area BCP1150 was significantly better ( $p < 0.01$ ) than BCP1300 for both area%b/pore and %b.cont.



Figure 9 illustrates histomorphometrical results of the percentage bone area occupying available pore area (area%b/pore) and percentage of available scaffold outline in contact with bone (%b.cont) in the total (figure 9a) and in the central (figure 9b) area of the iliac wing implants. BCP1150 showed more bone than BCP1300 ( $15.2\pm 4.2\%$  vs  $13.5\pm 5.1\%$ ), although this difference was not significant for the area%b/pore ( $p=0.494$ ). The bone apposition (%b.cont) however, was significantly higher in BCP1150 as compared to BCP1300 ( $p<0.01$ ) ( $13.9\pm 3.1\%$  vs  $8.1\pm 3.6\%$  respectively). These observations were amplified when only the middle of the implant was analyzed ( $11.0\pm 7.2\%$  vs.  $1.4\pm 2.8\%$  ( $p<0.01$ ) for area%b/pore and  $9.6\pm 5.8\%$  vs.  $1.1\pm 1.9\%$  ( $p<0.01$ ) for %b.cont.) in BCP1150 and BCP1300, respectively.

## 7.5 Discussion

In the current study, for the first time, bone formations in an osteoinductive and a non-osteoinductive porous CaP ceramic were compared in a clinically relevant critical-sized defect in goats.

The two ceramics used in this study had identical composition, crystallinity and macrostructure, but differed significantly in their microstructure. BCP1150 had a high microporosity and a small average crystal size, which consequently resulted in a high specific surface area. In contrast to BCP1150, the BCP1300 ceramic possessed a low microporosity, large average crystal size and hence a relatively low specific surface area. The differences in microstructures between the two ceramics were achieved solely by different temperatures at which they were sintered, as described previously [183].

The ectopic implantation of the two ceramics showed only bone formation in BCP1150 ceramic in all animals. This is in agreement with observations from previous studies in which it is suggested that the microstructure may be crucial and responsible for the osteoinductive potential of biomaterials [135, 136, 183, 209]. Although the exact mechanism of this process is still not unraveled, the fact is that in the used model BCP1150 somehow stimulated undifferentiated cells to generate bone at its surface. BCP1300 completely lacked this ability.

When implanted in the critical-sized iliac wing defects, the biological performances of the two ceramics differed as well. After twelve weeks of implantation, bone had grown deeply inside the BCP1150 discs, and in most animals the defect was even fully bridged by new bone. In contrast to BCP1150, in the BCP1300 discs new bone had only formed a small ridge along the host bone bed. Differences in the healing between the two ceramics were highly significant as demonstrated by the histomorphometrical results in the central area of the implants.

Besides differences in bone yield, we observed more Calcein green (4-week-label) on the periphery of the BCP1150 in comparison to the BCP1300 ceramic, which indicated that the new bone formation started earlier in the osteoinductive material. Furthermore, the presence of the 6-week Oxytetracycline marker in the center of the BCP1150 implants showed the start of the new bone formation deep inside the implant before the sixth week of implantation. Differences in bone formation onset observed between the two ceramics might be an explanation for the fact that the measured percentage of bone area in the available pores was not significant in the total implant area. Namely, after 12 week-implantation period bone formed in BCP1150 is likely to be in a different phase of remodeling from that formed in BCP1300. In particular on the edges of the implant along the host bone bed, where the earliest bone formation had taken place, bone may transfer to the structure of the surrounding cancellous bone. The parameter percentage of contact between the newly formed bone and the scaffold is less sensitive for the remodeling processes and highly sensitive for early bone apposition and might therefore be more appropriate for comparing the performance of different materials at one time point.

The findings of an earlier start and a higher amount of bone formation in the orthotopically implanted osteoinductive CaP ceramic in comparison to the non-osteoinductive ceramic, suggests the osteoinductive potential to be relevant for the performance of a material as a bone filler. However, it does not necessarily mean that osteoinduction itself is the cause for a better performance as it cannot be excluded that more micropores and consequent higher specific surface area lead to better osteoconduction. In other words, the presence of osteoinduction and increased osteoconduction might be two independent consequences of introducing microporosity in porous BCP.

Davies and Hosseini defined osteoconduction as “the recruitment and migration of osteogenic cells into the wound site” [243]. According to the authors, bone formation during either healing or the anabolic phase of bone remodeling comprises the two distinct phenomena: 1) de novo bone formation, preceded by osteoconduction, formed by the migrating osteogenic cells along the solid surface of the implant and 2) appositional bone growth by polarized cells and differentiated osteoblasts formed in the direction perpendicular to the solid surface of the implant. The former process is by far more important in the bone healing than the latter one.

During the process of osteoconduction, recruited osteogenic cells differentiate into osteoblasts and stop migrating as soon as they have reached the target surface (old bone or implant). The newly differentiated osteoblasts start producing bone matrix, while osteoconduction continues along the implant surface by new osteogenic cells. Thus, osteoconduction followed by de novo bone formation, takes place from the host bone bed towards the center of the (porous) implant. Osteoinductive BCP1150 ceramic might have the ability to attract more osteogenic cells than the non-osteoinductive ceramic, which could explain an earlier start of bone formation on the periphery of BCP1150.

However, neither de novo bone formation nor appositional bone growth can explain the early bone formation in the center of the BCP1150 implants in the critical sized iliac wing defect. It is therefore conceivable that osteoinduction plays an important role. However, if we assume that the process of osteoinduction is the same both ectopically and orthotopically, difference between percentage of bone contact in the central areas of BCP1150 and BCP1300 implanted orthotopically should have a maximum of about 2.9% (=average %b.cont. found in BCP1150 implants intramuscularly). The larger difference observed may be explained by the fact that there is a higher amount of IOPCs at orthotopic than at ectopic sites. This is conceivable, because, in addition to IOPCs from the surrounding muscle, it is known that bone marrow also contains IOPCs [244, 245].

The above described findings suggest that new bone formation in an orthotopic defect is reproducibly enhanced by the osteoinductive material, which is responsible for the “production” of new bone cells (effect of osteoinduction) and/or recruitment of a higher amount of osteogenic cells as compared to non-osteoinductive ceramic (enhancement of osteoconduction).

In summary, the results of this study show that the improvement of the intrinsic bone inductive properties of biomaterials can significantly improve their performance in the role of bone filler. Improving osteoinductive properties of biomaterials might be a way to make them a suitable substitute for autograft, with a similar performance to that of growth factors and tissue-engineered hybrids, but without disadvantages associated with their use.

## **7.6 Conclusion**

Although the exact mechanism of the effect of osteoinductivity on the performance of a biomaterial as bone filler is still largely unknown, this study has shown a significantly better performance of an osteoinductive CaP ceramic in comparison to a similar, but non-osteoinductive ceramic in a critical-sized orthotopic defect in a large animal model.

## **7.7 Acknowledgements**

Authors would like to thank Dr. Maarten Terlou from the Image Analysis Department of the University of Utrecht for developing the software used for the histomorphometry and Dr. Edwin Martens from the Biostatistics Department for his generous help with statistical analysis.

This study was financially supported by the EU “IntelliScaf” Project (G5RD-CT-2002-00697).

## Chapter 8

### General discussion

Pamela Habibovic, Clemens A. van Blitterswijk and Klaas de Groot

University of Twente, Institute for Biomedical Technology,  
Professor Bronkhorstlaan 10D, 3723 MB, Bilthoven, The Netherlands

#### 8.1 Discussion

In this chapter, a brief overview of the findings that have been discussed in detail in the chapters 2-7 are given.

In Chapter 2, we reviewed a number of existing *in vitro* models to assay bone formation in general and in relation to osteoinduction in particular. We discussed the limitations of the use of the existing *in vitro* systems to study the potential *in vivo* performance of biomaterials in terms of osteoconduction and osteoinduction. When biomaterials are introduced in an *in vitro* system, there is a risk of an interaction between the biomaterial and the cell culture medium in addition to the biomaterial-cells interaction that is being studied. Resorbable materials can release compounds into the medium. Similarly, contents of the medium, such as calcium- and phosphate ions can precipitate on the material with a high specific surface area. The biomaterial-cell culture medium interaction might be an artifact of the *in vitro* system, if a similar interaction between the material and body fluids is not expected *in vivo*. The use of bioreactors, by which changes of the medium composition are screened and adjusted in time, might be a way to avoid the artifact caused by the biomaterial-cell culture medium interaction. Without required adjustments, the existing *in vitro* systems are inadequate for the biomaterials research.

When trying to study complex and largely unknown biological phenomena *in vitro*, such as osteoconduction and osteoinduction by biomaterials, attention should be focused on the appropriate cell and assay choice. It is important to keep in mind that the

established in vitro systems are simplified models of the in vivo environment, and that, although in vitro studies can give some valuable information, only very careful conclusions can be drawn from their results. Preclinical in vivo studies remain therefore necessary in order to unravel complex biological phenomena.

In Chapters 3-7 of this thesis, attempts were made to get more insight into the mechanism underlying osteoinduction by biomaterials and into the relevance of osteoinductive biomaterials in bone repair. The achievements of the research described in this thesis will be attended by answering the specific questions given in the Introduction Chapter 1:

- What is the influence of chemical composition, microstructure and surface morphology on material osteoinductive properties?
- Is there an influence of implant size and implantation site on the amount of induced bone?
- What occurs on the surface of an osteoinductive material during ectopic implantation?
- What is the performance of osteoinductive biomaterials at orthotopic implantation sites?

### **8.1.1 Influence of physico-chemical parameters and microstructure**

In Chapter 3 of the thesis, we applied biomimetic octacalcium phosphate (OCP) coating on porous titanium alloy (Ti6Al4V), hydroxyapatite (HA) ceramic, biphasic calcium phosphate (BCP) ceramic consisting of hydroxyapatite (HA) and  $\beta$ -tricalcium phosphate ( $\beta$ -TCP) and polyethylene glycol terephthalate/polybutylene terephthalate (PEGT-PBT) copolymer. Uncoated materials were used as control.

After intramuscular implantation for 6 and 12 weeks in goats, bone was induced by all OCP-coated porous materials, apart from the OCP-coated PEGT-PBT copolymer. From the uncoated materials, only BCP ceramic showed ectopic bone formation, although bone incidence was higher when BCP ceramic was coated with OCP.

The results of this study showed that there was a difference in osteoinductive properties between different biomaterials. The tested materials differed not only in their chemical composition, but also in their macro- and microstructures. It was therefore difficult to conclude which of these factors influenced materials' osteoinductive properties.

It was further shown that biomimetic OCP coating could be applied on different porous materials, independent on their chemistry, and that therewith the osteoinductive properties of these materials can be improved. Ti6Al4V and HA, which did not induce bone when uncoated, showed ectopic bone formation in presence of the OCP coating. Bone incidence in BCP ceramic, which was osteoinductive without OCP coating, increased in the presence of the coating.

The fact that OCP-coated PEGT-PBT copolymer did not induce ectopic bone formation was probably due to poor mechanical properties of the chosen polymer composition, which caused a loss of porous structure and delamination of the OCP coating after implantation. The presence of macropores has previously been shown to be a prerequisite of osteoinduction by biomaterials [116, 117, 124, 125, 135, 220].

In conclusion, this study confirmed that chemistry does influence osteoinductivity of biomaterials [128, 129, 208], as previously suggested by different authors. In addition, it was confirmed that the presence of macroporosity [116, 117, 124, 125, 135, 220] is a prerequisite for osteoinduction. Finally, biomimetic OCP coating was shown to be osteoinductive when applied on porous surfaces of different materials, in analogy to the previously published results for porous tantalum [132].

In Chapter 4, we investigated the influence of microstructure on osteoinductive properties of two types of porous ceramic, HA and BCP, after intramuscular implantations in goats for 6 and 12 weeks. Different microstructures were achieved by changing the sintering temperatures of the ceramics. HA ceramic was sintered at 1150 °C and 1250 °C, while biphasic calcium phosphate BCP ceramic was sintered at 1100 °C, 1150 °C and 1200 °C.

Decrease of the sintering temperatures significantly increased microporosity and therewith also the specific surface area of the ceramics. Increase of the specific surface area consequently had a positive influence on the osteoinductive properties of the ceramics. While bone was not induced by HA sintered at 1250 °C, HA sintered at 1150

°C induced bone in 50% of the animals after 6 and in 70% of the animals after 12 weeks of implantation. All BCP ceramics induced bone, however, both bone incidence and the amount of induced bone were higher in BCP sintered at 1100°C and 1150°C as compared to the BCP ceramic sintered at 1200°C. Comparison of HA ceramic sintered at 1150°C with BCP ceramic sintered at 1150°C showed more bone in the latter.

In conclusion, the results of this study indicated that the presence of micropores, in addition to the presence of macropores, is a prerequisite for osteoinduction by biomaterials, and that this phenomenon is independent on the material chemistry. Furthermore, there seems to be a limit in the increase of microporosity solely by decreasing sintering temperature. Namely, difference in microporosity between BCP sintered at 1200°C and BCP sintered at 1150°C was much larger than difference between BCP sintered at 1150°C and BCP sintered at 1100°C. Finally, the finding that BCP ceramic sintered at 1150°C induced more bone than HA sintered at the same temperature indicated the importance of chemistry, and, in this particular case, the presence of the more soluble  $\beta$ -TCP phase in the ceramic.

In Chapter 5, we compared osteoinductive properties of four, slightly different porous BCP ceramics, consisting of HA and  $\beta$ -TCP and a porous carbonated apatite (CA) ceramic, after a 12-week intramuscular implantation in goats.

Results of the study confirmed observations from previous studies that the material needs a relatively high specific surface area, which is achieved by the increase of microporosity, in order to be able to induce ectopic bone formation. However, this study showed that if the surface area is too high, or material is too resorbable due to its chemical composition, the implants might degrade and lose their porous shape. In that case, ectopic bone formation does not occur, as a relatively stable surface is needed to facilitate new bone growth. These findings suggest that, for each type of material, there is an optimal specific surface area at which the osteoinductive potential is highest.



### **8.1.2 Implant size and implantation site dependence**

In Chapter 5, BCP ceramics sintered at 1150°C and 1300°C were intramuscularly implanted in two implant sizes for 12 weeks in goats. BCP1150 ceramic cylinders with the size of  $\text{Ø}6.5 \times 10 \text{ mm}^3$  induced bone in 90% of animals, while the cylinders with half the volume ( $\text{Ø}6.5 \times 10 \text{ mm}^3$ ) induced bone in 70% of animals. In addition, the amount of induced bone was higher, and the start of bone formation took place earlier in larger in comparison to smaller implants. As expected, BCP1300 ceramics did not induce bone in neither large nor small implants, as it lacked micropores, and had a relatively small specific surface area.

In Chapter 5, BCP ceramic implants sintered at 1150°C and 1300°C with a size of  $\text{Ø}6.5 \times 5 \text{ mm}^3$  were implanted both intramuscularly and subcutaneously in goats for 12 weeks. While intramuscularly implanted BCP1150 induced bone in 70% of animals, bone was not induced after subcutaneous implantation of BCP1150. As expected, BCP1300 did not induced bone at either implantation sites.

In conclusion, this study showed that there is an influence of the implant size on the materials' osteoinductive potential, namely, the larger the implant, the more bone is induced. This might explain the fact that ectopic bone formation by biomaterials is rarely found in rodents and other small animals [67, 116, 142-144], in which, obviously, only implants of a small size can be inserted. We observed differences in the amount of induced bone between intramuscular and subcutaneous locations, which contrasts a previous study in sheep [124], and might therefore be species dependent.

### **8.1.3 In vivo changes on the surface of osteoinductive materials**

In order to investigate changes occurring on the surface of osteoinductive implants after implantation, in Chapter 5 we implanted the osteoinductive BCP1150 ceramic and the non-osteoinductive BCP1300 ceramic inside diffusion chambers subcutaneously in goats for 1, 2 and 4 weeks. Consequently, thermogravimetry analysis on the explanted materials was performed.

The results of this study showed that, after explantation, more carbonate and organic compounds were present on the surface of osteoinductive ceramic as compared to the non-osteoinductive ceramic. These results suggested that, during implantation, on the surface of the osteoinductive ceramic more dissolution took place, followed by the reprecipitation of the carbonated-apatite layer and possible coprecipitation of the organic compounds such as endogenous proteins, than on the surface of the non-osteoinductive ceramic. This finding might be explained by the difference in the specific surface area between osteoinductive and non-osteoinductive ceramic.

#### **8.1.4 Performance of osteoinductive biomaterials at orthotopic implantation sites**

In Chapter 6, we implanted porous titanium alloy (Ti6Al4V), uncoated and coated with biomimetic OCP coating and porous BCP ceramic (all implants were cylinders with the size  $\varnothing 5 \times 10$  mm<sup>3</sup>), intramuscularly and in the diaphyseal femur of goats for 6 and 12 weeks.

As expected from the data described in Chapter 3, intramuscularly implanted uncoated porous Ti6Al4V did not induce bone in any of the animals. Bone was observed in intramuscularly implanted OCP-coated Ti6Al4V (in 40% of goats after 6 and in 60% after 12 weeks of implantation) and BCP ceramic (30% of goats after 6 and 60% after 12 weeks of implantation).

Orthotopically, after both 6 and 12 weeks of implantation, more bone was formed in OCP-coated Ti6Al4V and BCP implants as compared to the uncoated Ti6Al4V. BCP ceramic showed significantly more bone than OCP-coated Ti6Al4V after 6 weeks, however, this difference was no longer significant after 12 weeks of implantation.

In conclusion, this study showed that the presence of calcium-phosphates in the form of coating on metal implants or in the form of bulk ceramic had a significantly positive effect on the bone healing process as compared to the uncoated metal. Whether this positive effect is due to the fact that both OCP-coated Ti6Al4V and BCP were osteoinductive is hard to conclude from this study, as the uncoated Ti6Al4V was not only non-osteoinductive, but its osteoconductive properties were limited as well.

In Chapter 7, osteoinductive BCP ceramic sintered at 1150°C and the non-osteoinductive BCP ceramic sintered at 1300°C were implanted in paraspinal muscles and in a critical-sized iliac wing defect [29] in goats for 12 weeks.

As expected from the results of the study described in Chapter 5, intramuscularly implanted BCP1150 induced bone in all animals, while no ectopic bone formation was found in any of the implanted BCP1300 ceramic discs.

After 12 weeks of implantation in the critical-sized iliac wing defect, in BCP1300 implants only a small ridge of new bone had formed along the host bone bed. In contrast, in BCP1150 implants, bone had grown deeply inside the implants, and in most animals, the defect was fully bridged by new bone. In addition to a higher amount of bone formed in BCP1150 than in BCP1300 implants, analyses of fluorochrome markers, which were administered in order to visualize the bone growth dynamics, showed that new bone formation had started earlier in BCP1150 implants. In addition, fluorochrome markers illustrated that in BCP1150 implants, bone did not only grow from the host bone bed towards the center of the implant, as the new bone growth took place simultaneously in the center of the implant and on its periphery.

Results of this study showed a significantly positive effect of the osteoinductive ceramic in a clinically-relevant critical-sized defect as compared to the non-osteoinductive ceramic with the same chemical composition.

## **8.2 General observations**

There are two general observations from this research that need to be addressed. First of all, so far, all our trials to develop an *in vitro* study that might help unraveling the mechanism of osteoinduction or at least understanding certain aspects of this phenomenon were unsuccessful. Cultures of cells belonging to osteoblastic cell lines, pluripotent cell lines and primary cells, followed by assays for cell attachment, proliferation and differentiation all gave inconclusive results, which were often in contrast to the findings from the *in vivo* studies.

The second general observation concerns *in vivo* studies. We observed very large variations in the amount of induced bone between individual goats within a group. In all

performed studies, there were goats with “high” and “low” osteoinductive potential. In other words, the amount of bone induced by the same material in goat 1 and goat 2 could differ significantly. That the reason for these difference probably does not lie in materials themselves, or in any kind of coincidence, was shown by the trends within each animal, the analyses of which were possible due to paired implantations. It was namely observed, that, if smaller amount of bone was induced by material A in the goat with a “low” osteoinductive potential, the amount of bone induced by material B, C, etc. was relatively small in the same goat as well. Thus, there were inter-animal variations, but intra-animal consistencies. Much smaller variations were observed at orthotopic implantation sites, and these could not be related to the differences observed at ectopic sites.

## Chapter 9

### General conclusions and future perspectives

Pamela Habibovic, Clemens A. van Blitterswijk and Klaas de Groot

University of Twente, Institute for Biomedical Technology,  
Professor Bronkhorstlaan 10D, 3723 MB, Bilthoven, The Netherlands

#### 9.1 General conclusions

In Chapter 1, General introduction, it was indicated that the two main goals of this thesis were: (I) gathering relevant information on parameters which are important in the process of osteoinduction by biomaterials in order to unravel this, so far largely unknown, phenomenon and (II) investigating the performance of osteoinductive biomaterials orthotopically in order to get more insight into their potential use in the clinic.

##### 9.1.1 Mechanism of osteoinduction

With regard to the first goal, our research has shown that:

- various calcium-phosphate biomaterials are able of inducing ectopic bone formation depending on their chemical composition, making osteoinduction by biomaterials a general phenomenon;
- in addition to, previously demonstrated, macroporosity, our research has shown that presence of microporosity is an essential element in osteoinduction by biomaterials;
- there seems to be an optimum in specific surface area for each type of biomaterial, different for each chemical composition;

- besides the well known species dependence, we have demonstrated that implantation site as well as the implant size influence the osteoinductive potential of biomaterials;
- the high specific surface area of osteoinductive biomaterials is responsible for a high interaction with the in vivo surrounding resulting in a high level of dissolution and reprecipitation of more biological carbonated apatite layer, accompanied by coprecipitation of possibly relevant endogenous proteins. This typical surface reactivity is lower on non-osteoinductive biomaterials.

In General introduction of the thesis, we hypothesized a mechanism of osteoinduction. The presence of macropores, or well-defined three-dimensional concavities has previously been shown to be a prerequisite for osteoinduction by biomaterials [132, 135, 138, 140]. A well-interconnected macroporous structure is of importance for an adequate supply of the body fluids with nutrients throughout the implant. Accompanied with this supply, the release of calcium- and phosphate ions, believed to be the origin of the bioactivity of calcium-phosphate biomaterials [138, 171, 172, 210], takes place, followed by the precipitation of a biological carbonated apatite layer [211]. The precipitation of this apatite layer occurs when the concentration of calcium- and phosphate ions has reached the supersaturation level in the material vicinity. This might explain the experimental fact that the bone induction always takes place in the supersaturated pores in the center of implant and not at or near the, less saturated, implant periphery [205].

It is expected that a material with a higher dissolution rate releases calcium- and phosphate ions faster, and thus allows a faster formation of the biological layer [Chapter 5]. One way to influence the in vivo dissolution rate of a material is by changing its specific surface area. Increase of the specific surface area increases its surface reactivity [Chapters 5 and 6]. However, there seems to be an optimal specific surface area for each type of biomaterial. Materials with a specific surface area below the optimum have a consequent low surface reactivity and will therefore induce bone later or will not be inductive at all [Chapters 3, 4, 5 and 7]. Materials with a specific surface area above the optimum or materials with poor mechanical properties might degrade, losing thereby the shape and stability that is necessary to facilitate bone formation [Chapter 5].

Also the material chemical composition can influence its *in vivo* degradation. For example, presence  $\beta$ -TCP in BCP has a positive influence on the ceramics osteoinductive properties [Chapter 4]. In the biomaterials that initially do not contain CaPs, like alumina ceramic and titanium, the formation of the biological apatite layer needs more time. In this case, calcium- and phosphate ions from the body fluids precipitate onto the microporous surface of the material macropores which acts as a collection of nucleation sites for the precipitation.

Changes that occur after implantation on the surface of the osteoinductive biomaterial inside or around its micropores are obviously responsible for its ability to trigger undifferentiated cells to start forming osteoblasts. The formed bone-like biological carbonated apatite layer could be a physico-chemical trigger for the cells to differentiate into the osteogenic lineage similar to being in an orthotopic environment.

On the other hand, coprecipitated “relevant endogenous proteins” are also possible candidates for the role of inducer of osteogenic differentiation. The fact that the ectopic bone formation by biomaterials is very rarely found in rodents and other “small animals” [116, 141-144] and that osteoinduction by biomaterials is always intramembranous [121, 129] suggest that osteoinduction by biomaterials does not involve BMPs.

However, our research has shown that implant size is of large importance on osteoinduction by biomaterials [Chapter 5], which could be a reason for the lack of bone formation by biomaterials in rodents. Obviously, only small implants can be introduced in small animals. In addition, implantations in rodents are mostly subcutaneous, and our research has shown that for osteoinduction by biomaterials, subcutis is a less inductive site implantation site than muscle [Chapter 5]. Furthermore, in our research we observed large differences in osteoinductive potential between individual animals [Chapters 4 and 5], and these types of differences are also observed in response to BMPs [56, 112, 113]. Finally, whether bone induction by BMPs is endochondral or intramembranous depends on the carrier as well [104, 246, 247]. It is thus possible that, in combination with osteoinductive biomaterials, BMP always gives rise to intramembranous bone formation. It is therefore conceivable that BMPs play a role in osteoinduction by biomaterials, but as long as we did not find conclusive evidence, other possibilities should be left open.

### **9.1.2 Clinical relevance of osteoinductive biomaterials**

Regarding the second goal of our research, we have shown that osteoinductive biomaterials perform better orthotopically than the non-osteoinductive ones in small [Chapter 6] and large, critical-sized defects [Chapter 7].

In particular Chapter 7, in which a clinically relevant defect was chosen, showed an importantly better performance of osteoinductive in comparison to the non-osteoinductive ceramic with similar chemical composition. Analyses of fluorochrome markers gave valuable information on bone growth dynamics, and indicated that bone formation started rather early in the center of osteoinductive ceramic, which could not be explained by the phenomenon of osteoconduction. Although we did not completely unravel the exact mechanism of the effect of osteoinductive potential orthotopically, the results of this study suggest that osteoinductive biomaterials have the potency of becoming a good alternative for autologous bone grafts.

### **9.2 Recommendations for future research**

Although our research has given some new insights into the mechanism of osteoinduction by biomaterials as well as into its clinical relevance, a lot of work is still needed in order to be able to design a perfect synthetic alternative for autologous bone graft.

It is important to investigate in detail the exact events that take place on the surface of osteoinductive and non-osteoinductive biomaterials *in vivo*. A similar study could be performed as described in Chapter 5 of this thesis, in which materials are implanted intramuscularly or subcutaneously inside diffusion chambers for different periods of time. This implantation should be followed by the analysis of the organic compounds which are then present on the surface. For this type of study, the goat might not be the best model because of the lack of antibodies. Therefore, additional attention should be paid on interspecies differences. Understanding of reasons for lack of osteoinduction in rodents and other “small” animals can lead to the solution of the problem. The use of (transgenic) mice and rats would make the fundamental research into mechanism of osteoinduction much easier.



It is further important to investigate how relevant the formation of biological apatite layer and coprecipitation of organic compounds is for the material osteoinductive potential. In order to investigate this relevance, implantation of osteoinductive and non-osteoinductive materials inside diffusion chamber for short period of time in e.g. goats, could be followed by the reimplantation of these materials in soft tissues of rodents, where they are, so far, unable to induce bone.

More effort should be put in developing reliable in vitro systems to study certain aspects of osteoinduction. The use of fully pluripotent embryonic stem cells in combination with osteoinductive biomaterials, in a well controlled cell culture medium might give valuable information of molecular pathways involved in the process of osteoinduction by biomaterials.

Finally, further understanding of the effect of osteoinductivity at an orthotopic implantation site is the most important goal for the future research. Clinically relevant orthotopic implantations will give the answers to most important questions concerning the use of osteoinductive biomaterials for bone replacement and support of bone regeneration.

## Summary

The improvement in the quality of life and consequent increase of life expectancy are accompanied by the expanding demand for the repair of damaged and degraded organs and tissues. Bone tissue regeneration remains an important challenge in the field of orthopaedic- and maxillofacial surgery. Spinal fusions and repairs of bone defects caused by traumas, tumors, infections, biochemical disorders and abnormal skeletal development, are some examples of the frequently performed surgeries in the clinic. For most of these surgeries, there is a great need for grafting materials. In general, grafting materials can be divided into the categories of natural bone grafts (autograft, allograft, xenograft), synthetic bone graft substitutes (metals, ceramics, polymers and composites) and tissue-engineered hybrids (cell-based, bioactive molecules-based). Because of the drawbacks of natural bone grafts and tissue-engineering techniques, such as additional invasive surgical procedure which may lead to donor site morbidity, chronic post-operative pain, hypersensitivity and infection, there is a great need for further development of synthetic bone graft substitutes that are largely available, do not cause antigenic response and can easily be tailored depending on the intended application. Future research should focus on improving biological performance of synthetic bone graft substitutes, which is today still inferior to that of autografts. Fully synthetic “intelligent” biomaterials should be able to perform at least as good as autologous bone graft. A group of potentially “intelligent” biomaterials are osteoinductive biomaterials.

Osteoinduction can be defined as the induction of the undifferentiated osteoprogenitor cells that are not yet committed to the osteogenic lineage to form osteoprogenitor cells. In other words, osteoinduction is bone formation at ectopic sites such as muscle and subcutis. It has been known for a long time that certain growth factors, such as Bone Morphogenetic Proteins have the ability to induce ectopic bone formation. Recent research has shown that some synthetic biomaterials, which initially do not contain Bone Morphogenetic Proteins, also possess the ability to induce ectopic bone growth. It is hypothesized that osteoinductive biomaterials are better for bone grafts than the non-osteoinductive biomaterials. So far, the exact mechanism underlying osteoinduction by

biomaterials is largely unknown. Furthermore, the effect of osteoinductive potential of biomaterials on their performance orthotopically has not been fully investigated yet.

This thesis had two main goals: (I) to investigate parameters influencing osteoinductive potential of biomaterials in order to unravel the mechanism underlying osteoinduction and (II) to investigate performance of osteoinductive biomaterials orthotopically in order to get insight into their clinical relevance.

In Chapter 2 we reviewed different *in vitro* models that are used in bone research in general, and in bone research involving biomaterials in particular. It has been shown that *in vitro* organ- and cell culture systems, which were initially developed to study influence of growth factors, hormones and cytokines on cell behavior, are not always adequate for bone research involving biomaterials. Biomaterials might interfere with cell culture medium, which is an undesired effect, if similar interaction is not expected to occur *in vivo*. Besides, various cell types which are used in *in vitro* systems are often not representative for the *in vivo* situation, in particular when complex biological phenomena such as osteoinduction are studied. Because of these drawbacks of simplified *in vitro* models, in the present thesis, we used *in vivo* models in goats to study mechanisms and clinical relevance of osteoinductive biomaterials.

In Chapter 3 it was described that biomimetic octacalcium phosphate coating could be applied on different porous materials, independent on their chemistry, and that therewith the osteoinductive properties of these materials were improved.

The main conclusion from the study described in Chapter 4 was that the presence of micropores, in addition to the presence of macropores, is a prerequisite for osteoinduction by biomaterials, and that this phenomenon is independent on the material chemistry.

Chapter 5 showed that, for each type of material, there is an optimal specific surface area at which the osteoinductive potential is highest. We also described the influence of the implant size on the material osteoinductive potential, i.e. the larger the implant, the more bone is induced and that the same material is “more osteoinductive” intramuscularly than subcutaneously. Finally, in Chapter 5 it was demonstrated that, during implantation, on the surface of osteoinductive ceramic more dissolution took place, followed by the reprecipitation of the carbonated-apatite layer and possible coprecipitation of the organic compounds such as endogenous proteins, than on the

surface of non-osteoinductive ceramic. This finding might be explained by the difference in the specific surface area between osteoinductive and non-osteoinductive ceramic.

Chapter 6 showed that the presence of calcium-phosphates in the form of coating on metallic implants or in the form of bulk ceramic had a significantly positive effect on the bone healing process as compared to the uncoated metal. Whether this positive effect is due to the fact that both OCP coating on metallic implants and BCP ceramic used in this study were osteoinductive is hard to conclude, as the uncoated metallic implants were not only non-osteoinductive, but their osteoconductive properties were limited as well.

Finally, in Chapter 7 we demonstrated a significantly positive effect of an osteoinductive ceramic in a clinically-relevant critical-sized defect as compared to a non-osteoinductive ceramic with the same chemical composition.

In conclusion, the results described in the present thesis shed light upon parameters influencing osteoinductive properties of biomaterials, which is a step forward towards unraveling the mechanism underlying the phenomenon of osteoinduction. Furthermore, this thesis demonstrates that osteoinductive biomaterials have the potency of being an adequate substitute for autograft in bone tissue regeneration.

## Samenvatting

De verbetering van de gezondheidszorg en daarmee samenhangende toename van de leeftijd heeft als gevolg dat er steeds groter wordende behoefte is aan behandeling van beschadigde en zieke organen die veroorzaakt worden door slijtage. Reconstructie van botweefsel is een belangrijke uitdaging op het gebied van orthopedische- en kaakchirurgie. Wervelfusies en reparatie van botdefecten veroorzaakt door trauma's, tumoren, infecties, biochemische aandoeningen en abnormale skeletontwikkeling zijn voorbeelden van vaak uitgevoerde operaties. Voor de uitvoering van dit type chirurgie is er een grote behoefte aan vervangende botimplantaten. Op dit moment zijn er drie soorten veel gebruikte botimplantaten: natuurlijke implantaten (lichaamseigen bot, bot van andere (menselijke) donoren en bot van donoren van een andere soort), kunstmatige implantaten (metalen, keramieken, polymeren en composietmaterialen) en tissue-engineered botimplantaten (synthetische dragers gecombineerd met lichaamseigen cellen en/of bioactieve stoffen). Wegens de nadelen van natuurlijke- en tissue-engineered botimplantaten, zoals de extra operatie voor het wegnemen van bot of beenmerg, mogelijk gevolgd door chronische post-operatieve pijn, hypersensitiviteit en infecties, is er een grote behoefte aan kunstmatige materialen die onbeperkt beschikbaar zijn, niet afgestoten worden door het lichaam, gebruikt kunnen worden voor verschillende doeleinden en hetzelfde effect kunnen bereiken als de voornoemde alternatieven. Toekomstig onderzoek zou zich moeten richten op het verbeteren van biologische prestaties van kunstmatige materialen, die op dit moment nog inferieur zijn aan die van natuurlijke botimplantaten. Met andere woorden, er is behoefte aan volledig synthetische "intelligente" materialen die in het lichaam dezelfde prestatie kunnen leveren als bijvoorbeeld lichaamseigen bot. Een groep potentieel "intelligente" kunstmatige materialen zijn osteoinductieve biomaterialen.

Osteoinductie kan gedefinieerd worden als de inductie van ongedifferentieerde cellen die nog niet gecommitteerd zijn aan de osteogene lijn om osteogene cellen te vormen. In andere woorden, osteoinductie is het vermogen tot botvorming in een ectopische (niet-botrijke) omgeving zoals in de spier of onderhuids. Het is al langere tijd bekend dat sommige groeifactoren, zoals Bone Morphogenetic Proteins (BMPs), het vermogen hebben om botvorming te kunnen induceren in een ectopische omgeving. Recentelijk

onderzoek heeft aangetoond dat ook bepaalde kunstmatige biomaterialen, die initieel geen BMPs of andere groeifactoren bevatten, ook ectopische botvorming kunnen induceren. Onze verwachting is dat osteoinductieve materialen betere botimplantaten zijn dan de niet-osteoinductieve materialen vanwege de voornoemde eigenschap. Het is tot nu toe nog niet volledig bekend wat het onderliggende mechanisme van osteoinductie door biomaterialen is. Bovendien is het onduidelijk wat voor effect de mate van osteoinductiviteit van een materiaal heeft op de prestatie van dit materiaal in een orthotopische (botrijke) omgeving.

Ons onderzoek had twee hoofddoelen: (I) het onderzoeken van de parameters die van invloed zijn op het osteoinductieve potentieel van biomaterialen om de onderliggende mechanismen van osteoinductie te ontrafelen en (II) inzicht te krijgen in de prestaties van osteoinductieve biomaterialen in een orthotopische omgeving en de daarmee samenhangende klinische relevantie.

In Hoofdstuk 2 hebben we een overzicht gegeven van verschillende *in vitro* modellen die gebruikt worden in het onderzoek naar bot in het algemeen en in het onderzoek naar biomaterialen voor botvervanging in het bijzonder. We hebben laten zien dat sommige orgaan- en celkweek *in vitro* modellen, die oorspronkelijk ontwikkeld waren voor het bestuderen van effecten van hormonen en groeifactoren op het gedrag van botcellen, niet altijd optimaal zijn voor het botonderzoek met betrekking tot biomaterialen. Biomaterialen gaan soms een interactie aan met het gebruikte celkweekmedium in een *in vitro* modelsysteem. Dit kan ongewenste effecten hebben wanneer een soortgelijke interactie niet aanwezig is *in vivo*. Daarnaast zijn de cellen die in *in vitro* celkweek systemen gebruikt worden niet altijd representatief voor de, meer complexe, *in vivo* situatie, in het bijzonder wanneer men complexe biologische fenomenen zoals osteoinductie bestudeert. Wegens deze nadelen van de *in vitro* systemen hebben we in ons onderzoek gebruik gemaakt van een *in vivo* model in geiten om de mechanismen die een rol spelen bij osteoinductie door biomaterialen en hun klinische relevantie te kunnen bestuderen.

In Hoofdstuk 3 wordt beschreven dat biomimetische octacalcium fosfaat coatings gemaakt kunnen worden op verschillende soorten kunstmatige materialen en dat daardoor hun osteoinductieve eigenschappen verbeterd kunnen worden.

In Hoofdstuk 4 wordt beschreven dat microporiën (poriën met een diameter kleiner dan 10 micrometer), naast de aanwezigheid van macroporiën, een vereiste zijn voor osteoinductie door biomaterialen, en dat deze eigenschap onafhankelijk is van de chemische samenstelling van het materiaal.

Hoofdstuk 5 toont aan dat voor ieder materiaalsoort, er een optimale soortelijke oppervlakte bestaat waarbij de osteoinductieve potentie van een materiaal het hoogst is. Verder wordt duidelijk gemaakt dat de osteoinductieve potentie van een materiaal afhankelijk is van de grootte van een implantaat: hoe groter de implantaat, hoe meer bot geïnduceerd kan worden. Tevens blijkt er een verschil te bestaan in de hoeveelheid geïnduceerd bot afhankelijk van de plaats van implantatie: er wordt meer bot gevormd in een intramusculaire dan in een subcutane omgeving. Als laatste maakt hoofdstuk 5 duidelijk dat gedurende een implantatie periode aan het oppervlak van osteoinductieve keramieken meer dissolutie van calcium- en fosfaat ionen plaatsvindt, wat weer wordt gevolgd door de reprecipitatie van een biologisch gecarboneerde apatiet laag en coprecipitatie van endogene organische stoffen, dan aan het oppervlak de niet-osteinductieve keramieken. Deze bevinding kan worden verklaard door het verschil in de grootte van de soortelijke oppervlakte tussen osteoinductieve en niet-osteinductieve keramieken.

In Hoofdstuk 6 tonen we aan dat de aanwezigheid van calciumfosfaat in de vorm van een coating op het oppervlak van poreuze metalen of keramieken een significant positief effect heeft op het botgenezingsproces in vergelijking met de ongecoate materialen. Een belangrijk voordeel van biomimetische coatings is dat het een relatief eenvoudige methode is die gebruikt kan worden om biologische prestaties van verschillende materialen te verbeteren.

Uiteindelijk, in Hoofdstuk 7 hebben we aangetoond dat osteoinductieve keramieken significant beter presteren dan niet-osteinductieve keramieken in een botdefect van klinisch relevant grootte.

Concluderend, met dit onderzoek zijn we weer een stap dichterbij het ontrafelen van de mechanismen die een rol spelen bij het fenomeen osteoinductie gekomen. Daarnaast heeft ons onderzoek laten zien dat osteoinductieve materialen de potentie hebben adequate vervangers van lichaamseigen bot worden.

## Kratki sadržaj

Poboljšanje životnih uslova i doslijedna prognoza dužeg života nose sa sobom povećanu potrebu za popravkom oštećenih i degradiranih organa i tkiva. Rekonstrukcija kostiju je važan izazov u ortopedskoj i stomatološkoj hirurgiji. Spajanje kičmenih grebena, rekonstrukcija oštećenja kostiju izazvanih ozlijedom, rakom, infekcijama, hormonskim poremećajima i nepravilnim razvojem skeleta su primjeri često izvedenih operacija. Za većinu navedenih operacija potrebni su implantati. Implantati koji se često koriste mogu biti svrstani u tri grupe: prirodni (kost iz vlastitog tijela, iz tijela drugog (ljudskog) darodavca ili iz tijela životinje), sintetični (metalni, keramički, plastični ili mješavine) i "tissue-engineered" (kombinacija sintetičnih materijala sa ćelijama pacijenta ili sa bioaktivnim molekulama). Zbog nedostataka prirodnih i "tissue-engineered" implantata, kao što su dodatna operacija koja može uzrokovati hronični bol i infekcije, postoji velika potreba za sintetičnim materialima koji su lako dostupni, prihvaćeni u tijelu i mogu biti korišteni za različite namijene. Buduća ispitivanja se trebaju koncentrisati na poboljšanje bioloških dostignuća sintetičnih implantata, koji su još uvijek lošiji od dostignuća prirodnih implantata. Potpuno sintetični "inteligentni" implantati bi trebali imati dostignuće koje je jednako onom prirodnih implantata. Vrsta potencijalno "inteligentnih" materijala su takozvani osteoinduktivni biomaterijali.

Jednostavna definicija osteoindukcije je razvoj kostiju tamo gdje koštane ćelije nisu prisutne (na primjer u mišićima ili ispod kože). Već je godinama poznato da su određene molekule, kao na primjer "Bone Morphogenetic Proteins" (BMP) u mogućnosti da otpočnu razvoj kostiju u odsustvu kosti i njegovih ćelija. Skorašnje istrage su pokazale da i neki sintetični materijali, koji u početku ne posjeduju BMP, su takođe u mogućnosti da otpočnu razvoj kostiju, na primjer u mišićima. Naša hipoteza je da materijali, koji mogu da započnu razvoj kostiju tamo gdje su kosti odsutne (u mišićima ili pod kožom), bi trebali omogućiti brži i veći razvoj nove kosti tamo gdje postoji nedostatak zbog povrede ili raka. Tačni mehanizam koji leži na osnovi fenomena osteoindukcije biomaterijalima je još uvijek nepoznat. Takođe nije potpuno istraženo da li osteoinduktivni materijali uistinu prouzrokuju bolji razvoj kostiju nego materijali koji nisu osteoinduktivni.



Glavni ciljevi ove disertacije su: (I) istražiti koje osobine materijala imaju uticaj na njihov osteoinduktivni potencijal da bismo bolje razumjeli mehanizam fenomena osteoindukcije i (II) istražiti da li osteoinduktivni materijali prouzrokuju bolji razvoj nove kosti nego materijali koji nisu osteoinduktivni, da bismo mogli predskazati značaj osteoinduktivnih materijala u liječenju pacijenata sa oboljenjima kostiju.

U Poglavlju 2 smo opisali različite in vitro (izvan tijela) modele koji se mogu koristiti za opštu istragu kostiju i za specifičnu istragu koja obuhvata biomaterijale. Pokazali smo da postojeći in vitro modeli, koji su u početku bili stvoreni za istraživanje uticaja hormona i drugih razvojnih faktora na ponašanje koštanih ćelija, nisu uvijek adekvatni za istragu koja obuhvata biomaterijale. Biomaterijali mogu reagovati sa sredstvom u kojem ćelije rastu, a ove reakcija je nepoželjna, ukoliko nije očekivana u tijelu (in vivo). Pored toga, ćelije koje se koriste za istraživanja in vitro često nisu reprezentativne za ono što se dešava in vivo, posebno u istragama kompleksnih bioloških fenomena, kao što je osteoindukcija. Zbog navedenih nedostataka in vitro modela, mi smo u ovoj disertaciji koristili koze kao in vivo model za istragu mehanizma i kliničnog značaja osteoinduktivnih biomaterijala.

U Poglavlju 3 je opisano da sloj oktakalcijum-fosfata koji se može nanijeti na površinu različitih materijala bez obzira na njihov hemijski sadržaj poboljšava osteoinduktivne osobine biomaterijala.

Najvažniji zaključak iz Poglavlja 4 je da prisutvo mikropora (pora sa prečnikom manjim od 10 mikrometara) je, zajedno sa prisustvom većih makropora, preduslov za osteoindukciju uzročenu biomaterijalima, i da je ova osobina neovisna o hemijskom sadržaju biomaterijala.

U Poglavlju 5 je opisano da, za svaku vrstu materijala, postoji optimalna specifična površina (u  $m^2/g$ ) pri kojoj je osteoinduktivni potencijal materijala najveći. Pored toga je u Poglavlju 5 opisano da količina nove kosti koja je započeta osteoinduktivnim materijalom zavisi od veličine implantata: u većim implantatima raste relativno više kosti nego u manjim implantatima. Količina nove kosti takođe zavisi od mjesta gdje je material usađen: u mišićima raste više kosti nego pod kožom. Konačno, u Poglavlju 5 je opisano da je, za vrijeme implantacije, na površini osteoinduktivnih materijala više rastvaranja kalcijum i fosfat jonova nego na površini materijala koji nisu osteoinduktivni.

Ovi rastvoreni joni stoga stvaraju sloj novog, takozvanog, karbonisanog apatita koji je moguće odgovoran za začetak rasta kosti.

U Poglavlju 6 je opisano da prisutnost kalcijum fosfata u obliku sloja na površini metalnog implantata ili u obliku keramike, poboljšava zacijeljenje defekta kosti u poređenju sa metalom bez kalcijum fosfata.

Konačno, u Poglavlju 7 je dokazano da osteoinduktivna keramika uzrokuje bitno bolje zacijeljenje kosti nego jednaka, ali neosteoinduktivna keramika, u velikom, klinički važnom defektu kosti.

U zaključku, rezultati opisani u ovoj disertaciji su pokazali nove osobine materijala koji imaju uticaj na njihov osteoinduktivni potencijal. Na ovaj način smo došli korak bliže potpunom razumijevanju mehanizma osteoindukcije. Osim toga, ova teza je pokazala da osteoinduktivni biomaterijali imaju potenciju postati adekvatan zamjenik prirodnih implantata u liječenju bolesti kostiju.

---

## References

- [1] Lowenstam HA and Weiner S. "On biomineralization". Oxford University Press, New York, USA. **1989**; 336.
- [2] Addadi L and Weiner S. Control and design principles in biological mineralization. *Angew Chem Int Ed Engl*, **1992**; 31: 153-69.
- [3] Du C, Falini G, Fermani S, Abbott C, and Moradian-Oldak J. Supramolecular assembly of amelogenin nanospheres into birefringent microribbons. *Science*, **2005**; 307(5714): 1450-4.
- [4] Boskey AL. Matrix proteins and mineralization: an overview. *Connect Tissue Res*, **1996**; 35(1-4): 357-63.
- [5] Bonucci E. Role of collagen fibrils in calcification, in "Calcification in biological systems", E Bonucci, Editor. CRC Press, Boca Raton, USA. **1992**; 19-40.
- [6] Green M, Isaac DH, and Jenkins GM. Bone microstructure by collagenase etching. *Biomaterials*, **1985**; 6(3): 150-2.
- [7] Fawcett DW. Bone, in "A textbook of histology", W Bloom and DW Fawcett, Editors. W.B. Saunders Company, Philadelphia, USA. **1986**; 199-238.
- [8] Marks SC and Hermey DC, Jr. The structure and development of bone, in "Principles of bone biology", JP Bilezikian, LG Raisz, and GA Rodan, Editors. Academic Press, San Diego, USA. **1996**; 3-14.
- [9] Derx P, Nigg AL, Bosman FT, Birkenhager-Frenkel DH, Houtsmuller AB, Pols HA, and van Leeuwen JP. Immunolocalization and quantification of noncollagenous bone matrix proteins in methylmethacrylate-embedded adult human bone in combination with histomorphometry. *Bone*, **1998**; 22(4): 367-73.
- [10] Rey C. Calcium phosphate biomaterials and bone mineral. Differences in composition, structures and properties. *Biomaterials*, **1990**; 11: 13-5.
- [11] Rey C, Collins B, Goehl T, Dickson MR, and Glimcher MJ. The carbonate environment in bone mineral: a resolution-enhanced fourier transform infrared spectroscopy study. *Calcif Tissue Int*, **1989**; 45: 157-64.
- [12] Rey C, Lian J, Grynblas MD, Shapiro F, Zylberberg L, and Glimcher MJ. Nonapatitic environments in bone mineral: FT-IR detection, biological properties and changes in several disease states. *Connect Tissue Res*, **1989**; 21: 267-73.

- [13] Yaszemski MJ, Payne RG, Hayes WC, Langer R, and Mikos AG. Evolution of bone transplantation: molecular, cellular and tissue strategies to engineer human bone. *Biomaterials*, **1996**; 17(2): 175-85.
- [14] Brown KL and Cruess RL. Bone and cartilage transplantation in orthopaedic surgery. A review. *J Bone Joint Surg Am*, **1982**; 64(2): 270-9.
- [15] de Boer HH. The history of bone grafts. *Clin Orthop*, **1988**; 226(226): 292-8.
- [16] Coombes AG and Meikle MC. Resorbable synthetic polymers as replacements for bone graft. *Clin Mater*, **1994**; 17(1): 35-67.
- [17] Damien CJ and Parsons JR. Bone graft and bone graft substitutes: a review of current technology and applications. *J Appl Biomater*, **1991**; 2(3): 187-208.
- [18] Lane JM, Tomin E, and Bostrom MP. Biosynthetic bone grafting. *Clin Orthop*, **1999**; 367 Suppl: S107-17.
- [19] Urist MR. Bone: formation by autoinduction. *Science*, **1965**; 150(698): 893-9.
- [20] Cornell CN and Lane JM. Current understanding of osteoconduction in bone regeneration. *Clin Orthop*, **1998**; 355 Suppl: S267-73.
- [21] Prolo DJ and Rodrigo JJ. Contemporary bone graft physiology and surgery. *Clin Orthop*, **1985**; 200: 322-42.
- [22] Cowley SP and Anderson LD. Hernias through donor sites for iliac-bone grafts. *J Bone Joint Surg Am*, **1983**; 65(7): 1023-5.
- [23] Arrington ED, Smith WJ, Chambers HG, Bucknell AL, and Davino NA. Complications of iliac crest bone graft harvesting. *Clin Orthop*, **1996**; 329: 300-309.
- [24] Younger EM and Chapman MW. Morbidity at bone graft donor sites. *J Orthop Trauma*, **1989**; 3(3): 192-5.
- [25] Brantigan JW, Cunningham BW, Warden K, McAfee PC, and Steffee AD. Compression strength of donor bone for posterior lumbar interbody fusion. *Spine*, **1993**; 18(9): 1213-21.
- [26] Urist MR, Silverman BF, Buring K, Dubuc FL, and Rosenberg JM. The bone induction principle. *Clin Orthop*, **1967**; 53: 243-83.
- [27] Lane JM and Sandhu HS. Current approaches to experimental bone grafting. *Orthop Clin North Am*, **1987**; 18(2): 213-25.

- [28] Oikarinen J and Korhonen LK. The bone inductive capacity of various bone transplanting materials used for treatment of experimental bone defects. *Clin Orthop*, **1979**; 140: 208-15.
- [29] Anderson M, Dhert W, de Bruijn J, Dalmeijer R, Leenders H, van Blitterswijk C, and Verbout A. Critical size defect in the goat's os ilium. A model to evaluate bone grafts and substitutes. *Clin Orthop*, **1999**; 364: 231-9.
- [30] Oklund SA, Prolo DJ, Gutierrez RV, and King SE. Quantitative comparisons of healing in cranial fresh autografts, frozen autografts and processed autografts, and allografts in canine skull defects. *Clin Orthop*, **1986**; 205: 269-91.
- [31] Progress in biomedical engineering, 4: Definitions in Biomaterials. *Trans Consensus Conference of the European Society for Biomaterials*. **1986**. 67.
- [32] LeGeros RZ. Properties of osteoconductive biomaterials: calcium phosphates. *Clin Orthop*, **2002**; 395: 81-98.
- [33] Ducheyne P and Qiu Q. Bioactive ceramics: the effect of surface reactivity on bone formation and bone cell function. *Biomaterials*, **1999**; 20(23-24): 2287-303.
- [34] Hench LL and Wilson J. Surface-active biomaterials. *Science*, **1984**; 226(4675): 630-6.
- [35] Tengvall P and Lundstrom I. Physico-chemical considerations of titanium as a biomaterial. *Clin Mater*, **1992**; 9(2): 115-34.
- [36] Hildebrand HF and Hornez JC. Biological response and biocompatibility, in "Metals and biomaterials", JA Helsen and HJ Breme, Editors. John Wiley & Sons, Chichester, UK. **1998**; 265-290.
- [37] Agrawal CM. Reconstructing the human body using biomaterials. *JOM*, **1998**; 50: 31-35.
- [38] Turner TM, Sumner DR, Urban RM, Rivero DP, and Galante JO. A comparative study of porous coatings in a weight-bearing total hip-arthroplasty model. *J Bone Joint Surg Am*, **1986**; 68(9): 1396-409.
- [39] Zardiackas LD, Teasdall RD, Black RJ, Jones GS, St John KR, Dillon LD, and Hughes JL. Torsional properties of healed canine diaphyseal defects grafted with a fibrillar collagen and hydroxyapatite/tricalcium phosphate composite. *J Appl Biomater*, **1994**; 5(4): 277-83.

- [40] Guan L and Davies JE. Preparation and characterization of a highly macroporous biodegradable composite tissue engineering scaffold. *J Biomed Mater Res A*, **2004**; 71(3): 480-7.
- [41] Zhang R and Ma PX. Poly(alpha-hydroxyl acids)/hydroxyapatite porous composites for bone-tissue engineering. I. Preparation and morphology. *J Biomed Mater Res*, **1999**; 44(4): 446-55.
- [42] Havelin LI, Engesaeter LB, Espehaug B, Furnes O, Lie SA, and Vollset SE. The Norwegian Arthroplasty Register: 11 years and 73,000 arthroplasties. *Acta Orthop Scand*, **2000**; 71(4): 337-53.
- [43] Ducheyne P, van Raemdonck W, Heughebaert JC, and Heughebaert M. Structural analysis of hydroxyapatite coatings on titanium. *Biomaterials*, **1986**; 7(2): 97-103.
- [44] Ong JL, Lucas LC, Lacefield WR, and Rigney ED. Structure, solubility and bond strength of thin calcium phosphate coatings produced by ion beam sputter deposition. *Biomaterials*, **1992**; 13(4): 249-54.
- [45] Ben-Nissan B, Chai CS, and Gross KA. Effect of solution aging on sol-gel hydroxyapatite coatings. *Bioceramics*, **1997**; 10: 175-178.
- [46] Du C, Klasens P, Haan RE, Bezemer J, Cui FZ, de Groot K, and Layrolle P. Biomimetic calcium phosphate coatings on Polyactive 1000/70/30. *J Biomed Mater Res*, **2002**; 59: 535-546.
- [47] Leeuwenburgh S, Layrolle P, Barrere F, de Bruijn J, Schoonman J, van Blitterswijk CA, and de Groot K. Osteoclastic resorption of biomimetic calcium phosphate coatings in vitro. *J Biomed Mater Res*, **2001**; 56(2): 208-15.
- [48] Liu Y, Hunziker EB, Randall NX, de Groot K, and Layrolle P. Proteins incorporated into biomimetically prepared calcium phosphate coatings modulate their mechanical strength and dissolution rate. *Biomaterials*, **2003**; 24(1): 65-70.
- [49] Liu Y, Hunziker, E. B., Layrolle, P., de Bruijn, J. D. and de Groot, K. Bone morphogenetic protein 2 incorporated into biomimetic coatings retains its biological activity. *Tissue Eng*, **2004**; 10(1-2): 101-8.
- [50] Blokhuis TJ, Wippermann BW, den Boer FC, van Lingen A, Patka P, Bakker FC, and Haarman HJ. Resorbable calcium phosphate particles as a carrier material

- for bone marrow in an ovine segmental defect. *J Biomed Mater Res*, **2000**; 51(3): 369-75.
- [51] Boden SD, Martin GJ, Jr., Morone M, Ugbo JL, Titus L, and Hutton WC. The use of coralline hydroxyapatite with bone marrow, autogenous bone graft, or osteoinductive bone protein extract for posterolateral lumbar spine fusion. *Spine*, **1999**; 24(4): 320-7.
- [52] Zdeblick TA, Cooke ME, Kunz DN, Wilson D, and McCabe RP. Anterior cervical discectomy and fusion using a porous hydroxyapatite bone graft substitute. *Spine*, **1994**; 19(20): 2348-57.
- [53] Langer R and Vacanti JP. Tissue engineering. *Science*, **1993**; 260(5110): 920-6.
- [54] Kirker-Head CA. Potential applications and delivery strategies for bone morphogenetic proteins. *Adv Drug Deliv Rev*, **2000**; 43(1): 65-92.
- [55] Johnson EE, Urist MR, and Finerman GA. Repair of segmental defects of the tibia with cancellous bone grafts augmented with human bone morphogenetic protein. A preliminary report. *Clin Orthop*, **1988**(236): 249-57.
- [56] Geesink RG, Hoefnagels NH, and Bulstra SK. Osteogenic activity of OP-1 bone morphogenetic protein (BMP-7) in a human fibular defect. *J Bone Joint Surg Br*, **1999**; 81(4): 710-8.
- [57] Johnson EE and Urist MR. Human bone morphogenetic protein allografting for reconstruction of femoral nonunion. *Clin Orthop*, **2000**; 371: 61-74.
- [58] Nefussi JR, Brami G, Modrowski D, Oboeuf M, and Forest N. Sequential expression of bone matrix proteins during rat calvaria osteoblast differentiation and bone nodule formation in vitro. *J Histochem Cytochem*, **1997**; 45(4): 493-503.
- [59] Wada Y, Kataoka H, Yokose S, Ishizuya T, Miyazono K, Gao YH, Shibasaki Y, and Yamaguchi A. Changes in osteoblast phenotype during differentiation of enzymatically isolated rat calvaria cells. *Bone*, **1998**; 22(5): 479-85.
- [60] Miura Y and O'Driscoll SW. Culturing periosteum in vitro: the influence of different sizes of explants. *Cell Transplant*, **1998**; 7(5): 453-7.
- [61] Takushima A, Kitano Y, and Harii K. Osteogenic potential of cultured periosteal cells in a distracted bone gap in rabbits. *J Surg Res*, **1998**; 78(1): 68-77.

- [62] Robey PG and Termine JD. Human bone cells in vitro. *Calcif Tissue Int*, **1985**; 37(5): 453-60.
- [63] Gundle R, Joyner CJ, and Triffitt JT. Interactions of human osteoprogenitors with porous ceramic following diffusion chamber implantation in a xenogeneic host. *J Mater Sci Mater Med*, **1997**; 8(8): 519-23.
- [64] Bruder SP and Fox BS. Tissue engineering of bone. Cell based strategies. *Clin Orthop*, **1999**; 367 Suppl: S68-83.
- [65] Doherty MJ, Ashton BA, Walsh S, Beresford JN, Grant ME, and Canfield AE. Vascular pericytes express osteogenic potential in vitro and in vivo. *J Bone Miner Res*, **1998**; 13(5): 828-38.
- [66] Owen M. Marrow stromal stem cells. *J Cell Sci Suppl*, **1988**; 10: 63-76.
- [67] Ohgushi H and Okumura M. Osteogenic capacity of rat and human marrow cells in porous ceramics. Experiments in athymic (nude) mice. *Acta Orthop Scand*, **1990**; 61(5): 431-4.
- [68] Friedenstein AJ, Chailakhyan RK, and Gerasimov UV. Bone marrow osteogenic stem cells: in vitro cultivation and transplantation in diffusion chambers. *Cell Tissue Kinet*, **1987**; 20(3): 263-72.
- [69] Maniopoulos C, Sodek J, and Melcher AH. Bone formation in vitro by stromal cells obtained from bone marrow of young adult rats. *Cell Tissue Res*, **1988**; 254(2): 317-30.
- [70] Beresford JN. Osteogenic stem cells and the stromal system of bone and marrow. *Clin Orthop*, **1989**(240): 270-80.
- [71] Muschler GF, Boehm C, and Easley K. Aspiration to obtain osteoblast progenitor cells from human bone marrow: the influence of aspiration volume. *J Bone Joint Surg Am*, **1997**; 79(11): 1699-709.
- [72] Allay J, Dennis J, Haynesworth S, Majumdar M, Clapp D, Shultz D, Caplan A, and Gerson S. LacZ and interleukin-3 expression in vivo after retroviral transduction of marrow-derived human osteogenic mesenchymal progenitors. *Hum Gene Ther*, **1997**; 8(12): 1417-27.
- [73] Friedenstein AJ, Latzinik NW, Grosheva AG, and Gorskaya UF. Marrow microenvironment transfer by heterotopic transplantation of freshly isolated and cultured cells in porous sponges. *Exp Hematol*, **1982**; 10(2): 217-27.



- [74] Bruder SP, Kurth AA, Shea M, Hayes WC, Jaiswal N, and Kadiyala S. Bone regeneration by implantation of purified, culture-expanded human mesenchymal stem cells. *J Orthop Res*, **1998**; 16(2): 155-62.
- [75] Cui Q, Ming Xiao Z, Balian G, and Wang GJ. Comparison of lumbar spine fusion using mixed and cloned marrow cells. *Spine*, **2001**; 26(21): 2305-10.
- [76] Krebsbach PH, Mankani MH, Satomura K, Kuznetsov SA, and Robey PG. Repair of craniotomy defects using bone marrow stromal cells. *Transplantation*, **1998**; 66(10): 1272-8.
- [77] Anselme K, Noel B, Flautre B, Blary MC, Delecourt C, Descamps M, and Hardouin P. Association of porous hydroxyapatite and bone marrow cells for bone regeneration. *Bone*, **1999**; 25(2 Suppl): 51S-54S.
- [78] Kruyt MC, de Bruijn JD, Wilson CE, Oner FC, van Blitterswijk CA, Verbout AJ, and Dhert WJ. Viable osteogenic cells are obligatory for tissue-engineered ectopic bone formation in goats. *Tissue Eng*, **2003**; 9(2): 327-36.
- [79] Kruyt MC, Dhert WJ, Oner C, van Blitterswijk CA, Verbout AJ, and de Bruijn JD. Optimization of bone-tissue engineering in goats. *J Biomed Mater Res*, **2004**; 69B(2): 113-20.
- [80] Kruyt MC, Dhert WJ, Yuan H, Wilson CE, van Blitterswijk CA, Verbout AJ, and de Bruijn JD. Bone tissue engineering in a critical size defect compared to ectopic implantations in the goat. *J Orthop Res*, **2004**; 22(3): 544-51.
- [81] Bruder SP, Kraus KH, Goldberg VM, and Kadiyala S. The effect of implants loaded with autologous mesenchymal stem cells on the healing of canine segmental bone defects. *J Bone Joint Surg Am*, **1998**; 80(7): 985-96.
- [82] Petite H, Viateau V, Bensaid W, Meunier A, de Pollak C, Bourguignon M, Oudina K, Sedel L, and Guillemain G. Tissue-engineered bone regeneration. *Nat Biotechnol*, **2000**; 18(9): 959-63.
- [83] Winn SR, Uludag H, and Hollinger JO. Carrier systems for bone morphogenetic proteins. *Clin Orthop*, **1999**; 367 Suppl: S95-106.
- [84] Boden SD. Bioactive factors for bone tissue engineering. *Clin Orthop*, **1999**; 367 Suppl: S84-94.

- [85] Hollinger JO, Uludag H, and Winn SR. Sustained release emphasizing recombinant human bone morphogenetic protein-2. *Adv Drug Deliv Rev*, **1998**; 31(3): 303-318.
- [86] Kruyt MC, Tissue engineering of bone: the applicability of cell-based strategies. *Thesis*, Department of Orthopaedics, University Medical Center Utrecht: Utrecht, The Netherlands. **2003**; 186.
- [87] Bertelsen A. Experimental investigations into post-foetal osteogenesis. *Acta Orthop Scand*, **1944**; 15: 139-181.
- [88] Huggins C. The formation of bone under the influence of epithelium of the urinary tract. *Arch Surg*, **1931**; 22: 377-408.
- [89] Urist MR and McLean FC. Osteogenetic potency and new-bone formation by induction in transplants to the anterior chamber of the eye. *J Bone Joint Surg Am*, **1952**; 34-A(2): 443-76.
- [90] Levander G. On the formation of new bone in bone transplantation. *Acta Chir Scand*, **1934**; 74: 425-426.
- [91] Urist MR, Grant TT, Lindholm TS, Mirra JM, Hirano H, and Finerman GA. Induction of new-bone formation in the host bed by human bone-tumor transplants in athymic nude mice. *J Bone Joint Surg Am*, **1979**; 61(8): 1207-16.
- [92] Bridges JB and Pritchard JJ. Bone and cartilage induction in the rabbit. *J Anat*, **1958**; 92(1): 28-38.
- [93] Friedenstein AY. Induction of bone tissue by transitional epithelium. *Clin Orthop Relat Res*, **1968**; 59: 21-37.
- [94] Urist MR and Strates BS. Bone morphogenetic protein. *J Dent Res*, **1971**; 50(6): 1392-406.
- [95] Urist MR, Granstein R, Nogami H, Svenson L, and Murphy R. Transmembrane bone morphogenesis across multiple-walled diffusion chambers. New evidence for a diffusible bone morphogenetic property. *Arch Surg*, **1977**; 112(5): 612-9.
- [96] Groeneveld EH and Burger EH. Bone morphogenetic proteins in human bone regeneration. *Eur J Endocrinol*, **2000**; 142(1): 9-21.

- [97] Kessler E, Takahara K, Biniaminov L, Brusel M, and Greenspan DS. Bone morphogenetic protein-1: the type I procollagen C-proteinase. *Science*, **1996**; 271(5247): 360-2.
- [98] Schmitt JM, Hwang K, Winn SR, and Hollinger JO. Bone morphogenetic proteins: an update on basic biology and clinical relevance. *J Orthop Res*, **1999**; 17(2): 269-78.
- [99] Wozney JM and Rosen V. Bone morphogenetic protein and bone morphogenetic protein gene family in bone formation and repair. *Clin Orthop Relat Res*, **1998**; 346: 26-37.
- [100] Wozney JM. Molecular biology of the Bone Morphogenetic Proteins, in "Bone grafts, derivatives and substitutes", MR Urist, BT O'Connor, and RG Burwell, Editors. Butterworth-Heinemann Ltd., Oxford, UK. **1994**; 397-406.
- [101] Reddi AH. Cell biology and biochemistry of endochondral bone development. *Coll Relat Res*, **1981**; 1(2): 209-26.
- [102] Sasano Y, Ohtani E, Narita K, Kagayama M, Murata M, Saito T, Shigenobu K, Takita H, Mizuno M, and Kuboki Y. BMPs induce direct bone formation in ectopic sites independent of the endochondral ossification in vivo. *Anat Rec*, **1993**; 236(2): 373-80.
- [103] Kuboki Y, Saito T, Murata M, Takita H, Mizuno M, Inoue M, Nagai N, and Poole AR. Two distinctive BMP-carriers induce zonal chondrogenesis and membranous ossification, respectively; geometrical factors of matrices for cell-differentiation. *Connect Tissue Res*, **1995**; 32(1-4): 219-26.
- [104] Liu Y, de Groot K, and Hunziker EB. BMP-2 liberated from biomimetic implant coatings induces and sustains direct ossification in an ectopic rat model. *Bone*, **2005**; 36(5): 745-57.
- [105] Caplan AL. Cartilage begets bone versus endochondral myelopoiesis. *Clin Orthop Relat Res*, **1990**; 261: 257-67.
- [106] Ripamonti U, Ma S, and Reddi AH. The critical role of geometry of porous hydroxyapatite delivery system in induction of bone by osteogenin, a bone morphogenetic protein. *Matrix*, **1992**; 12(3): 202-12.
- [107] Okubo Y, Bessho K, Fujimura K, Konishi Y, Kusumoto K, Ogawa Y, and Iizuka T. Osteoinduction by recombinant human bone morphogenetic protein-2 at

- intramuscular, intermuscular, subcutaneous and intrafatty sites. *Int J Oral Maxillofac Surg*, **2000**; 29(1): 62-6.
- [108] Yoshida K, Bessho K, Fujimura K, Kusumoto K, Ogawa Y, Tani Y, and Iizuka T. Osteoinduction capability of recombinant human bone morphogenetic protein-2 in intramuscular and subcutaneous sites: an experimental study. *J Craniomaxillofac Surg*, **1998**; 26(2): 112-5.
- [109] Aspenberg P, Wang E, and Thorngren KG. Bone morphogenetic protein induces bone in the squirrel monkey, but bone matrix does not. *Acta Orthop Scand*, **1992**; 63(6): 619-22.
- [110] Hosny M and Sharawy M. Osteoinduction in rhesus monkeys using demineralized bone powder allografts. *J Oral Maxillofac Surg*, **1985**; 43(11): 837-44.
- [111] Ripamonti U. The induction of bone in osteogenic composites of bone matrix and porous hydroxyapatite replicas: an experimental study on the baboon (*Papio ursinus*). *J Oral Maxillofac Surg*, **1991**; 49(8): 817-30.
- [112] Miyamoto S, Takaoka K, and Ono K. Bone induction in monkeys by bone morphogenetic protein. A trans-filter technique. *J Bone Joint Surg Br*, **1993**; 75(1): 107-10.
- [113] Marusic A, Katavic V, Grcevic D, and Lukic IK. Genetic variability of new bone induction in mice. *Bone*, **1999**; 25(1): 25-32.
- [114] Winter GD and Simpson BJ. Heterotopic bone formed in a synthetic sponge in the skin of young pigs. *Nature*, **1969**; 223(201): 88-90.
- [115] de Groot K. Some considerations about bone-induction. *Calc Tiss Res*, **1973**; 13: 335-7.
- [116] Klein C, de Groot K, Chen W, Li Y, and Zhang X. Osseous substance formation induced in porous calcium phosphate ceramics in soft tissues. *Biomaterials*, **1994**; 15(1): 31-4.
- [117] Ripamonti U. Osteoinduction in porous hydroxyapatite implanted in heterotopic sites of different animal models. *Biomaterials*, **1996**; 17(1): 31-5.
- [118] Yamasaki H. Heterotopic bone formation around porous hydroxyapatite ceramics in the subcutis of dogs. *Jpn J Oral Biol*, **1990**; 32: 190-192.

- [119] Yamasaki H and Sakai H. Osteogenic response to porous hydroxyapatite ceramics under the skin of dogs. *Biomaterials*, **1992**; 13(5): 308-12.
- [120] Zhang X. A study of porous block HA ceramics and its osteogenesis, in "Bioceramics and the human body", A Ravaglioli and A Krajewski, Editors. Elsevier Science, Amsterdam, The Netherlands. **1991**; 692-703.
- [121] Ripamonti U. The morphogenesis of bone in replicas of porous hydroxyapatite obtained from conversion of calcium carbonate exoskeletons of coral. *J Bone Joint Surg Am*, **1991**; 73(5): 692-703.
- [122] Vargervik K. Critical sites for new bone formation, in "Bone grafts and bone substitutes", MB Habal and AH Reddi, Editors. WB Saunders, Philadelphia, USA. **1992**; 112-120.
- [123] Pollick S, Shors EC, Holmes RE, and Kraut RA. Bone formation and implant degradation of coralline porous ceramics placed in bone and ectopic sites. *J Oral Maxillofac Surg*, **1995**; 53(8): 915-22.
- [124] Gosain AK, Song L, Riordan P, Amarante MT, Nagy PG, Wilson CR, Toth JM, and Ricci JL. A 1-year study of osteoinduction in hydroxyapatite-derived biomaterials in an adult sheep model: part I. *Plast Reconstr Surg*, **2002**; 109(2): 619-30.
- [125] Yuan H, Yang Z, Zou P, Li Y, and Zhang Z. An investigation of the osteoinduction of synthetic porous phase-pure hydroxyapatite ceramic. *Biomed Eng Appli Bas Com*, **1997**; 9: 274-278.
- [126] Yuan H, Yang Z, Li Y, Zhang Z, de Bruijn JD, and de Groot K. Osteoinduction by calcium phosphate biomaterials. *J Mater Sci Mater Med*, **1998**; 9: 723-726.
- [127] Yuan H, Kurashina K, de Bruijn JD, Li Y, de Groot K, and Zhang X. A preliminary study on osteoinduction of two kinds of calcium phosphate ceramics. *Biomaterials*, **1999**; 20(19): 1799-806.
- [128] Yuan H, de Bruijn JD, Li Y, Feng Z, Yang K, de Groot K, and Zhang X. Bone formation induced by calcium phosphate ceramics in soft tissue of dogs: a comparative study between alpha-TCP and beta-TCP. *J Mater Sci Mater Med*, **2001**; 12: 7-13.
- [129] Yuan H, van den Doel M, Li SH, van Blitterswijk CA, de Groot K, and de Bruijn JD. A comparison of the osteoinductive potential of two calcium phosphate

- ceramics implanted intramuscularly in goats. *J Mater Sci Mater Med*, **2002**; 13: 1271-5.
- [130] Le Nihouannen D, Daculsi G, Saffarzadeh A, Gauthier O, Delplace S, Pilet P, and Layrolle P. Ectopic bone formation by microporous calcium phosphate ceramic particles in sheep muscles. *Bone*, **2005**; 36(6): 1086-93.
- [131] Yuan H, Li Y, de Bruijn JD, de Groot K, and Zhang X. Tissue responses of calcium phosphate cement: a study in dogs. *Biomaterials*, **2000**; 21(12): 1283-90.
- [132] Barrere F, van der Valk CM, Dalmeijer RA, Meijer G, van Blitterswijk CA, de Groot K, and Layrolle P. Osteogenicity of octacalcium phosphate coatings applied on porous metal implants. *J Biomed Mater Res*, **2003**; 66A(4): 779-88.
- [133] de Bruijn JD, Yuan H, Dekker R, Layrolle P, de Groot K, and van Blitterswijk CA. Osteoinductive biomimetic calcium-phosphate coatings and their potential use as tissue-engineering scaffolds, in "Bone engineering", JE Davies, Editor. em squared, Toronto, Canada. **2000**; 421-431.
- [134] Yuan H, de Bruijn JD, Zhang X, van Blitterswijk CA, and de Groot K. Osteoinduction by porous alumina ceramic. *Trans European Conference on Biomaterials*. **2001**. 209.
- [135] Fujibayashi S, Neo M, Kim HM, Kokubo T, and Nakamura T. Osteoinduction of porous bioactive titanium metal. *Biomaterials*, **2004**; 25(3): 443-50.
- [136] Takemoto M, Fujibayashi S, Matsushita T, Suzuki J, Kokubo T, and Nakamura T. Osteoinductive ability of porous titanium implants following three types of surface treatment. *Trans 51st Annual Meeting of the Orthopaedic Research Society*. **2005**. Poster No: 0992.
- [137] Yuan H, de Bruijn JD, Zhang X, van Blitterswijk CA, and de Groot K. Bone induction by porous glass ceramic made from Bioglass (45S5). *J Biomed Mater Res*, **2001**; 58(3): 270-6.
- [138] Ripamonti U, Crooks J, and Kirkbride AN. Sintered porous hydroxyapatites with intrinsic osteoinductive activity: geometric induction of bone formation. *South African J Sci*, **1999**; 95: 335-343.

- [139] Ripamonti U. Smart biomaterials with intrinsic osteoinductivity: geometric control of bone differentiation, in "Bone engineering", JM Davies, Editor. em squared Corporation, Toronto, Canada. **2000**; 215-221.
- [140] Yuan H, Osteoinduction of calcium phosphates. *Thesis*, Biomaterials Research Group, University of Leiden: Leiden, The Netherlands. **2001**; 159.
- [141] Ohgushi H, Dohi Y, Tamai S, and Tabata S. Osteogenic differentiation of marrow stromal stem cells in porous hydroxyapatite ceramics. *J Biomed Mater Res*, **1993**; 27(11): 1401-7.
- [142] Ohgushi H, Goldberg VM, and Caplan AI. Heterotopic osteogenesis in porous ceramics induced by marrow cells. *J Orthop Res*, **1989**; 7(4): 568-78.
- [143] Yang Z, Yuan H, Tong W, Zou P, Chen W, and Zhang X. Osteogenesis in extraskelentially implanted porous calcium phosphate ceramics: variability among different kinds of animals. *Biomaterials*, **1996**; 17(22): 2131-7.
- [144] Goshima J, Goldberg VM, and Caplan AI. The osteogenic potential of culture-expanded rat marrow mesenchymal cells assayed in vivo in calcium phosphate ceramic blocks. *Clin Orthop Relat Res*, **1991**; 262: 298-311.
- [145] Reddi AH. Regulation of cartilage and bone differentiation by bone morphogenetic proteins. *Curr Opin Cell Biol*, **1992**; 4(5): 850-5.
- [146] Reddi AH. Bone and cartilage differentiation. *Curr Opin Genet Dev*, **1994**; 4(5): 737-44.
- [147] Wozney JM. The bone morphogenetic protein family and osteogenesis. *Mol Reprod Dev*, **1992**; 32(2): 160-7.
- [148] Yuan H, de Bruijn JD, Zhang X, van Blitterswijk CA, and de Groot K. Use of an osteoinductive biomaterial as a bone morphogenetic protein carrier. *J Mater Sci Mater Med*, **2001**; 12(9): 761-6.
- [149] Toth JM, Lynch KL, and Hackbarth DA. Ceramic-induced osteogenesis following subcutaneous implantation of calcium phosphates. *Bioceramics*, **1993**; 6: 9-13.
- [150] Shehab D, Elgazzar AH, and Collier BD. Heterotopic ossification. *The Journal of Nuclear Medicine*, **2002**; 43(3): 346-53.
- [151] Mohler ER, 3rd, Gannon F, Reynolds C, Zimmerman R, Keane MG, and Kaplan FS. Bone formation and inflammation in cardiac valves. *Circulation*, **2001**; 103(11): 1522-8.

- [152] Kaplan FS, Glaser DL, Hebel N, and Shore EM. Heterotopic ossification. *J Am Acad Orthop Surg*, **2004**; 12(2): 116-25.
- [153] Mahboubi S, Glaser DL, Shore EM, and Kaplan FS. Fibrodysplasia ossificans progressiva. *Pediatr Radiol*, **2001**; 31(5): 307-14.
- [154] Kaplan FS and Shore EM. Progressive osseous heteroplasia. *J Bone Miner Res*, **2000**; 15(11): 2084-94.
- [155] Anderson DG, Putnam D, Lavik EB, Mahmood TA, and Langer R. Biomaterial microarrays: rapid, microscale screening of polymer-cell interaction. *Biomaterials*, **2005**; 26(23): 4892-7.
- [156] Gronowicz G and Raisz LG. Bone formation assays, in "Principles of bone biology", JP Bilezikian, LG Raisz, and GA Rodan, Editors. Academic Press, San Diego, USA. **1996**; 1253-1265.
- [157] Kartsogiannis V and Ng KW. Cell lines and primary cell cultures in the study of bone cell biology. *Mol Cell Endocrinol*, **2004**; 228(1-2): 79-102.
- [158] Majeska RJ. Culture of osteoblastic cells, in "Principles of bone biology", JP Bilezikian, LG Raisz, and GA Rodan, Editors. Academic Press, San Diego, USA. **1996**; 1229-1237.
- [159] Doetschman TC, Eistetter H, Katz M, Schmidt W, and Kemler R. The in vitro development of blastocyst-derived embryonic stem cell lines: formation of visceral yolk sac, blood islands and myocardium. *J Embryol Exp Morphol*, **1985**; 87: 27-45.
- [160] Resnick JL, Bixler LS, Cheng L, and Donovan PJ. Long-term proliferation of mouse primordial germ cells in culture. *Nature*, **1992**; 359(6395): 550-1.
- [161] Buttery LD, Bourne S, Xynos JD, Wood H, Hughes FJ, Hughes SP, Episkopou V, and Polak JM. Differentiation of osteoblasts and in vitro bone formation from murine embryonic stem cells. *Tissue Eng*, **2001**; 7(1): 89-99.
- [162] Kawaguchi J, Mee PJ, and Smith AG. Osteogenic and chondrogenic differentiation of embryonic stem cells in response to specific growth factors. *Bone*, **2005**; 36(5): 758-69.
- [163] Phillips BW, Belmonte N, Vernochet C, Ailhaud G, and Dani C. Compactin enhances osteogenesis in murine embryonic stem cells. *Biochem Biophys Res Commun*, **2001**; 284(2): 478-84.



- [164] zur Nieden NI, Kempka G, Rancourt DE, and Ahr HJ. Induction of chondro-, osteo- and adipogenesis in embryonic stem cells by bone morphogenetic protein-2: effect of cofactors on differentiating lineages. *BMC Dev Biol*, **2005**; 5(1): 1.
- [165] Hyakuna K, Yamamuro T, Kotoura Y, Kakutani Y, Kitsugi T, Takagi H, Oka M, and Kokubo T. The influence of calcium phosphate ceramics and glass-ceramics on cultured cells and their surrounding media. *J Biomed Mater Res*, **1989**; 23(9): 1049-66.
- [166] Norman ME, Elgendy HM, Shors EC, el-Amin SF, and Laurencin CT. An in-vitro evaluation of coralline porous hydroxyapatite as a scaffold for osteoblast growth. *Clin Mater*, **1994**; 17(2): 85-91.
- [167] Suzuki T, Yamamoto T, Toriyama M, Nishizawa K, Yokogawa Y, Mucalo MR, Kawamoto Y, Nagata F, and Kameyama T. Surface instability of calcium phosphate ceramics in tissue culture medium and the effect on adhesion and growth of anchorage-dependent animal cells. *J Biomed Mater Res*, **1997**; 34(4): 507-17.
- [168] Knabe C, Gildenhaar R, Berger G, Ostapowicz W, Fitzner R, Radlanski RJ, and Gross U. Morphological evaluation of osteoblasts cultured on different calcium phosphate ceramics. *Biomaterials*, **1997**; 18(20): 1339-47.
- [169] Knabe C, Ostapowicz W, Radlanski RJ, Gildenhaar R, Berger G, Fitzner R, and Gross U. In vitro investigation of novel calcium phosphates using osteogenic cultures. *J Mater Sci Mater Med*, **1998**; 9(6): 337-45.
- [170] Davies JE. Mechanisms of endosseous integration. *Int J Prosthodont*, **1998**; 11(5): 391-401.
- [171] Geesink RG, de Groot K, and Klein CP. Bonding of bone to apatite-coated implants. *J Bone Joint Surg Br*, **1988**; 70(1): 17-22.
- [172] Hanawa T, Kamiura Y, Yamamoto S, Kohgo T, Amemiya A, Ukai H, Murakami K, and Asaoka K. Early bone formation around calcium-ion-implanted titanium inserted into rat tibia. *J Biomed Mater Res*, **1997**; 36(1): 131-6.
- [173] de Bruijn JD, Klein CPAT, de Groot K, and van Blitterswijk CA. Influence of crystal structure on the establishment of the bone-calcium phosphate interface in vitro. *Cells and materials*, **1993**; 3: 407-17.

- [174] de Bruijn JD, Bovell YP, and van Blitterswijk CA. Structural arrangements at the interface between plasma sprayed calcium phosphates and bone. *Biomaterials*, **1994**; 15(7): 543-50.
- [175] ter Brugge PJ, Wolke JG, and Jansen JA. Effect of calcium phosphate coating crystallinity and implant surface roughness on differentiation of rat bone marrow cells. *J Biomed Mater Res*, **2002**; 60(1): 70-8.
- [176] Hulshoff JE, van Dijk K, van der Waerden JP, Wolke JG, Ginsel LA, and Jansen JA. Biological evaluation of the effect of magnetron sputtered Ca/P coatings on osteoblast-like cells in vitro. *J Biomed Mater Res*, **1995**; 29(8): 967-75.
- [177] Hulshoff JE, van Dijk K, van der Waerden JP, Wolke JG, Kalk W, and Jansen JA. Evaluation of plasma-spray and magnetron-sputter Ca-P-coated implants: an in vivo experiment using rabbits. *J Biomed Mater Res*, **1996**; 31(3): 329-37.
- [178] Gaillard ML and van Blitterswijk CA. Pre-operative addition of calcium ions or calcium-phosphate layer to PEO/PBT copolymers (Polyactive™) stimulates bone mineralization *in vitro*. *J Mater Sci Mater Med*, **1994**; 5: 695-701.
- [179] Gaillard ML, van den Brink J, van Blitterswijk CA, and Luklinska ZB. Applying a calcium phosphate layer on PEO/PBT copolymers affects bone formation in vivo. *J Mater Sci Mater Med*, **1994**; 5: 424-8.
- [180] Wang C, Duan Y, Markovic B, Barbara J, Howlett RC, Zhang X, and Zreiqat H. Proliferation and bone-related gene expression of osteoblasts grown on hydroxyapatite ceramics sintered at different temperature. *Biomaterials*, **2004**; 25(15): 2949-56.
- [181] Habibovic P, Yuan H, van den Doel M, Sees TM, van Blitterswijk CA, and de Groot K. Relevance of osteoinductive biomaterials in a critical-sized orthotopic defect. **2005**; *submitted*.
- [182] Habibovic P, van der Valk CM, Meijer G, van Blitterswijk CA, and de Groot K. Influence of octacalcium phosphate coating on osteoinductive properties of biomaterials. *J Mater Sci Mater Med*, **2004**; 15(4): 373-380.
- [183] Habibovic P, Yuan H, van der Valk CM, Meijer G, van Blitterswijk CA, and de Groot K. 3D microenvironment as essential element for osteoinduction by biomaterials. *Biomaterials*, **2005**; 26(17): 3565-75.

- [184] Adkisson HD, Strauss-Schoenberger, J., Gillis, M., Wilkins, R., Jackson, M. and Hruska, K. A. Rapid quantitative bioassay of osteoinduction. *J Orthop Res*, **2000**; 18(3): 503-11.
- [185] Zhang M, Powers RM, Jr., and Wolfinbarger L, Jr. A quantitative assessment of osteoinductivity of human demineralized bone matrix. *J Periodontol*, **1997**; 68(11): 1076-84.
- [186] Wolfinbarger L, Jr. and Zheng Y. An in vitro bioassay to assess biological activity in demineralized bone. *In Vitro Cell Dev Biol Anim*, **1993**; 29A(12): 914-6.
- [187] Carnes DL, Jr., De La Fontaine J, Cochran DL, Mellonig JT, Keogh B, Harris SE, Ghosh-Choudhury N, Dean DD, Boyan BD, and Schwartz Z. Evaluation of 2 novel approaches for assessing the ability of demineralized freeze-dried bone allograft to induce new bone formation. *J Periodontol*, **1999**; 70(4): 353-63.
- [188] Han B, Tang B, and Nimni ME. Quantitative and sensitive in vitro assay for osteoinductive activity of demineralized bone matrix. *J Orthop Res*, **2003**; 21(4): 648-54.
- [189] Yuan H, Li Y, Yang Z, Feng J, and Zhang X. Calcium phosphate ceramic induced osteogenesis in rabbits, in "Biomedical materials research in the Far East (III)", X Zhang and Y Ikada, Editors. Kobunshi Kankokai, Kyoto, Japan. **1997**; 228-229.
- [190] Kokubo T, Kushitani H, Sakka S, Kitsugi T, and Yamamuro T. Solutions able to reproduce in vivo surface-structure changes in bioactive glass-ceramic A-W. *J Biomed Mater Res*, **1990**; 24(6): 721-34.
- [191] Barrere F, Layrolle P, van Blitterswijk CA, and de Groot K. Biomimetic calcium phosphate coatings on Ti6Al4V: growth study of OCP. *J Mater Sci Mater Med*, **2001**; 12: 529-534.
- [192] Habibovic P, Barrere F, van Blitterswijk CA, de Groot K, and Layrolle P. Biomimetic hydroxyapatite coating on metal implants. *J Amer Ceram Soc*, **2002**; 85(3): 517-522.
- [193] Li JP, Li SH, de Groot K, and Layrolle P. Preparation and characterization of porous titanium. *Key Eng Mat*, **2002**; 218-222: 51-54.

- [194] Magan A and Ripamonti U. Geometry of porous hydroxyapatite implants influences osteogenesis in baboons (*Papio ursinus*). *J Craniofac Surg*, **1996**; 7(1): 71-8.
- [195] Yuan H, de Bruijn JD, van Blitterswijk CA, and de Groot K. Osteoinductive biomaterials and bone repairs. *Trans European Conference on Biomaterials*. **2002**. 156.
- [196] Reddi AH and Huggins C. Biochemical sequences in the transformation of normal fibroblasts in adolescent rats. *Proc Natl Acad Sci U S A*, **1972**; 69(6): 1601-5.
- [197] Urist MR, DeLange RJ, and Finerman GA. Bone cell differentiation and growth factors. *Science*, **1983**; 220(4598): 680-6.
- [198] Cook SD and Rueger DC. Osteogenic protein-1: biology and applications. *Clin Orthop*, **1996**; 324: 29-38.
- [199] Reddi AH. Bone morphogenetic protein, bone marrow stromal cells and mesenchymal stem cells. *Clin Orthop*, **1995**; 313: 115-119.
- [200] Riley EH, Lane JM, Urist MR, Lyons KM, and Lieberman JR. Bone morphogenetic protein-2: biology and applications. *Clin Orthop*, **1996**; 324: 39-46.
- [201] Ruys AJ, Wei M, Sorrell CC, Dickson MR, Brandwood A, and Milthorpe BK. Sintering effects on the strength of hydroxyapatite. *Biomaterials*, **1995**; 16(5): 409-15.
- [202] Kitsugi T, Yamamuro T, Nakamura T, Kokubo T, Takagi M, Shibuya T, Takeuchi H, and Ono M. Bonding behavior between two bioactive ceramics in vivo. *J Biomed Mater Res*, **1987**; 21(9): 1109-23.
- [203] Wang FR. Experimental study of osteogenic activity of sintered hydroxyapatite--on the relationship of sintering temperature and pore size. *Nippon Seikeigeka Gakkai Zasshi*, **1990**; 64(9): 847-59.
- [204] Villarreal DR, Sogal A, and Ong JL. Protein adsorption and osteoblast responses to different calcium phosphate surfaces. *J Oral Implantol*, **1998**; 24(2): 67-73.
- [205] Kruyt MC, de Bruijn JD, Yuan H, van Blitterswijk CA, Verbout AJ, Oner FC, and Dhert WJ. Optimization of bone tissue engineering in goats: a peroperative

- seeding method using cryopreserved cells and localized bone formation in calcium phosphate scaffolds. *Transplantation*, **2004**; 77(3): 359-65.
- [206] Hollander M and Wolfe DA. "Nonparametric statistical inference". John Wiley & Sons, New York, USA. **1973**; 139-146.
- [207] Mendenhall W. "Nonparametric statistics: introduction to probability and statistics". Duxbury Press, Belmont, UK. **1971**; 379-382.
- [208] Yuan H, Yang Z, de Bruijn JD, de Groot K, and Zhang X. Material-dependent bone induction by calcium phosphate ceramics: a 2.5-year study in dog. *Biomaterials*, **2001**; 22(19): 2617-23.
- [209] Habibovic P, Li J, van der Valk CM, Meijer G, Layrolle P, van Blitterswijk CA, and de Groot K. Biological performance of uncoated and octacalcium phosphate-coated Ti6Al4V. *Biomaterials*, **2005**; 26(1): 23-36.
- [210] Kay JF and Cook SD. Biological profile of calcium phosphate coatings, in "Hydroxyapatite coatings in orthopaedic surgery", RG Geesink and MT Manley, Editors. Raven Press, New York, USA. **1993**; 89-106.
- [211] Le Huec JC, Clement D, Brouillaud B, Barthe N, Dupuy B, Foliguet B, and Basse-Cathalinat B. Evolution of the local calcium content around irradiated beta-tricalcium phosphate ceramic implants: in vivo study in the rabbit. *Biomaterials*, **1998**; 19(7-9): 733-8.
- [212] Elliot JC. "Studies in inorganic chemistry: structure and chemistry of the apatites and other calcium orthophosphates". Elsevier Science, Amsterdam, The Netherlands. **1994**; 389.
- [213] Heughebaert M, LeGeros RZ, Gineste M, Guilhem A, and Bonel G. Physicochemical characterization of deposits associated with HA ceramics implanted in nonosseous sites. *J Biomed Mater Res*, **1988**; 22(3 Suppl): 257-68.
- [214] Kohri M, Miki K, Waite DE, Nakajima H, and Okabe T. In vitro stability of biphasic calcium phosphate ceramics. *Biomaterials*, **1993**; 14(4): 299-304.
- [215] Koerten HK, van der Meulen J, and Verhoeven MCH. Degradation of calcium phosphate ceramics: a comparative study on three types of calcium phosphate, in "Bone-bonding materials", P Ducheyne, T Kokubo, and CA van Blitterswijk, Editors. Reed Healthcare Communications, Leiderdorp, The Netherlands. **1992**; 85-94.

- [216] Lacroix P. Recent investigation on the growth of bone. *Nature*, **1945**; 156: 576.
- [217] Karageorgiou V and Kaplan D. Porosity of 3D biomaterial scaffolds and osteogenesis. *Biomaterials*, **2005**; 26(27): 5474-91.
- [218] Hulbert SF, Young FA, Mathews RS, Klawitter JJ, Talbert CD, and Stelling FH. Potential of ceramic materials as permanently implantable skeletal prostheses. *J Biomed Mater Res*, **1970**; 4(3): 433-56.
- [219] Ripamonti U, van den Heever B, and van Wyk J. Expression of the osteogenic phenotype in porous hydroxyapatite implanted extraskelentially in baboons. *Matrix*, **1993**; 13(6): 491-502.
- [220] Yang Z, Yuan H, Zou P, Tong W, Qu S, and Zhang X. Osteogenic response to extraskelentially implanted synthetic porous calcium phosphate ceramics: an early stage histomorphological study in dogs. *J Mater Sci Mater Med*, **1997**; 8: 697-701.
- [221] Manley MT. Calcium phosphate biomaterials: a review of the literature, in "Hydroxyapatite coatings in orthopaedic surgery", RGT Geesink and MT Manley, Editors. Raven Press, New York, USA. **1993**; 1-19.
- [222] Osborn JF. The biological profile of hydroxyapatite ceramics with respect to the cellular dynamics and human soft tissue and mineralized tissue under loaded and unloaded conditions, in "Biomaterials degradation", MA Barbosa, Editor. Elsevier Science, Amsterdam, The Netherlands. **1991**; 185-225.
- [223] Hollinger JO, Brekke J, Gruskin E, and Lee D. Role of bone substitutes. *Clin Orthop*, **1996**; 324: 55-65.
- [224] Daculsi G, Laboux O, Malard O, and Weiss P. Current state of the art of biphasic calcium phosphate bioceramics. *J Mater Sci: Mater Med*, **2003**; 14: 195-200.
- [225] Pilliar RM. Porous-surfaced metallic implants for orthopedic applications. *J Biomed Mater Res*, **1987**; 21(A1 Suppl): 1-33.
- [226] Pilliar RM. Overview of surface variability of metallic endosseous dental implants: textured and porous-structured designs. *Implant Dent.*, **1998**; 7(4): 305-314.
- [227] Jaffe WL and Scott DF. Total hip arthroplasty with hydroxyapatite-coated prostheses. *J Bone Joint Surg Am*, **1996**; 78(12): 1918-34.

- [228] Bhardwaj T, Pilliar RM, Grynblas MD, and Kandel RA. Effect of material geometry on cartilaginous tissue formation in vitro. *J Biomed Mater Res*, **2001**; 57(2): 190-9.
- [229] Wu B and Guo F. A study of preparation of man-made hipbone by using composite porous titanium. *The Technology of Powder Metallurgy*, **1990**; 8(4): 145-149.
- [230] Jansen JA, von Recum AF, van der Waerden JP, and de Groot K. Soft tissue response to different types of sintered metal fibre-web materials. *Biomaterials*, **1992**; 13(13): 959-68.
- [231] Ferretti C and Ripamonti U. Human segmental mandibular defects treated with naturally derived bone morphogenetic proteins. *J Craniofac Surg*, **2002**; 13(3): 434-44.
- [232] Vehof JW, Takita H, Kuboki Y, Spauwen PH, and Jansen JA. Histological characterization of the early stages of bone morphogenetic protein-induced osteogenesis. *J Biomed Mater Res*, **2002**; 61(3): 440-9.
- [233] van den Dolder J, Farber E, Spauwen PH, and Jansen JA. Bone tissue reconstruction using titanium fiber mesh combined with rat bone marrow stromal cells. *Biomaterials*, **2003**; 24(10): 1745-50.
- [234] Sikavitsas VI, van den Dolder J, Bancroft GN, Jansen JA, and Mikos AG. Influence of the in vitro culture period on the in vivo performance of cell/titanium bone tissue-engineered constructs using a rat cranial critical size defect model. *J Biomed Mater Res*, **2003**; 67A(3): 944-51.
- [235] Zardiackas LD, Parsell DE, Dillon LD, Mitchell DW, Nunnery LA, and Poggie R. Structure, metallurgy, and mechanical properties of a porous tantalum foam. *J Biomed Mater Res*, **2001**; 58(2): 180-7.
- [236] Bobyn JD, Stackpool GJ, Hacking SA, Tanzer M, and Krygier JJ. Characteristics of bone ingrowth and interface mechanics of a new porous tantalum biomaterial. *J Bone Joint Surg Br*, **1999**; 81(5): 907-14.
- [237] Sidhu KS, Prochnow TD, Schmitt P, Fischgrund J, Weisbrode S, and Herkowitz HN. Anterior cervical interbody fusion with rhBMP-2 and tantalum in a goat model. *Spine J*, **2001**; 1(5): 331-40.

- [238] Cavagna R, Daculsi G, and Bouler JM. Macroporous calcium phosphate ceramic: a prospective study of 106 cases in lumbar spinal fusion. *J Long Term Eff Med Implants*, **1999**; 9(4): 403-12.
- [239] Ducheyne P, Bianco P, Radin S, and Schepers E. Bioactive materials: mechanism and bioengineering considerations, in "Bone-bonding materials", P Ducheyne, T Kokubo, and CA van Blitterswijk, Editors. Reed Healthcare Communications, Leiderdorp, The Netherlands. **1993**; 1-12.
- [240] LeGeros RZ, Orly I, Gregoire M, and Daculsi G. Substrate surface dissolution and interfacial biological mineralization, in "The bone-bonding interface", JE Davies, Editor. University of Toronto Press, Toronto, Canada. **1991**; 76-87.
- [241] Gosain AK, Riordan PA, Song L, Amarante MT, Kalantarian B, Nagy PG, Wilson CR, Toth JM, and McIntyre BL. A 1-year study of osteoinduction in hydroxyapatite-derived biomaterials in an adult sheep model: part II. Bioengineering implants to optimize bone replacement in reconstruction of cranial defects. *Plast Reconstr Surg*, **2004**; 114(5): 1155-63.
- [242] Banwart JC, Asher MA, and Hassanein RS. Iliac crest bone graft harvest donor site morbidity. A statistical evaluation. *Spine*, **1995**; 20(9): 1055-60.
- [243] Davies JE and Hosseini MM. Histodynamics of endosseous wound healing, in "Bone engineering", JE Davies, Editor. em squared Inc., Toronto, Canada. **2000**; 1-14.
- [244] Burwell RG. The function of bone marrow in the incorporation of a bone graft. *Clin Orthop Relat Res*, **1985**; 200: 125-41.
- [245] Friedenstein AJ. Stromal cells responsible for transferring the microenvironment of the homopoietic tissues. Cloning in vitro and retransplantation in vivo. *Transplantation*, **1974**; 17: 331-40.
- [246] King GN. The importance of drug delivery to optimize the effects of bone morphogenetic proteins during periodontal regeneration. *Curr Pharm Biotechnol*, **2001**; 2(2): 131-42.
- [247] Stoeger T, Proetzel GE, Welzel H, Papadimitriou A, Dony C, Balling R, and Hofmann C. In situ gene expression analysis during BMP2-induced ectopic bone formation in mice shows simultaneous endochondral and intramembranous ossification. *Growth Factors*, **2002**; 20(4): 197-210.



## Acknowledgements

First of all, I would like to thank my promoters Prof. Klaas de Groot and Prof. Clemens van Blitterswijk. I am thankful to both of you for giving me the opportunity to pursue my PhD within your group. Dear Klaas, I greatly appreciate your availability, guidance and feedback, even when I needed to discuss some less scientific matters. You taught me that a lot can be said with very few words, and for me, that is worth a million. I couldn't wish for a better supervisor for my PhD time. Dear Clemens, although we often disagree on the answer to the question "how big the steps should be to reach the goal?", I always enjoyed your inspiring scientific ideas. Your criticism and your compliments were always "right on the nose" and your sharp and thorough corrections of the manuscripts taught me that there are many ways to write something, but only one to be read.

I would also like to thank my old colleagues from IsoTis' Rainbow team, and in particular Dr. Pierre Layrolle, who helped and stimulated me to start my PhD.

To all my fellow PhD students, and all the other members of the "PhD Pool" over the past four years: thank you all for creating such a great environment to work in. My special thanks goes to my office mates and my housemate: I hope I did not bother you too much with "the making of" my thesis.

To the personnel of the "Afdeling Groot" at the GDL: thank you all for being so helpful and taking good care of "my" goats. My special thanks goes to the three ladies without whom my animal studies wouldn't have been possible: Chantal, Tara and Mirella. I enjoyed my time working with you, and you taught me (at least you tried to) how to stop being such a control freak.

For the preparation of my "more" and "less" osteoinductive biomaterials I am very grateful to my Chinese friends, Jiaping and Yuan. I am also thankful for the dinners you prepared for me, which were, if possible, even better than your materials.

My great appreciation goes to Moyo Kruyt. Dear Moyo, you are, without doubt, a great scientist. Thank you very much for all the fruitful discussions.

In a great working environment such as IsoTis and "PhD Pool", it happens that some colleagues become more than that: Jeanine, Ineke, Shihong, Inge, Chang, Peter, Paul, Jeroen, Frederic, Roka, Lorenzo, Linda, Remco, Peter Paul, Mireille, Jan, Joost, Jérôme,

Fabiënne, Steven, Tim, Aart, Jos, Clay, thank you for all the nice times in and outside the lab.

I would also like to thank my dear friends Eva, Jessica, Seka, Sajo, Darko, Silvana, Biserica, Mirela, Edin: thanks for showing me that there is so much more in the world than osteoinduction alone.

Some of my very little friends deserve thanks too: Emma, David, Levi, Thijmen, Nienke, Jade, Yoëlle, Cas and especially Rémi, thank you for reminding me how surprising and beautiful the world can be.

My special thanks goes to two quite different people, both very special to me. Dear Flo, you are the best friend a person can have. Thanks for all the great times together. I hope our friendship will last for a long time. Dear Mirella, it is a great feeling to know that I can tell you everything anytime. I hope you have the same feeling too. You are a great friend!

To my family, which has, although scattered all over the world, always been very supportive: hvala! I would also like to thank family Verburg for their hospitality and friendship.

A very special thanks goes to Pim: for the cover, help with layout, for your patience, support, inspiration, criticism and love. Thank you for being my best friend!

To my sister and her husband: thank you both for all the support and love.

To my mother: thank you for being the best mom in the world. Your unconditioned love and your cooking are priceless. Draga mama, puno ti hvala na svemu!

Finally, a very special thanks goes to my father, who was the most inspiring person I have ever known. Dragi tata, nadam se da si ponosan na mene. Hvala na svemu.

Pamela

## Curriculum Vitae

Pamela Habibovic was born on March 12<sup>th</sup> 1977 in Tuzla, Bosnia and Herzegovina. After the graduation from high school (HAVO, Roncalli SG, Bergen op Zoom, The Netherlands) in 1996, she joined The Hague University (The Hague, The Netherlands) whereby she was awarded a BEng. degree in Chemical Engineering and Industrial Management, with honors, in 2000. During her studies, she performed two internships, one at the University of San Carlos, Department of Chemical Engineering, Cebu City, Philippines, where she worked on adsorption of hexavalent chromium from waste waters by using the seaweed *Sargassum siliquosum* and one at IsoTis NV, Bilthoven, The Netherlands where she worked on optimization and upscaling of the biomimetic calcium-phosphate coating process. The latter internship resulted in the first authorship of the paper Habibovic P. et.al., Biomimetic hydroxyapatite coating on metal implants, J Amer Cerm Soc, 2002; 85(3): 517-22. From July 2000 until October 2001 she worked as a research technician at IsoTis NV, Bilthoven, The Netherlands on improvement of biomimetic calcium-phosphate coatings. In October 2001 she started as a PhD student at University of Twente, Institute for Biomedical Technology on the EU funded project "Intelligent scaffolds for tissue engineering of bone, skin and cartilage" under supervision of Prof. Klaas de Groot and Prof. Clemens A. van Blitterswijk. The subject of her research was the mechanism and clinical relevance of osteoinductive biomaterials. From November 2005, she will continue her scientific work at the Institute for Biomedical Technology of the University of Twente.

## Selected colour figures

### Chapter 2

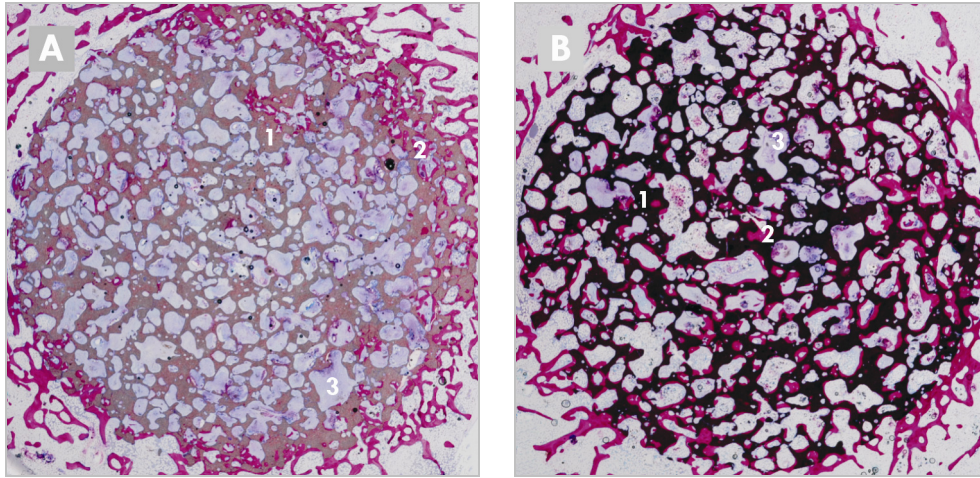


**Figure 2:** digital photographs of BCP1300 (A) and BCP1150 (B) after implantation in goat iliac wing defect for 12 weeks.  
(1) = ceramic, (2) = bone, (3) = fibrous tissue.

Only a small ridge of new bone has formed along the host bone bed in the BCP1300 disc (A), while bone has grown deeply inside the BCP1150 disc (B).

## Chapter 2

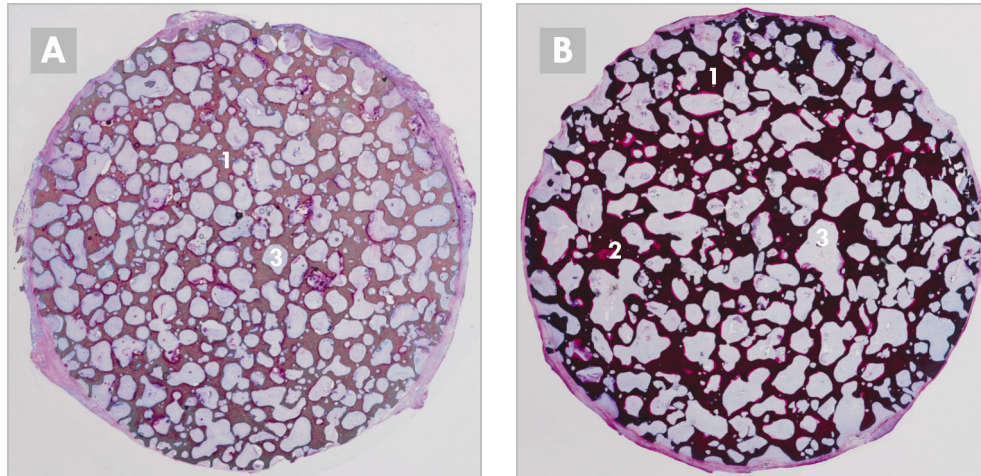


**Figure 3:** digital photograph of histological slides of BCP1300 (A) and BCP1150 (B) after 12-week intramuscular implantation in goat.

(1) = ceramic, (2) = bone, (3) = fibrous tissue.

In BCP1300, the ceramic is extensively filled with fibrous tissue, but no signs of bone formation are observed.

In BCP1150 (B) bone has formed in the pores of the implants, aligning its surface.

Chapter 3

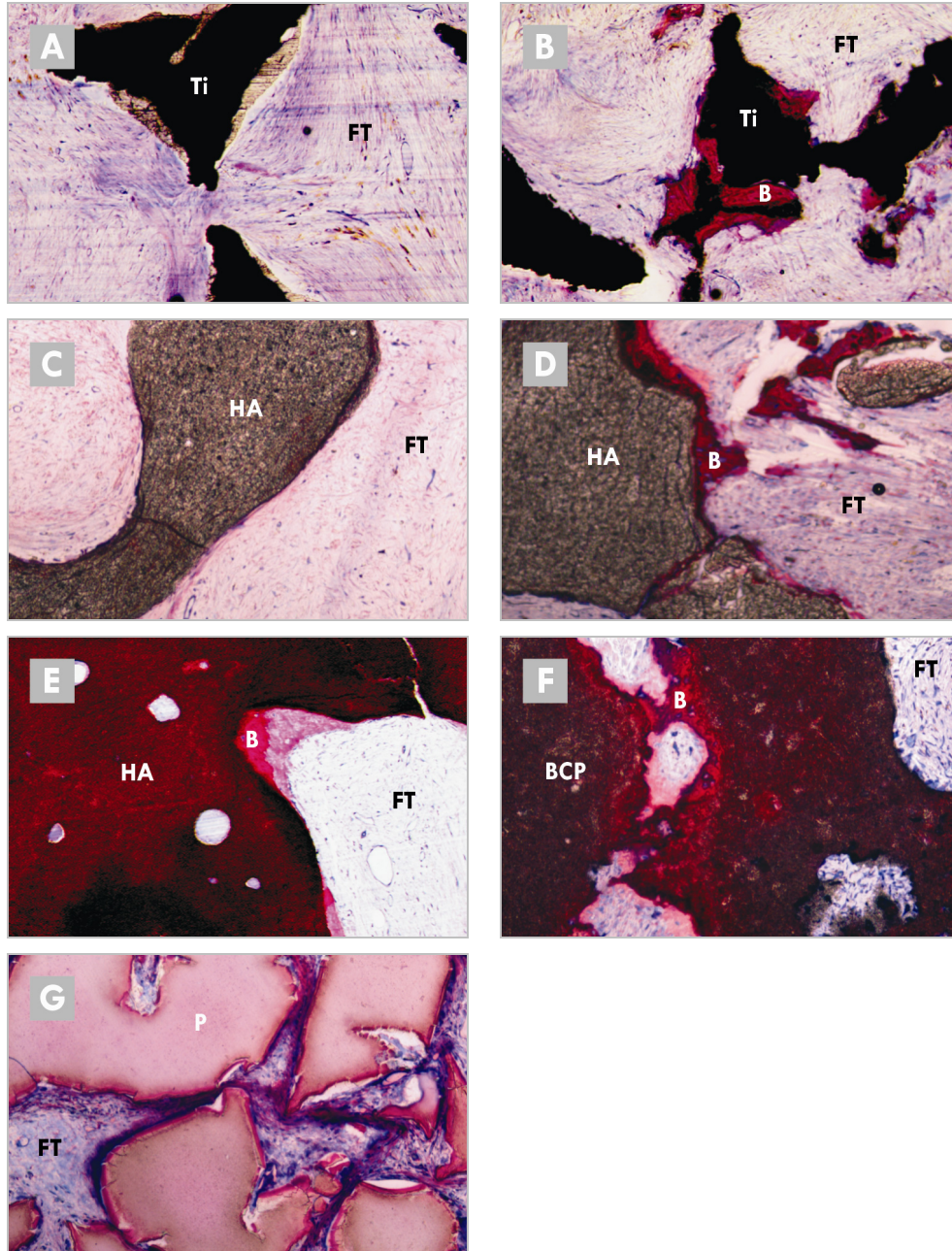


**Figure 2:** LM photographs (magnification 10x) after 12 weeks of intramuscular implantation of Ti6Al4V (A), OCP Ti6Al4V (B), HA (C), OCP HA (D), BCP (E), OCP BCP (F) and OCP PEGT-PBT (G).

Ti=titanium alloy, HA=hydroxyapatite, BCP=biphasic calcium phosphate, P=PEGT-PBT, FT=fibrous tissue and B=bone.



## Chapter 4

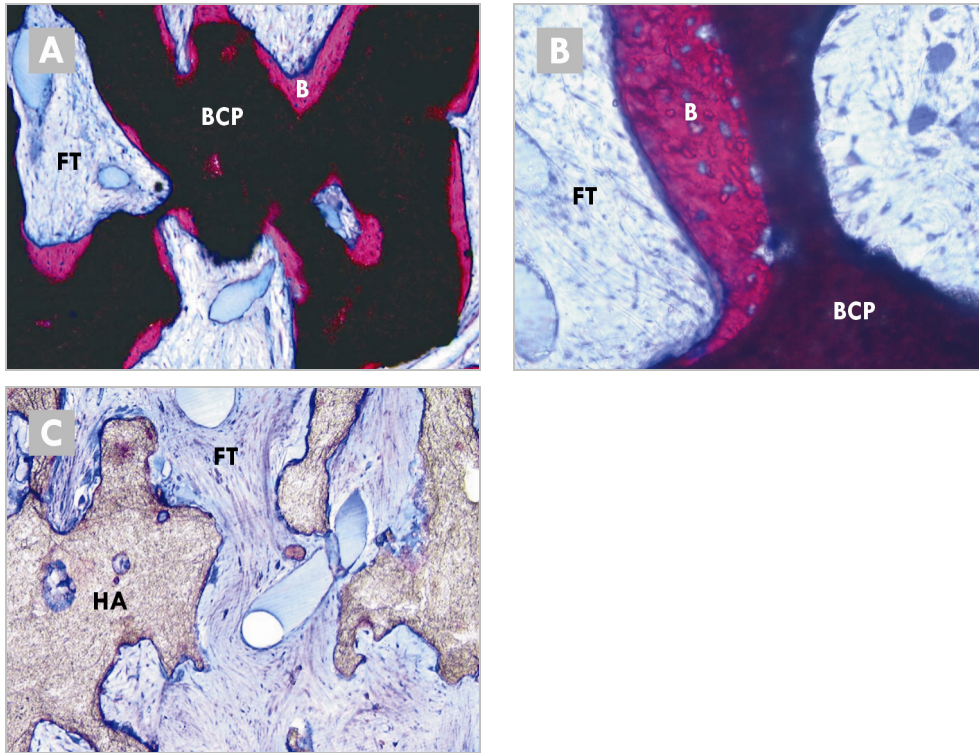


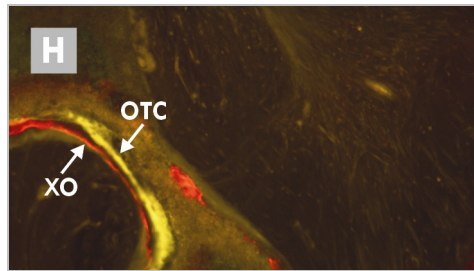
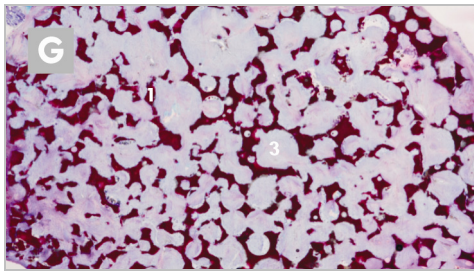
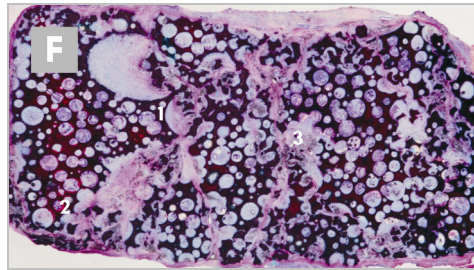
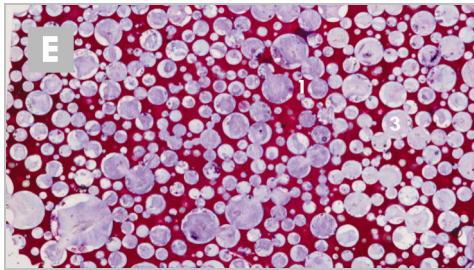
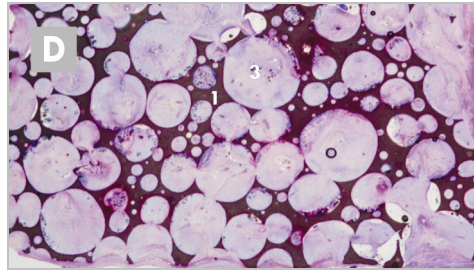
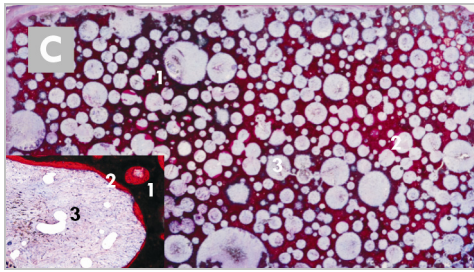
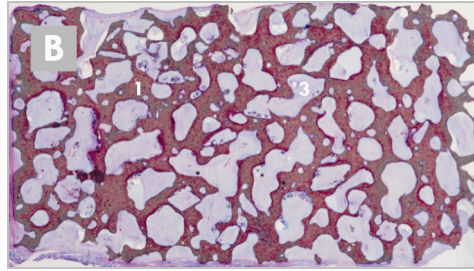
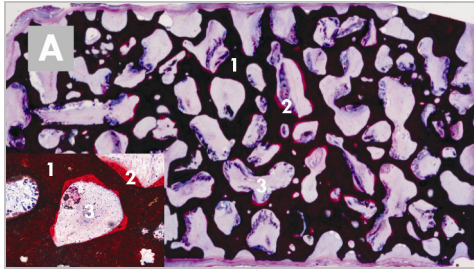
**Figure 7:** LM photographs of BCP1150 (magnification 4x) (A), BCP1150 (magnification 20x) (B), and HA1250 (magnification 4x) (C) after 12 weeks of implantation.

B=bone, FT=fibrous tissue BCP=BCP1150 ceramic, HA=HA1250 ceramic.

The induced bone is formed in the pores of the implant, aligning its surface (A). The formed bone is normal in appearance, aligned with osteoblasts and with osteocytes and osteoid clearly visible (B).

The non-inductive ceramic is filled with fibrous tissue, but no signs of bone formation are observed (C).

Chapter 5





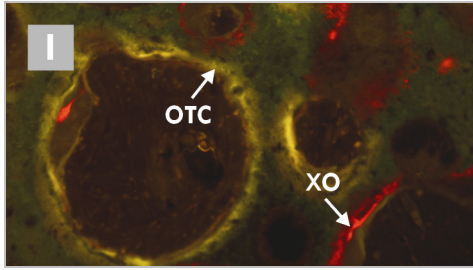


**Figure 5:** digital photograph of histological slides of intramuscularly implanted BCPA (A) (inset = LM photograph magnification 10x), BCPB (B), BCPC (C) (inset = LM photograph magnification 10x), BCPD (D), CA (E), BCPA (F), CA (G) and fluorochrome markers of BCPA (H) and BCPC (I).

(1) = ceramic, (2) = bone, (3) = fibrous tissue, OTC = Oxytetracycline, XO = Xylenol orange.

The induced bone in BCPA and BCPC (A and C respectively) is formed in the pores of the implants, aligning their surface. The bone is normal in appearance, aligned with osteoblasts and with osteocytes and osteoid clearly visible (insets of A and C). BCPB, BCPD and CA ceramics (B, D and E respectively) are extensively filled with fibrous tissue, but no signs of bone formation are observed. In some animals, BCPC ceramic was fragmented and mechanical degradation was observed. Note bone formation only in the non-fragmented part of the implant (F). In some animals, chemical dissolution of CA ceramic was observed (G). Presence of both Oxytetracycline and Xylenol orange marker shows that the bone formation in both BCPA and BCPC (H and I respectively) had started before the sixth week of implantation.

Chapter 6

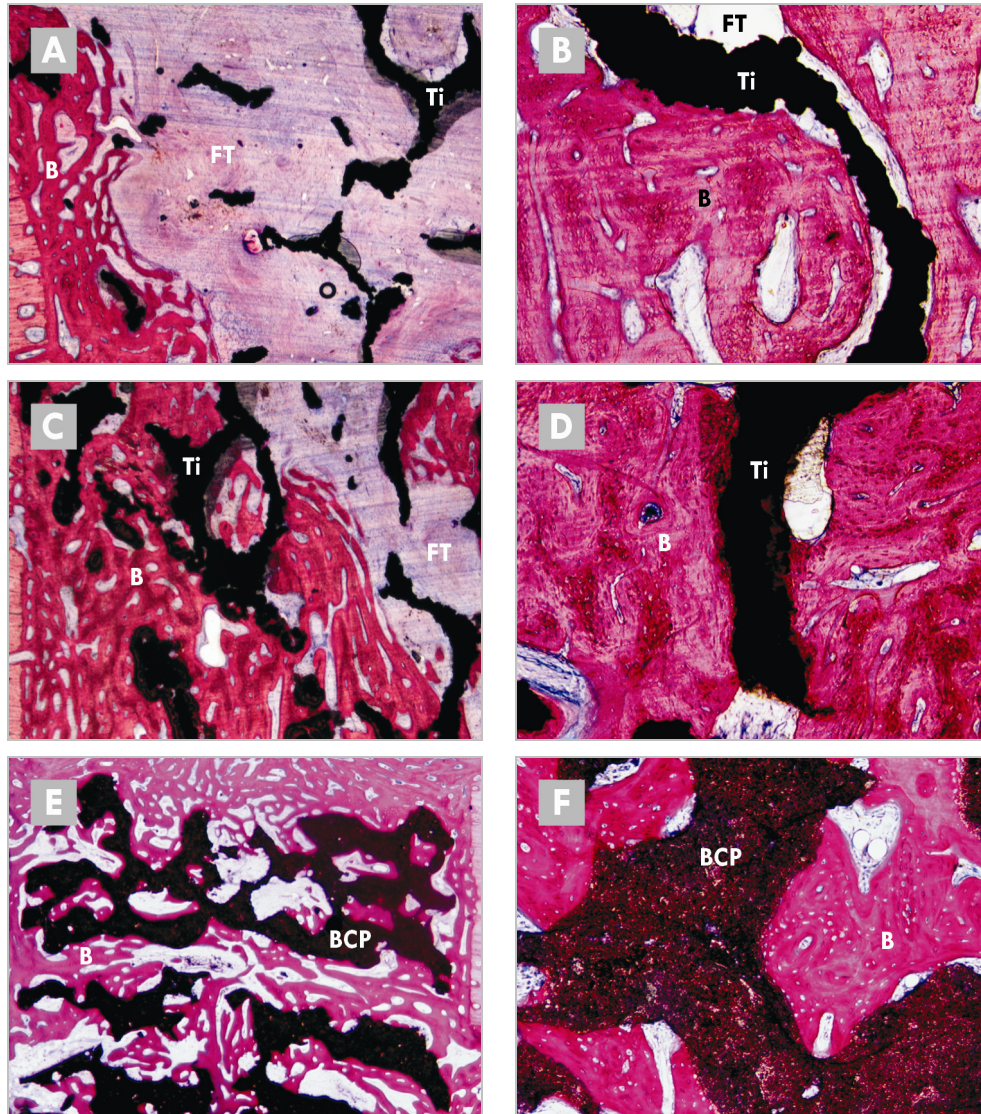


**Figure 9:** LM photographs of histological slides of uncoated Ti6Al4V after 6 weeks (magnification 2x) (A) and 12 weeks (magnification 10x) (B); OCP coated Ti6Al4V after 6 weeks (magnification 2x) (C) and 12 weeks (magnification 10x) (D) and BCP after 6 weeks (magnification 2x) (E) and 12 weeks (magnification 10x) (F) of transcortical implantation.

Ti=Ti6Al4V, B=bone, FT=fibrous tissue, BCP=ceramic.

More bone has grown in the OCP Ti6Al4V and BCP (A and C) implants in comparison to the uncoated Ti6Al4V implant (E). Similarly, there is more direct bone contact between the newly formed bone in OCP Ti6Al4V and BCP implants (B and D) in comparison with the uncoated Ti6Al4V implants (F).

## Chapter 6

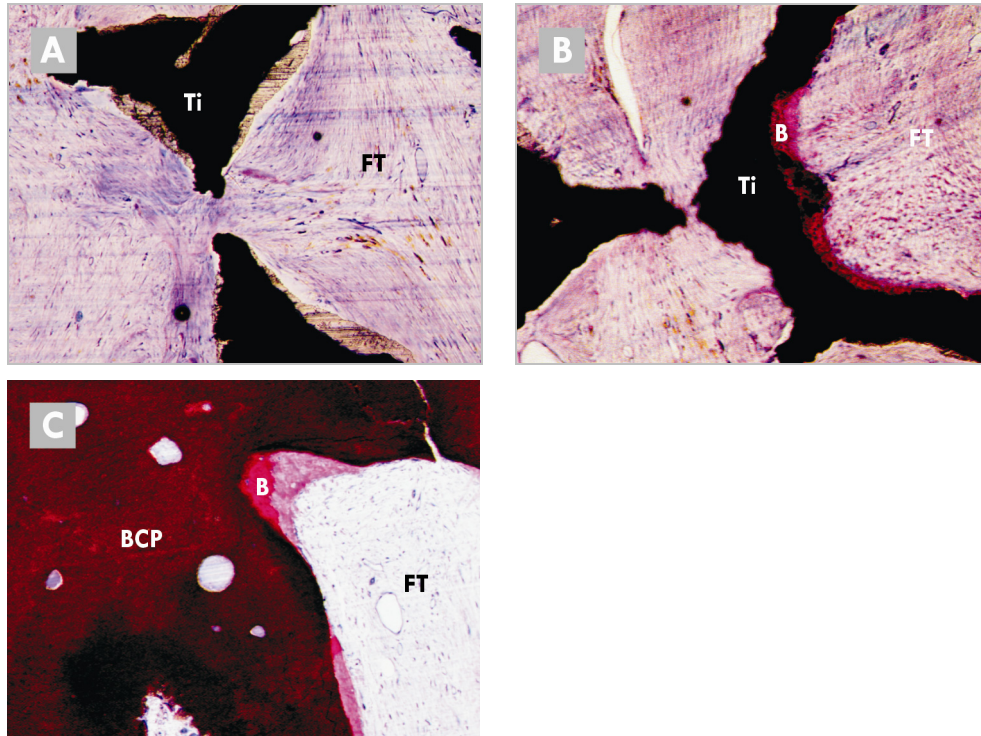


**Figure 11:** LM photographs of histological slides magnification 10x of uncoated Ti6Al4V (A), OCP coated Ti6Al4V (B) and BCP (C) after 12 weeks of intramuscular implantation.

Ti=Ti6Al4V, B=bone, FT=fibrous tissue, BCP=ceramic.



Chapter 6

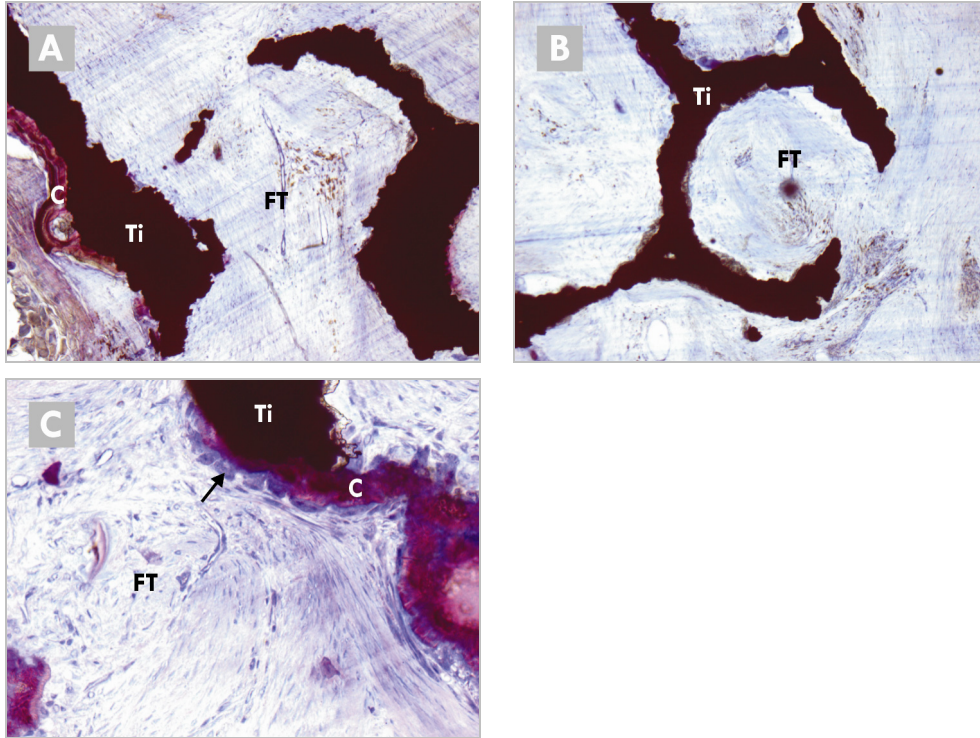


**Figure 12:** LM photographs of histological slides magnification 5x of the OCP Ti6Al4V after 6 weeks (A) and 12 weeks (B) of implantation, and magnification 20x after 6 weeks of implantation.

Ti=Ti6Al4V, B=bone, FT=fibrous tissue, C=OCP coating; BCP=ceramic.

In (A) there is still some coating present on the periphery of the implant after 6 weeks of implantation, in (B) after 12 weeks of implantation the coating is further degraded, in (C) multinucleated cells (see arrow) are resorbing the coating left after 6 weeks of implantation.

## Chapter 7

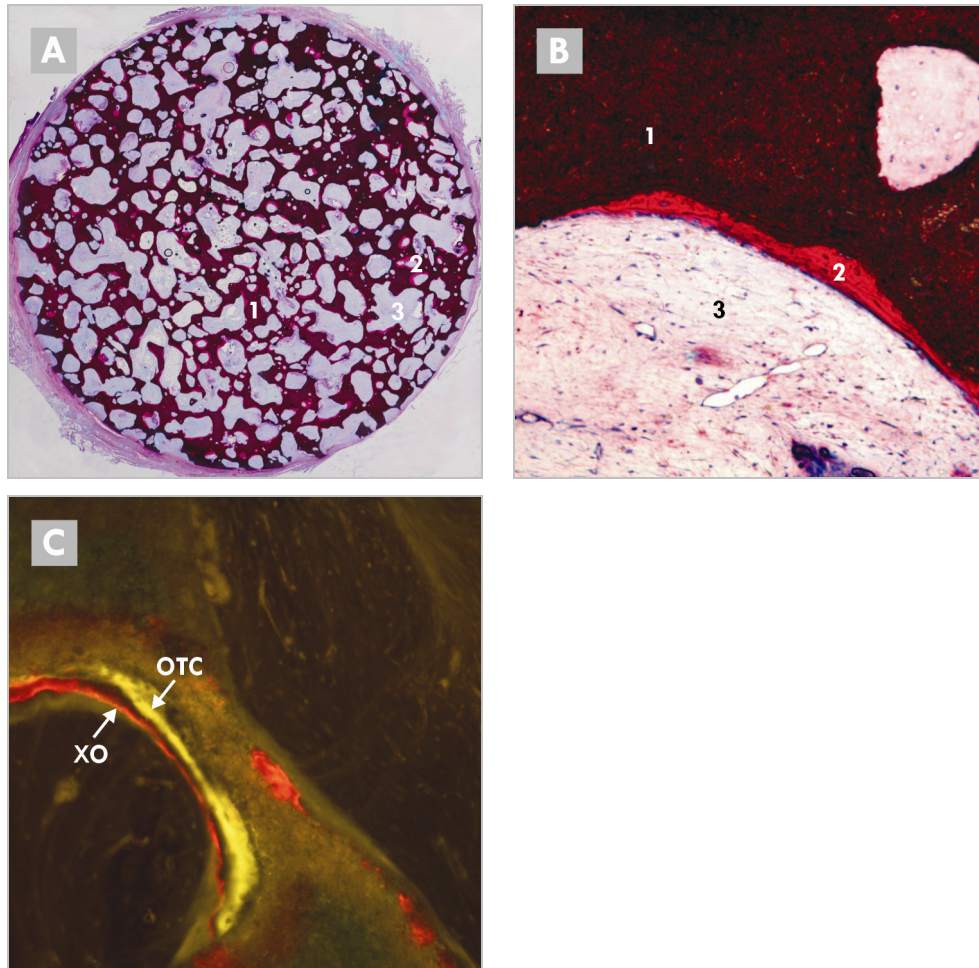


**Figure 5:** digital photograph (A), LM photograph (magnification 10x) of a histological slide (B) and fluorochrome markers (C) of intramuscularly implanted BCP1150.

(1) = ceramic, (2) = bone, (3) = fibrous tissue, OTC = Oxytetracycline, XO = Xylenol orange.

The induced bone is formed in the pores of the implant, aligning its surface (A). The bone is normal in appearance, aligned with osteoblasts and with osteocytes and osteoid clearly visible (B). The presence of both Oxytetracycline and Xylenol orange marker shows that the bone formation had started before the sixth week of implantation (C).

Chapter 7

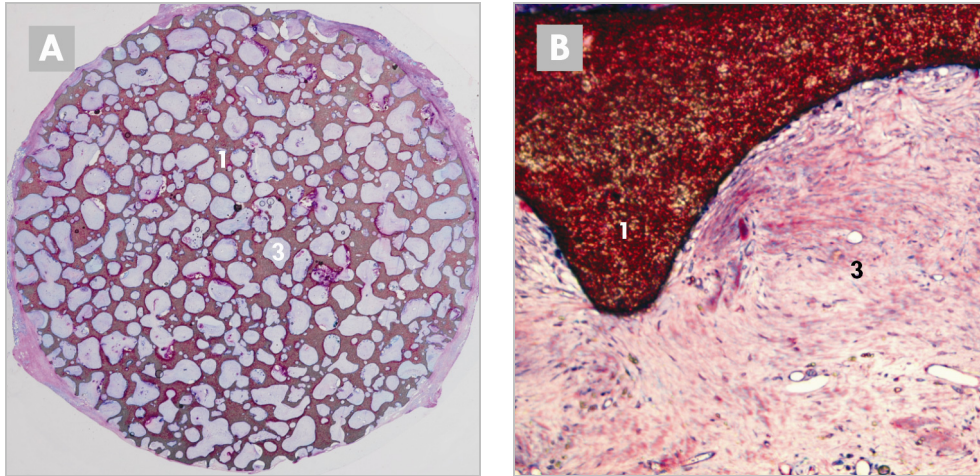


**Figure 6:** digital photograph (A) and LM photograph (magnification 10x) (B) of a histological slide of the intramuscularly implanted BCP1300.

(1) = ceramic, (3) = fibrous tissue.

The ceramic is extensively filled with fibrous tissue, but no signs of bone formation are observed.

## Chapter 7

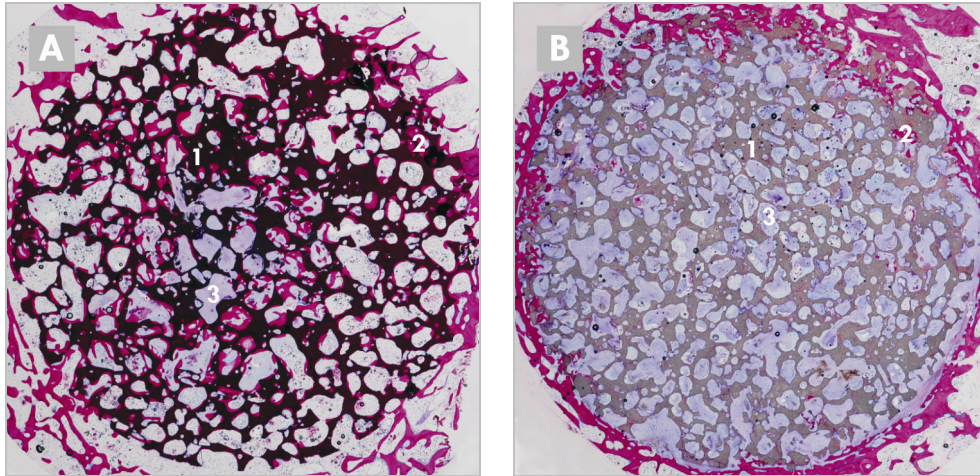


**Figure 7:** digital photographs of BCP1150 (A) and BCP1300 (B) after explantation from the iliac wing defect.

(1) = ceramic, (2) = bone, (3) = fibrous tissue.

Bone has grown deeply inside the BCP1150 disc (A) while only a small ridge of new bone has formed along the host bone bed in the BCP1300 disc (B).



Chapter 7

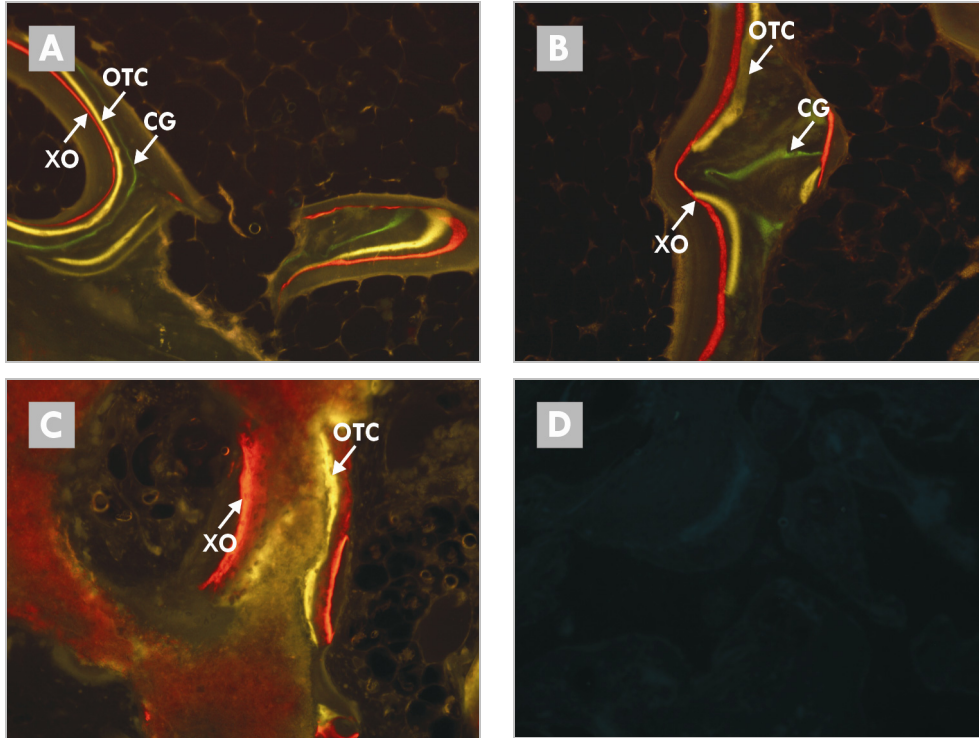


**Figure 8:** LM photographs (magnification 10x) of the fluorochrome markers on the periphery of BCP1150 (A) and BCP1300 (B) and in the center of BCP1150 (C) and BCP1300 (D) discs explanted from the iliac wing defects.

CG = Calcein green, OTC = Oxytetracycline, XO = Xylenol orange.

On the peripheries of both BCP1150 (A) and BCP1300 (B) all markers can be seen, which shows that in both ceramics bone formation near the host bone bed had started before the fourth week of implantation.

The presence of the Oxytetracycline and Xylenol orange marker in the center of BCP1150 disc (C) shows that the bone formation far away from the host bone bed had started before the sixth week of implantation. Absence of any of the markers in the center of BCP1300 (D) illustrates the absence of new bone within the first eight weeks of implantation.